National and Kapodistrian University of Athens
Medical School
Department of Pharmacology

Ph.D. Thesis

"*Crocus sativus* L. – derived bioactive compounds: Development and holistic evaluation of their biological role in neurodegenerative diseases"

«Ανάπτυξη και ολιστική αξιολόγηση του βιολογικού ρόλου βιοδραστικών ουσιών από το φυτό *Crocus sativus* L. σε νευροεκφυλιστικές νόσους»

Ph.D. Candidate

Evangelia Karkoula

Pharmacist M.Sc.

Athens 2018

1	Ημερομηνία Αιτήσεως υποψηφίου	22/01/2014
2	Ημερομηνία ορισμού 3μελούς Συμβουλευτικής επιτροπής	18/03/2014
3	Μέλη 3μελούς Συμβουλευτικής επιτροπής	Τσαρμπόπουλος Αντώνιος (Επιβλέπων) Αναπλ. Καθηγητής Ιατρικής σχολής Αθηνών
		Σκαλτσούνης Αλέξιος- Λέανδρος Καθηγητής Φαρμακευτικής σχολής Αθηνών
		Γκίκας Ευάγγελος Επικ. Καθηγητής Φαρμακευτικής σχολής Αθηνών
4	Ημερομηνία ορισμού του Θέματος	17/04/2015
5	Ημερομηνία καταθέσεως της Διδακτορικής Διατριβής	28/06/2018

Scientific Examining Committee

1. **Anthony Tsarbopoulos (Supervisor, Member of the Three-member Advisory Committee)**
   Associate Professor
   National and Kapodistrian University of Athens, Medical School, Department of Pharmacology

2. **Alexios-Leandros Skaltsounis (Member of the Three-member Advisory Committee)**
   Professor
   National and Kapodistrian University of Athens, Department of Pharmacy, Division of Pharmacognosy

3. **Evagelos Gikas (Member of the Three-member Advisory Committee)**
   Assistant Professor
   National and Kapodistrian University of Athens, University of Athens, Department of Pharmacy, Division of Pharmaceutical Chemistry

4. **Constantinos Pantos**
   Professor (Director of Department of Pharmacology)
   National and Kapodistrian University of Athens, Medical School, Department of Pharmacology

5. **Jonas Bergquist**
   Professor
   Department of Chemistry - BMC, Uppsala University, Uppsala, Sweden.

6. **Nikolaos Skarmeas**
   Associate Professor of Neurology
   National and Kapodistrian University of Athens, Eginition Hospital

7. **Christina Dalla**
   Assistant Professor
   National and Kapodistrian University of Athens, Medical School, Department of Pharmacology

Dean of the School of Medicine
Professor Petros P. Sfikakis

Πρόεδρος Ιατρικής Σχολής Αθηνών
Καθηγητής Πέτρος Π. Σφηκάκης

ΟΡΚΟΣ ΙΠΠΟΚΡΑΤΟΥΣ

"Ορκίζομαι στον Απόλλωνα τον Ιατρό και στον Ασκληπιό και στην Υγεία και στην πανάκεια και σ΄ όλους τους Θεούς επικαλούμενος την μαρτυρία τους, να τηρήσω πιστά κατά τη δύναμη και την κρίση μου αυτό τον όρκο και το συμβόλαιό μου αυτό. Να θεωρώ αυτόν που μου δίδαξε αυτή την τέχνη ίσο με τους γονείς μου και να μοιραστώ μαζί μου τα υπάρχοντά μου και τα χρήματά μου αν έχει ανάγκη φροντίδας.

Να θεωρώ τους απογόνους του ίσους με τ΄ αδέλφια μου και να τους διδάξω την τέχνη αυτή αν θέλουν να τη μάθουν, χωρίς αμοιβή και συμβόλαιο και να μεταδώσω με παραγγελίες, οδηγίες και συμβουλές όλη την υπόλοιπη γνώση μου και στα παιδιά μου και στα παιδιά εκείνου με δίδαξε και στους άλλους μαθητές που έχουν κάνει γραπτή συμφωνία μαζί μου και σ΄ αυτούς που έχουν ορκισθεί στον ιατρικό νόμο και σε κανέναν άλλο και να θεραπεύω τους πάσχοντες κατά τη δύναμή μου και την κρίση μου χωρίς ποτέ, εκουσίως, να τους βλάψω ή να τους αδικήσω. Και να μη δώσω ποτέ σε κανένα, έστω κι αν μου το ζητήσει, θανατηφόρο φάρμακο, ούτε να δώσω ποτέ τέτοια συμβουλή. Ομοίως να μη δώσω ποτέ σε γυναίκα φάρμακο για ν΄ αποβάλει. Να διατηρήσω δε τη ζωή μου και την τέχνη μου καθαρή και αγνή. Και να μη χειρουργήσω πάσχοντες από λίθους αλλά ν΄ αφήσω την πράξη αυτή για τους ειδικούς. Και σ΄ όποια σπίτια κι αν μπω, να μπω για την ωφέλεια των πασχόντων αποφεύγοντας κάθε εκούσια αδικία και βλάβη και κάθε γενετήσια πράξη και με γυναίκες και με άνδρες, ελεύθερους και δούλους. Και ό,τι δω ή ακούσω κατά την άσκηση του επαγγέλματός μου, ή κι εκτός, για τη ζωή των ανθρώπων, που δεν πρέπει ποτέ να κοινοποιηθεί, να σιωπήσω και να το τηρήσω μυστικό. Αν τον όρκο μου αυτό τηρήσω πιστά και δεν τον αθετήσω, είθε ν΄ απολαύσω για πάντα την εκτίμηση όλων των ανθρώπων για τη ζωή μου και για την τέχνη μου, αν όμως παραβώ και αθετήσω τον όρκο μου να υποστώ τα αντίθετα από αυτά".

CURRICULUM VITAE

PERSONAL INFORMATION

Karkoula Evangelia

Nikitara 52, Chiliomodi Korinthias, PostCode 20008 Greece

+30 6978581894

evakarkoula@gmail.com

evakarkoula@med.uoa.gr

Date of birth 23/01/1989 | Nationality Greek

PERSONAL STATEMENT

Pharmacist, Ph.D Candidate of Athens Medical School, M.Sc. in Pharmacognosy & Natural Products Chemistry and specialized researcher on the fields of Natural Products' Isolation and Analysis. Practical experience in targeted isolation of bioactive natural compounds in analytical and preparative scale using modern techniques and state-of-the-art equipment. Experience in analytical methods' development and validation. Supervisor of undergraduate and postgraduate students and capable of imparting knowledge to them. Efficient, highly-organised with multi-tasking skills, quick decision maker and capable of handling and overcoming stressful situations in the laboratory. Pleasant company to my colleagues and friends and able to create a friendly ambience in my workplace.

WORK EXPERIENCE

March 2017– December 2017

Participation in the program "Development and Validation of analytical methodologies for the determination of *Crocus*-derived bioactive compounds in mice brain and plasma"

The Goulandris Natural History Museum

- Pharmacist - Analytical researcher

March 2016– December 2016

Participation in the program "Development of an industrial process for the integrated sustainable management of winemaking waste through the recovery of high added value and composting polyphenols"

Faculty of Pharmacy, National and Kapodistrian University of Athens, Greece

- Pharmacist - Analytical researcher

May 2014 – July 2015

Participation in the program "SYNERGASIA" − Development and Scanning of new *Amyloid Beta* Peptide inhibitors against Alzheimer's disease

Medical School, Athens

- Pharmacist - Analytical researcher

January 2011 – June 2011

Internship in a homeopathic Pharmacy

Markos Filianos Pharmacy, Krisila 16, Pangrati

- Assistant in homeopathic medicines' preparation and pharmaceutical cosmetic products production

July 2010 – December 2010

Internship in Hospital's Pharmacy

General Hospital of Nafplio

- Assistant in providing the clinics with the necessary medicines for the patients' treatment.

EDUCATION AND TRAINING

March 2014 – today

Ph.D. Candidate, Medical School

EQF Level 8

Medical School, National and Kapodistrian University of Athens, Greece

- Ph.D. Thesis: *Crocus sativus* L. – derived bioactive compounds: Development and holistic evaluation of their biological role in neurodegenerative diseases

November 2011 – July 2013

M.Sc. Graduate of Pharmacognosy

EQF level 7

Faculty of Pharmacy, National and Kapodistrian University of Athens, Greece (Degree: Excellent 9,73/ 10)

- M.Sc. Thesis: *New method of direct quantitative measurement of four secoiridoids in olive oil using NMR spectroscopy*

October 2011

Licence to practise pharmacy

September 2006 – July 2011

Graduate of Faculty of Pharmacy

EQF level 6

Faculty of Pharmacy, National and Kapodistrian University of Athens, Greece (Degree: Very Good 7,81/ 10)

- Diploma Thesis: A c*hemotaxonomic study of Greek extra virgin olive oils*

2006

Graduate of Greek High School

Degree: Excellent: 19,1/20)

PERSONAL SKILLS

Mother tongue Greek

Other languages

	UNDERSTANDING		SPEAKING		WRITING
	Listening	Reading	Spoken interaction	Spoken production	
English	C2	C2	C2	C2	C2
	Certificate of Proficiency in English-University of Michigan (C2)				
German	B2	B2	B2	B2	B2
	Mittelstufe−Goethe Institut of Athens (C1)				

Communication skills

- good communication skills gained through my experience as a researcher in pharmaceutical laboratory
- ability to impart knowledge, collaborative research
- ability to cooperate in a multicultural environment

Organisational / managerial skills

- leadership (laboratory supervisor at bachelor students)
- consistency, will, laboratory organization, taking initiatives

Job-related skills

- Natural products analysis and isolation of bioactive compounds
- Extraction, isolation and structural elucidation of bioactive metabolites of natural products
- Chromatographical techniques (UPLC, HPLC, CPC)
- Development of quantitative analytical methods based on NMR and UPLC/MS techniques
- Development and validation of bioanalytical methodologies (ICH,FDA, EMA)
- Pharmacokinetic Studies
- Metabolomic studies in animal models

Digital competence

SELF-ASSESSMENT				
Information processing	Communication	Content creation	Safety	Problem solving
Proficient user	Proficient user	Proficient user	Proficient user	Proficient user

- ECDL Profile Certificate
- excellent command of Microsoft office suite (Word, Excel, PowerPoint, Internet, Outlook), Internet tools
- excellent command of several functional systems available in pharmaceutical laboratories:
  TopSpin, Mestrenova & ACD/ NMR Processor (NMR Spectroscopy), Empower (UPLC), ChromQuest (HPLC), Wincats (CAMAG Visualiser), SciFinder & Reaxys (Data Bases), MarvinSketch (Chemical Molecules Drawing), Simca, XCMS, R-Language

Other skills

Flute diploma (Degree: Excellent 10/10)

Driving licence

Driving licence category: B

Hobbies/ Other Activities

I usually participate in many concerts as a flutist and I also teach flute in two conservatoires

ADDITIONAL INFORMATION

Publications

- **06/2018 Submitted**
  "Analytical *methodologies used for the determination of colistin in biological fluids. Still a challenge? ", Dagla I.V.;* ***Karkoula E.****; Tsarbopoulos A.; Gikas E.;* ***Journal of Pharmaceutical and Biomedical Analysis***
- **09/2018**
  "Rapid isolation and characterization of crocins, picrocrocin and crocetin from saffron using centrifugal partition chromatography and LC-ESI MS", ***Karkoula E.****; Angelis A.; Koulakiotis N.S.; Gikas E.; Halabalaki M.; Tsarbopoulos A.; Skaltsounis A.L.;* ***Journal of Separation Science*** *OI:10.1002/jssc.201800516*
- **06/2018**
  "Trans-crocin 4 is not hydrolyzed to crocetin following i.p. administration in mice, while it shows penetration through the blood brain barrier", ***Karkoula E.****; Lemonakis N.; Kokras N.; Dalla C.; Gikas E.; Skaltsounis A.L.; Tsarbopoulos A.;* ***Fitoterapia****, 2018, https://doi.org/10.1016/j.fitote.2018.06.012*
- **01/2014**
  "*Quantitative measurement of major secoiridoid derivatives in olive oil using qNMR. Proof of the artificial formation of aldehydic oleuropein and ligstroside aglycon isomers",* ***Karkoula E.****; Skantzari A.; Melliou E.; Magiatis P.;* ***J. Agric. Food Chem.****, 2014,* ***DOI:*** *10.1021/jf404421p*
- **04/2013**
  "*A new method for the estimation of olive oil healthfulness",* ***Karkoula E.****;*

Melliou E.; Magiatis P.; ***Journal of the American oil Chemists' Society****, 2013, 24 (4) , pp. 266-270*

- **11/2012**
  "*Direct Measurement of Oleocanthal and Oleacein Levels in Olive Oil by Quantitative ^{1}H NMR. Establishment of a New Index for the Characterization of Extra Virgin Olive Oils",* ***Karkoula E.****; Skantzari A.; Melliou E.; Magiatis P.;* ***J. Agric. Food Chem.****, 2012, 60 (47), pp 11696–11703*

Presentations

- **Oral presentation**

05/2013, 16th Panhellenic Pharmaceutical Congress
"New method of direct quantitative measurement of four secoiridoids in olive oil using NMR spectroscopy"

- **Poster presentations**

3-7/6/18, ASMS Conference on Mass Spectrometry and Allied Topics, San Diego, California
"Bioavailability and Metabolomic Studies of Crocus-derived bioactive compounds following i.p. administration in mice"

3-7/9/17, 65th International Congress and Annual Meeting of the Society for Medicinal Plant and Natural Product Research (GA), Basel, Switzerland
"Application of a novel UPLC-HRMS-based plasma metabolomics approach reveals differences between male and female mice following i.p. administration of trans-crocin-4."

24-28/7/16, 9th Joint Natural Products Conference 2016, Denmark
"Development and validation of a UPLC method for quantifying trans-crocin 4 and crocetin from saffron in plasma: A pharmacokinetic study"

28/6-2/7/15, MedMSIII
"Rapid isolation and characterization of crocins, picrocrocin and crocetin from saffron extract using hydrostatic countercurrent chromatography and ESI MS"

4-6/2/15, 22th Young Research Fellows Meeting, Paris
"Rapid and effective isolation of crocins, picrocrocin and crocetin from Saffron extract using step-gradient Hydrostatic Countercurrent Chromatography"

31/5-3/6/13, 16th Panhellenic Pharmaceutical Congress
"New method of direct quantitative measurement of four secoiridoids in olive oil using NMR spectroscopy"

Conferences Seminars

- **3-7/9/17**
  65th International Congress and Annual Meeting of the Society for Medicinal Plant and Natural Product Research (GA), Basel, Switzerland
- **24-8/7/16**
  9th Joint Natural Products Conference 2016, Denmark
- **8-11/10/15**
  MedMSIII (Mediterranean Sea Region Countries Mass Spectrometry Workshop)
- **26-28/6/15**
  TreatAD Workshop (European Commission Funded Program)
- **4-6/2/15**
  22th Young Research Fellows Meeting, Paris
- **31/5-3/6/14**
  16th Panhellenic Pharmaceutical Congress (Hellenic Union of Pharmacists)

Honours and awards

- Travel grant from the Society for Medicinal Plants and Natural Product Research (GA) to participate in the 65th International Congress and Annual Meeting of GA in Basel, Switzerland
- Best poster presentation in the 22th Young Research Fellows Meeting, Paris

Memberships

- Member of Society for Medicinal Plant and Natural Product Research
- Member of Hellenic Mass Spectrometry Society

SUMMARY

Crocus sativus is a species of flowering plant of the *Crocus* genus in the Iridaceae family. Saffron, the dried stigmas of the flower *Crocus sativus* L. is considered to be among the most expensive spices in the world, and it is mainly used as a traditional herbal medicine but also as a flavoring and food coloring agent in everyday life. The main saffron constituents include crocins, which are mono- and bis-esters of crocetin with glucose and/or gentiobiose. Saffron is considered to be a potential weapon against neurodegenerative diseases since saffron, crocin, crocetin and saffranal have shown remarkable anti-oxidant activity. Moreover, saffron has exhibited significant activity against Parkinson's and Alzheimer's disease.

The overview of the current study was to isolate the most abundant crocin, *trans*-crocin-4 (TC4) from *Cr. Sativus* in sufficient quantities in order to perform a Pharmacokinetic study in mice and subsequently assess the bioavailability of TC4, in mice plasma after *i.p.* administration, as well as its capability to cross the Blood Brain Barrier (BBB). The final goal of this study was to explore the alterations to the metabolic fingerprint after the *i.p.* administration of TC4 and to annotate the features that were significantly altered.

Initially, this study demonstrates a simple and effective method for one-step isolation of the main secondary metabolites of a Methanol-Water 50:50 v/v saffron extract employing step-gradient centrifugal partition chromatography (CPC) performed both in dual mode and elution−extrusion mode, using five biphasic solvent systems. In total, from all the CPC experiments performed, 6185 mg of pure TC4 were isolated, 15 saffron constituents have been isolated and characterized leading to the establishment of the developed CPC methodology, as a suitable approach for the saffron stigmas analysis in the laboratory as well as the natural products industry.

The subsequent step of the current study included the development and full validation of two UPLC-PDA methodologies, according to U.S-FDA and EMA guidelines, for the rapid and accurate quantification of TC4 and crocetin (CRC) in mice plasma and brain after *i.p.* administration. The two UPLC-PDA methods were successfully applied for the determination of CRC and TC4 in mouse plasma and brain after *i.p.* administration of TC4 (50 and 150 mg/kg) in a time range of 0-240 minutes. Due to the selection of *i.p.* administration route, the first-pass metabolism and/or gastric hydrolysis were bypassed, a fact that enhanced the bioavailability of TC4. Furthermore, TC4 was found to be capable of crossing the Blood Brain Barrier

(BBB) and build up levels in the mouse brain, regardless of its highly hydrophilic character. Interestingly, CRC was not detected in any plasma or brain sample, although it has been reported that TC4 quickly hydrolyzes to CRC after *p.o.* administration. Therefore *i.p.* administration could be used in the case of TC4 for the accurate determination of its biological role.

In the last step of the current study, the metabolic fingerprint and its associated alterations following *i.p.* administration of TC4 in male and female mice were determined by an untargeted UPLC-HRMS metabolomics approach. Statistical evaluation of the results was achieved by multivariate analysis (MVA), i.e., Principal Component Analysis (PCA), and (sparse) Partial Least Squares–Discriminant Analysis (sPLS-DA). Due to the high variability imposed by various factors e.g. sex, administration dose, and time points, the ML-(s)PLS–DA has proven to be the only effective approach. Furthermore, a preliminary sex-related effect on the metabolome has been proven to exist, denoting that the administration in both genders is indispensable in order to acquire safe conclusions as reliable metabolome pictures. Finally, this UPLC-HRMS-based methodology clearly demonstrated that the time sequence of metabolome changes was due to the administration of TC4. In accordance with the results provided by various statistical softwares, the selected features were further implemented to online databases so as to annotate them and to identify potential metabolites.

ΠΕΡΙΛΗΨΗ

Το φυτό *Crocus sativus* (Κρόκος Κοζάνης) είναι ένα ανθοφόρο είδος του γένους *Crocus* που ανήκει στην οικογένεια Iridaceae. Το σαφράν είναι τα αποξηραμένα στίγματα του φυτού *Crocus sativus* L. και συγκαταλέγεται ανάμεσα στα πιο ακριβά μπαχαρικά του κόσμου. Κυρίως χρησιμοποιείται σαν φάρμακο της παραδοσιακής ιατρικής καθώς και ως αρωματικό και χρωστική τροφίμων στην καθημερινή ζωή. Στα κυριότερα συστατικά του σαφράν περιλαμβάνονται οι κροκίνες, οι οποίες είναι μονο- και δις-εστέρες κροκετίνης με γλυκόζη ή/και γεντιοβιόζη. Το σαφράν θεωρείται δυνητικό όπλο ενάντια στις νευροεκφυλιστικές ασθένειες αφού οι ουσίες που περιέχει (κροκίνη, κροκετίνη και σαφρανάλη) έχουν δείξει αξιοσημείωτη αντιοξειδωτική δράση. Επιπλέον, ο κρόκος έχει παρουσιάσει σημαντική δραστικότητα έναντι της νόσου του Πάρκινσον και του Αλτσχάιμερ.

Ο κεντρικός σχεδιασμός της τρέχουσας μελέτης ήταν η απομόνωση από τον κρόκο της πιο άφθονης κροκίνης, *trans*-crocin-4 (TC4) σε επαρκείς ποσότητες προκειμένου να πραγματοποιηθεί μια Φαρμακοκινητική μελέτη σε ποντίκια και στη συνέχεια να εκτιμηθεί η βιοδιαθεσιμότητα της TC4, σε πλάσμα ποντικών μετά από ενδοπεριτοναϊκή (*i.p.*) χορήγηση καθώς και η ικανότητά της να διασχίσει τον αιματοεγκεφαλικό φραγμό (ΑΕΦ). Ο τελικός στόχος αυτής της μελέτης ήταν να διερευνηθούν οι μεταβολές στο μεταβολικό δακτυλικό αποτύπωμα μετά τη χορήγηση της TC4 και να εντοπιστούν τα χαρακτηριστικά που μεταβλήθηκαν σημαντικά.

Αρχικά, αυτή η μελέτη παρουσιάζει μια απλή και αποτελεσματική μέθοδο απομόνωσης σε-ένα-βήμα των κύριων δευτερογενών μεταβολιτών ενός εκχυλίσματος κρόκου με μεθανόλη-νερό 50:50 v/v χρησιμοποιώντας χρωματογραφία κατανομής με φυγοκέντρηση (Centrifugal Partition Chromatography-CPC) που εκτελέστηκε τόσο σε dual-mode όσο και σε elution-extrusion mode, χρησιμοποιώντας πέντε διφασικά συστήματα διαλυτών. Συνολικά, από όλα τα πειράματα CPC που πραγματοποιήθηκαν, απομονώθηκαν 6185 mg καθαρής TC4 ενώ απομονώθηκαν και χαρακτηρίστηκαν 15 επιμέρους συστατικά του εκχυλίσματος του σαφράν. Συνεπώς, η μεθοδολογία CPC που αναπτύχθηκε, θεωρήθηκε κατάλληλη προσέγγιση για την ανάλυση του σαφράν τόσο στο εργαστήριο όσο και στη βιομηχανία των φυσικών προϊόντων.

Το επόμενο βήμα της τρέχουσας μελέτης περιελάμβανε την ανάπτυξη και την πλήρη επικύρωση δύο μεθοδολογιών με χρήση υγρής χρωματογραφίας υπερυψηλής απόδοσης (Ultra High Performance Liquid Chromatography–UHPLC-PDA), σύμφωνα με τις οδηγίες των U.S-FDA και EMA, για την ταχεία και

ακριβή ποσοτικοποίηση της TC4 και της κροκετίνης (CRC) σε πλάσμα και εγκέφαλο ποντικιών μετά από *i.p.* χορήγηση. Οι δύο μέθοδοι UPLC-PDA εφαρμόστηκαν επιτυχώς για τον προσδιορισμό των CRC και TC4 σε πλάσμα και εγκέφαλο ποντικιών μετά από *i.p.* χορήγηση TC4 (50 και 150 mg/kg) σε χρονικό διάστημα 0-240 λεπτών. Η επιλογή της *i.p.* οδού χορήγησης εξυπηρετούσε την παράκαμψη του μεταβολισμού πρώτης διόδου ή/και της γαστρικής υδρόλυσης, γεγονός που ενίσχυσε τη βιοδιαθεσιμότητα της TC4. Επιπλέον, διαπιστώθηκε ότι η TC4 ήταν ικανή να διασχίσει τον ΑΕΦ και να αυξήσει τα επίπεδά της στον εγκέφαλο ανεξάρτητα από τον ιδιαίτερα υδρόφιλο χαρακτήρα της. Είναι ενδιαφέρον ότι η CRC δεν ανιχνεύθηκε σε κανένα δείγμα πλάσματος ή εγκεφάλου, αν και έχει αναφερθεί ότι η TC4 υδρολύεται γρήγορα σε CRC μετά από χορήγηση από το στόμα. Συνεπώς η *i.p.* χορήγηση θα μπορούσε να χρησιμοποιηθεί στην περίπτωση της TC4 ώστε να είναι εφικτός ο ακριβής προσδιορισμός του βιολογικού της ρόλου.

Στο τελευταίο στάδιο της τρέχουσας μελέτης, το μεταβολικό δακτυλικό αποτύπωμα και οι σχετικές μεταβολές του μετά την *i.p.* χορήγηση της TC4 σε αρσενικά και θηλυκά ποντίκια, προσδιορίστηκε με μεταβολομική μελέτη βασισμένη σε φασματομετρία μάζας συζευγμένη με υγροχρωματογραφία υπερυψηλής απόδοσης (UHPLC-HRMS). Στη συνέχεια εφαρμόστηκε πολυπαραμετρική στατιστική ανάλυση (MVA), με σκοπό να προσδιορισθούν τυχόν επιδράσεις της TC4 στο μεταβόλωμα των ποντικιών. Λόγω της μεγάλης μεταβλητότητας που επιβάλλεται από διάφορους παράγοντες, π.χ. το φύλο, η δόση χορήγησης και τα χρονικά σημεία, η ML-(s)PLS-DA αποδείχθηκε η μόνη αποτελεσματική προσέγγιση. Επιπλέον, ανιχνεύθηκε μια φυλοσύνδετη πρωταρχική επίδραση στο μεταβόλωμα των ζώων, υποδηλώνοντας ότι η χορήγηση και στα δύο φύλα είναι απαραίτητη προκειμένου να έχουμε σαφή εικόνα των μεταβολικών αλλαγών. Τέλος, με αυτή τη UPLC-HRMS μεθοδολογία, καταδείχθηκε σαφώς ότι η χρονική αλληλουχία των μεταβολών στο μεταβόλωμα οφειλόταν στη χορήγηση TC4. Σύμφωνα με τα αποτελέσματα που παρήχθησαν από διάφορα στατιστικά λογισμικά, οι επιλεγμένες μεταβλητές εφαρμόστηκαν περαιτέρω σε ηλεκτρονικές βάσεις δεδομένων, ώστε να ταυτοποιηθούν και να εντοπιστούν πιθανοί μεταβολίτες.

CHAPTER ONE

Natural products:
A “key-tool” to “unlock” aspects of emerging scientific fields and their application in the treatment of modern diseases

1.1 NATURAL PRODUCTS: A "KEY-TOOL" TO "UNLOCK" ASPECTS OF EMERGING SCIENTIFIC FIELDS

Natural Products (NP) are defined as small molecules produced naturally by any organism (from marine and/or terrestrial sources) including primary and secondary metabolites. They are comprised of very low molecular weight molecules such as urea as well as really complex chemical structures such as Vancomycin and Erythromycin (isolated from microorganisms *Amycolatopsis orientalis* and *Saccharopolyspora erythraea* respectively) and Taxol®/paclitaxel, the most widely used drug against breast cancer (isolated from the bark of the plant *Taxus brevifolia*). These secondary metabolites own many promising biological activities thus they are considered as a potential source of successful drug leads.

In the past few decades, the urgent need to discover eco-friendly alternatives to replace the toxic chemicals utilized in almost everything around us, has initiated a vivid and constant research in order to exploit natural products as substitutes for the synthetic and potentially hazardous chemical compounds. These natural approaches result from a modern trend which enables the use of as much eco-friendly materials as possible and the return to the initial roots and origins.

As a result, NP and the plethora of products deriving from them, receive an increasing attention of the consuming audience, since their applications range from food and textiles to medicines and holistic healthcare in general. Furthermore, the ever increasing improvement of biotechnology has provided solutions to the successful isolation of the NP of interest from the producing sources (e.g. plants, marine organisms etc.) and has also encouraged the development of optimized procedures so as to afford selective cultivation and production of the optima secondary metabolites.

1.1.1 Natural products in the treatment of ailments through the centuries

Since ancient times, NP have been employed for the treatment of several diseases and illnesses. In a brief historical flashback, the first records of NP originated from Mesopotamia (from about 2600 B.C) and were written on clay tablets in cuneiform while these records reported various compounds that were used for the treatment and relief of several diseases and medical situations. Among the documented compounds are essential oils from *Glycyrrhiza glabra* (licorice), *Cedrus* species (cedar), *Commiphora* species (myrrh), and *Papaver somniferum* (poppy juice), while all of them are still in use today for the treatment of several ailments ranging from simple coughs to inflammations and severe pain. [1]

Moreover, there are several more pharmaceutical records demonstrating the application of NP against diseases e.g. *Ebers Papyrus* dating from 1500 B.C (best known Egyptian pharmaceutical record) and Chinese *Materia Medica* with its first record dating from about 1100 B.C.[1]

A major and substantial chapter of the employment of herbal drugs as therapeutic agents was recorded by the ancient Greeks as well. Theophrastus (~300 B.C.) was a philosopher and natural scientist who in his books, *Enquiry into Plants* and *Causes of Plants*, demonstrated the classification of plants according to their modes of generation, their localities, their sizes and according to their practical application as foods, juices, herbs. [2] Furthermore, Pedanius Dioscorides (c. 40-90 A.D.) was a Greek physician, pharmacologist, botanist, and author of *De Materia Medica* (Ancient Greek: Περὶ ὕλης ἰατρικῆς); a 5-volume Greek encyclopedia which was a monumental reference work about herbal medicine and related medicinal substances (a pharmacopeia), that was widely read and remained the ultimate authority on the subject for more than 1500 years. Dioscorides in *De Materia Medica* managed to organize the drugs into major categories based on observed similarities on their medicinal activity and was the first association of the science of pharmacy with the science of medicine. (Figure 1)

Figure 1: Pages from Dioscorides encyclopedia "*De Materia Medica*"

In the Medieval Period (5th to 15th century), this precious knowledge was preserved with carefulness and devotion by the monks in the monasteries of countries like England, Ireland, Germany and France. However, the Arabs were responsible not only for the maintenance of the knowledge but also for the incorporation of their resources as well as Chinese and Indian traditions and herbs with the Western knowledge. [1]

1.1.2 Application of Natural Products in the treatment of modern diseases

It is evident that in the past few decades, regarding the treatment of current ailments, Natural Products have been constantly gaining ground towards the employment of chemical drugs and they are steadily entering the battle against a variety of modern diseases. Moreover, although the valuable pharmacologically active secondary metabolites are sometimes produced in extremely low quantities which might have hindered the wide application of these compounds in the medicinal fields, so far, the evolution of the genetic engineering and the biotechnology have offered large-scale cultivation techniques as well as novel biosynthesis pathways so as to afford the cultivation and isolation of the desired secondary metabolites in large quantities. [3]

1.1.3 Anti-cancer activity of Natural Products

Cancer is considered to be a major and confusing challenge to the global healthcare system and also has a major impact on society across the world. According to the National Cancer Institute, cancer is among the leading causes of death worldwide highlighting that in 2012, there were 14 million new cases and 8.2 million cancer-related deaths worldwide whilst approximately 39.6% of men and women will be diagnosed with cancer at some point during their lifetimes (based on 2010-2012 data). Furthermore, it is well known that cancer has a devastating physiological and psychological impact on patients and their families. Unfortunately, cancer does not make discriminations between people thus it might affect men, women and also children and in any case the occurring stress is inevitable. For example, pediatric cancer is considered to be a highly stressful situation for parents as it includes several stressors such as the financial strain, the life threat and many treatment-related events. [4] Regarding the adult cancer patients, the disease also has devastating impacts on patients' everyday lives such as finances, work and family roles. [5]

Based on these horrifying data, researchers all over the world have been constantly trying to decode its hidden aspects and to discover potential drugs that would inhibit the progress or even provide a cure of this disease. Hopefully, the persistent research of the scientists has led to the development or the discovery of many potential drugs while many of them have proved to be actually effective towards the treatment of this illness. The majority of anti-cancer drugs are derived from synthetic or hemi-synthetic sources and can be classified into many different

categories such as 1) Alkylating agents 2) Antimetabolites 3) Antitumor antibiotics 4) Mitosis inhibitors 5) Molecular targeting agents which alter gene expression, monoclonal antibodies, kinase inhibitors, proteasome inhibitors 6) Topoisomerase I & II inhibitors 7) Hormonal antagonists 8) Telomerase blockers 9) Biological response modifiers. [6] However, except from the synthetic drugs, a constantly evolving research on the abundant supply of herbal medicinal products has revealed many promising pharmacologically active secondary metabolites produced by plants e.g. the mitostatic drug paclitaxel® (Taxol). The scientific achievements as well as the advent of genetic engineering have offered an expansion of plants' capability to produce anti-cancer medicinal products. [7] The most promising anti-cancer compounds derived from plants are considered to be the phenolic compounds. [8]–[10] Alkaloids is another major category of anti-tumor agents deriving from plants. These metabolites are extremely abundant in nature and are normally produced by plants as toxic constituents. Amongst the most famous cytotoxic alkaloids that are in clinical use for the treatment of cancer worldwide are vinblastine, vincristine, topotecan and taxol while the constant screening for novel anti-tumor alkaloids has revealed many more alkaloids with promising apoptotic activities in particular cancer cell lines. [11] These have been only two prime examples of the plethora of NP with anti-cancer activities since numerous compounds of several NP categories have also shown remarkable anti-tumor activity. Furthermore, given that carcinogenesis is a really complex process comprised of abnormal successive cellular events such as anomalous proliferation and differentiation which is regulated by mutations and epigenetic alterations, epigenetically active compounds could be estimated as promising anti-tumor agents since these epigenetic modifications are present during the early progression of cancer. [12]

1.1.4 Medicinal plants against cardiovascular diseases

According to the World Health Organization (WHO), Cardiovascular diseases (CVD) are a group of heart and blood vessels disorders that include: coronary heart disease, cerebrovascular disease, peripheral arterial disease, rheumatic heart disease, congenital heart disease and deep vein thrombosis and pulmonary embolism. As a result, some of the most commonly occurring consequences of cardiovascular diseases are heart failure, diffuse atherosclerosis, cognitive impairment and dementia. The clinical treatment of the several aspects of cardiovascular diseases has been performed with synthetic medicines

e.g. anti-hypertensive and anti-arrhythmic drugs, however, the numerous side effects of the aforementioned medicines in combination with their low effectiveness towards the CVD, have turned the scientists' interest to a more natural approach. As a result, a lot of progress is observed regarding the research about medicinal plants that afford anti-hypertensive properties. Since plants are a wealthy source of biomolecules such as flavonoids, alkaloids, terpenoids etc. with cardio-promoting effects, the effort to detect and isolate non-toxic natural compounds with health benefits is indispensable. [13]

In the past decades, the exhausting pace of everyday living in combination with the adoption of an unhealthy lifestyle have contributed to the appearance of another serious disease, closely related to the CVD. The cluster of biochemical and physiological abnormalities (increased blood pressure, high blood sugar, excess body fat around the waist, and abnormal cholesterol or triglyceride levels) associated with the development of cardiovascular disease and type 2 diabetes is called Metabolic Syndrome (MetS) and it is considered to be one of the major causes of heart diseases and fatal strokes. However, an extensive research about this syndrome has pointed out that the aggressive alteration of the unhealthy life habits as well as the incorporation of NP in the everyday routine (i.e. use of neutraceuticals such as omega-3 fatty acids, macroelements and vitamins) has shown remarkable effects with clinically demonstrated advances on more than one component of MetS. [13]

A prime example of NPs capable of modifying the effects of MetS is the polyphenols included in olive oil since the biological activity of polyphenols is strongly related to their antioxidant properties. Hydroxytyrosol (HT), an antioxidant phenolic compound of olive oil has been found to be a promising factor for the amelioration of the MetS as it is associated with increased unsaturated lipid acids levels and decreased free polyunsaturated lipid acids levels and reduced glucose levels which establish HT as a promising lead compound for the development of pharmaceuticals against MetS. [14]

1.1.5 Natural Products against Inflammatory Diseases

Inflammatory diseases include a vast array of disorders and conditions that are characterized by inflammation. Typical examples of inflammatory diseases are allergies, asthma, autoimmune diseases, hepatitis, transplant rejection etc. Inflammatory conditions are important and extremely common threatening situations. Every day, each individual is exposed to one or more inflammatory

disorders that given the overall health condition of the organism, they are regarded as temporary, chronic or even life threatening ones. From a simple headache to extensive rheumatopathy, inflammatory diseases are affecting millions of individuals around the world thus indicating the necessity to invent more specific drugs with more targeted mechanism of action. However, a major problem occurring from the extensive use of anti-inflammatory drugs is how to overcome the numerous side effects. A brief example illustrating the situation is the following; Nonsteroidal anti-inflammatory drugs (NSAIDs) are a drug class that are utilized in order to relieve pain, to decrease fever and to curb inflammation. Their use should be under medical prescription while the doctor defines the dose and the treatment period. NSAIDs are powerful drugs that offer instant pain relief and allow the patients to feel comfortable and readjust themselves to their life pace, however, NSAIDs should be taken in low doses for a short period of time especially due to the side effects that most commonly occur after overdosing for a longer period of time (e.g. stomach pain and heartburn, stomach ulcers, liver or kidney problems, high blood pressure, leg swelling etc. The severity of the side-effects ranges from mild symptoms that disappear when reducing the administration dose to serious ones, that demand medical attention. All the above described complications have led to the exploration of alternative approaches that would ideally overcome the unfortunate side-effects.

Since ancient times, natural products play a significant role in human health considering the prevention and treatment of inflammatory conditions. It is common knowledge that several herbal NP, and most of the times easily accessible, significantly affect cellular mechanisms thus offer a beneficial effect in inflammatory diseases. Nowadays, due to the pollution of the atmosphere as well as the adoption of unhealthy habits such as smoking, an increase in pulmonary diseases rate has been observed. Chronic obstructive pulmonary diseases (COPD), asthma and acute respiratory distress syndrome (ARDS) are the most common ones and they are related to high mortality rates. [15], [16] However, several herbal-originated NP have shown remarkable effect against these diseases. Flavonoids, a supreme NP category comprised of compounds with outstanding pharmacological actions in many medicinal fields, have proved to be effective in the treatment of lung inflammation and diseases. More specifically, nariginin, a compound isolated from the dried unripe or ripe fruit peel of *Citrus grandis* and apigenin, a common dietary flavonoid that is abundantly present in many fruits, have shown action against asthma by causing reduction of IL-4, IL-5, IL-13, and INF-δ levels (nariginin) [17] and reduction of eosinophil infiltration in lung tissue and IL-6, TNF-α, and IL-17A

levels (apiginin).[18] Furthermore, taking into consideration that anti-inflammatory effects could be associated with anti-oxidant capacity, red wine, a rich source of anti-oxidant bioactive compounds, could be incorporated in the everyday routine so as to prevent several inflammations. As demonstrated in the literature, treatment with resveratrol, a stilbene present in the red wine, has shown inhibition of lung cancer cell growth since it was capable of inducing premature senescence through ROS-mediated DNA damage. [19] Finally, as the examples of NP with anti-inflammatory effects are countless, propolis, a honey bee product well-known for its anti-inflammatory and anti-oxidant activity has been found to offer dose-dependent protection against adhesive surgical complications therefore it could be utilized as protective factor against them. [20]

1.1.6 Natural Products with antiviral activity

The cure of infections from viruses is a crucial point in the global medicinal strategy. The viruses have been accused of several human pathogeneses from a common cold or a flu to even cancer. In the last decades, there are several studies suggesting that many syndromes and diseases such as Alzheimer's Disease [21] or Diabetes-Type I [22] have been associated with viral infections. Nowadays, the "mixing" of populations and cultures is easier than ever with the constant and effortless travelling around the world as well as the global trade advances. However, a common observation is that the transportation of viruses that might have been fought-off or hibernated in a place but extremely infectious in another continent or country, is inevitable. Thus the WHO sounds the alarm about the prevention of the virus spread with the promotion of vaccination, one of the most cost-effective health interventions that offers protection against a variety of serious diseases and improves the life quality.

Along with the synthetic and hemi-synthetic drugs, herbal medicinal products as well as purified compounds isolated from plants and formulated into drugs, could offer a wealthy supply of novel antiviral lead-compounds in the current and future drug development. [23] A common observed type of virus is *Herpes simplex* virus type 1 and type 2 (HSV-1 and HSV-2). HSV is responsible for mucocutaneous lesions in the oral/perioral area (HSV-1) and in the genital areas (HSV-2) as well as other body areas. Meanwhile, the infection of HSV is everlasting as the virus is permanently located in the sensory neurons and it can be reactivated by several stimuli including fever, stress or menstruation. [24], [25] Unfortunately, despite 100 years of research there is still not a vaccine for HSV available, indicating

the difficulty in discovering and developing new drugs. Hence, so far, the antiviral drugs (nucleoside analogs such as acyclovir, penciclovir, and their prodrugs) are the only treatment approved by the EMA and FDA as a suitable approach for HSV infections. However, the problem of the formation of drug-resistant types of viruses is major, thus further research is definitely required. [26]

Nevertheless, along with the conventional methods of treatment, the application of NP has also shown remarkable results.(Figure 2) *Phyllanthus urinaria* L. Euphorbiaceae or so called “Chamber Bitter” is a traditional plant with numerous biological activities that is commonly used in Eastern countries and it is widely found in all tropical regions of the world. The plant is a popular herbal remedy and also available for legal sale on the internet. Recent studies demonstrated that Hippomanin A, a compound isolated from the aceton extract of *P. urinaria*, impeded HSV-2 but not HSV-1 infection. [23]

Figure 2: Commercial herbal product from Italy with immunostimulant action against infection from HSV. The formulation of the product is enriched with plant extracts of Echinacea and “Witch-hazel” (*Hamamelis virginiana*), plants with recognized antifungal, immunostimulant and soothing effects [27]–[29].

Another typical example is the blackberry ethanol extract (*Rubus eubatus* cv. “Hull”) which was capable of significantly reducing the HSV-1 yield probably by interfering with the adsorption of the virus or the entry into host cells. In combination with the high percentage of blackberries in the polyphenolic compounds anthocyanins and ellagitannins which also possess antiviral activity, the synergistic effect is inevitable. [30] To sum up, many plants-derived compounds and extracts have shown remarkable anti-viral activity, thus they have been incorporated into ointments and/or other galenic formulations and have succeeded in treating the infection efficiently.

Finally, *Artemisia annua* L. Asteraceae, is a famous plant containing the antimalarial compound artemisinin which is chemically categorized as a sesquiterpene lactone. Research indicated that Artemisinin-based combination therapies are the most effective drugs to treat *Plasmodium falciparum* malaria, a theory adopted by the WHO as well. [31] However, mostly based on ethnopharmacological observations, researchers have recently demonstrated that the *Artemisia annua* tea infusion was found to be highly active with $IC_{(50)}$ values as low as 2.0 μg/mL against Human Immunodeficiency Virus (HIV) thus providing a different but equally important aspect on this plant. [32]

In conclusion, these were only a few examples, out of hundreds, of the wide utilization of NP in the everyday living thus undeniably indicating that the application of NP has been successfully expanded to numerous experimental and commercial fields. (Figure 3) Nevertheless, the perpetual necessity for novel treatments, novel materials as well as alternative approaches for the beneficial improvement of the everyday routine and the common needs, would definitely unlock many hidden aspects of the Natural Products’ world.

Figure 3: Applications of Natural Products in everyday aspects of life

1.2 NEURODEGENERATIVE DISEASES: THAT CONTEMPORARY SCOURGE

According to the definition provided by the International Journal of Science 'Nature', "*Neurodegenerative Diseases (ND) are a heterogeneous group of disorders that are characterized by the progressive degeneration of the structure and function of the central nervous system or peripheral nervous system."*

At the moment, neurodegenerative diseases are considered to be incurable and devastating conditions resulting in progressive neurons' degeneration and finally nerve-cell death. As a result, since neurons, the building blocks of the nervous system, are not capable of being reproduced or replaced when damaged, a potential degeneration of the neurons leads to the progressive loss of the brain function. Given that the brain is the central organ of the human nervous system which controls almost every function of the human body such as movement, senses, language, memory and learning, emotions, cognition etc., a potential brain dysfunction will definitely affect some of the above mentioned aspects. If the progressive neurons' degeneration causes movement problems and lack of voluntary coordination of muscle movements, this is called 'ataxia' while if it causes mental dysfunction with long-term and steady decrease in the memory, thinking and speaking capability, this is called 'dementia'.

The most common neurodegenerative diseases include Alzheimer's disease (AD), Parkinson's disease (PD), Huntington's disease (HD), Amyotrophic lateral sclerosis (ALS), Multiple sclerosis (MS), Spinal muscular atrophy (SMA), and Spinocerebellar ataxia (SCA). [33] Amongst them, AD, PD, MS, ALS and HD seemed to be at the top five positions of the neurodegenerative diseases that affect a huge number of the mid- to late-life population worldwide.(Figure 4)

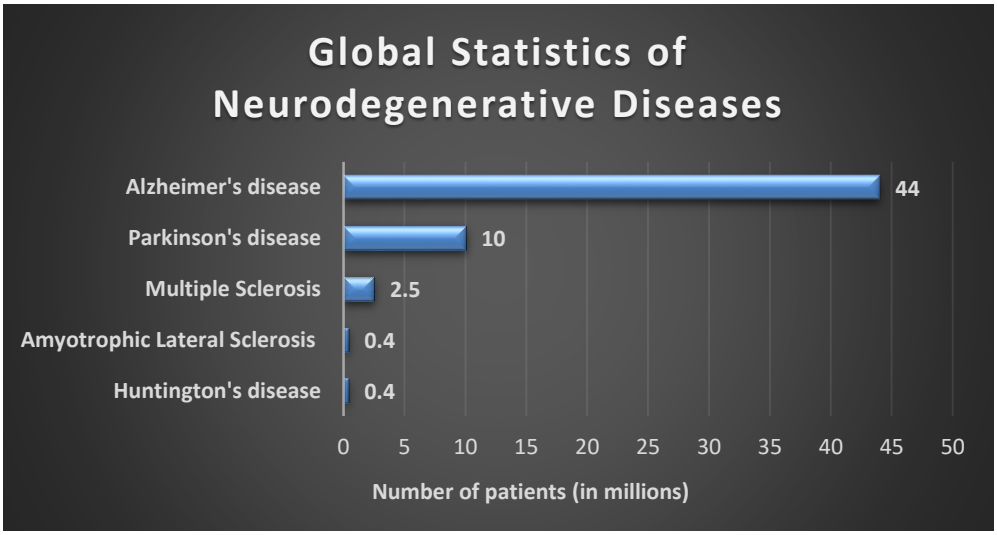

Figure 4: Global statistics of the most common neurodegenerative diseases

1.2.1 Parkinson's Disease (PD)

Parkinson's Disease (PD) is a chronic progressive neurodegenerative disorder that affects predominately dopamine-producing (dopaminergic) neurons in a specific area of the brain called substantia nigra while the etiology of PD is mostly unknown. The insufficient levels of dopamine in the basal ganglia lead to the appearance of the PD motor symptoms viz. resting tremor, rigidity, postural instability, asymmetric manifestations and bradykinesia. However, the motor symptoms co-exist with non-motor symptoms including disorders of mood, apathy, anhedonia, depression and cognitive dysfunction. [34] As a result, the term "Parkinson's complex" has been proposed, comprising both motor and non-motor symptoms. [35] After the diagnosis of the disease and during the progression of PD, the non-motor symptoms become gradually permanent, however, in most cases the non-motor symptoms e.g. depression and/or hyposmia preexisted before the initial observation of the motor ones, thus indicating the necessity for constant awareness from each individual and their families. [34]

1.2.1.1 Neuropathology of PD

The pathophysiology of PD comprises of degeneration or complete loss of the dopaminergic neurons in the pars compacta of substantia nigra (SNpc) [36] and formation of immunoreactive neuronal inclusions containing proteins like alpha-synuclein (αSyn) which are called Lewy bodies (LBs). [37] However, α-synuclein pathology is not a necessary prerequisite in all parkinsonian disorders since, although the neuronal loss in the SNpc is a common characteristic feature in all types of PD, α-synuclein is not always observed, leading to a broader classification of PD into α-synucleinopathies and non-α-synucleinopathies. [37][38][39]

1.2.1.2 Genetics of PD

The etiology of PD is not clearly identified and described, however in recent years, the aspect that the majority of patients suffer from genetic forms of the disease has been made apparent. To date, common variant genome-wide association studies (GWASs) have identified >24 risk loci for PD while a constantly increasing number of novel loci has been identified [40] highlighting novel pathways associated with the PD pathogenesis. [41] The risk-genes involved in the PD have

been found to play a crucial role in the lysosomal biology and autophagy [40] thus indicating that the potential consequent studies regarding the PD etiology should definitely include the genes involved in these procedures as an attempt to determine PD contributory genes and potential therapeutic agents. Nevertheless, although there are several genes involved in hereditary PD, the most important one is the SNCA gene encoding for α-synuclein, which is considered to be the major causative gene implicated in the PD since five described point mutations of the gene locus result in autosomal dominant PD. Furthermore, the SNCA gene is considered as a key feature of several other neurodegenerative diseases such as AD, Lewy bodies' disease (LBD) and Muscular System Atrophy (MSA). [42]

In an attempt to support the global GWAS efforts, the scientists around the world have tried to perform genotyping of risk agents in PD patients. According to recent arguments, there was a hypothesis that isolated populations would perhaps afford limited genetic heterogeneity [43], [44] thus allowing a targeted studying of the genetic aspect of the disease. However, this assumption was rejected since the performed studies failed to detect alterations or modifications of similar gene patterns. [43]

In Greece, according to a screening performed to PD patients, the A53T mutation in the SNCA gene has been found to be the most common one [45] along with mutations in the glucocerebrosidase1 (GBA1) gene encoding for the lysosomal enzyme that is deficient in Gaucher's disease (GD-a rare lysosomal storage disorder characterized by inherited deficiency of the enzyme glucocerebrosidase). [46][47] The unexpectedly close association of the GD with the PD that has been observed, since GBA mutations have been accused of altering the binding of α-synuclein to the cell membrane thus leading to its aggregation, abnormal conformation and formation of LBs [48], has opened new horizons to the interpretation of the PD pathogenesis. [49]

1.2.1.3 Pharmacological therapeutic approaches against PD

The patients suffering from PD face both motor and non-motor symptoms. However, since the mostly preexisting non-motor symptoms could easily be misinterpreted and probably underestimated by the patients as well as their families, in most cases the early diagnosis of the PD is not possible. So far, there is no specific test capable of diagnosing PD thus neurologists diagnose PD based on the patient's medical history, the observation of the (non)-motor symptoms and finally

neurological and physical examination. Unfortunately, at this time, there is no cure for PD, however, a proper medication as well as aerobic exercise along with specialized sessions with trained speech-therapists would contribute to the deceleration of the PD progression.

Regarding the treatment of PD, huge progress has been made in the last 50 years, however, Levodopa is still considered to be the most effective drug for the elimination of PD symptoms. [50]

(a) Carbidopa-Levodopa

Levodopa (L-Dopa) is the first-line drug for PD since it is turned into dopamine into the body and therefore increases the dopamine levels and compensates the insufficient levels of dopamine in a patient with PD. Levodopa is combined with carbidopa, a peripheral decarboxylase inhibitor, which inhibits the decarboxylation of levodopa to dopamine in the systemic circulation, thus allowing a greater levodopa distribution into the central nervous system. Nevertheless, although the combination of Levodopa-Carbidopa offers the best antiparkinsonian advantage for the motor signs its continuous use, is often linked to motor complications such as fluctuations ("wearing-off") and dyskinesias (involuntary movements), [51] situations that once fully established, then it is extremely difficult to be resolved.

Dyskinesia is primarily associated with the dose as well as the duration of the treatment with Levodopa while is a complication observed after 5 years of treatment. As a result, since it is a powerful drug with known and standard side-effects, the initiation of the therapeutic scheme should be performed wisely. [51] The main therapeutic approaches employed in order to enhance levodopa-induced dyskinesias are: 1) reduction of the levodopa dosage; 2) amelioration of dyskinesia with suitable drugs; 3) surgery. [52]

(b) Carbidopa-levodopa infusion

Duopa™ is a prescription medicine approved by the U.S. Food and Drug Administration in 2015 which is used to treat motor fluctuations in advanced Parkinson's disease. Duopa™ is a suspension form of Carbidopa/Levodopa that is continuously administered directly into the small intestine over 16 hours through a tube with the aid of a small portable pump carried or wore by the patient. This drug is suitable for patients still responding to the treatment with Carbidopa/Levodopa but with many fluctuations in their response since the constant infusion of Duopa allows stable levels of the two drugs in the blood circulation. [53]

(c) Dopamine receptor agonists

Dopamine agonists are compounds that activate dopamine receptors therefore they resemble the dopamine effects in the brain. They last longer than levodopa, although they are not that effective yet they are used in combination with levodopa in order to delay the development of dyskinesia compared with levodopa.[54]

(d) Monoamine Oxidase B (MAO-B) inhibitors

Compounds such as selegiline and rasagiline are inhibitors of the brain enzyme monoamine oxidase B (MAO-B) which metabolizes brain dopamine. As a result MAO-B inhibitors extend the dopamine activity in the brain and improves the symptoms of Parkinson's disease. Furthermore, MAO-B inhibitors are key drugs in the treatment of PD since they have shown remarkable efficacy as well limited side-effects. As a result they have been utilized as initial monotherapy in the onset of the PD and as parallel therapeutic scheme with levodopa in advanced stages of PD. [55][54]

(e) Catechol-O-methyltransferase (COMT) inhibitors

Catechol-O-methyltransferase (COMT) is an enzyme involved in the degradation of neurotransmitters, e.g. catecholamines, catecholestrogens and various drugs and/or substances having a catechol structure. COMT inhibitors are employed against PD since they inhibit the peripheral degradation of levodopa outside the central nervous system thus increasing the available amount of levodopa. Normally they are used in combination with levodopa treatment. The primary drug of this category is entacapone however the main side-effect of this drug is dyskinesia, probably resulting from the enhanced levodopa activity. [56][57]

(f) Nondopaminergic therapy

Along with the dopaminergic drugs, nondopaminergic drugs e.g anticholinergics (e.g. trihexyphenidyl or benztropine) and amantadine offer acceptable relief of the unwanted PD symptoms especially in the onset of the disease. The younger the patient, the more important is to follow correct strategies so as to afford a long-term anti-PD effect. Furthermore, since the life expectancy of the younger patients is longer, the probability of them to suffer from motor fluctuations and dyskinesias increases. As a result nondopaminergic therapy, the use of MAO-B inhibitors and DA agonists are critical steps in the early onset of PD. [52], [54]

Finally, the most crucial step regarding the construction of the treatment strategy against PD, is to individualize therapy and to focus on the relief of the most discomforting symptoms, while the long-term target should be to hinder the progression of the disease in general.

1.2.1.4 Therapeutic strategies against α-synuclein's toxicity

As already mentioned, α-synuclein (a-Syn) is a 14-kDa (A-140 amino acid) protein and the major compound found in the abnormal neuronal aggregates observed in PD, the Lewy bodies. [58] The synuclein protein family comprised of α-, β- and γ-syn, although α-syn is the most studied member .[59] A-syn however, is abnormally accumulated not only in PD but also in other neurodegenerative disorders such as multiple system atrophy and Lewy bodies dementia. [38] Furthermore, it has been demonstrated that α-Syn plays a substantial role in the formation of the *beta*-amyloid and tau protein, while both of them are the key proteins involved in the Alzheimer's disease pathogenesis. [60] [39] As a result, since α-synuclein has proven to be not only toxic but also involved in more than one neurodegenerative diseases, it could potentially be the key feature for the assessment of alternative therapeutic approaches against several neurodegenerative diseases. (Figure 5)

There are various pathways proposed in order to effectively manipulate the decrease of α-synuclein's toxicity. Scientists have made efforts to combat the α-synuclein's side-effects by trying to alter several stages including its synthesis as well as its toxic accumulation. Initially, the first reasonable approach was the reduction of a-synuclein's synthesis. With the employment of direct infusion small interfering RNA (siRNA) in mice, the scientists have managed to decrease the α-synuclein levels for a week after infusion [61] and the protein's aggregation in SNpc. [62] The second strategy was the minimization of α-synuclein's aggregation. This has been performed with the application of porphyrin phtalocyanine tetrasulfonate which acts as an α-synuclein stabilizer thus leading to its incapability of further accumulation. [63][64] Furthermore there are many small molecules in early to late stages of clinical development such as; in Phase I: glycerol phenylbutyrate (as a Biomarker for a-Syn Clearance From the Brain) [65], Nilotinib (in Cognitively Impaired Parkinson Disease Patients) [66] while in Phase III, there is polyphenol (-)-epi-gallocatechine gallate (EGCG), a polyphenol contained in

green tea, against Multiple System Atrophy (as anti-aggregation approach) thus indicating that EGCG is an effective remodeling agent of mature amyloid fibrils. [67]

Consequently, another approach is to delay or hinder the α-synuclein's proliferation. Therefore, passive immunization studies have been proposed with the employment of antibodies against the C-Terminal region of α-synuclein with really promising results. [68]

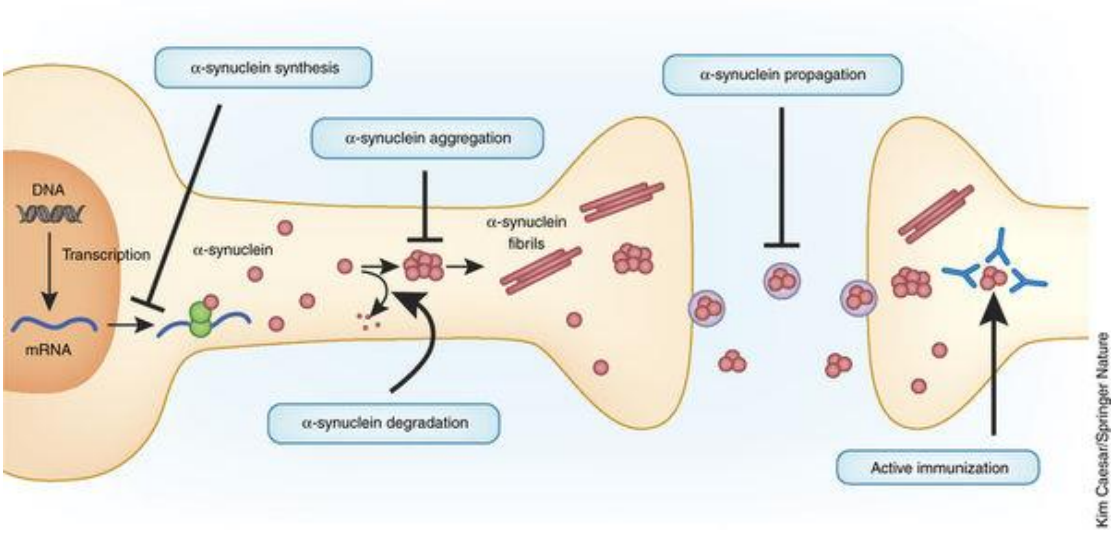

Figure 5: Therapeutic targets of a-synuclein toxicity
Source: Y. C. Wong and D. Krainc, "α-synuclein toxicity in neurodegeneration: mechanism and therapeutic strategies," Nat. Med., vol. 23, no. 2, pp. 1–13, Feb. 2017.

1.2.2 Alzheimer's Disease (AD)

Alzheimer's disease (AD), also referred to simply as *Alzheimer's*, is a chronic, progressive and debilitating neurodegenerative disease. It is an irreversible brain disorder that gradually destroys memory and thinking skills hence eventually the brain ability fades.[69] AD is categorized as a part of the wide term *'Dementia'* which is a syndrome where deterioration in memory, thinking, behaviour and the ability to perform everyday activities are observed. As a result, the patients eventually become unable to perform even the simplest tasks. According to the WHO, Alzheimer's disease is the most common form of dementia and may contribute to 60–70% of cases.

Regarding the symptoms and diagnosis of AD, scientists declare that the irreversible brain damage initiates a decade before the observation of the memory and cognitive complications while in most people with AD, symptoms first appear in their mid-60s. The initial symptoms of AD range from simple memory difficulties to

cognitive impairments such as difficulty in finding the correct words to describe things, vision/spatial issues or aggression/mood changes and insufficient arguments while speaking. As the disease progresses, patients experience greater memory loss and other cognitive difficulties and while they are on the moderate stages of the disease they might suffer from hallucinations, delusions, and paranoia or they might behave impulsively (e.g. undressing at inappropriate times or places or using vulgar language). [69], [70] Finally at the late and last stage of the AD, people with severe Alzheimer's cannot communicate and are completely dependent on others for their care. [71]

1.2.2.1 Statistics of AD

According to the **World Alzheimer Reports** published by Alzheimer's Disease International (ADI) in London, the global dementia developing rate is 1 person / 3sec and the estimated population living with dementia worldwide in 2017 is 50 million people. This number will almost double every 20 years, reaching 75 million in 2030 and 131.5 million in 2050. The majority of dementia cases will be observed in developing countries, since already 58% of people suffering from dementia come from low and middle income countries while this percent will rise to 65% by 2050. (Figure 6, Figure 7, Figure 8)

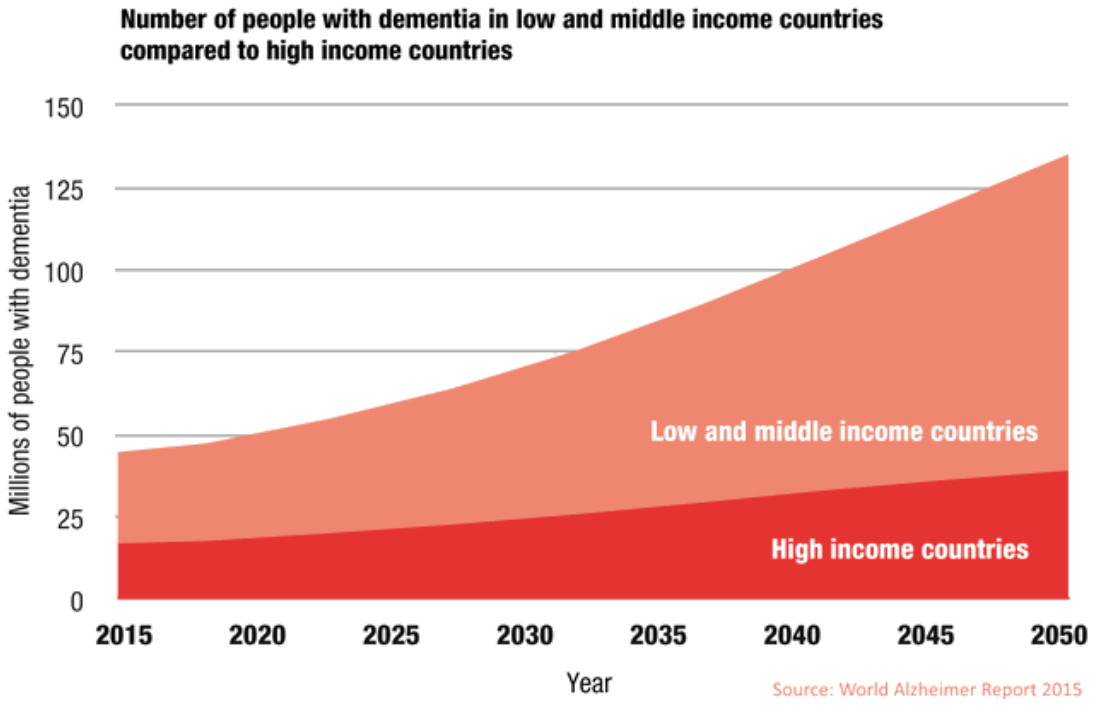

Figure 6: Number of people with dementia in low and middle income countries compared to high income countries. Source: World Alzheimer Report 2015

Regarding the prevalence of AD by gender, women are more likely to develop dementia in their lifetimes mainly since they have a longer life expectancy. In United Kingdom where they have performed statistical analysis of the patients as far as their gender is concerned, they have resulted that 65% of people living with dementia are women while 35% are men.

(Source: Prince, M et al (2014) Dementia UK: Update Second Edition report produced by King's College London and the London School of Economics for the Alzheimer's Society)

Furthermore, 15.4% of women died due to Alzheimer's disease and other dementias in 2016 in the UK thus it was considered to be the leading cause of death for women. On the other hand, 8.0% of men died due to Alzheimer's disease and other dementias in 2016 in the UK thus it was considered to be the second leading cause of death for men.

(Source: England and Wales; Mortality Statistics: Deaths Registered in England and Wales (Series DR). Scotland: National Records of Scotland Vital Events Reference Tables. Northern Ireland; Northern Ireland Statistic & Research Agency Registrar General Annual Report 2015)

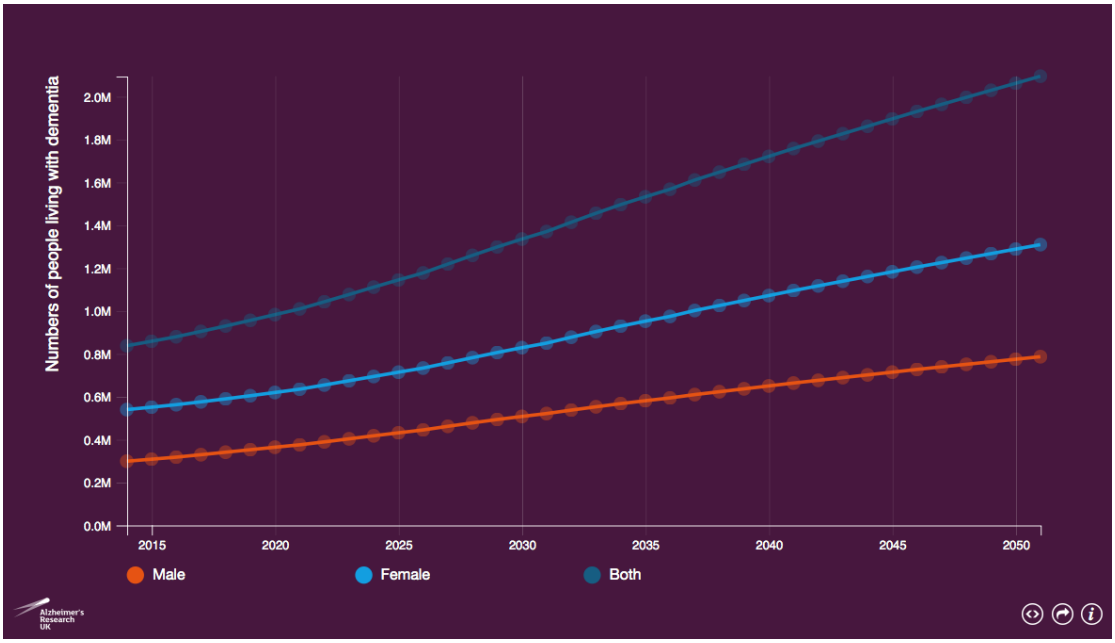

Figure 7: Numbers of people living with dementia in UK in both genders.
Source: Prince, M et al (2014) Dementia UK: Update Second Edition report produced by King's College London and the London School of Economics for the Alzheimer's Society

In Greece, the HELIAD epidemiological study (Hellenic Longitudinal Investigation of Aging and Diet) was conducted so as to estimate the incidence (frequency) of dementia in the Greek population. This was the first large-scale

epidemiological study on dementia in Greece, which makes its results very important for the design of disease management actions at national level. According to the findings of the study, every 3 seconds someone shows dementia which in half cases is due to AD while seven out of ten (74%) of those taking care of people with AD are middle-aged women (56%) and care for the patient for an average of 40 hours a week. Finally, regarding the cost of the neurodegenerative diseases in the countries of the world, it is outrageous to declare that a neurodegenerative disease is “as expensive as a war” since in the US the annual cost outweighs the cost of war in Iraq, while in Greece the annual cost varies between 3 and 6 billion euros.

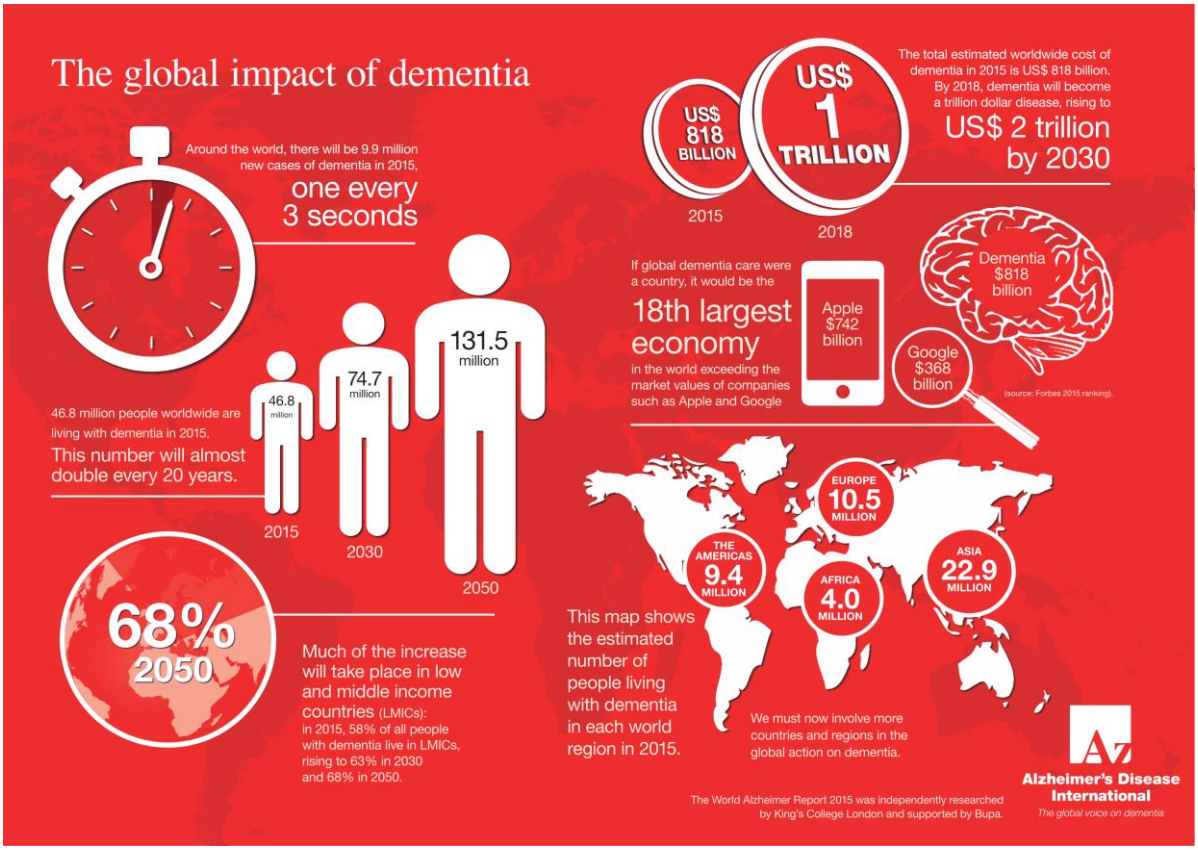

Figure 8: The global impact of Dementia in numbers.
Source: World Alzheimer Report 2015

1.2.2.2 Neuropathology of AD

The two principal cardinal lesions related to Alzheimer's disease are the neurofibrillary tangles and the senile plaques while both of these aberrant structures have been found in the brains of patients with Alzheimer’s disease.

The flame-shaped neurofibrillary tangles are abnormal aggregates of hyperphosphorylated tau protein located in the perikaryal cytoplasm of certain neurons. These aggregates are also observed in numerous other neurodegenerative diseases characterized by the presence of phosphotau aggregates, known as tauopathies. [72] Under pathological conditions, an increase in tau phosphorylation is observed, which reduces its affinity for microtubules, resulting in cytoskeleton destabilisation, principally in neurons. [73] However, to date, the numerous tau phosphorylation sites contributing to the disease pathogenesis have not been made apparent as well as the sites that become phosphorylated only after the formation of tau pathology in the tauopathies. [73]

To date, these neurofibrillary tangles are closely associated with the AD. The senile plaques (also known as neuritic plaques) are extracellular deposits of amyloid beta in the grey matter of the brain consisted of a central core of beta-amyloid (Aβ), a 4-kDa peptide. [74]

This ~ 4 kDa Aβ , a 39-42 residue peptide, is formed through the “amyloidogenic pathway” after a consecutive cleavage of the amyloid precursor protein (APP), a transmembrane glycoprotein whose activity and function remains unclear. The proteolytic enzymes cleaving APP are α-, β- and γ-secretase. Cleavage of APP by β-secretase leads to the generation of a C-terminal fragment (APP-CTFbeta), and subsequently γ-secretase cleaves it within the transmembrane region of APP, thus Aβ is produced. However, the degradation of APP-CTFbeta in the primary cortical neurons is performed in two separate mechanisms; the first one includes γ-secretase which produces Aβ while the second major pathway involves direct cleavage of APP-CTFbeta within the cytoplasmic domain by the proteasome.[75] Once Aβ is produced, it is subsequently either degraded within the brain, or transported out into the periphery. The final amount of Aβ accumulating in the brain as amyloid deposits, results from the interaction between the two procedures. [76]

The pathological aggregation of hyperphosphorylated tau protein and Aβ are sequential procedures. Initially, intraneuronally, the monomers accumulate and form the oligomers which afterwards aggregate in order to form the fibrils found in the senile plaques and Neurofibrillary tangles (NFTs). The structural and biophysical properties of the Aβ and tau protein oligomers are closely resembling to each other in terms of owning a high β-sheet content, showing resistance to proteolytic degradation by enzymes and causing neuronal toxicity. These oligomers are considered to be the most neurotoxic species in AD since they largely affect the cognitive function; even more than senile plaques or NFTs. The transmission of

these neurotoxic oligomers can be performed via “prion-like” mechanisms thus explaining the spread of AD pathology through specific brain regions. [77], [78]

Attempts to explain the progression of the neuropathology of Alzheimer's disease have been performed by the neuroanatomists Eva and Heiko Braak who introduced a classification of AD into six distinct pathoanatomical stages (the so called Braak and Braak stages) which was based on the characteristic distribution pattern of the neurofibrillary changes. [79], [80] Stages I-II demonstrated mild or severe modification of the transentorhinal cortex virtually limited to a single layer of the transentorhinal region, stages III-IV were characterized by serious involvement of the entorhinal and transentorhinal layer while stages V-VI are marked by the obliteration of all isocortical association areas.

1.2.2.3 Genetics of AD

There are numerous factors contributing to AD inception and progression with genes playing a crucial role. Both types of AD (early-onset and late-onset AD) are supposed to have a genetic component. A child from a mother who carries a genetic mutation for early-onset familial Alzheimer’s disease (FAD) has 50/50 possibility to inherit that mutation or not. Furthermore, an actual inheritance of such a mutation would boost the probability of developing early-onset FAD. Early-onset FAD is caused by some different single-gene mutations on chromosomes 21, 14, and 1. These mutations are located either in the precursor protein for Aβ (mutation in chromosome 21) or in presenilin-1 (PS1) or presenilin-2 (PS2) (mutations to chromosomes 14 and 1 respectively) while PS1 or PS2 is the catalytic subunit of γ-secretase. However, regardless of the genetic evidence and the fact that Aβ is involved in synaptic dysfunction and causes neuronal death there is a feeble correlation between the amounts and spread of Aβ and the expression of AD. [76]

Regarding the late-onset form of the disease, no gene directly causing the late-onset form of AD has been found yet. However, having one form of the apolipoprotein E (APOE) gene on chromosome 19 is considered to be one major genetic risk factor. APOE functions as a ligand in receptor-mediated endocytosis of lipoprotein particles while this susceptibility gene comes in several different forms (APOE ε2, APOE ε3, APOE ε4) with the ε4 allele to be the main contributing genetic risk factor for AD. [81]

Finally it was in early 2017 when the personal genetics company 23andMe announced that they received FDA approval to offer genetic information for 10 health risks including one for late-onset Alzheimer's (APOE gene variant). A blood

test can detect which APOE alleles a person has, although the prediction of AD development is still impossible. Hence, 70% of the population have APOE ε3 allele which is basically neutral, APOE ε2 is found in 5-10% of the people and is actually associated with lower risk of developing AD while APOE ε4 which is found in 10-15% of the population is the major risk factor for AD. [81], [82]

1.2.2.4 Pharmacological therapeutic approaches against AD

As already mentioned before, to date, there is no cure for AD, however, there are five prescription drugs approved by the U.S. Food and Drug Administration (FDA). Three of the five commercially available drugs belong to the class 'acetylcholinesterase inhibitors' and the fourth drug is memantine. Finally the fifth one is a combination of an acetylcholinesterase inhibitor with memantine. [83]

1.2.2.4.1 Conventional methods of AD treatment

(a) Acetylcholinesterase inhibitors

Acetylcholin (Ach) is the first discovered neurotransmitter and it is found in the autonomic ganglia, at many autonomically innervated organs, at the neuromuscular junction, and at many synapses in the central nervous system. On the other hand, Acetylcholinesterase (AChE) is a serine hydrolase mainly located at neuromuscular junctions and cholinergic brain synapses. The main role of AChE is to hydrolyze Ach to acetate and choline so as to terminate the transmission at the cholinergic synapses. [84]

The three Acetylcholinesterase inhibitors available to be prescribed are Donepezil, Galantamine and Rivastigmine. The main function of this drug class is to increase the levels of circulating acetylcholine by reducing its peripheral degradation. Ach is involved in almost all mind and thinking processes such as memory, speaking or judgment working as a neurotransmitter that delivers messages to the neighbor cells. By the end of the neurotransmitting procedure, the enzyme Acetylcholinesterase signals the abortion of the transmission and allows the hydrolysis of Ach. As a result, since in AD the neurons employing Ach are progressively destroyed, the available amount of Ach capable for transmitting messages is extremely limited. Thus, the Acetylcholinesterase inhibitors block the activity of acetylcholinesterase and help the maintenance of the necessary Ach levels in order to perform the neurotransmission and to compensate for the loss of functioning brain cells. However, since the AD symptoms are gradually evolving,

their capability to offer deceleration of the disease's progression is steadily fading as brain damage progresses. [83], [85]–[87]

(b) Memantine

Memantine is an uncompetitive antagonist of the N-methyl-D-aspartate glutamate receptor and also an approved drug only for treatment of moderate-to-severe Alzheimer's disease which enhances memory, attention, reason, language and the ability to perform simple tasks. Memantine's activity is based on the ability to regulate the activity of glutamate, the most abundant neurotransmitter involved in the cell signaling, information processing, storage and recovery. Glutamate is the principal excitatory neurotransmitter in brain. Its' main role is to trigger NMDA receptors and to increase membrane permeability for Ca^{2+}. The NMDA receptor channels contribute to the synaptic plasticity however, overactivating the receptor results in excessive influx of Ca^{2+} which causes excitotoxicity, a dysfunction involved in some neurodegenerative disorders. As a result, the excess glutamate has the ability to overstimulate the NMDA receptor thus leading to excessive entrance of Ca^{2+} into the nerve cells and cell death. Hence memantine's ability to partially block NMDA receptor establishes it as a potent drug for treating neurodegenerative diseases such as AD.

(c) Memantine + Donepezil combination therapy

Namzaric™ is a fixed-dose combination of memantine hydrochloride extended-release, a NMDA receptor antagonist, and donepezil hydrochloride, an acetylcholinesterase inhibitor which was recently approved by the FDA (December 2014) for the treatment of moderate-to-severe Alzheimer's in people who are taking donepezil hydrochloride 10 mg. According to the results of the clinical trials, Namzaric™ offered an enhancement of cognition and overall mental function and a provisional slowdown in the worsening of symptoms. [88] However, like all four drugs mentioned before, Namzaric™ has no evidence of preventing or decelerating the AD progression.

1.2.2.5 Alternative Approaches against AD

(a) Amyloid-β Immunotherapy for Alzheimer's Disease

Aβ peptide, the main characteristic compound found in the senile plaques in AD is characterized as a potential treatment target against AD since they are considered to own a major contribution to the pathogenesis of the disease. The

initial concept of the potential employment of immunization against AD derived from the observation that anti-Aβ monoclonal antibodies dissolve Aβ aggregates *in vitro*. [89] Hence, both active and passive vaccination procedures resulted in reduction and prevention of plaque deposition and enhancement of cognitive function in FAD mutant amyloid precursor protein (APP) transgenic mice. [90], [91]

Aβ immunotherapy has enhanced cognitive function in animal models and has afforded a reduction in amyloid fraction. However, despite the successful outcome of the preclinical studies, once the active Aβ vaccine was administered to humans, the vaccination was aborted since ~ 6% of the vaccinated AD patients developed meningoencephalitis. [92] Nevertheless, signs of cognitive improvement as well as obvious plaque clearance were observed in patients that generated antibody titers thus indicating that there might be hope.

Currently, there is no effective treatment for AD. However, there is a plethora of various active and passive immunization potential therapeutic approaches under construction and many of them under investigation in clinical trials. Nevertheless, unfortunately many of these therapeutic strategies are successively halted. A typical example is the “Solanezumab-case”, a humanized monoclonal IgG1 antibody directed against the mid-domain of the Aβ peptide by the pharmaceutical company Eli Lilly. In June 2016 Eli Lilly began a Phase III study in prodromal AD under the name ExpeditionPRO. This trial had started enrolling in up to 223 locations worldwide; however, in January 2017, Lilly terminated the study since it was demonstrated that Solanezumab had no effect on Aβ and tau PET biomarkers.[93]

A phase III randomized trial of Gantenerumab in prodromal Alzheimer's disease was conducted from Hoffman-La Roche. The study was halted as the administration proved futile, however, the dose-dependent effects observed in exploratory analyses on select clinical and biomarker endpoints might indicate that administration with higher doses of Gantenerumab is indispensable in order to achieve more efficacy. [93] Another effort is performed by Biogen Inc. with the Aducanumab which is currently at an ongoing Phase III clinical trial. Nevertheless, on February 2018 Biogen Inc declared that they observed more variability on the primary endpoint than initially assumed thus planning to expand the trial, which is considered to be a bad-sign from many.

(b) Tau-based therapies in neurodegeneration

Taking into consideration the inefficiency of the Aβ targeted therapies so far, tau has gained ground as a latent alternative target so as to defeat the disease. Therefore, there are several drugs participating in preclinical and clinical trials aiming to reduce tau levels as well as to abolish the aggregation of pathological modifications of the protein. [94] The approaches under clinical development include direct strategies pointing towards tau either by hindering its' aggregation or by vaccination. On the other hand, indirect tactics include microtubules stabilizing, kinase manipulating and reduction of tau oligomerization as well as targeting oxidative stress and autophagy.

Regarding Tau aggregation blockers, the initial drug tested against the formation of tau-filaments was methylene blue, a tricyclic phenothiazine drug which was capable of blocking the tau–tau interaction through the microtubule-binding domain (MBD). [95] This drug has been found to induce autophagy and attenuate tauopathy *in vitro* and *in vivo*, although its exact mechanism of action is still not understood. [96] However, at higher doses, it exhibited poor absorbance by the stomach which was induced by the presence of food and also it was accused of causing toxicity and haemolysis due to haemoglobin oxidation. [94]

Another recent drug that made it to Phase III of clinical trials but did not exhibit any promising results was intravenous immunoglobulin (IVIg) which has been examined in patients with mild-to-moderate AD. However, despite the fact that the initial theory of endorsing amyloid clearance would be advantageous, IVIg proved to be incapable of reversing the AD effects thus indicating that focus should be made on relevant mechanisms of action other than the removal of amyloid plaques. [97]

(c) Human induced pluripotent stem cell (iPSC) technology

The advent of human induced pluripotent stem cell (iPSC) technology is one of the most revolutionary and modern approaches available in the battle against AD. This technique initiated only a decade ago and since then, enormous progress has been made in terms of drug discovery, disease modelling and cell therapy development. [98] Based on iPSC technology, a team of Japanese researchers employed human iPSC-derived neurons, which afford human-specific drug responsiveness in order to perform screening and evaluation of potential anti-AD drugs. Consequently, after the screening procedure, the compounds possessing anti-Aβ effect combined so as to enhance their anti-Aβ activity. *In vitro* evaluation of the compounds was performed on iPSC-derived neurons including all types of

AD patients while the final results confirmed that the combination of anti-Aβ compounds could reduce Aβ efficiently in all participants beyond the differences in drug responsiveness among multiple individuals.[99] The final ‘drug-cocktail’ tested consisted of bromocriptine, cromolyn, topiramate (BCroT) which was proved to be the most potent anti-Aβ combination. These drugs were found to synergistically improve Aβ phenotypes of AD in cells. The results deemed worthy, thus further verification steps are necessary in order to export safe conclusions such as pharmacokinetic data and evaluation of the interaction of the iPSC neurons with the BBB and the vascular cells. [99]

1.2.3 Application of Natural Products for the treatment of Neurodegenerative Diseases

As it was previously described, the neurodegenerative diseases are ailments that are incurable and especially for AD and PD there is no current therapeutic approach available. As a consequence of many years of scientific research, there are many well-established (semi-)synthetic drugs employed for the deceleration of the AD and PD progression however most of them bare several side-effects as well. Thus, along with the chemical drugs, traditional medicine provides numerous lead-compounds that have shown remarkable action against neurodegenerative diseases. Although the plant-originated compounds are usually a second option in comparison to the chemical ones, we should always highlight and bear in mind that one of the five drugs approved by the US FDA against AD in total, galantamine, also known as galanthamine, is an isoquinoline alkaloid produced by plants from Amaryllidaceae family with a specific, competitive, and reversible activity to inhibit acetylcholinesterase. (Figure 9) [86][100]

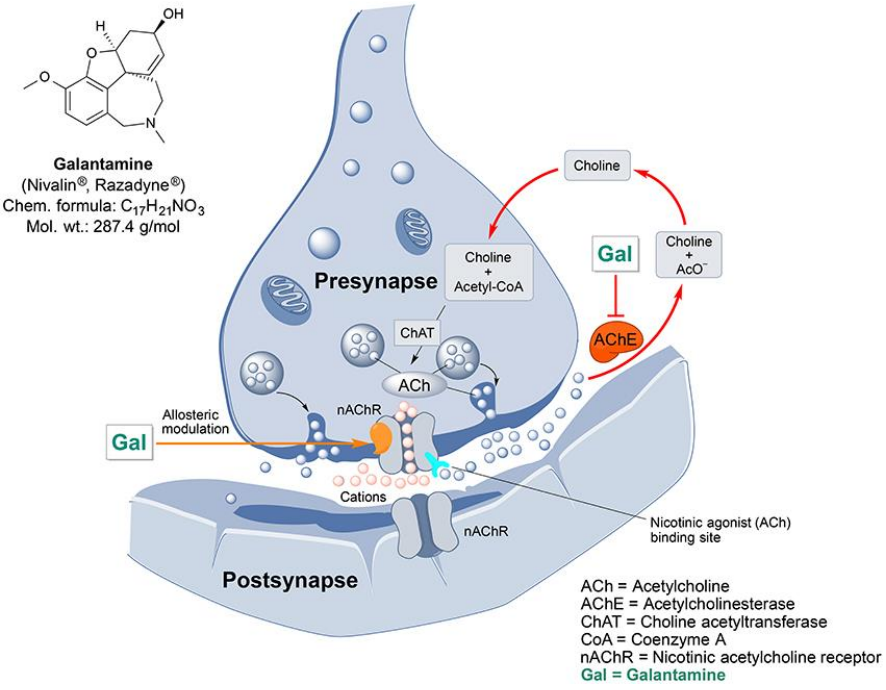

Figure 9: Chemical structure and targeted mechanisms of galantamine (Gal) against AD and dementia. *Source: D. Tewari et al., Front. Aging Neurosci., vol. 10, p. 3, Feb. 2018.*

An extensive search at the web for medicinal plants employed against dementia and neurodegenerative diseases in general, resulted in more than 70 plants. However, mainly based on the number of hits observed, the most “famous” plants have been selected and will be thoroughly discussed below.

(a) *Gingko biloba* L.

Ginkgo biloba fam. Ginkgoaceae, commonly known as ginkgo is the only living species in the division Ginkgophyta. It is an extremely old species since it has remained unaltered in terms of gross morphology for more than 200 million years. [101] The extract of *Gingko biloba* (EGb 761) is regarded one of the most widely used herbal remedy for dementia. It is employed as a symptomatic treatment for cerebral insufficiency observed during normal ageing or due to neurodegenerative dementia. [102] The main constituents of the EGb belong to three principal classes; flavonoids (e.g. kaempferol), terpenoids (e.g. ginkgolides A, B, C, bilobalide) and ginkolic acid. *Ginkgo biloba* is extensively studied thus there are numerous reports indicating the substantial contribution of EGb 761 into the prevention and treatment of neurodegenerative diseases since it enhances memory and cognitive function.[103] The flavonoid fraction of EGb 761 is responsible for interaction with neuronal receptors involved in memory and learning procedures. [104] The terpen lactones of Ginkgo own some really important pharmacological activities such as platelet-activating factor (PAF) receptor antagonism and neuroprotective properties. [105] As a result the EGb 761 has the potential to enhance memory and learning and to decelerate cognitive deterioration in patients with AD or dementia since it exhibits neuroprotective effect underlined by its antioxidant and antiplatelet activity.[100] It is noteworthy that it is the only herbal remedy considered a phytomedicine, which is recommended by international authorities to be used as a beneficial supplement against dementia. [106] Furthermore, it has been demonstrated that EGb761 could boost amyloid precursor protein (APP) metabolism towards the enhancement of α-secretase pathway, thereby increasing the release of the soluble form of APP (sAPPα). [107] In conclusion, the beneficial effects of EGb at doses greater than 200 mg/day, are well supported by several systematic reviews and scientific evidence. Nevertheless, the interpretation of the results should be careful since many methodological limitations are observed. [106][102]

(b) *Panax ginseng* L.

Panax ginseng fam. Araliaceae is a slow-growing perennial plant renowned for its remarkable neuroprotective activity. Traditionally it has been used in Chinese medicine for >2000 years as a tonic for fatigue, weakness and aging. The main compounds of the ginseng extract are ginsenosides Rg1 and Rg3 and ginseng polysaccharides which have all been explored so as to identify their therapeutic potential. [100] Given the ancient and traditional information of the ginseng's

capability to improve age-related memory impairments as well as the current use for the co-treatment of AD symptoms in China, numerous studies have tried to investigate its' role in the treatment of primary AD signs. As a result, the analysis of ethanol-derived extracts of different types of ginseng extract have demonstrated that a significant reduction in the Aβ has occurred. [108], [109] The main compound contributing to the neuroprotective effect of ginseng is 20(S)-ginsenoside Rg3 which enabled a significant reduction in the amount of Aβ-40 and Aβ-42 peptide in the brains of transgenic mice. [109]

Given the fact that we live in a Mediterranean country where the so-called "Mediterranean Diet" (MD) plays a crucial role in our everyday lives, it would be appropriate to mention the supreme neuroprotective properties of two major constituents included in our daily nutrition habits; extra virgin olive oil (EVOO) and red wine. [110]

(c) *Olea europaea* and Olive Oil

The adoption of the MD in the everyday routine has been widely associated with a significant reduction of the neurodegenerative disorders in the Mediterranean population. Extra virgin olive oil is an indispensable part of the MD and it is rich in numerous pharmacological compounds which are mainly minor phenolic compounds. Hydroxytyrosol (HT) is a strong anti-oxidant molecule possessing anti-inflammatory activity thus contributing to the neuroprotective effect of olive oil. [111] Furthermore, another minor compound of EVOO, the secoiridoid oleocanthal, is responsible for enhanced clearance of Aβ from the brain via up-regulation of P-glycoprotein (P-gp) and LDL lipoprotein receptor related protein-1 (LRP1) which are major Aβ transport proteins, at the blood-brain barrier (BBB). [112]

(d) *Vitis vinifera* and Red wine

Another major part of a holistic MD is the moderate consumption of red wine thus the potential protective role of the Red Wine Polyphenols (RWP) has been thoroughly investigated. Red wine is considered to be a rich source of specific polyphenolic compounds such as quercetin, tannins, anthocyanidins, resveratrol, and ferulic acid, compounds that seem to interfere with the AD and PD molecular mechanisms. [113] It has been demonstrated that RWP reduce oxidative stress since they have strong anti-oxidant capacity. The central nervous system is highly vulnerable to oxidative stress (OS) since it demands high levels of oxygen consumption. [114] Furthermore, the accumulation of redox-active metals such as

zinc, copper, and iron [114] in combination with the presence of polyunsaturated fatty acids in the neuronal membranes contribute to the exposure of the neurons to OS. As a result, OS is a major contributing factor to the neurodegenerative diseases pathogenesis thus the direct antioxidant and metal-complexing properties of RWP may be of vital importance. [113] Nevertheless, the RWP and their metabolites do not simply act as anti-oxidants but they are also capable of interacting with signaling pathways involved in adaptive stress responses. Therefore, phenolic compounds included in red wine are capable of defeating OS and neuroinflammation thus they are major contributors in the arsenal against neurodegenerative diseases. [113]

As a result, there are several drugs of natural origin that may serve as potential therapeutical approaches against dementia and AD, however, in most cases, the lack of adequate evidence is a black-point. Therefore, these promising plant-oriented drugs should be involved in advanced clinical trials in order to deeply investigate their therapeutic efficacy. In conclusion, the numerous promising natural products and semi-synthetic compounds represent a wealthy source of “major lead compounds” for the development of new therapeutic strategies and for the treatment of neurodegenerative diseases.

1.2.4 Natural and synthetic neuroprotective steroids against Neurodegenerative Disorders

The leading cause of neuronal loss in many neurodegenerative diseases is not completely understood. Neuroprotective steroids comprise an interesting approach and could potentially play a crucial role against the molecular mechanisms involved in several neurodegenerative disorders since the natural endogenous steroids have the ability to protect the nerve cells from being injured through multiple mechanisms. The endogenous neuroactive steroids derive from the steroidogenic peripheral glands and they include dehydroepiandrosterone (DHEA), itself a prohormone of the sex steroids, DHEA sulfate (DHEAS), testosterone, estradiol, pregnenolone, and progesterone etc. [115]

Steroids have neuroprotective activity since they have the ability to shield the neurons against oxidative stress, excitotoxicity, and neuroinflammation which are considered amongst the most crucial causes of neuronal cell death. Furthermore, steroids enhance the neurotransmission as well as repair neurogenesis. [116] Furthermore, the steroids are able to modify the phosphatases and kinases expression and also, they can decrease the release of pro-inflammatory cytokines such as IL1b, TNF-a, IL6. As a result, the progression

of the neurodegenerative diseases is hindered, hence these steroids are effectively contributing to the therapeutic management of neurodegenerative disorders. [117]

The neuroprotective steroids' activity is primarily regulated by endogenous interaction with neurotransmitter receptors such as gamma-amino-butyric acid type A and B (GABA-A receptor, GABA-B receptor), serotonin type 3 (5-HT3), NMDA etc. [118] It is inevitable that sex plays a crucial role in the neuroprotective activity of steroids in the CNS since sex differences affect the structural and functional activities of neuronal cells in the brain and cause different pathologies in terms of symptomatology and neurodegenerative outcome.[119] Numerous examples indicate that steroidal hormones have a major contribution on the brain response to pathological conditions [118], [119] while some theories confirming these observations are that during the estrous cycle, the variations in the hormonal levels affect the neuronal loss. [120][121]

A typical example is the 17α-Hydroxypregnenolone which is considered a *prohormone* in the formation of dehydroepiandrosterone (DHEA). Furthermore, through the activity of 3α-hydroxysteroid dehydrogenase, 17α-Hydroxypregneolone is also converted to 17α-hydroxyprogesterone, a prohormone for glucocorticosteroids and androstenedione. Dehydroepiandrosterone and its sulfate ester (DHEAS) are regarded as neuroprotective factors thus they are capable of protecting neurons against a plethora of harmful events including excitotoxicity. The defending character of DHEA is probably linked to its' capability to inhibit the NMDA-induced nitric oxide (NO) production in hippocampal cells or modulation of the calcium/NO signaling pathway. [116]

In conclusion, the neuroactive steroids exhibit differential effects in the male and female neuronal cells thus indicating that this could be associated with major differences in steroid receptors or in the steroid signaling mechanisms. They have proved to significantly affect neuro-inflammation by offering a wide range of compounds capable of diverting the neuro-inflammation pathways and improve the anti-inflammatory response.

1.3 *Crocus sativus*: THE HUMBLE FLOWER AND THE ROYAL SPICE

Crocus sativus is a species of flowering plant of the *Crocus* genus in the Iridaceae family which grows in the Mediterranean, East Asia and Irano-Turanian region. *Crocus* is a perennial spicy herb which is difficult to be cultivated since it demands special climate and soil conditions. In details, *Crocus* shows resistance to cold temperatures below -18 ^{o}C and to hot temperatures of no more than 35-40 ^{o}C explaining its' cultivation capability in dry, moderate and continental climate types. Regarding the soil characteristics, *Crocus sativus* grows in many different soil types but thrives best in calcareous, humus-rich and well-drained soil with a pH between 6 and 8. [122] Given that the plant itself has no seed propagation capability, the underground parts of the plant, corms or bulbs, can be used to produce new plant. [123] *Saffron,* is the spice deriving from the flower of *Crocus sativus* which is comprised of the three red stigmas included in the flower that are consequently collected and dried under special conditions so as to produce the final saffron as a spice. (Figure 10) Cultivation of *Cr. sativus* requires intensive labour thus explaining its' significantly high price.

This flower is considered to be the "Prince and the Pauper" at the same time since on the one hand *Crocus sativus* is a humble, small and sometimes ignored flower but on the other hand, it contains the most precious spice in the world which is considered to be the most valuable spice by weight while it is characterized as "Red Gold" in producer countries.

Figure 10: Flower and Tripartite stigmas of *Crocus sativus* (original stigmas length 25–30 mm)

1.3.1 Pharmacological properties of saffron

Saffron is a wealthy source of numerous pharmacologically active compounds. The main constituents of saffron are carotenoids, glycosides, monoterpenes, aldehydes, flavonoids, anthocyanins, vitamins (especially riboflavin and thiamine), amino acids, proteins, starch, and gums. [124] In the last 20 years there is an increasing amount of data regarding saffron or its' constituents use for the treatment of several diseases mainly due to the plethora of pharmacological actions. Some of the most important pharmacological effects of saffron and/or its active components include: anticonvulsant [125], anti-inflammatory [126], anti-tumor [127] and anti-oxidant activity [128], [129] as well as enhancement of learning and memory capacity [130]–[132] etc. (Figure 11)

Figure 11: Pharmacological applications of saffron and its' major constituents

(a) Cardiovascular

The effects of saffron aqueous extract containing the polar fraction of saffron including crocins as well as saffranal, the major constituent of the essential oil of saffron, have been studied in isoproterenol-induced cardiotoxicity in rats. [133] A potential cardioprotective effect of crocin in isoproterenol-induced cardiac toxicity

was highlighted mainly due to the modulation of oxidative stress so as to keep the redox cell status stable. [134] Furthermore, the aqueous extract of saffron has been demonstrated that offered hypotensive effect in rats which is mainly based on the action of crocin and saffranal. [135] Crocetin, another carotenoid constituent, has been found to prevent the induced atherosclerosis in rabbits mainly by enhancing the tissues oxygenation. [136] Finally, taking into consideration the high content of saffron in well-known antioxidants such as flavonoids, a potential synergistic effect of all these compounds with anti-oxidant properties, might decrease the risk of cardiovascular diseases. [136] The capability of saffron extract to strengthen the blood circulatory system as well as the presence of minerals and vitamins such as riboflavin and thiamine may eliminate the heart-disease risk and prevent the occurrence of cardiovascular ailments.

(b) Anti-inflammatory

Inflammation is the defense mechanism of the body. As soon as the immune system realizes occurring damage, irritants or pathogens then a complex procedure trying to restore the health condition and to enhance the healing process begins. Saffron extract has shown strong anti-inflammatory activity in several models including xylene induced ear edema in mice as well as formaldehyde induced arthritis. [137] According to *in vitro* analysis results, crocin has been found to have strong anti-inflammatory activity since it was capable of altering the cyclooxygenase pathway by inhibition of both cyclooxygenase 1 (COX1), cyclooxygenase 2 (COX2) enzyme as well as by preventing the production of prostaglandin E dose-dependently. [138] Finally, another illustrating example is the capability of crocin to ameliorate cartilage degeneration *in vivo* in osteoarthritic condition. As a result, crocin is considered to be a potentially effective anti-arthritic factor. [139]

(c) Anti-tumor

Cancer is regarded to be one of the major mortality causes globally and normally is treated with synthetic drugs interfering with many different molecular mechanisms. However, along with the synthetic drugs, the use of medicinal plants and herbs has proven to be a promising strategy as well as a potential cancer-preventing approach. Saffron has shown remarkable anti-tumor activity and also chemoprotective activity when co-administered with amino acid cysteine and the antioxidant vitamin E against the toxicity of cisplatin and also exhibited a synergistic effect regarding the effective inhibition of colony formation. [140]

Considering the saffron constituents, saffranal has been found to have anti-genotoxic activity by offering significant protection of the Methyl Methanesulfonate induced DNA damage. [141] Crocin on the other hand, is suggested as one of the most putative and effective therapeutic components included in saffron extract although its' exact underlying molecular mechanism of action is not fully explained and understood. Therefore, there are several studies indicating that crocin exhibited significant anti-proliferative effects on cell lines from many different types of human cancer without affecting the growth of non-cancer cells. [142] Furthermore, another proposed mechanism of action is that crocin interacts with DNA topoisomerase enzymes thus resulting into the antiproliferation activity of crocin. [143] Finally crocin has been found to promote the apoptosis of cancer cells thus indicating that it has the potential to reduce the amount of malignant cells in the tumor cell lines. [142]–[144]

1.3.2 Saffron and nervous system

The nervous system is a complex and sophisticated system capable of regulating and coordinating all the activities of an organism. Normally, the nervous system acts like a well-rounded clock however, the nervous system is also susceptible to numerous disorders such as trauma, infections, degeneration, structural defects, depression and autoimmune diseases. Saffron and its constituents have shown remarkable activity in reversing some of the aforementioned symptoms. It has been demonstrated that saffron aqueous extract and its constituent, crocin, improved the sexual activity in male rats. [145] Furthermore, crocin has been found to have anti-depressant effects since the forced swimming test performed in rodents demonstrated that crocin (50–600 mg/kg) reduced immobility time while increased climbing time. [146][147] Another interesting observation was that administration with saffron aqueous extract and crocin (both at 15 mg twice a day) caused no serious side effects and were safely tolerated in patients with schizophrenia thus indicating its' safe potential use to humans, especially in patients suffering from chronic mental illnesses. [148]

Saffron is considered to be a potential weapon against neurodegenerative diseases since saffron, crocin, crocetin and saffranal have shown remarkable anti-oxidant activity. [149] Moreover, saffron has exhibited significant anti-PD and anti-AD activity which is highlighted by several recent studies including animal models with neurodegenerative diseases. Regarding PD, crocin and safranal have demonstrated inhibition on apo alpha-lactalbumin (a- alpha-LA) fibrillation under amyloidogenic conditions resulting in further inhibition of the formation of the toxic soluble amyloid oligomers causing the neurotoxicity in AD and PD. [150] Another study examined the potential protective effect of pre-treatment on dopaminergic cells in the substantia nigra pars compacta (SNpc) and retina in a mouse model of acute MPTP (1-methyl-4-phenyl-1,2,3,6- tetrahydropyridine)-induced PD where after a five-day treatment with saffron extract 0.01% w/v the results indicated that pre-treatment with saffron has saved many dopaminergic cells in the SNpc and retina from Parkinsonian. [151] Furthermore, there are studies indicating that saffron aqueous extract and crocin have significantly inhibited the amyloid fibril formation present in AD. [128] Finally, saffron has shown up to 30% inhibition of the acetyl-cholinesterase (AChE) activity hence, since this is the main therapeutic approach for AD, a parallel treatment with this extract would enhance the capability of the synthetic acetyl-cholinesterase inhibitors that are commercially available against the treatment of AD. [152]

1.4 SCREENING OF THE NONCOVALENT INTERACTIONS AMONG SELECTED NATURAL PRODUCTS AND SAFFRON-ISOLATED COMPONENTS AND Aβ PEPTIDE

To date, the pathogenesis of AD has not yet been clarified and the understanding of the disease mechanism remains obscure. Nonetheless, the amyloid-beta peptide formation leading to the cerebral deposition of amyloid plaques and the tau-protein containing neurofibrillary tangles are considered to be the main pathological hallmarks of AD. These disease-specific aggregated proteins and peptides have apparent diagnostic and even therapeutic implications[153]. In particular, $A\beta_{1-40}$ and $A\beta_{1-42}$ are the predominant components in amyloid plaques, with the formation of Aβ oligomers leading to either neuronal death and/or disruption of synaptic function. [154], [155] Regarding the Aβ's neurotoxicity, the main proposed mechanisms are oxidative stress and neuroinflammation. [156]

In general, it has been well-demonstrated that cellular functions are often activated by weak noncovalent interactions, such as those between enzyme and substrate, protein and ligand, antibody and antigen etc. Abnormal interruption of these noncovalent interactions can lead to a disease's initiation and progression. Therefore, the clarification of the formation mechanism of these noncovalent complexes can lead to a better elucidation of the disease process, and provide insights towards the design of a therapeutic approach.

Considering the suggested mechanistic link between oxidative stress, inflammation and neurodegeneration [157], it makes imperative to study the neuroprotective effect of plant-derived and dietary antioxidants and investigate the potential of antioxidants as putative neuroprotective agents. As a matter-of-fact, there are several *in vitro* and epidemiological studies demonstrating the positive impact of natural products on the progression and incidence of age-related disorders, such as dementia and AD. [158] [159][160]

An important example is that of the melatonin hormone, which is regarded as a strong cellular antioxidant while it possesses neuroprotective activity against neurodegenerative diseases and especially AD, as it affected the processing of amyloid precursor protein (APP) in cell lines. [161] Incidentally, it has been found that melatonin is significantly reduced in AD patients. [162] Therefore, it was essential to investigate the interactions between Aβ and melatonin and its inhibitory effect on the formation of Aβ fibrils in order to elucidate the noncovalent interactions, determine its relative binding strength to Aβ peptide and localize its binding site using enzymatic digestion mapping protocols. [163] The detection of the noncovalent interactions

between the Aβ peptide and melatonin was demonstrated by electrospray ionization (ESI) Mass Spectrometry (MS). [163]

In a subsequent study, Bazoti *et.al* [158] has also indicated the establishment of the noncovalent interactions between Aβ (1-40) and Oleuropein (OE) by means of ESI MS while suggesting the possibility to lock the Aβ-OE complex in a non-toxic conformation, thus acting as potential anti-amyloidogenic agent since the complex was well-preserved even at extreme conditions (i.e., high percentage of organic co-solvent) indicating its high binding energy. Furthermore, the powerful tool of ESI MS, enhances the detection of noncovalent interactions between biomolecules and natural products, even if they are present in small amounts since it was demonstrated that OE has the ability to interact with Aβ and its oxidized forms, with Aβ amino acid segments [4–11], [12–22], and [17–28] being involved in the interaction with OE. [164]

In a modified integrated approach for screening and identifying potential inhibitors for the Aβ peptide aggregation, the anti-amyloidogenic activity of isolated components from the stigmas of saffron has been evaluated. [165] The formation of similar 1:1 noncovalent interactions between the Aβ peptide and the main *Crocus* components have been demonstrated. The screening of several bioactive compounds in terms of binding to Aβ as well as their relative binding strength was performed employing ESI MS-based methodologies. It has been demonstrated that natural products could be effective towards the inhibition of Aβ fibrillogenesis without limiting neuronal cell viability at low concentrations. Such an integrated approach (real-time *in vitro* screening for noncovalent association with Aβ by ESI MS and cell viability assays) could further support any upcoming *in vivo* studies. [165]

Finally, these really promising results could be the leading hits into the design and synthesis of novel compounds with targeted anti-amyloidogenic activity and be utilized effectively against AD. Thus, the main goal of such studies was to provide some insights into the key pathways of AD development and pathology, along with the identification of potential anti-amyloidogenic agents. As a result, the *Crocus*-derived bioactive compounds could lead to the discovery of novel aggregation inhibitors for the prevention, or treatment of AD. [165]

CHAPTER TWO

Rapid isolation and characterization of major and minor Crocins, Picrocrocin and Crocetin from saffron extract employing step-gradient Countercurrent Partition Chromatography (CPC)

2.1 ABSTRACT

In the present study we describe a simple and effective method for one-step isolation of the main secondary metabolites of a Methanol-Water (MeOH−H_2O) 50:50 v/v extract of *Crocus sativus* stigmas by using step-gradient countercurrent partition chromatography (CPC). The step-gradient CPC analysis was performed both in dual mode and elution−extrusion mode, using five biphasic systems of the solvents n-Heptane−Ethyl acetate−Butanol−Ethanol−Water (n-Hept/ EtOAc/ BuOH/ EtOH/ H_2O) in ratio 4:10:0:4:10, 1:13:0:4:10, 1:12:1:4:10, 1:10:3:4:10 and 1:7:6:4:10 respectively. Five major crocins, picrocrocin and crocetin (CRC) were directly isolated in one step. Scaling up from semi preparative to preparative, led to the recovery of significantly high quantities of pure compounds and especially of *trans*-crocin 4 (TC4), which is the major crocin of saffron. Comparing the two methods of CPC analysis (elution-extrusion and dual mode), it was proven that in dual mode CPC, due to the analytical procedure (change from ascending mode to descending mode), the fractions containing TC4 did also include a high amount of free D-glucose. An absence of free D-glucose was observed on the elution-extrusion mode, which makes elusion-extrusion the most effective method compared to dual-mode method. Furthermore an effort to start the analysis with the 4^{th} solvent system (1:10:3:4:10) proved to be particularly selective for the effective isolation of *trans*-crocin 4 (TC4) with significant reduction in experimental time and solvent consumption. Structure elucidation of the *Crocus*-isolated components was carried out by HPLC and NMR experiments. In total, from all the CPC experiments that have been performed, 6185 mg of pure TC4 were isolated, 15 saffron constituents have been isolated and characterized leading to the establishment of the developed CPC methodology, as a suitable approach for the saffron stigmas analysis in the laboratory as well as the natural products industry.

Keywords:

Centrifugal Partition Chromatography; Crocetin; Crocin; Saffron

2.2 INTRODUCTION

Saffron is the dried stigmas of the flower *Crocus sativus* L. Apparently it is originated in Greece, Turkey, Iran and it is also successfully cultivated in many other countries such as France, Spain, Italy, Egypt, Israel, and Pakistan. [166] The quality and chemical composition of saffron are affected by the region in which saffron is grown, the drying process, the conditions of packaging and storage and the analytical extraction methods which have been used. [167] Saffron is considered to be the most expensive spice and it is mainly used as traditional herbal medicine or food coloring and flavoring agent in different parts of the world. [168] It has also been suggested to be effective in the treatment of a wide range of disorders including coronary artery diseases, hypertension, stomach disorders, dysmenorrhea and learning and memory impairments. [169] Several studies indicate that saffron or its' main constituents, possess numerous pharmacological properties such as antioxidant, anticonvulsant,[125] anti−schizophrenia [170] and protective against DNA damage [170] activities. Moreover, saffron has shown remarkable action against some of the most important neurodegenerative diseases such as Alzheimer's (AD) and Parkinson's (PD), [152][171][172] as well as a dose−dependent inhibitory response on breast cancer cells. [173]

Over the past years, there have been many studies, regarding the major and minor compounds of *Cr. sativus*. The main saffron constituents (Figure 12) include crocins, which are mono− and bis−esters of crocetin (apocarotenoid) with glucose and/or gentiobiose, and monoterpenes, mainly picrocrocin and safranal.[174] Picrocrocin, a colorless glycoside, is the β−d−glucoside of hydroxysafranal (4−hydroxy−2,6,6−trimethyl−1− cyclohexene−1−carboxaldehyde) and mainly responsible for saffron's well−known bitterness.[124] Safranal is the principal substance of saffron's aroma. The major components of *Cr. sativus* stigmas' are the crocins as well as crocetin esters (*cis*−crocetin and *trans*−crocetin) which provide saffron with its' intense red color. The crocins are a mixture of highly water−soluble carotenoid metabolites which are chemically categorized as sugar esters of the dicarboxylic acid crocetin (2,6,11,15−tetramethylhexadeca−2,4,6,8,10,12,14− heptaenedioic acid). [124] According to recent studies, the main crocins that have been identified in saffron are *trans*−crocin−2 (TC2), *trans*− crocin−2' (TC2'), *trans*−crocin−3 (TC3), *trans* crocin−4 (TC4), *cis*−crocin−1 (CC1), *cis*−crocin−2 (CC2), *cis*−crocin−3 (CC3), *cis*−crocin−4 (CC4), *cis*−crocin−5 (CC5). *Trans*−crocin 4 (TC4) is found to be the most abundant ingredient in the majority of the investigated saffron samples followed by *trans*−crocin−3 (TC3) and *cis*−crocin−4 (CC4), however *trans*−crocin−2

(TC2) and *cis*−crocin−2 (CC2) were present in all cultivated samples, although produced in lower concentrations. [166][173][128]

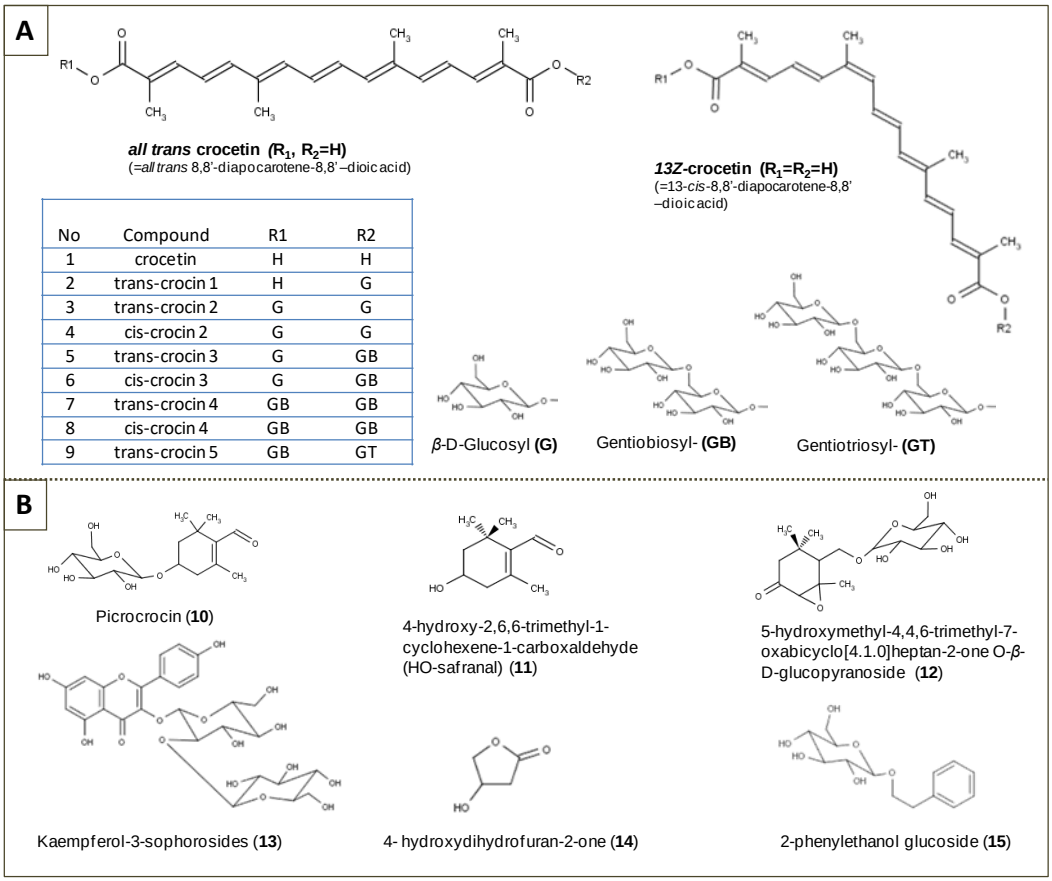

Figure 12: Structures of the main components isolated from Saffron extract

As natural products extracts are usually mixtures of bioactive compounds and also characterized by high complexity, their purification is normally a time consuming and surely challenging task. Some years before, this procedure used to require a high amount of working hours in the laboratory, as well as a comprehensive range of techniques and often led to the isolation of an extremely limited percentage of pure compounds. Thus, considering the natural products chemistry, there was an indefinite need for more sufficient isolation techniques that could lead to the production of pure or almost pure compounds, ready to be utilized in further experiments.

Centrifugal Partition Chromatography (CPC) is a liquid-liquid chromatography technique developed by Murayama et al. [175], and constitutes a constantly evolving separation, enrichment and purification technique. Its function is based on the principles of liquid/liquid partitioning chromatography were the individual solutes are isolated based on the different partitioning in the two

immiscible liquid phases of a biphasic system. [176]–[179] The one liquid phase (stationary phase) is fed into the CPC column and maintained inside due to the centrifugal force generated by rotor spinning (at moderate rotational speed) while the other one (mobile phase), is pumped through the stationary phase. The separation of the solutes is achieved as a function of the specific partitioning coefficient (K_D) of each solute between the mobile and stationary phases. The CPC technique faces two major problems; first to find the appropriate biphasic liquid system to obtain the anticipated purification of the compounds of interest; and second, to retain enough stationary phase inside the CPC column in order to achieve sufficient separation of the analytes. [180]

A crucial point to highlight while working on CPC experiments is the fact that, the stationary phase volume inside the CPC column is much larger than in classical silica-based high performance liquid chromatography (HPLC) columns. In CPC the stationary phase comprises up to 80% of the column volume, but it is not constant. Various parameters like the centrifugal filed strength (rotor's rotation speed), the mobile-phase flow rate as well as the biphasic liquid system utilized, affect the distribution of the stationary phase. Furthermore, the physicochemical properties of the system e.g. phase density difference, phase mutual solubility and interfacial tension affect the retention of the stationary phase inside the column as well. Thus, the stationary phase retention ratio, S_f, is an excellent way to model the CPC chromatograms obtained. [181] The absence of solid chromatographic support results in avoidance of irreversible adsorption, degradation or denaturation of compounds induced by solid stationary phases, thus CPC is characterized as an excellent alternative to more traditional solid support chromatographic techniques.[177] CPC is also considered a "green" technology, especially in preparative level, due to the absence of solid packing phase, while it affords short analysis time and low solvent consumption. Most importantly, it is easily scalable for the analysis of milligrams to multi-grams of starting material.

However, the selection of an appropriate two-phase solvent system is by far the most important part when it comes to the running of an effective CPC experiment and that is the reason why it is mainly the most time-consuming aspect of the technique. [182] Nevertheless, a careful selection of both solvents ratio and type of CPC experiment, potentially leads to a successful and effective isolation of the compounds of interest. CPC is an extremely useful tool for the separation of complex mixtures while, the aid of new advances such as pH refining zone CPC and step gradient CPC, made possible the successful separation of almost all

chemical categories of natural products (triterpenoids, saponins, phenolic compounds, flavonoids, alkaloids, peptides, etc.). [177], [179], [183]–[185]

Herein it is described a simple and fast method using countercurrent partition chromatography, leading to a rapid isolation of the main compounds of *Crocus sativus* stigmas' extract and enabling the high recovery of a large range of some pure compounds and some requiring an additional simple purification procedure, in practically one step.

2.3 MATERIALS AND METHODS

2.3.1 Apparatus

Semi-preparative separation was performed on a Fast Centrifugal Partition Chromatograph FCPC200®, purchased from the Rousselet-Robatel Kromaton company (Anonay, France). The rotor is made of 20 circular partition disks engraved with 1320 partition cells (130 µL per cell) and the total column volume capacity is 205 mL. The preparative separations were performed on a Fast Centrifugal Partition Chromatograph FCPC1000® (Rousselet-Robatel Kromaton, Anonay, France) equipped with a rotor of 955 mL total volume capacity (45 circular partition disks engraved with 32 partition cells). Rotation speed could be adjusted from 200 to 2000 rpm, producing a stable centrifugal force up to 161 g at 1000 rpm. The solvents were pumped through the CPC columns with a Prep36 LabAlliance dual piston pump (State College, PA, USA). The sample injected via a 10 mL sample loop for semi-prep analysis and 30 mL sample loop for the preparative separations. Fractions were collected with a Büchi B−684 fraction collector (Flawil, Switzerland). Chromatograms were recorded at 254, 320 and 440 nm using a UV detector SPECTRASYSTEM UV 2000, Thermo Scientific (Illkirch, France) and a ChromQuest® chromatography station. All experiments were performed at room temperature (20 ± 2 °C).

2.3.2 Reagents and materials

Methanol (MeOH) used for the extraction of the plant material (saffron) was of analytical grade (Merck, Darmstadt, Germany) while the water (H_2O) that was used was distilled by a Water Pro PS system, LABCONCO (Kansas city, Missouri, USA). Considering the isolation, Acetonitrile (ACN) and MeOH were of analytical grade (Merck, Darmstadt, Germany). Analytical thin layer chromatography (TLC) was performed on precoated silica gel 60 F254 plates (Merck), and spots were

visualized using UV light and vanillin−H_2SO_4 reagent. HPLC−grade ACN was used for the HPLC-diode-array-detector (DAD) analysis, while MS-grade H_2O and ACN (Merck, Darmstadt, Germany) were used for the HPLC−UV−HRMS analysis. H_2O acidified with 0.1% (v/v) ultrapure Formic acid for mass spectrometry ~98% from Sigma Aldrich. CPC separations were performed using organic solvents of analytical grade (Sigma−Aldrich).

Plant material *Cr. sativus* stigmas (saffron) was kindly supplied by the *Cooperative De Safran* (Krokos Kozanis, West Macedonia, Greece). After harvesting the saffron, stigmas were dehydrated first at 20°C and later at 30 to 35°C until moisture reaches the level of 10-12%, packed and kept in the dark until used.

2.3.3 Extraction of *Crocus sativus* stigmas

According to previous experiments in our laboratory [174], we have established the optimum extraction conditions in order to obtain a saffron extract that contains all the compounds of interest (either polar or unpolar). In detail, 30 g of dried *Cr. sativus* stigmas were extracted with 50 mL/g petroleum ether for 15 min (at 4 ^oC). Afterwards, the stigmas were extracted with 75 mL/g diethylether for 2 h (at 4 ^oC). Finally, the stigmas were extracted with 2,5 L of Methanol and Water (MeOH:H_2O) 50:50 for 24 h at 25°C in the absence of light. The final extract was filtered through filter funnel (por.4), then evaporated to dry under vacuum at 40°C and re-diluted with Water in order to be lyophilized. The yield of the *Cr. sativus* extract was 17.5 g (~58.4% of 30 g starting material). The whole procedure was performed four times, in order to produce the necessary amount of *Cr. sativus* extract for all the following experiments. The yield of the second extraction was 16.5 g (~54.9% of 30 g starting material), the third extraction produced 17.0 g (~56.8% of 30 g starting material) while the yield of the fourth extraction was 22.2 g (~55.4% of 40 g starting material). Consequently, the total amount of produced saffron extract was ~73.2 g.

2.3.4 CPC separation procedure

2.3.4.1 Determination of partition coefficients

The suitability of biphasic systems was first evaluated by Thin Layer Chromatography (TLC) (Figure 13) and then the solvent systems were further analyzed by High-performance liquid chromatography (HPLC) in order to calculate the partition coefficient values (K_D). The procedure was as follow: an aliquot of

saffron extract (10 mg) was weighed into a 20 mL glass tube, 4 mL of each phase of the pre-equilibrated biphasic solvent systems were added to the sample and shaken vigorously. After equilibration of the two phases (t<1 min), 1 mL of each layer was taken out and evaporated to dry. The residues were diluted in 1 mL of methanol, filtered on Nylon 0.45 mm and analyzed by HPLC-DAD. (Figure 14)

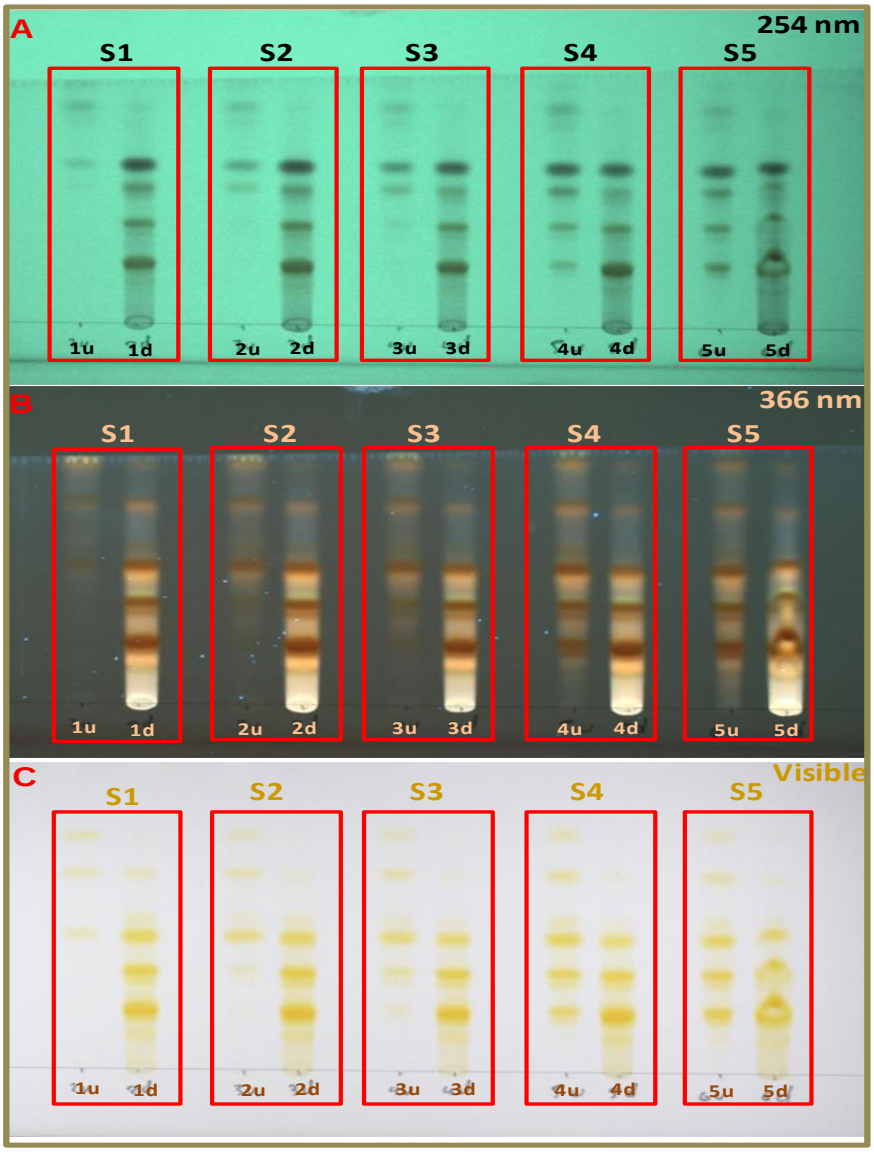

Figure 13: Monitoring of saffron extract compounds' partition in the five suggested Biphasic Solvent Systems (S1, S2, S3, S4 and S5) by reversed phase TLC analysis (ACN/H_2O 8/2 v/v) at (A) 254 nm, (B) 366 nm and (C) Visible. Upper phase of each solvent system is depicted on the left and lower phase is on the right of each red rectangle.

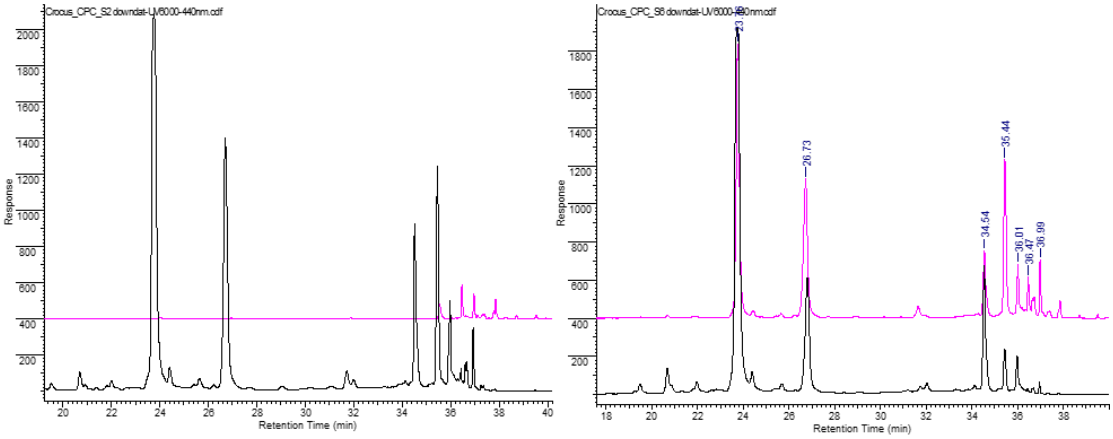

Figure 14: Representative HPLC chromatograms of the saffron compounds' partition in the solvent system 1 (which has an unpolar upper phase) and the solvent system 5 (which has a polar upper phase). Regarding Solvent System 1, almost all compounds have been retained by the polar lower phase whereas the far more polar upper phase of Solvent System 5, has managed to extract the majority of the extracts' compounds

K values ware expressed as the ratio between the peak area of each compound of interest in the stationary phase and the peak area in the mobile phase. The K value of the target compounds in all biphasic systems are demonstrated in Table 1.

SYSTEM/ COMPOUND	TC4	TC3	CC4	TC2	CC3
S1	309	248.10	212.4	11.29	43.7
S2	120.77	12.61	70.4	1.09	5.37
S3	20.62	3.91	11.99	0.20	2.04
S4	4.28	1.20	3.45	-0.67	0.59
S5	1.29	0.21	1.04	-1.26	-0.13

Table 1: Calculation of partition coefficients K_D for each analyte separately. Estimation of the appropriate elution solvent system for each analyte.

2.3.4.2 Semi−Preparative CPC analysis

The CPC experiments were carried out in step-gradient mode by using a series of five biphasic solvent systems consisting of n-heptane−ethyl acetate−butanol−ethanol−water in ratios: 4:10:0:4:10 (S1), 1:13:0:4:10 (S2), 1:12:1:4:10 (S3), 1:10:3:4:10 (S4), 1:7:6:4:10 (S5). Initially the column was filled with the stationary phase by pumping the lower phase of S1 at a flow−rate of 10 mL/min and setting the rotation speed at 200 rpm. Then the rotation speed of the column was increased to 1000 rpm and the upper phase of the S1 was pumped in, at a flow rate of 6.5 mL/min in ascending mode in order to equilibrate the two phases into the column. After the system equilibration, the retention volume of the stationary phase into the column was calculated at 130 mL giving a high S_f value of 65%.

In this experiment, 500 mg of the saffron's extract, diluted in a mixture of 7 mL of lower phase and 3 mL of upper phase of S1, were injected into the column via a 10 mL injection loop. The fractionation was achieved by pumping successively the upper phases of the five biphasic systems (S1 to S5) in ascending mode and completed by passing the lower phase of S5 in descending mode (dual-mode). The volumes of mobile phases used for the experiment are presented in Table 2. The flow rate and rotation speed were set at 6.5 mL/min and 1000 rpm respectively during the fractionation, while the automatic fraction collector was programmed to collect fractions every 93 sec. The total analysis time was 200 min and finally 125 fractions of 10 mL were collected.

2.3.4.3 Preparative CPC analysis

2.3.4.3.1 Dual mode

The semi preparative method was scaled−up to the preparative mode with 1000 mL rotary column adjusting all the experimental parameters to the larger scale. After filling the column with the stationary phase (lower phase of S1) at 200 rpm with a flow rate of 20 mL/min, the rotation speed was increased to 850 rpm and the upper phase of the same system was pumped at 20 mL/min in ascending mode in order to equilibrate the biphasic system into the column (S_f was calculated at 76 %). Then, ~7 g of the extract were diluted in a mixture of the two phases of S1 (ratio 7/3 lower phase/ upper phase) and were injected into the column via a 30 mL injection loop. The fractionation was performed employing the same method (step gradient elution in dual-mode process) and the corresponding mobile phases

(higher volume) as in the semi-preparative CPC experiment. The volumes of mobile phases used for the preparative dual-mode fractionation are presented in Table 2. Fractions of 20 mL/min were collected every minute as soon as an intense yellow color is noticed in the elution tube. The total analysis time was 270 min and finally 250 fractions of 20 mL were collected.

2.3.4.3.2 Elution−Extrusion mode

The preparative CPC fractionation of saffron extract was repeated by using step-gradient elution-extrusion mode instead of step-gradient dual mode experiment. The experiment started by filling the column with the lower phase of the system S1 and equilibration of the two phases was achieved by pumping the upper phase of S1 in the same conditions as in preparative dual mode procedure. After injecting ~9 g of saffron extract, the elution step of the experiment was achieved by pumping successively the five mobile phases in the same volumes as in the previously described dual mode preparative model (Table 2). The last step of the procedure was the extrusion of the column content by pumping the lower phase of the S5 in ascending mode. The flow rate and rotation speed were set at 20 mL/min and 850 rpm respectively during the whole experimental procedure while, the automatic fraction collector was set to collect fractions every 1 min resulting totally in 250 fractions of 20 mL.

2.3.4.3.3 Targeted Preparative CPC analysis

The experimental parameters were modified in order to achieve targeted isolation of TC4 in short time and with less solvent consumption. The experiment was performed in preparative CPC column with a step-gradient elution-extrusion method by using a series of two biphasic systems (S4 to S5) instead of five that have been employed in the previous experiments. Initially, the column was filled with the stationary phase (lower phase of S4, at 200 rpm and 30 mL/min) followed by pumping the upper phase of the same system at 850 rpm and 20 mL/min in ascending mode until the equilibrium of the two phases into the column was reached. Then ~8 gr of saffron extract (diluted in a mixture of 7/3 lower to upper phase of S4) was injected via a 30 mL injection loop. The elution step of the experiment was achieved by passing 1500 mL of upper phase of S4 followed by 1000 mL of the upper phase of S5 (Table 2). The last step of the procedure, was the extrusion of the column content by inserting 1000 mL of the lower phase of S5

in ascending mode at the same flow rate and rotation speed (20 mL/min and 850 rpm respectively. The fractionation lasted approximately 3 h and 150 fractions (20 mL) were collected in total.

Experiment	Volume of Mobile Phase (mL)						
	1 Upper phase	**2** Upper phase	**3** Upper phase	**4** Upper phase	**5** Upper phase	**5** Lower phase	
semi-prep CPC	200	200	300	200	200	200	Dual mode
	ascending					descending	
prep CPC	800	800	1200	800	800	1000	Dual mode
	ascending					descending	
prep CPC	800	800	1200	800	800	1000	Elution-Extrusion
	ascending					ascending	
Targeted prep CPC				1500	1000	1000	Elution-Extrusion
	ascending					ascending	

Table 2: Volume of mobile phases and analysis mode of the four step gradient CPC experiments. (Solvent systems: nHept−EtOAc−BuOH−EtOH−H_2O in ratios: 4:10:0:4:10 (S1), 1:13:0:4:10 (S2), 1:12:1:4:10 (S3), 1:10:3:4:10 (S4), 1:7:6:4:10 (S5))

2.3.5 TLC, HPLC-DAD and NMR analysis

Saffron's partition and CPC fractionations were monitored by TLC, using a solvent system consisting of Acetonitrile (ACN) and Water (H_2O). TLC plates (Silica gel 60 F_{254}, Merck) were developed with ACN−H_2O in ratio 75:25 (v/v) and then sprayed with cold vanillin stain (vanillin is dissolved in methanol together with conc. H_2SO_4) following heating the plate with hot air in order to visualize the spots. HPLC was used for the qualitative analysis of saffron extract, CPC fractions and pure compounds as well as the determination of partition coefficient. The analyses were conducted using a Spectra SYSTEM apparatus (ThermoFinnigan, San Jose, CA, USA) with a Rheodyne 7125 injector (Rheodyne, Ronhert Park, CA, USA) fitted with a 20-μL loop, equipped with a photo-diode array and operated with ChromQuest 4.1 software. For the separation of the compounds, a Discovery SUPELCO Analytical HS C-18 column (250 × 4.6 mm, 5 μm particle size) was used. Samples of 1 mg/mL (1:1 v/v MeOH:H_2O) of the dried extract were prepared and

then analyzed. Prior to the analysis, the samples were filtered through a nylon acrodisc filter (0.45 μm; Whattman-Merck, Darmstadt, Germany). The analyses were carried out employing a binary mobile phase gradient with a flow rate of 1 mL/min. Solvent A consisted of aqueous TFA (0.05%, v/v) and solvent B consisted of acetonitrile (with 0.05% TFA) HPLC grade (Fisher Scientific, Loughborough, UK). The deionized water was purified by a WaterPro PS system (Labconco, Kansas City, MO, USA). The gradient method used for the profiling initially started with 10% B which was kept for 2.5 min. For the next 18.5 min the percentage of solvent B was increased linearly to 27% and then was maintained isocratically for 4 min. It was then increased to 40% B in 7 min and to 100% in 2.5 min, and then maintained at 100% for 2 min. Finally, the percentage of B was decreased back to initial conditions (10%) in 0.5 min and kept for 5 more min for the system equilibration. The detection wavelengths were set at 254, 308 and 440 nm.

Regarding the NMR analysis, all the obtained CPC fractions as well as the pure compounds were analyzed in a Bruker Avance AVIII-600 spectrometer, by using standard Bruker pulse programs in order to elucidate the structures of the isolated compounds as well as their purity.

2.4 RESULTS AND DISCUSSION

2.4.1 CPC fractionation of saffron extract and recovery of high added value compounds

2.4.1.1 Selection of CPC method, solvent systems and determination of partition coefficients

Saffron extract obtained from the extraction of *Cr. sativus* stigmas is a complex mixture of secondary metabolites with a broad range of polarity such as simple compounds (picrocrocin, safranal etc.), *cis* and *trans* crocins, crocetin and phenolic compounds. TC4 is the most abundant constituent of Saffron's stigmas' extract although usually it is commercially found with impurities or in a mixture with other major or minor crocins. The most common protocols that have been published so far for the isolation of TC4 and other crocins include HPLC, MPLC, prepTLC, Molecularly imprinted polymer solid−phase extraction [186], crystallization method [187] and extraction with different solvents (water, methanol, ethyl acetate) from *Gardenia jasminoides* (Rubiaceae), a plant that also contains TC4 [188]. CRC on the other hand is difficult to be obtained by the above mentioned procedures, thus it is mainly produced by hydrolysis of crocins (acidic and/ or alkaline).[189][190] However all the developed processes present some limitation because either they produce mixtures that require many further steps of purification, or the production is in analytical till semi preparative grade.

Separation of crocins either from saffron or from the fruits of *Gardenia jasminoides* with MLCCC systems [191], [192] or HSCCC systems have also been reported in the literature [193][194][195]. There are two major reports for the separation of crocins on CPC systems using single elution methods leading to the isoltation of only the major compounds. In the first method, only the major crocin (*trans*-crocin-4) was isolated [194] whereas the second one, allowed the isolation of three major crocins (*trans*-crocin-4, *trans*-crocin-3, *trans*-crocin-2) and picrocrocin [196]. In the present work, the goal is not only to isolate the major crocins, but also the minor ones and the other ''valuable'' compounds of the extract. Due to the complexity of saffron extract, this dual aim is difficult to be achieved by using a single step CPC process. On the other hand, gradient CPC elution has been mentioned as "method-of-choice" for the analysis of complex mixtures offering an efficient fractionation of the analyzed extract and facilitating the isolation of the sum of constituents in a more effective manner. This method has been successfully applied to numerous cases for the direct separation of compounds with wide range

of polarities from complex mixtures [197]–[199]. Therefore, a fast, specific and selective CPC method was developed by using five sets of biphasic solvent systems composed of n-heptane, ethyl acetate, butanol, ethanol and water in a step-gradient elution mode. (Table 2)

The distribution of the target compounds in all selected biphasic systems was measured by HPLC-DAD. The study of K_D values led to the conclusion that the chosen systems enabled a selective elution of the different compounds according to their hydrophobicity and partition coefficient. Moreover, the measurement of separation factor α of the target compounds showed that there is at least one biphasic system enabling the efficient separation of each compound of interest (α>1.5). As given in Table 2, the fractionations were performed using as stationary phase the aqueous phase of S1 and as mobile phase the organic phases of the biphasic solvent systems in step-gradient elution. The experiments completed by pumping the aqueous phase of S5 either in descending (dual-mode) or ascending mode (elution-extrusion).

2.4.1.2 Fractionation of saffron extract by dual mode and elution-extrusion CPC experiments

The capability of the selected biphasic systems to effectively fractionate the saffron extract was initially tested in semi preparative column. After filling the column with the aqueous phase of biphasic system 1 (stationary phase) and equilibrium of the two phases into the column, 500 mg of the saffron's extract were injected via a 10 mL injection loop. The step gradient elution included the successive pumping of the five mobile phases (upper phases of systems S1 to S5). The dual mode experiment was completed by pumping the lower phase of S5 in descending mode (see experimental part). The total process duration was 200 min while the separation process was monitored by UV at 440 nm. (Figure 15) All resulting fractions (125 fractions of 10 mL) were evaluated using TLC. The obtained result regarding the step-gradient dual mode analysis was very promising thus separation was scaled-up to preparative CPC mode. Reports about scalability of countercurrent chromatography methods demonstrate that scaling-up can be easily and successfully applied for the preparative purification of natural compounds. [200][201][202] The total volume of the preparative CPC column is 5-fold larger than the semi-preparative one. To keep a high "g" field and a good resolution, the rotational speed of the preparative centrifuge was set at 850 rpm while the flow-rate

of the mobile phases was fixed at 20 mL/min. Under these conditions, the retention factor of stationary phase (S_f) was approx. 75% in contrast with the semi−preparative CPC where the S_f was calculated at 65%. The assay was conducted on ~7 g of saffron extract and the compounds of interest were separated according to their K_D values in the biphasic systems used for the step gradient analysis. After the completion of elution step and elution of all possible compounds, the pumping direction of the mobile phase switched from ascending to descending mode so the compounds having strong affinity to the stationary phase could also be recovered. The above described experimental procedure was continuously monitored with a UV detector and the chromatogram (at *λ*=440 nm) is presented in Figure 15.

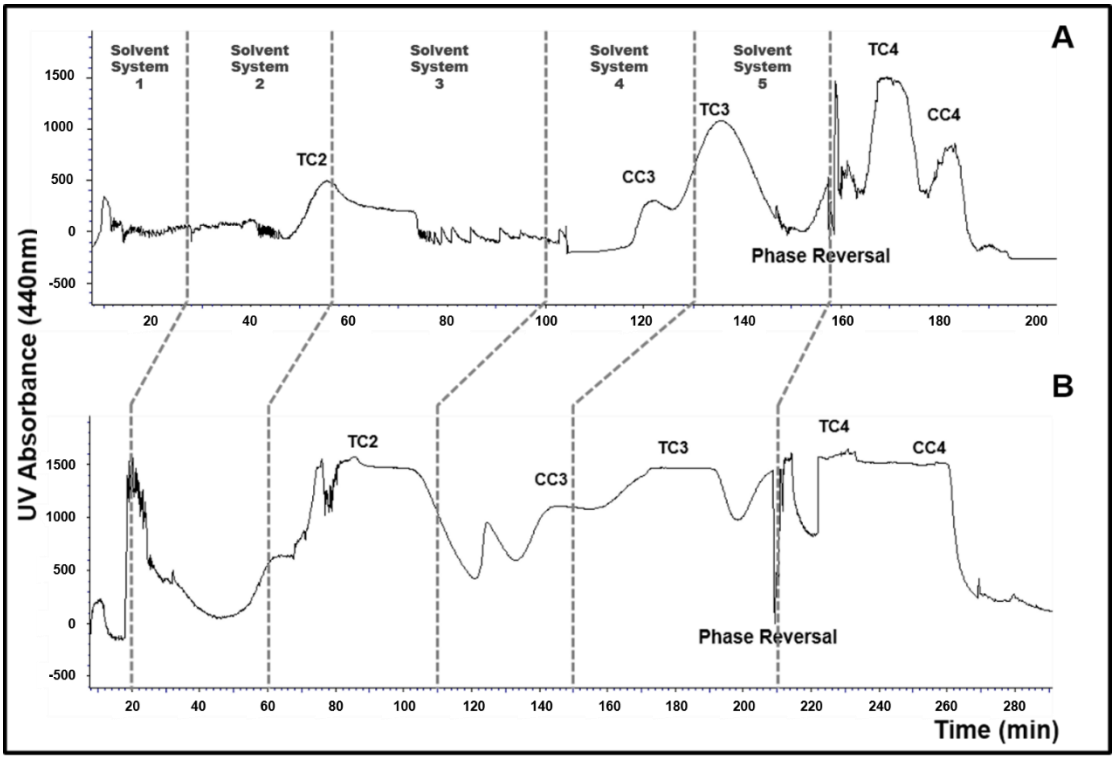

Figure 15: UV Chromatogram of semi prep CPC in comparison to prep CPC, indicating the high repeatability of the scaling up from semi preparative to preparative mode in accordance with the substances‘ elution. (λ=440 nm) (A) Semi-preparative CPC, dual mode, first mobile phase-upper phase, (B) Preparative CPC dual mode, first mobile phase-upper phase.

The fraction collector was set to collect 20 ml fractions during the experiment resulting in total 250 fractions 200 of which were collected in ascending mode (step-gradient elution part of the experiment) and 50 in descending mode (dual mode CPC). (Figure 16) All fractions were analyzed by TLC and pooled, based on chemical composition similarity, resulting in 34 combined fractions. The analysis of combined CPC fractions with HPLC-DAD, LC-HRMS and NMR resulted in the isolation and characterization of 15 saffron's constituents which are chemically categorized to crocins, crocetin, picrocrocin, flavonoids and phenolic compounds. (Figure 12)

In more details, the analysis of fractions collected during the elution step led to the identification of **(1)** crocetin (fr. 12-16), **(11)** 4-hydroxy-2,6,6-trimethyl-1-cyclohexene-1-carboxaldehyde (fr. 17-29), **(14)** 4- hydroxydihydrofuran-2-one (fr. 30-35), **(2)** *trans*-crocin 1 (fr. 45-52), **(4)** *cis*-crocin 2 (fr. 59-65), **(3)** *trans*-crocin 2 (fr. 66-83), **(15)** 2-phenylethanol glucoside (fr. 84-97), **(10)** picrocrocin (fr. 110-118), **(12)** 5-hydroxymethyl-4,4,6-trimethyl-7-oxabicyclo[4.1.0] heptan-2-one O-β-D-glucopyranoside (fr. 119-128), **(13)** kaempferol-3-sophorosides (fr. 129-139), **(6)** *cis*-crocin 3 (fr. 155-159) and **(5)** *trans*-crocin 3 (fr. 177 183). It is noticeable that three of the major compounds of saffron extract, TC2, TC3 and picrocrocin were isolated in purity higher than >90% (based on HPLC-DAD and NMR analysis) and in an one-step separation procedure. (Figure 17)

Figure 16: CPC fractions from semi-prep CPC (up) and prep-CPC (down) indicating the power of CPC technique to efficiently separate, enrich and purify complex mixtures of natural compounds

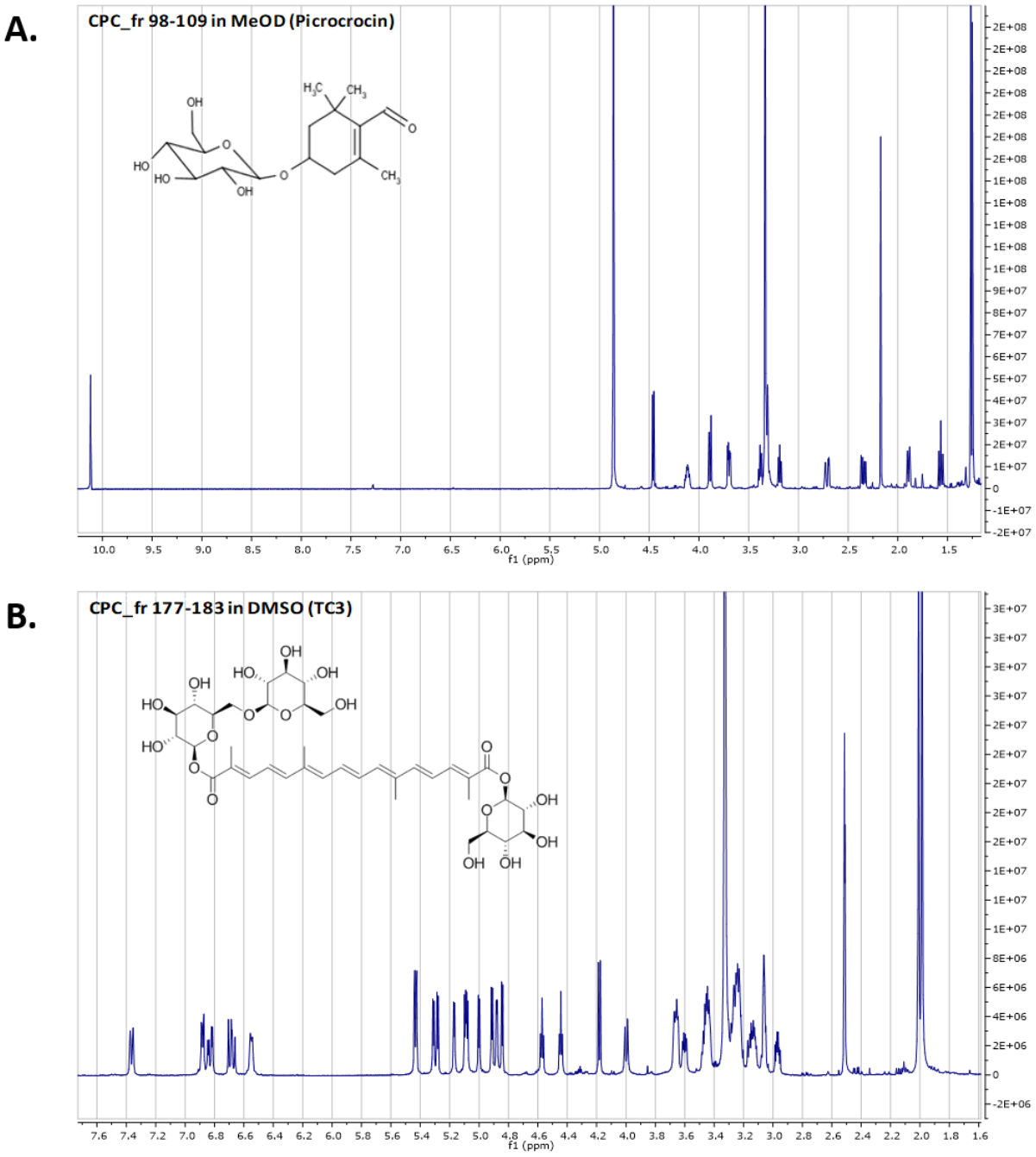

Figure 17: ^{1}H-NMR spectrum of A. CPC fraction 98-109 in MeOD including picrocrocin and B. CPC fraction 177-183 in DMSO including *trans*-crocin 3 both of them in pure form. The results are based on correlation between the obtained spectra with those described in the literature.

Interestingly, the main compound of interest, TC4, was unable to be recovered during the elution step due to its high polarity. Nevertheless, TC4 was fully eluted after switching the pumping direction to descending mode and was collected in fractions 206-215. (Figure 18) In the same mode two more crocins, **(9)** *trans*-crocin 5 (fr. 200-203) and **(8)** *cis*-crocin 4 (fr. 222-227), were also collected. TLC and NMR analysis thereof revealed the presence of an important amount of unconjugated sugars, thus reducing the purity of the isolated compounds. (Figure 18) This is due to the complete distribution of the free sugars in the aqueous stationary phase and their elution right after switching to descending mode, thus contaminating the targeted polar crocins of saffron extract. This fact necessitated further purification of TC5 and TC4 fractions with other chromatographic techniques and rendered the employed dual-mode CPC method inappropriate for the one-step isolation of those compounds.

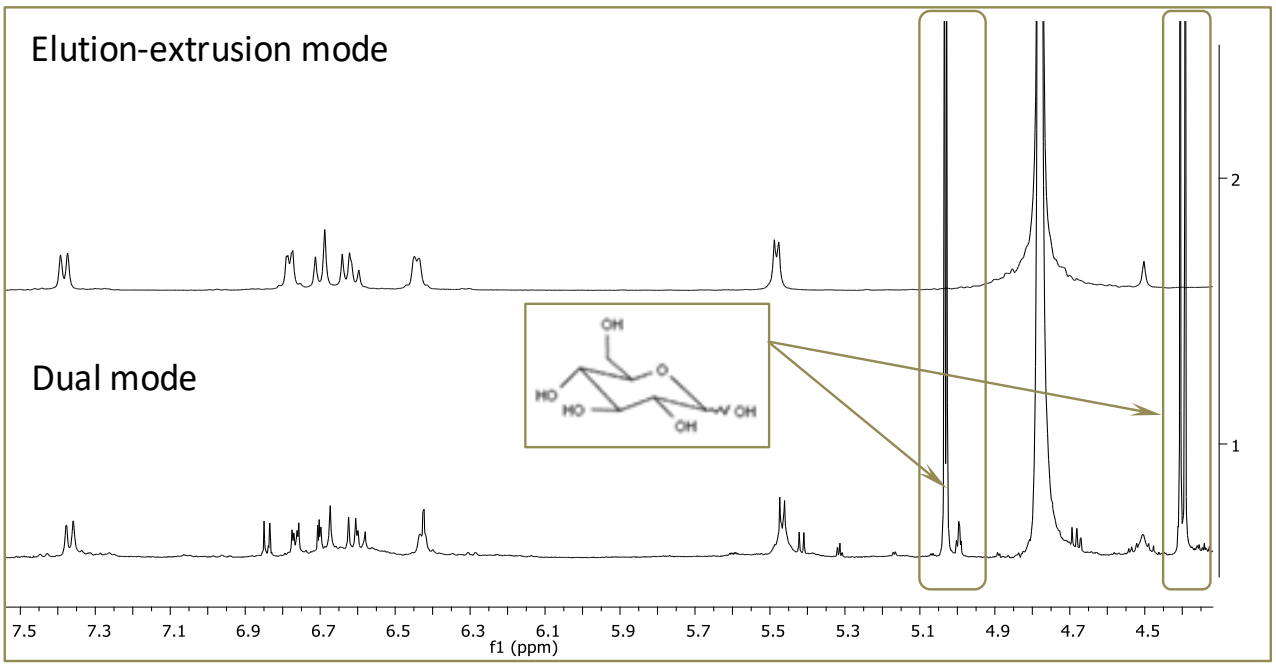

Figure 18: Correlation between NMR spectra of TC4 from elution-extrusion CPC and TC4 from dual mode CPC showing the existence of free D-glucose as a result of the analytical procedure

2.4.1.3 Fractionation of saffron extract by step-gradient elution-extrusion CPC experiment

In order to avoid the co-elution of impurities in TC4 fractions, the CPC experiment was repeated in step-gradient elution-extrusion mode. The difference between the two isolation procedures is that in elution−extrusion mode, when the run reaches a certain point, instead of switching from ascending to descending mode using the lower phase as mobile phase, the stationary phase (lower phase) is pumped in the instrument as the new mobile phase without changing flow direction.

In the preparative step-gradient elution−extrusion CPC experiment, ~9 g of the saffron's extract were fractionated. The total analysis time was 270 min and finally 250 fractions of 20 mL were collected. The introduction of the last solvent system's upper phase, followed the last solvent system's lower phase leading to the full elution of TC4 at 210−230 min. The TLC and NMR analysis of the corresponding fractions revealed that TC4 was eluted as pure compound, as all the free sugars were retained by the column due to their higher polarity than TC4. It is worth noting that pure TC4 obtained from the above process was found to be 920 mg representing almost the 10% of the extract.

Given that both methods offered an excellent fractionation of metabolites during the elution step, the conclusion was that the elution-extrusion mode is considered prior separation method compared to dual-mode due to the production of more pure compounds in the same experimental time and with equal solvent consumption.

Beyond the recovery of TC4 in pure form, the CPC fractionation led also to the isolation of the other saffron's constituents such as the other crocins, CRC, picrocrocin, flavonoids and phenolic compounds. (Figure 12) All fractions obtained from elution-extrusion CPC experiment (240 fractions) were analyzed by TLC and pooled, based on chemical composition similarity, leading to 35 combined fractions. Further analysis of the combined fractions with HPLC, LC-HRMS and NMR revealed an excellent fractionation of the total-amount of metabolites. As it is well demonstrated in Figure 19 and Figure 20, the CPC fractionation resulted in the isolation of many other compounds of saffron extract beyond TC4 and the majority of them was in pure form requiring no further purification procedures.

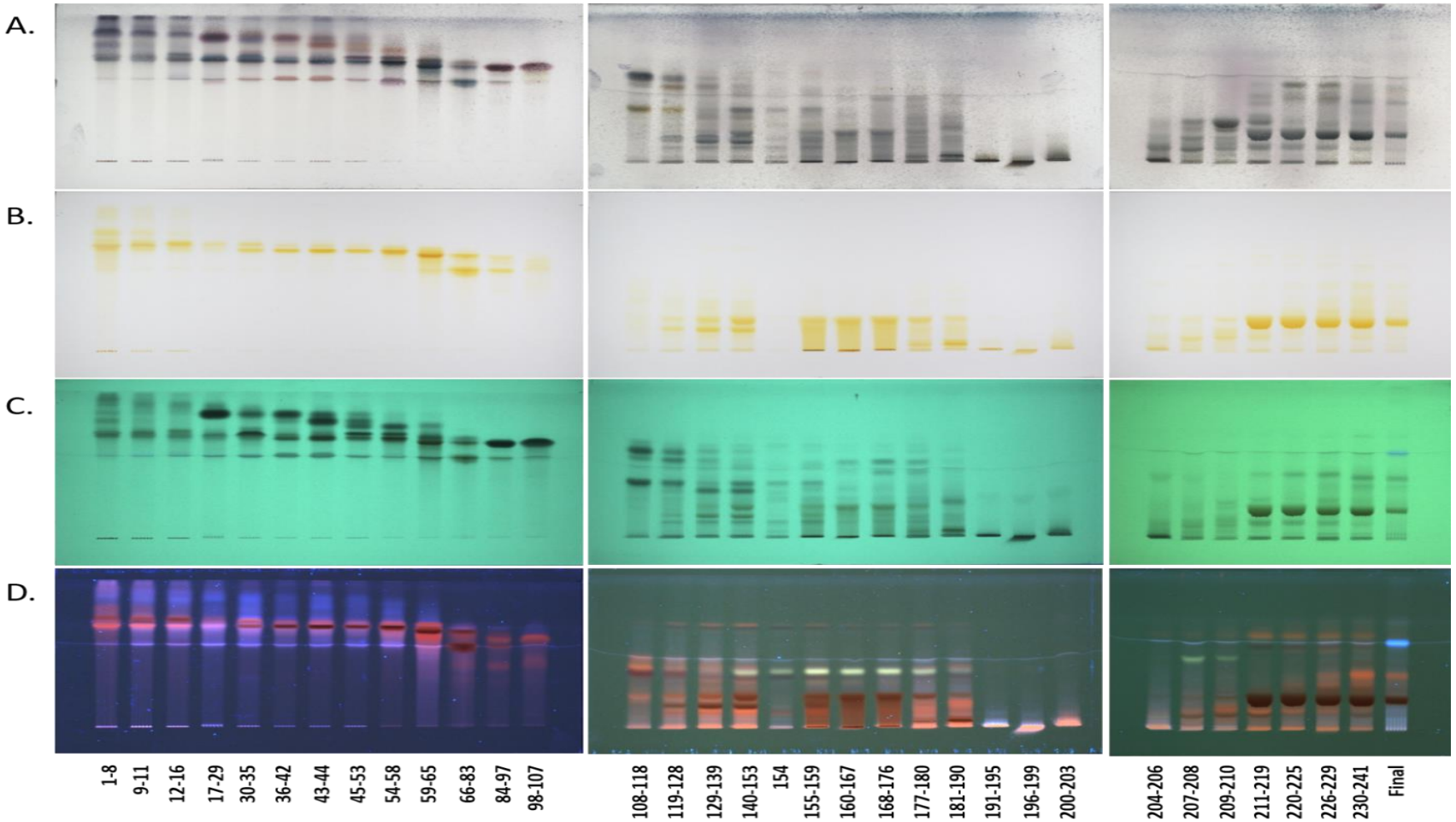

Figure 19: TLCs of all the fractions occurring from the preparative CPC procedure demonstrating the power of this analytical technique in analyzing complex mixtures and extracts. A. Visible observation in day-light after spraying with vanillin-H_2SO_4 reagent; B. Observation in day-light; C. λ=254 nm and D. λ=365 nm

Nº	Isolated Compound	Rt (min)
1	Crocetin	37.66
2	Hydroxysafranal **(11)**	21.5
3	*trans* -crocin 1	36.26
4	*cis* -crocin 2	36.57
5	*trans* -crocin 2	34.74
6	2-phenylethanol glucoside **(15)**	*no abs*
7	4-hydroxydihydrofuran-2-one **(14)**	*no abs*
8	Picrocrocin **(10)**	14.5
9	kaempferol 3-sophorosides **(13)**	15.97
10	5-hydroxymethyl-4,4,6-trimethyl-7-oxabicyclo[4.1.0]heptan-2-one O-β-d-glucopyranoside **(12)**	*no abs*
11	*cis* -crocin 3	35.76
12	*trans* -crocin 3	25.8
13	*trans* -crocin 4	22.8
14	*cis* -crocin 4	33.84

Fractions (No)	**12**	**17**	**54**	**59**	**66**	**84**	**98**	**110**	**119**	**129**	**154**	**155**	**168**	**177**	**184**	**206**	**210**	**222**
	16	29	58	65	83	97	109	118	128	139		159	176	183	190	209	215	227

Figure 20: The power of CPC in isolating the compounds of interest in pure form or in mixtures of two or maximum three compounds that require only one further step of purification.

2.4.2 Purification of isolated compounds from dual mode and elution-extrusion CPC

2.4.2.1 Recovery of Pure TC4 from the dual mode CPC-Generated Fractions

As mentioned above, during the dual mode CPC, TC4 was co-eluted with unconjugated sugars, a fact that led to the production of TC4 with reduced purity. This was an undesired side effect of the experimental procedure and resulted from the fact that the flow direction was altered from ascending to descending mode. As a result, despite the fact that the sugars could probably have been separated from the TC4 inside the CPC column during the ascending mode, the flow reversal from ascending to descending mode, resulted in the remixing of the compounds. Consequently, a further purification procedure in order to obtain TC4 in a pure form was indispensable. The method of choice in order to separate TC4 from unconjugated sugars was size exclusion chromatography. This technique is used in order to separate low and high molecular weight molecules. Since TC4 and free glucose are quite different compounds regarding their molecular weight, size partition chromatography was selected as a potentially effective purification technique. As a result, fractions of CPC containing TC4 and sugars (100-300 mg each) were further purified by column chromatography (diameter 1.2 cm, height 30 cm) on Sephadex® LH-20, (Sigma-Aldrich Chemie GmbH, Taufkirchen, 10 mm × 285 mm) using MeOH/H_2O (90:10) as mobile phase and 80 fractions of 1 mL were collected. All fractions were then analyzed with TLC and those of similar chemical content were combined. TLC plates (Silica gel 60 F_{254}, Merck) were developed with ACN−H_2O in ratio 80:20 (v/v) and then sprayed with cold vanillin stain (vanillin is dissolved in methanol together with conc. H_2SO_4) following heating the plate with hot air in order to visualize the spots. The above described procedure was repeated ten (10) times leading to the production of 718 mg of TC4 (purity>95%) in total. The purity of the isolated compound was determined by HPLC−DAD and ^{1}H-NMR analysis.

2.4.2.2 Isolation and purification of *trans*-crocin 2 (TC2)

Trans-crocin 2 (TC2) is another valuable crocin included in saffron stigmas extract. This high-added value compound was isolated from all the CPC experiments in both dual mode and elution-extrusion mode. According to the K_D of TC2, as it was expected to be eluted while Solvent System 2 was inside the column.

However, TC2 was isolated as a mixture with other compounds in ratio ~ 90/10. As a result, a further purification step was definitely required in order to utilize TC2 in upcoming experiments. For this reason, after performing a number of attempts to separate TC2 from the impurities (e.g. preparative TLC, Sephadex® LH-20) that proved to be unsuccessful, semi-preparative HPLC was selected as the most suitable technique for the purification of TC2. In more details, 10 mg/mL of dry CPC fraction containing TC2 in 1:1 MeOH:H_2O (v/v) were analyzed with Spectra System apparatus and a DAD detector on a Sigma-Aldrich Supelcosil RP−C18 column (25 × 10mm, 5 μm). A linear gradient of water (Solvent A) and ACN (Solvent B) was employed for the separation of the compounds with a flow rate of 4 mL/min. The initial conditions of the method were 10% B, then increased linearly to 27% for the next 8 min; increased to 40% B for 4 min; then increased to 70% B for 2 min and was kept there isocratically for additional 3 min; then increased linearly to 75% B for 6 min, afterwards linearly to 80% B for 2 min and finally to 90% B for 3 min. At last the system returned to initial conditions and was kept there for 10 min. The detection wavelength was set to 440 nm for TC2 and 250nm for all the impurities. Individual fractions were collected manually after close observation of the chromatogram. Furthermore, TC2 bears an intense yellow color, easily noticeable, that allows the accurate collection of the fraction containing this compound at the exact time of elution. The purity was found to be > 98% verified by HPLC‑DAD and ^{1}H-NMR [Avance AVIII-600 spectrometer (Bruker, Karlsruhe, Germany)] experiments.

2.4.3 Targeted isolation of TC4

As already mentioned, *trans*−crocin 4 is a compound of high interest due to its' promising pharmacological properties. In order to investigate TC4 thoroughly *in vitro* as well as in preclinical and clinical pharmacokinetic trials, a quick and effective isolation protocol is necessary in order to isolate TC4 in large quantities with no need of further purification. Based on the K_D study of the target compounds in the five biphasic systems (Table 1) and considering our previous results, the experimental approach was further optimized. Effort was also given towards a more "green" methodology i.e. short time and less solvent consumption.

In details, the step-gradient elution-extrusion experiment was repeated by choosing a more polar solvent system (S4) as the initial one. As a result, all the compounds with low K values were co−eluted in a mixture during the first (S4 upper phase) and second (S5 upper phase) mobile phase pumping (elution step of the

experiment). According to previous experiments, TC4 was expected to be eluted by the lower phase of the last system during the extrusion step of the experiment. Thus, after starting the extrusion of the column, all the out−coming fractions were separately collected. The following TLC and HPLC-DAD analysis of all the fractions demonstrated that the recovered TC4 was of equal purity to TC4 from elution–extrusion mode. These results denote the efficacy of TC4 targeted isolation method in isolating compounds of interest in a more effective way with reduced experimental time and solvents' consumption.

2.4.4 Overall assessment of CPC experiments

The current study was designed in order to fulfil two interrelated core goals. The first priority was to isolate the main crocin (*trans*-crocin-4, TC4) from the methanol/aqueous extract of saffron stigmas in order to be utilized in consequent animal experiments that would take place in the next steps of this study. As a result, TC4 ought to be isolated in the purest possible form. Consequently, the second essential goal of the study was to optimize the experimental conditions in order to obtain TC4 in pure condition avoiding any further purification procedure. Taking into consideration the large amount of TC4 that was required for the upcoming experiments as well as the experimental cost (e.g. solvent consumption) there was a vast necessity to develop an isolation method capable of accomplishing both goals. However, with commitment to the necessary prerequisite that the so far discussed methodologies could be adopted by the pharmaceutical and natural products industries in a scaled-up level, but at the same time could lead to the production of as many pure compounds as possible, the developed methodologies offer the ability to directly identify and isolate up to 15 secondary metabolites by an optimized experimental procedure. Regarding the complete analysis of saffron stigmas extract with CPC, as it is clearly depicted in Table 3, 70.8 g of saffron extract were analyzed with step-gradient CPC employing three different experimental procedures (10 CPC experiments including: dual mode CPC, elution-extrusion CPC and a targeted approach) resulting in the production of 6.19 g of pure TC4, a quantity that has never been isolated so far and especially from saffron.

FCPC Mode		Saffron extract (g)	TC4 isolated (mg)	Comments
FCPC 1	Dual mode	5.7	718	Further purification of the initial FCPC fractions containing TC4 with Sephadex® LH 20 was required 
FCPC 2	Dual mode	6.5		
FCPC 3	Elution-Extrusion	3	296	Direct isolation of pure TC4 in one step
FCPC 4	Elution-Extrusion	8.6	805	
FCPC 5	Elution-Extrusion	5	567	
FCPC 6	Elution-Extrusion	9.9	918	
FCPC 7	Elution-Extrusion	7.7	733	
FCPC 8	Elution-Extrusion	8.2	758	
FCPC 9	Targeted	8.2	757	
FCPC 10	Targeted	8	633	
Total amount of analyzed saffron extract (g)		Total amount of pure TC4 isolated with FCPC (mg)		
70.8		6185		

Table 3: Overall assessment of the CPC experiments regarding TC4 isolation.

2.5 CONCLUSION

Saffron extract is an important source of natural bioactive compounds with many potential beneficial pharmacological properties. Hence, there is a strong need for a rapid and effective isolation procedure in order to produce TC4 of high purity and quality to support the commercial availability. As TC4 is a compound with many important pharmacological properties, the hereby described CPC experimental procedure offers the opportunity to obtain the necessary TC4 for all the pharmacokinetic, preclinical and clinical studies with a rapid and effective way. Employing the aforementioned saffron's extract fractionation protocol, it is now possible not only to perform the TC4 isolation but also to afford a complete analysis of the whole extract, leading to the isolation of many other major and minor secondary metabolites of saffron as well, in quite pure condition. The purity of isolated TC4 was particularly high as proven by the HPLC-UV-HRMS method. All the above described results contribute to potential usage of this technique in a more industrial level allowing the production of enriched fractions of TC4 with potential use in either cosmetic or pharmaceutical industries with interest in natural products.

2.6 ACKNOWLEDGEMENTS

We would like to acknowledge Cooperative De Safran (Krokos Kozanis, West Macedonia, Greece) for providing saffron stigmas.

2.7 FUNDING

This research was funded by the TreatAD SYN21-1003 ESPA Grant.

CHAPTER THREE

Development of two rapid and sensitive UPLC-PDA methodologies for the assessment of the bioavailability of *trans*-crocin 4 and crocetin in mice Brain and Plasma after *i.p.* administration.

Evidence of crocin's penetration through the Blood Brain Barrier.

3.1 ABSTRACT

A novel, fit-for-purpose, highly sensitive, analytical UPLC-PDA methodology was developed and fully validated, according to ICH, FDA and EMA guidelines, for the rapid and accurate quantification of *trans*-crocin 4 (TC4) and crocetin (CRC) in mice plasma and brain after *i.p.* administration. A PDA based methodology shows a wider applicability as it is cost effective and can be easily and seamlessly adopted by the pharma industry. The separation of the analytes was performed on a C18 Hypersil Gold column with 2.5 min run time, employing the internal standard (ISTD) methodology. The two methods were successfully applied for the determination of CRC and TC4 in mouse plasma and brain after *i.p* administration of TC4 (50 and 150 mg/kg) in a time range of 0-240 minutes. Due to the selection of *i.p.* administration route, the first-pass metabolism and/or gastric hydrolysis were bypassed, a fact that enhanced the bioavailability of TC4. Furthermore, TC4 was found to be capable of crossing the Blood Brain Barrier (BBB) and build up levels in the mouse brain, regardless of its highly hydrophilic character. CRC was not detected in any plasma or brain sample, although it has been reported that TC4 quickly hydrolyzes to CRC after *p.o.* administration. Therefore *i.p.* administration could be used in the case of TC4 for the accurate determination of its biological role. Overall, the developed methodology offers important information about the bioavailability of TC4 in mouse plasma and for the first time, demonstrates the ability of TC4 to penetrate the BBB and localize inside the brain.

KEYWORDS

UPLC; bioavailability; *trans*-crocin 4; crocetin; mice plasma; mice brain

3.2 INTRODUCTION

Saffron, the dried stigmas of the flower *Crocus sativus* L. is considered to be among the most expensive spices in the world. *Crocus sativus* L., a stemless perennial herb of the Iridaceae family which is native to Greece and Southwest Asia, was first cultivated in Greece for its' red stigmas (style branches). Saffron is mainly used as a traditional herbal medicine but also as a flavoring and food coloring agent in everyday life. Chemical analysis of *Crocus sativus* L. stigmas has shown the presence of a wide variety of different constituents including carotenoids (e.g., a- and b-carotene), mono- and bis-esters of crocetin, picrocrocin and safranal [166]. Picrocrocin, a colorless glycoside, is the *β*−d−glucoside of hydroxysafranal (4−hydroxy−2,6,6−trimethyl −1−cyclohexene−1−carboxaldehyde) and its mainly responsible for saffron's well−known bitterness. Safranal on the other hand, is the principal substance of saffron's aroma. [124] The main bioactive saffron constituents are the crocins, which are mono− and bis−esters of crocetin (apocarotenoid) with glucose, gentiobiose and/or gentiotriose. [174] Depending on the type and amount of sugar(s) conjugated with crocetin as well as the space-configuration, there are many different crocins produced i.e. *cis/trans*−crocin−2 (CC2/TC2), *cis/trans*−crocin−3 (CC3/TC3), *cis/trans*−crocin−4 (CC4/TC4) while TC4 is found to be the most abundant crocin in all saffron species studied so far. [174]

Several studies indicate that saffron's constituents have been proven to be effective against a wide range of common disorders including coronary artery disease [203] [204][205] stomach disorders, hypertension [206], learning and memory impairment [169], dysmenorrhea and premenstrual syndrome (PMS) [207]. Furthermore, saffron or its main constituents have shown remarkable activity against some neurodegenerative diseases that nowadays affect significant percentages of the general population such as Alzheimer's Disease (AD)[208][209][128] , Parkinson's Disease (PD) [172], depression [210] and schizophrenia. [170] Finally, saffron exhibits dose−dependent inhibitory response on breast cancer cells [173]. Due to its plethora of pharmacological properties saffron is not only regarded to be a precious spice but also a highly valuable and health-promoting herb. [168]

TC4 is of raising interest due to its' promising pharmacological properties as well as its' nontoxic character. [211][212] Interestingly *i.p.* administration of crocin up to 3g/kg in mice did not show any mortality after 24 and 48 hrs. Therefore TC4 has been considered to be a practically low-toxic substance. [213] Anti-oxidant and

anti-inflammatory activity of TC4 suggest its therapeutic potential against various nervous system disorders. [169] It has been shown that TC4 enhances the sexual activity of male rats [145], exhibits antidepressant effects in rodents [131], prevents oxidative stress in the hippocampus contributing to the prevention of deficits in spatial learning and memory [214] and also enhances the learning ability and improves memory. [132] However, recent studies have demonstrated that TC4 also possesses anti-AD and anti-PD activity as it has shown significant inhibitory effect on the fibrillation of apo-alpha-lactalbumin (a-alpha-LA), under amyloidogenic conditions [215] and also on beta-amyloid (A*β*) fibrillogenesis. [128] CRC, the main metabolite of TC4, has been shown to inhibit A*β* fibrillization and attributed to the stabilization of A*β* oligomers [216], enhanced the angiogenesis in rats [217] and it is considered to be a potent antitumor agent as it has been shown to act as scavenger of free radicals. [218] Furthermore, CRC has shown neuroprotective effects against brain injuries as it inhibited apoptosis at early stages of the injury as well as promoted the angiogenesis step. [217]

However despite the broad bioactivity of crocins, there are only few studies focused on the pharmacokinetic properties of TC4 and CRC while most of them include plasma and/or urine.[219][220][221][222][223][224] Many of the methods reported in previous studies did not exhibit adequate sensitivity for the quantitation of crocin in biological samples, and only its metabolite, CRC, could be detected and assessed. Despite the fact that LC-MS/MS methodologies developed are slightly more sensitive [223], the incorporation of the PDA detector offers a wider linear range as well as wider laboratory applicability because of its lower cost. Therefore, there is a need to develop low-cost, fast and sensitive methodologies in order to assess the bioavailability of crocin and its metabolites in brain and plasma.

Moreover, several factors contribute to a compound's bioavailability such as the administration route, its lipophilicity, sex, age, genotype, hormonal status etc. of the dosed organism as well as the individuality of each subject etc. [225]–[227]. So far there has been no other study describing the bioavailability of TC4 and CRC after *i.p*. administration in mice plasma, as well as the bioavailability of these compounds in mice brain. Given that saffron extracts have shown neuroprotective effects, it is of a great importance to discover the correlation between plasma and brain circulation levels following TC4 administration. In this study, we describe the development of two fully validated UPLC analytical methodologies for the simultaneous quantification of TC4 and CRC in both mice plasma and brain. This is a rapid, robust and fully automated procedure, with a simple sample pretreatment and a high sample turnover with only 2.5 min run time.

Although there is a more sensitive methodology appearing in the literature [223], the currently developed methodology shows comparably low detection limits (2 vs 10 ng/mL of plasma). Nevertheless, the UPLC-PDA methodology for plasma is fit-for-purpose, as it exhibits a broader linear range (10-6000 ng/mL), whereas the levels determined by the bioavailability study are well higher than the LLOQ. Preliminary pilot studies concerning the concentration levels of TC4 in plasma showed the circulation of relatively high levels (>400 ng/mL in plasma) indicating that a method's sensitivity in the low ng/mL area is not actually required. Furthermore, a PDA based methodology receives wider applicability as it is cost effective and can be easily and seamlessly adopted by the pharma industry. Considering the administration route, an *i.p.* administration methodology has been adopted in order to bypass the first-pass metabolism and/or gastric hydrolysis and gain a more holistic bioavailability profile of the substance (elimination of the liver-induced metabolism as well as exposure of TC4 in the low pH of the stomach).[228] Hence, this study demonstrates for the first time, the absence of hydrolysis of TC4 to CRC in plasma after *i.p.* administration, and provides preliminary evidence on the ability of TC4 to penetrate the Blood Brain Barrier (BBB) and localize inside the brain.

3.3 MATERIALS AND METHODS

3.3.1 Study design

The mice study was conducted under medical supervision at National and Kapodistrian University of Athens Medical School. Fifty-six (56) wild type (C57BL/6J) mice were divided into three groups. The treatment groups were as follow: 21 mice (15 female-6 male) were treated with 50 mg/kg pure TC4 (dissolved in 0.9% aqueous NaCl) through *i.p.* administration; 30 mice (18 female-12 male) were treated with 150 mg/kg pure TC4 (dissolved in 0.9% aqueous NaCl) through *i.p.* administration; 5 mice (3 female-2 male) were used as control animals. Plasma samples of the mice were collected at predefined time points (0, 15, 30, 60, 120 and 240 minutes after administration). The protocol was approved by the ethical committee of the National and Kapodistrian University of Athens and was conducted according to the ICH-GCP guidelines (ICH GCP, 1996). The study received a permit from the Veterinary Directorate of the Prefecture of Athens (Approval #: 478/ 2014) according to the Greek legislation conforming to the 2010/53/ EU Council Directive.

3.3.2 Chemicals and analytical reagents

The analytical reference standard of TC4 was isolated from *Crocus sativus* stigmas following a procedure previously developed and described in our laboratory [229]. Plant material *Cr. sativus* dried stigmas (saffron) was kindly provided by the Cooperative De Safran (Krokos Kozanis, West Macedonia, Greece). The purity of TC4 was found to be more than 95% by HPLC-PDA using the continuous peak purity approach and its structure was verified by ^{1}H Nuclear Magnetic Resonance (NMR) spectroscopy. Crocetin (CRC) was produced after saponification of TC4 with aq. sodium hydroxide (10% w/v) at 60ºC for 4 hr. The solution was then acidified with phosphoric acid and the yielded precipitate was washed with water. CRC was recrystallized from dimethylformamide [168] and its purity was better than 95% (HPLC). The internal standard (ISTD) 4-nitro-aniline (Figure 21) was purchased from Sigma-Aldrich ® (Darmstad, Germany). All solvents were of LC-MS grade. Acetonitrile, methanol and water, were purchased from Avantor ® (Gliwice, Poland) whereas trifluoroacetic acid (TFA) was purchased from Sigma-Aldrich ®. Blank mice serum and brain for the validation of the PK studies were obtained from healthy animals (wild type mice) under written consent.

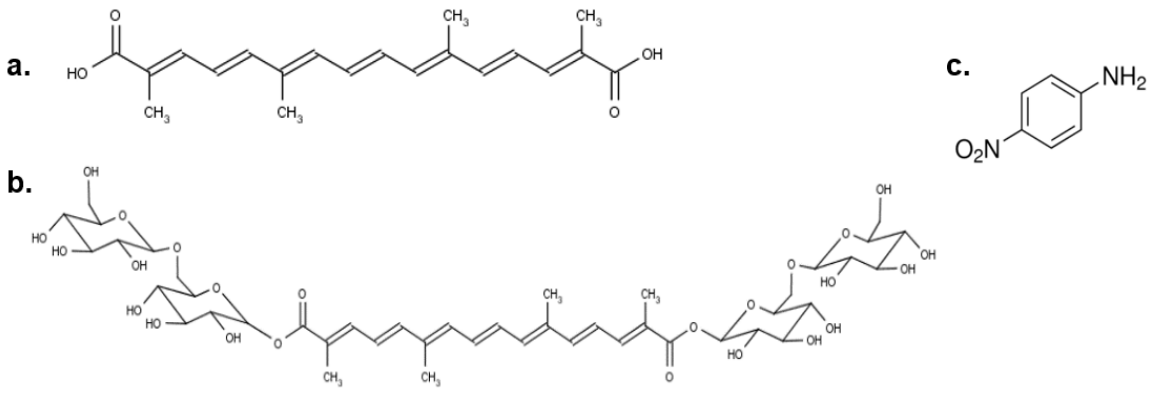

Figure 21: Chemical structures of (a.) crocetin (CRC) (b.) *trans*-crocin 4 (TC4) and (c.) ISTD (4-nitro-aniline)

3.3.3 Stock solutions, calibrators and QCs preparation

Stock solutions of TC4, CRC and ISTD were prepared at a concentration of 1 mg/mL in methanol and stored at dark place at -20 ^{o}C. Working solutions were prepared in a daily basis by diluting appropriate volumes of the stock solutions in methanol in order to achieve the following concentration levels: 100, 10, 1 μg/mL and 100 ng/mL for both TC4 and CRC in the same initial solution and 100 μg/mL for the ISTD. The TC4 and CRC calibration curve in mouse plasma was constructed in the dynamic range of 10-6000 ng/mL (10, 25, 50, 100, 250, 500, 1000, 2000, 4000, 6000 ng/mL) while the concentration of the ISTD was kept at 100 μg/mL. In order to proceed to the validation of the described methodology, a different set of solutions were used as Quality Control (QC) samples in concentrations 30, 80, 3000, 4600 ng/mL (LQC1, LQC2, MQC and HQC respectively). For the construction of the calibration curve in mice brain the dynamic range was set from 0.05-5 ng/mg (0.05, 0.125, 0.25, 0.5, 1.25, 2.5, 4, 5 ng/mg) while the concentration of the ISTD was also kept at 100 μg/mL. The concentrations of the QC samples were 0.2, 0.35, 3, 3.5 ng/mg (LQC1, LQC2, MQC and HQC respectively).

3.3.4 Instrumentation

For the quantitation study, UPLC-PDA analysis was performed on an ACQUITY UPLC ® System. The core system comprises of a Binary Solvent Manager, a Sample Manager with an integral Column Heater and a PDA Detector

(180-550 nm). Centrifugation of the serum samples was performed in a Mikro 200R centrifuge (Hettich Lab Technology, Germany). For the instrument control and the data processing the Waters® Empower™ 3.0 software suite has been employed using the QuanLynx data manager for all the quantification procedures employed. When needed, the SPSS 22.0 statistics software and R statistical language have also been used.

3.3.5 Sample pretreatment

3.3.5.1 Serum Samples

Serum standards were prepared for UPLC-PDA analysis by direct protein precipitation with acetonitrile:methanol (ACN:MeOH) 2:1 (v/v). A 50 µL aliquot of plasma spiked with 5 µL of 100 µg/mL ISTD was treated with 150 µL ACN:MeOH 2:1 leading to the precipitation of the plasma proteins. This procedure was followed by a vortexing step for 30 sec. and the mixture was centrifuged at 12000 rpm for 10 min. Subsequently, 150 µL of the supernatant were transferred into an 220 µL insert and were instantly analyzed as described below.(Figure 22)

3.3.5.2 Brain Samples

Brain standards were prepared in a blank brain homogenate which was prepared by homogenization of brain in methanol (10mg brain in 500mL MeOH). Brain homogenates were spiked with appropriate quantities of TC4 and CRC stock solution and 5 µL of 100 µg/mL ISTD and followed by a vortexing and centrifugation step. Subsequently, 150 µL of the supernatant were transferred into an insert and were instantly analyzed as described below. (Figure 22)

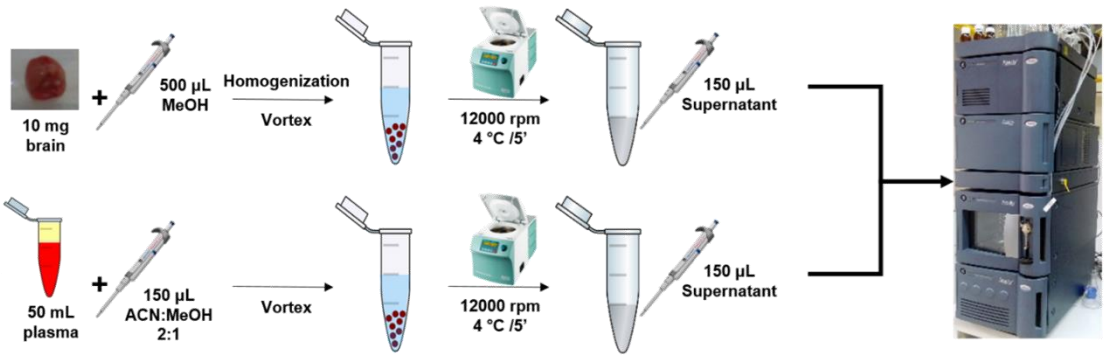

Figure 22: Final plasma and brain samples pretreatment protocol

3.3.6 Chromatographic conditions

All analyses were performed on an Acquity UPLC system (Waters Corp., Milford, MA, USA) comprised of a Binary Solvent Manager, a sample manager and a PDA detector. An RP-C18 Hypersil Gold column (50 x 2.1 mm, 1.9 µm; Supelco, Darmstadt, Germany) preceded by a precolumn (Waters Van- Guard 5 mm × 2.1 mm, 1.7 µm) of the same packing material and an on-line filter were used for the chromatographic separation of TC4, CRC and ISTD. A flow rate of 0.5 mL/min has been used throughout all chromatographic experiments. The mobile phase consisted of 0.01% aq. TFA (% v/v - solvent A) and acetonitrile (solvent B). A gradient elution method with a total run time of 2.5 min including the column equilibration time was used as follows: initial conditions 95% A: 5%B, 0 to 0.7 min, 40%A: 60% B; 0.7 to 1.1 min, 15%A: 85% B; 1.1 to 1.3 min, 0%A: 100% B; 1.30 to 1.50 min, 0%A: 100% B; 1.5 to 1.9 min, 60%A: 40% B; 1.9 to 2.1 min, 95%A: 5% B; 2.1 to 2.5 min, 95%A: 5% B. The column temperature maintained stable at 40 ^{o}C throughout all experiments while the autosampler tray temperature was set at 4 ^{o}C avoiding direct light exposure as crocins are photo-sensitive and could be easily degraded when exposed to light. The injection volume was 5 µL.

3.3.7 Validation of the bioanalytical method

Assay validation was performed according to the ICH (http://www.ich.org/fileadmin/Public_Web_Site/ICH_Products/Guidelines/Quality/Q2_R1/Step4/Q2_R1__Guideline.pdf), FDA (https://www.fda.gov/downloads/drugs/guidancecomplianceregulatoryinformation/guidances/ucm368107.pdf) and EMA (http://www.ema.europa.eu/docs/en_GB/document_library/Scientific_guideline/2011/08/WC500109686.pdf) guidelines for bioanalytical methods validation employing the ISTD methodology. All responses were measured as the ratio between the peak areas of the compounds of interest (TC4, CRC) and the ISTD. The assays were validated by evaluating the specificity, selectivity, calibration model, precision and accuracy (intra- and inter-day), lower limit of quantification (LLOQ), recovery from spiked mice plasma and brain samples, carry over-effect, stability (short- and long-term, autosampler and freeze–thaw), robustness, sample dilution and incurred sample reanalysis.

3.3.7.1 Selectivity and specificity

Selectivity was studied by comparing chromatograms of six blank substance-free mice plasma and brain samples from six subjects with blank samples spiked with TC4, CRC and ISTD. All plasma and brain samples were subjected to the above described pretreatment procedure and were further analyzed by the aforementioned methodology in order to test for potential interferences or co-elution of the compounds of interest and endogenous plasma substances. Selectivity was tested in different concentrations as well as the lower limit of quantification (LLOQ).

3.3.7.2 Calibration Curves-Regression model

In order to estimate the validation parameters, three different types of calibration curves were constructed (in solvent, in pre-spiked and post-spiked plasma and brain samples). For plasma analysis, this procedure included analysis of the calibration standards at ten concentration levels ranging from 10 to 6000 ng/mL (n=10) and calculating the analyte/ ISTD ratio. Curve fitting was achieved by non-linear regression analysis employing a quadratic model with $1/x^2$ weighting factor for TC4 and CRC. The method demonstrated acceptable accuracy for the concentration range studied, as the back calculated concentrations of the calibration standards did not exceed ±15% of the nominal value. Pre- and post-spiked serum samples were prepared for UPLC analysis by direct protein precipitation as described above. For brain analysis, the dynamic range was set from 0.05-5 ng/mg (n=8) followed by calculation of the analyte/ISTD ratio. Curve fitting was achieved by non-linear regression analysis employing a quadratic model with $1/x^2$ weighting factor for both TC4 and CRC. The method demonstrated acceptable accuracy for the concentration range studied where the back calculated concentrations of the calibration standards were within ±15% of the nominal value.

3.3.7.3 Carry-over study

The potential carry-over effect has been evaluated by injecting blank samples after the injection of the Upper Limit of Quantification (ULOQ)

3.3.7.4 Incurred sample reanalysis

All the samples have been reanalyzed with the aforementioned methodology.

3.3.7.5 Stability

Stability testing (assessed according to EMA, FDA, ICH procedures) was applied in order to evaluate the stability of the analytes during sample treatment, after long-term (frozen at -80 ^{o}C) and short-term (bench-top at room temperature) storage, after three freeze and thaw cycles and during the analytical process. All stability tests in plasma and brain have been performed at three spiked levels for TC4 and CRC (n=5) simultaneously [i.e. HQC=4600ng/mL, LQC1=80ng/mL and LQC2=30ng/mL for plasma and HQC=3.5ng/mg, LQC1=0.35ng/mg and LQC2=0.2ng/mg for brain]. Short-term stability has been evaluated by reinjecting spiked samples that have been left for 6h at room temperature away from artificial light in an effort to simulate the precise working conditions. Long-term stability has been estimated by storing spiked samples at -80 ^{o}C for 1 month and re-injecting them, whereas the freeze-and-thaw stability has been evaluated by analyzing the spiked samples after three consecutive cycles of freezing and thawing at room temperature. Autosampler stability has been evaluated after reanalyzing spiked samples that have remained in the autosampler's tray for 12h at 5 ^{o}C.

3.3.7.6 Precision and accuracy (Intra-day and inter-day)

Five replicates (n=5) of each QC sample (LQC, MQC, HQC, were repeatedly analyzed in order to evaluate the intra- and inter-day precision and accuracy expressed as relative standard deviation (%) (RSD%) and relative error (%) (RE%) respectively. The inter-day precision and accuracy were assessed by analyzing five sets including all QC samples on three consecutive days.

3.3.7.7 Lower Limit of Quantification (LLOQ)

LLOQ defined as the lowest TC4 and CRC concentration of the calibration curve that could be determined with %RSD, %RE <20% (n=5) and signal-to-noise ratio (S/N) at least 5. Therefore, five blank samples were prepared and the (S/N) was found to be >5 which has been determined by comparison between the measured signals (heights) from samples spiked at the LLOQ levels and those of blank plasma samples leading to the determination of the minimum concentration that the analytes can be reliably quantified.

3.3.7.8 Robustness

In order to evaluate the method's robustness, three experimental conditions (the flow rate of the mobile phase, the column temperature and the pH of the mobile phase) were altered by ± 5% compared to the established values. The LQC1, LQC2 and HQC were analyzed in five replicates by altering one parameter per time followed by calculation of the chromatographic peak area and retention time according to the previously described methodology. The results were expressed as % RSD.

3.3.7.9 Dilution Integrity

For the demonstration of the ability to dilute and analyze samples that contain TC4 and CRC above ULOQ, a set of 2-fold and 10-fold spiked plasma compared to the ULOQ i.e. 12000 and 60000 ng/ mL were analyzed. The spiked samples were diluted with appropriate volumes of blank drug-free human plasma, processed according to the sample pretreatment procedure and analyzed by the developed methodology. For this reason, matched samples in human and mouse plasma have been prepared and analyzed. It has been demonstrated that the interchange of mice plasma with human plasma to the dilution integrity study did not significantly affect the result as it has been shown that the specificity and selectivity have been remained unaltered under the experimental conditions employed in the current study (%RSD =1.41). The substitution of mice plasma with human plasma has been rendered necessary due to the lack of adequate quantities of mice or rat plasma for the dilution integrity study. Regarding the brain dilution integrity study, it has not been performed, due to the lack of brain homogenate in appreciable amount. Nevertheless, this has been compensated by the fact that no sample has exhibited higher concentrations than the ULOQ of the corresponding calibration curve.

3.3.7.10 Plasma regression model

Non-linear regression analysis has been employed, using a quadratic model with $1/x^2$ weighting fitted to the TC4 and CRC calibration curves over the range of 10 to 6000 ng/mL (n=5). The models produced, exhibited adequate fitting (correlation coefficient R^2 better than 0.995 for both TC4 and CRC, whereas the back-calculated values exhibited % RE lower than the 15% margin in all cases. The

results show that the model is acceptable for the quantitation of the analytes in mice plasma.

The equation for the calibration curve used for the quantification of TC4 in the plasma sample is:

y=1.860e-004(±4.287e-005)+5.277e-005(±1.835e-006)*x+3.998e-011(±6.590e-010)*x^2 using 1/x^2 weighting [mean±(SD)].

The equation for the calibration curve used for the quantification of CRC in the plasma sample is:

y=0.03273(±3.532e-004)+1.572e-004(±1.512e-005)*x+8.053e-010 (±5.429e-009)*x^2 using 1/x^2 weighting [mean±(SD)].

3.3.7.11 Brain regression model

The quadratic model with 1/x^2 weighting that was fitted to the TC4 and CRC calibration curves in brain over the range of 0.05 to 5 ng/mg (n=5) had a correlation coefficient R^2 of better than 0.996 for both TC4 and CRC whereas the back calculated values did not exceed the 15% (RE%) margin in all cases. The equation for the calibration curve used for the quantification of TC4 in the brain samples is:

y= 3.160e-007 (±2.162e-005)+2.092e-004(±1.161e-005)*x+ 6.023e-007 (±1.923e-007)*x^2 using 1/x^2 weighting [mean±(SD)].

The equation for the calibration curve used for the quantification of CRC in the brain samples is:

y= 3.423e-003(±3.525e-004)+ 1.132e-003(±1.892e-004)*x+ 5.557e-006 (±3.135e-006)*x^2 using 1/x^2 weighting [mean±(SD)].

3.4 RESULTS AND DISCUSSION

In every step of the validation procedure, all calculations were constructed by plotting the area ratios of TC4/ISTD and CRC/ISTD versus the added concentration of both substances.

3.4.1 Analytical method development and optimization of UPLC-PDA conditions

The chromatographic conditions employed for the determination of TC4 and CRC in mouse plasma and brain were thoroughly optimized by varying parameters such as the column chemistry (C18, C18-NPS, C8 and Hilic), column geometry (100 x 2.1 mm, 1.9μm; 50 x 2.1 mm, 1.9μm; 100 x 2.1 mm, 1.7 μm), mobile phase (organic modifiers and buffers), gradient elution type, column temperature and flow rate. The best results in terms of peak resolution and shape as well as speed of analysis have been achieved employing a Hypersil Gold (C18, 50 x 2.1 mm, 1.9 μm) reversed-phase column with acetonitrile as the organic modifier of the mobile phase. The addition of 0.01% TFA in the mobile phase, improved the analyte peak shape, therefore it has been used throughout all analyses (sharpness, width, symmetry). Moreover, the total analysis time was limited to 2.5 min. (incl. equilibration conditions) offering a rapid chromatographic methodology with adequate resolution (TC4 eluted at 0.91 min, ISTD at 1.02 min and CRC at 1.64 min with resolution $R_{TC4/ISTD}$=4 and $R_{ISTD/CRC}$=6.15). In order to enhance the separation of the compounds of interest as well as to maintain the life duration of the column, it was necessary to utilize a precolumn so as to absorb all the unwanted endogenous compounds of both plasma and brain that would hinder the experimental procedure. Given the fact that both TC4 and CRC are extremely colored compounds lying to the red region of the visible spectrum, the optimum λ_{max} chosen for the quantification of TC4 and CRC was 440 nm after careful observation with the PDA [174] whereas the ISTD exhibits λ_{max} at 373 nm. Thus, the developed UPLC-PDA methodology included 3 observation channels (440, 373, 220 nm) the last one being used to assess the methodology's performance for species that do not bear double bonds.

3.4.2 Sample preparation and extraction protocol

In order to efficiently remove any unwanted impurities from plasma and brain samples, many sample pretreatment protocols were evaluated. The main criteria of acceptance for the sample pretreatment methodology were its efficiency, measured

by the % recovery and the convenience of the employed procedure in terms of cost and time. Therefore, an SPE-based sample preparation procedure was rejected, as the protein precipitation employed in this study exhibited faster sample preparation with minimal cost and quantitative recovery efficiency as well. The quantitative recovery of the analytes along with the simplicity and rapidity of this sample pretreatment protocol, rendered the method compatible with high-throughput analysis of clinical samples.

For the sample preparation of the serum, various solvents such as methanol, ethanol, ACN and mixtures of ACN and methanol in various ratios (2:1, 3:1, 1:1) were tested. After thorough examination of the analytes' recovery (%) in each case, acetonitrile:methanol 2:1 (v/v) mixture (at 0 ^{o}C) was chosen as extraction solvent system, as it ensured satisfactory protein precipitation, good extraction recovery and high reproducibility for both TC4 and CRC as well as the ISTD, without interfering with various co-eluting endogenous components.

In order to proceed to the sample preparation of the brain samples, a homogenization step was required. In accordance with the literature, a variety of protocols have been proposed to extract analytes from the brain. [230] According to the adopted protocol, 10mg of brain are homogenized with 500μL of a precipitation solvent. Water was rejected in favor of the organic solvents in order to shorten the evaporation step followed homogenization. Various solvents were tested and ice-cold methanol (0 ^{o}C) has been proven to be the most effective in terms of recovery. Furthermore, in an effort to simplify and accelerate the experimental procedure, homogenization was performed in the entire amount of brain needed for the set of experiments planned to occur during the day i.e. calibration curve and QCs with appropriate amount of precipitation solvent (500μL acetonitrile for each 10mg of brain) as it was proven that there was no difference between the peak areas deriving from samples spiked and then homogenized separately and samples that have been pre-homogenized and afterwards spiked (TC4: %RSD= 2.33 and %RE= −3.27 and CRC: %RSD= 2.57 and %RE= −1.52).

3.4.3 Quantification of *trans*-crocin 4

4-nitro-aniline was chosen as the ISTD because it meets all the necessary prerequisites for this selection i.e. it exhibited high and repeatable recovery, suitable chromatographic properties under the described experimental conditions, it has not been reported as an endogenous plasma and brain metabolite and had no interference with the compounds of interest (TC4 and CRC). Representative UPLC–

PDA at λ=440 nm (λ_{max} for TC4 and CRC) chromatograms of plasma and brain samples are shown in Figure 23 and Figure 24**,** whereas the corresponding chromatograms of plasma and brain samples at λ=373 nm (λ_{max} for ISTD) are shown in Figure 25 and Figure 26. Processed blank samples, exhibited no observable peaks for none of the three compounds.

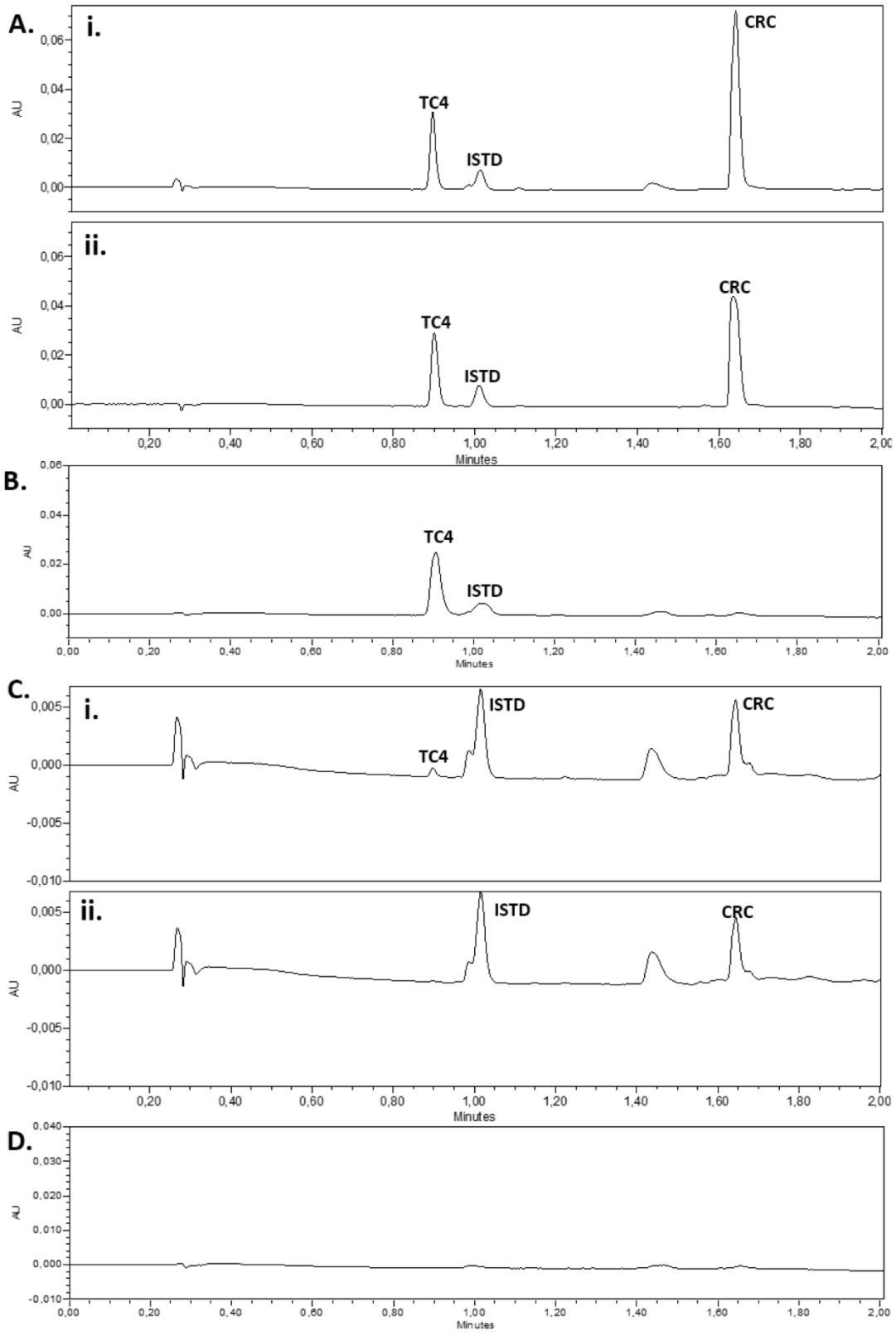

Figure 23: Representative UPLC–PDA (λ=440 nm) chromatograms of: A. HQC sample spiked with TC4 and CRC (4600ng/mL) and ISTD (100ug/mL) (i) in mice plasma; (ii) in MeOH; B. Plasma sample from mouse treated with 50 mg TC4 (*i.p.*) collected 30 min after administration; C. LLOQ (i) TC4 (25 ng/mL); (ii) CRC (10ng/mL) D. blank mice plasma. The t_R for TC4, CRC and ISTD are 0.91, 1.64 and 1.02 min, respectively.

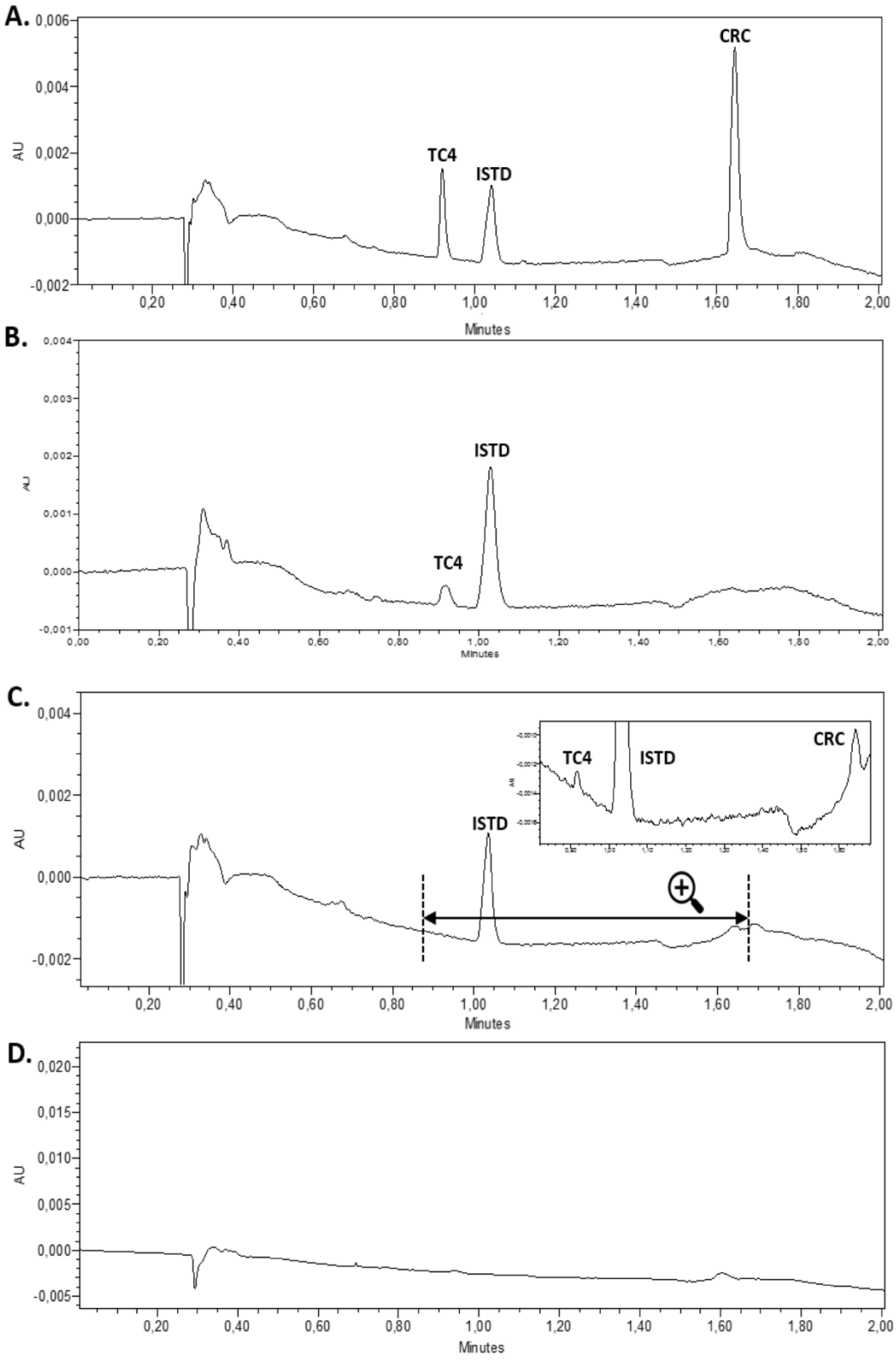

Figure 24: Representative UPLC–PDA (λ= 440 nm) chromatograms of: A. HQC mice brain sample spiked with TC4 and CRC (3.5 ng/mg) and ISTD (100 ug/mL); B. Brain sample from mouse treated with 50 mg TC4 (*i.p.*) collected 30 min after administration; C. LLOQ of TC4 and CRC (0.05 ng/mg) D. blank mice brain. The t_R for TC4, CRC and ISTD are 0.91, 1.64 and 1.02 min, respectively.

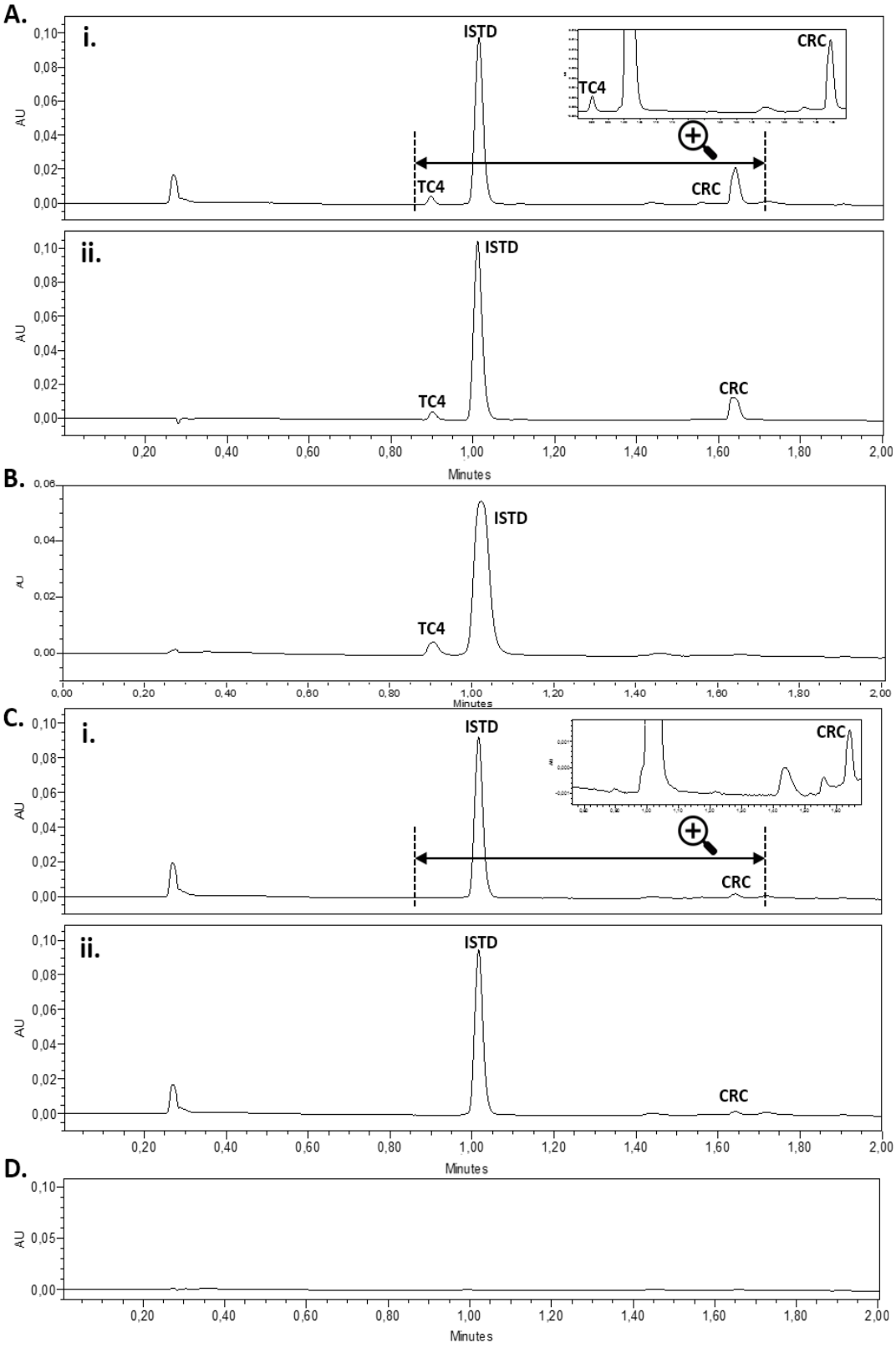

Figure 25: Representative UPLC–PDA (λ= 373 nm) chromatograms of: A. HQC sample spiked with TC4 and CRC (4600ng/mL) and ISTD (100ug/mL) (i) in mice plasma; (ii) in MeOH; B. Plasma sample from mouse treated with 50 mg TC4 (*i.p.*) collected 30 min after administration; C. LLOQ (i) TC4 (25 ng/mL); (ii) CRC (10ng/mL) D. blank mice plasma. The t_R for TC4, CRC and ISTD are 0.91, 1.64 and 1.02 min, respectively.

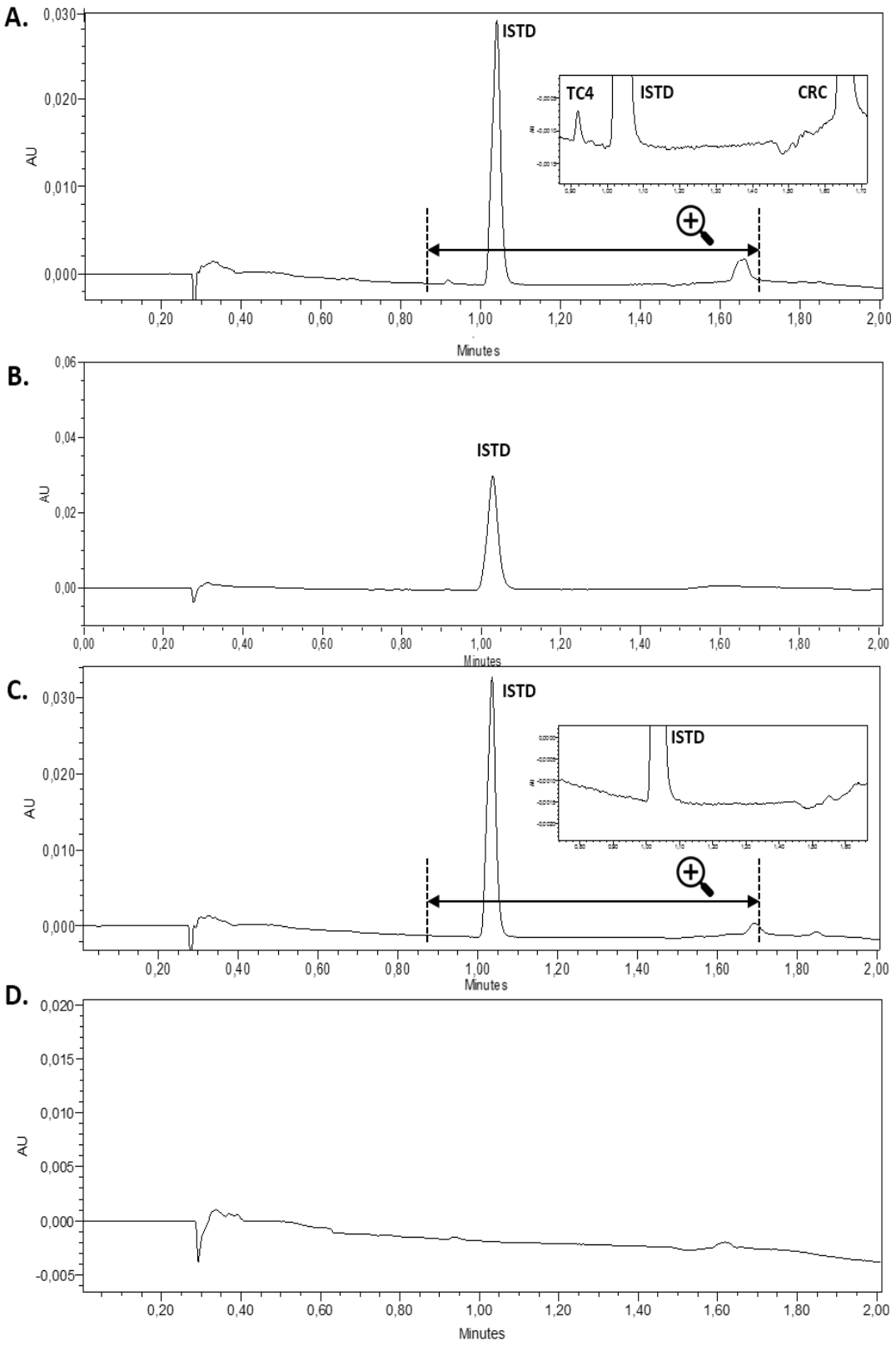

Figure 26: Representative UPLC–PDA (λ= 373 nm) chromatograms of: A. HQC sample spiked with TC4 and CRC (3.5 ng/mg) and ISTD (100 ug/mL) in mice brain; B. Brain sample from mouse treated with 50 mg TC4 (*i.p.*) collected 30 min after administration; C. LLOQ of TC4 and CRC (0.05 ng/mg) D. blank mice brain. The t_R for TC4, CRC and ISTD are 0.91, 1.64 and 1.02 min, respectively.

3.4.4 Validation of the bioanalytical method

3.4.4.1 Specificity

In order to evaluate the presence of potential endogenous metabolites that would interfere with the quantification of the analytes the specificity of the method has been evaluated. The gradient UPLC method developed, allowed the baseline separation of the analytes, without the presence of any interferences from endogenous plasma or brain compounds at the corresponding retention times of the analytes and ISTD. The addition of the ISTD has been made at the protein precipitation step in order to ensure that any potential interference the analytes might have with the plasma proteins, would not have any effect on the ratio between analyte/ISTD. This step, offers an additional level of confidence to the proposed methodology as it eliminates potential analytical errors.

3.4.4.2 Regression model

Non-Linear regression analysis has been employed for the assessment of the calibration analysis for TC4 and CRC in both plasma and brain. The range used for both analytes in plasma was 10 to 6000 ng/mL (n=10) whereas in brain, where lower concentrations were expected, the corresponding range has been set to be 0.05 to 5 ng/mg (n=8).

3.4.4.3 Lower Limit of Quantification (LLOQ)

The lower limit of quantification (LLOQ) is the lowest analyte concentration of the calibration curve that could be determined with precision <20% and accuracy between 80% and 120%, showing a signal-to-noise (S/N) ratio better than 5. The LLOQ for each analyte was determined as the concentration of the analyte that led to a peak with a S/N ratio of at least 5 times the response compared to that of a blank sample. The LLOQ have been determined to be 25 ng/mL for TC4 and 10 ng/mL for CRC for plasma and 0.05 ng/mg for TC4 and CRC for brain while %RE and %RSD were less than %20 margin and the S/N was at least 5 times the signal of a blank sample. The data indicate that the sensitivity of the described methodologies for the analysis of TC4 and CRC in mice plasma and brain is acceptable.

3.4.4.4 Carry-over study

No carry-over effect was observed during the study as there was no chromatographical peak of the analytes following the injection of a blank plasma or brain sample.

3.4.4.5 Incurred sample reanalysis

In order to assess the validity of the results in successive days, the total number of samples was reanalyzed. The results demonstrated that the % difference between the two measurements was <20% of their mean, indicating that the developed methodology can afford accurate data on the concentration of TC4 and CRC in plasma and brain.

3.4.4.6 Stability

The stability of the QC samples was compared to that of freshly prepared and instantly analyzed one while the %RSD and %RE values obtained were within the 15% margin. TC4 and CRC were found to be stable enough for at least 3 freeze and thaw cycles and also for the investigated time periods.

The %RSD values of short- and long-term stability of the QC plasma samples were found to be less than 2.8% (short-term) and 7.9% (long-term) for TC4 and 0.9% (short-term) and 5.0% (long-term) for CRC respectively (Table 4). Autosampler stability was found to be less than 9.7% for TC4 and 9.3 for CRC whereas the %RSD values of the QC samples included in the 3 freeze and thaw cycles were no more than 1.6% for TC4 and 1.4% for CRC. The %RSD values of short- and long-term stability of the QC brain samples were found to be less than 5.4% (short-term) and 9.2% (long-term) for TC4 and 1.0% (short-term) and 7.2% (long-term) for CRC respectively. Autosampler stability was found to be less than 5.8% for TC4 and 5.3% for CRC whereas the %RSD values of the QC samples included in the 3 freeze and thaw cycles were no more than 9.2% for TC4 and 7.2% for CRC. Corresponding %RE values could be found in Table 4. Our results show that the samples could remain for at least 30 days at -80 ^{o}C as no out-of-limit degradation can be observed.

TC4 **Plasma** Storage conditions	Nominal Concentration (ng/mL)	RSD%	RE%
Short-term (6h, 25°C)	4600	3.1	6.7
	80	0.1	1.5
	30	2.8	-6.3
Freeze-thaw (from -80°C to 25°C, 3 cycles)	4600	0.4	-4.9
	80	0.5	-10.5
	30	1.6	-14.1
Long-term (30 days, -80°C)	4600	3.7	-12.9
	80	2.9	-8.1
	30	7.9	-11.8
Autosampler (12h, 5°C)	4600	4.9	2.9
	80	5.6	1.7
	30	9.7	-1.3

CRC **Plasma** Storage conditions	Nominal Concentration (ng/mL)	RSD%	RE%
Short-term (6h, 25°C)	4600	0.3	3.3
	80	0.9	-4.8
	30	0.9	-6.9
Freeze-thaw (from -80°C to 25°C, 3 cycles)	4600	0.3	-4.0
	80	0.5	0.9
	30	1.4	-6.7
Long-term (30 days, -80°C)	4600	1.3	-14.0
	80	3.7	-11.1
	30	5.0	-10.1
Autosampler (12h, 5°C)	4600	3.0	1.6
	80	9.0	-1.8
	30	9.3	-1.2

TC4 **Brain** Storage conditions	Nominal Concentration (ng/mg)	RSD%	RE%
Short-term (6h, 25°C)	3.5	0.5	-10.9
	0.35	1.2	-11.8
	0.2	5.4	-14.3
Freeze-thaw (from -80°C to 25°C, 3 cycles)	3.5	0.5	-2.4
	0.35	4.6	-13.5
	0.2	4.9	-15.8
Long-term (30 days, -80°C)	3.5	9.2	-10.5
	0.35	3.0	-9.2
	0.2	4.7	-13.5
Autosampler (12h, 5°C)	3.5	3.0	-1.3
	0.35	5.8	2.8
	0.2	2.8	-1.9

CRC **Brain** Storage conditions	Nominal Concentration (ng/mg)	RSD%	RE%
Short-term (6h, 25°C)	3.5	0.5	-7.6
	0.35	1.0	-3.7
	0.2	0.7	-2.2
Freeze-thaw (from -80°C to 25°C, 3 cycles)	3.5	0.6	-2.5
	0.35	3.2	15.3
	0.2	3.2	6.0
Long-term (30 days, -80°C)	3.5	6.5	-12.7
	0.35	7.2	-12.0
	0.2	2.7	-11.4
Autosampler (12h, 5°C)	3.5	2.9	1.4
	0.35	4.6	1.4
	0.2	5.3	-2.0

Table 4: Stability study of TC4 and CRC in mice plasma and brain

3.4.4.7 Intra-day and Inter-day precision and accuracy

Intra- (n = 5) and inter-day (n = 15) precision and accuracy were evaluated for both substances at the three QC levels (HQC, MQC, LQC1, LQC2) (Table 5). The intra-day precision in plasma did not exceed 6.7% (TC4) and 13.9% (CRC) whereas the inter-day did not exceed 6.1% (TC4) and 3.7% (CRC). On the other hand, the intra-day precision in brain did not exceed 9.5% (TC4) and 14.9% (CRC) whereas the inter-day did not exceed 8.8% (TC4) and 7.0% (CRC). At the LLOQ level, the accuracy, expressed as the relative percentage error (%RE) was found to be within ±12.3% whereas the precision, expressed as the %relative standard deviation (%RSD) was found to be less than 13.9% The above results demonstrate that the developed methodology offers acceptable reliability and accuracy for the most part.

3.4.4.8 Robustness

In order to certify that the developed analytical methodology is not affected by minor alterations to the experimental conditions the robustness of the method was extensively studied as described above. The results indicated that none of the changes performed caused an alteration of more than 3.6% for all the parameters tested certifying that, the developed methodology has sufficient robustness in order to allow quality control measurements. Hence, %RSD of the resolution between TC4, CRC and ISTD was estimated as less than 3.6% after the application of the predefined robustness alterations, whereas changing the column temperature from 40 ^{o}C to 38 ^{o}C and 42 ^{o}C had no significant alteration to the resolution between peaks (%RSD less than 1.9%) as well as to the sensitivity (%RSD 2.4%). Finally, changing the flow rate of the mobile phase from 0.5 mL/min to 0.475 and 0.525 mL/min the %RSD of the resolution between peaks did not exceed 3.6% and the sensitivity was less than 1.4%. Furthermore, by altering the percentage of TFA in the stationary phase neither the peak area and shape nor the resolution between peaks were considerably affected.

TC4 PLASMA		Intra Day (n=5)			Inter Day (n=15)		
QC Level	Spiked Concentration (ng/mL)	Mean concentration found (ng/mL)	RE%	RSD %	Mean concentration found (ng/mL)	RE%	RSD%
HQC	4600	4427	3.8	5.4	4750	-3.3	0.8
MQC	3000	2877	4.1	4.6	2886	3.8	1.3
LQC1	80	91	-14.3	5.1	76	4.5	6.1
LQC2	30	31	-2.2	6.7	26	12.1	4.1
CRC PLASMA		Intra Day (n=5)			Inter Day (n=15)		
QC Level	Spiked Concentration (ng/mL)	Mean concentration found (ng/mL)	RE%	RSD %	Mean concentration found (ng/mL)	RE%	RSD%
HQC	4600	4543	1.2	2.1	4719	-2.6	1.2
MQC	3000	2744	8.5	1.5	2859	4.7	1.3
LQC1	80	72	10.3	4.6	76	4.8	2.1
LQC2	30	26	13.5	13.9	29	3.9	3.7
TC4 BRAIN		Intra Day (n=5)			Inter Day (n=15)		
QC Level	Spiked Concentration (ng/mg)	Mean concentration found (ng/mg)	RE%	RSD %	Mean concentration found (ng/mg)	RE%	RSD%
HQC	3.5	3.5	1.4	2.6	3.5	0.7	0.9
MQC	3	3.1	-4.6	4.4	3.0	0.3	1.5
LQC1	0.35	0.4	-6.3	7.6	0.3	12.3	2.9
LQC2	0.2	0.2	-2.9	9.5	0.2	5.1	8.8
CRC BRAIN		Intra Day (n=5)			Inter Day (n=15)		
QC Level	Spiked Concentration (ng/mg)	Mean concentration found (ng/mg)	RE%	RSD %	Mean concentration found (ng/mg)	RE%	RSD%
HQC	3.5	3.5	0.1	1.4	3.4	4.1	0.6
MQC	3	3.1	-3.7	5.0	2.8	5.3	0.5
LQC1	0.35	0.4	-1.3	14.9	0.3	11.3	5.5
LQC2	0.2	0.2	-4.0	13.0	0.2	13.7	7.0

Table 5: Precision and accuracy data (Intra-day and Inter-day) for TC4 and CRC in mice plasma and brain

3.4.5 Bioavailability of *trans*-crocin 4 in Brain and Plasma

The two proposed analytical methodologies were applied to the analysis of mice plasma and brain samples obtained after *i.p* administration of TC4. In particular, fifty-six (56) wild type (C57BL/6J) mice were divided into three groups. The treatment groups were as follow: 21 mice (15 female-6 male) were treated with 50 mg/kg pure TC4 (dissolved in 0.9% aqueous NaCl) through *i.p.* administration; 30 mice (18 female-12 male) were treated with 150 mg/kg pure TC4 (dissolved in 0.9% aqueous NaCl) through *i.p.* administration; 5 mice (3 female-2 male) were used as control animals. Plasma samples and the whole brain of the mice were collected by authorized personnel at predefined time points (0, 15, 30, 60, 120 and 240 minutes after administration). Thus, whole plasma samples were gently shaken and centrifuged at 4000 rpm for 10 min at 25 ^{o}C and after the collection of serum were stored immediately in EDTA containing vacutainers at -80 ^{o}C. The brains were immediately stored at -80 ^{o}C until analysis.

Plasma:

Experimentally determined TC4 plasma levels of the studied mice in the predefined time points regarding both administration doses are depicted in Figure 27 and Figure 28. Given the fact that the *i.p.* administration route was selected in order to bypass the first-pass effect and/or its gastric hydrolysis, it is well demonstrated that TC4 was found to be in considerably high circulating levels regarding both studied administration doses i.e. 2600 ng/mL with a $t_{1/2}$ of 120 min (50 mg/kg-Female mice). These results show high accumulation of crocin in plasma in accordance with the *i.v.* results obtained by Yue Zhang *et.al.* [223] which exhibited ~ 6300 ng/mL showing a $t_{1/2}$ = 3.4 h. In that respect, it should be pointed out that *i.p.* administration is resembling more the *p.o.* administration. [228]

Furthermore, regarding the first administration dose (50 mg/kg) the experimentally determined TC4 levels of the female population were significantly higher than the male ones in all time points whatsoever, however, the male mice exhibited their C_{max} values 30 min after the TC4 administration (T_{max}) in contrast with the female individuals that exhibited their C_{max} values 60 min after the TC4 administration (T_{max}). (Figure 27) Similar to the previously described results regarding the administration of 50 mg/kg, after the treatment with 150 mg/kg TC4, female mice exhibited higher levels of circulating TC4 than the male population. **(**Figure 28**)**

The observed differences in the C_{max} between male and female mice could possibly occur due to the higher amount of fat accumulating in the female population. It is well known that female, compared to male, have higher percent body fat and deposit it in a different pattern while sex differences in fat distribution and correlations to metabolic health are well established in the clinical and epidemiological literatures. [231] As a result, it is indispensable to take into consideration the significance of sex differences regarding an ailment's treatment, however, it remains unclear to what extent pharmacokinetics contribute to these differences. Consequently, it is substantial to clarify the role of sex in pharmacokinetics in order to reach safe conclusions and to develop a gender-based optimized treatment.[232]

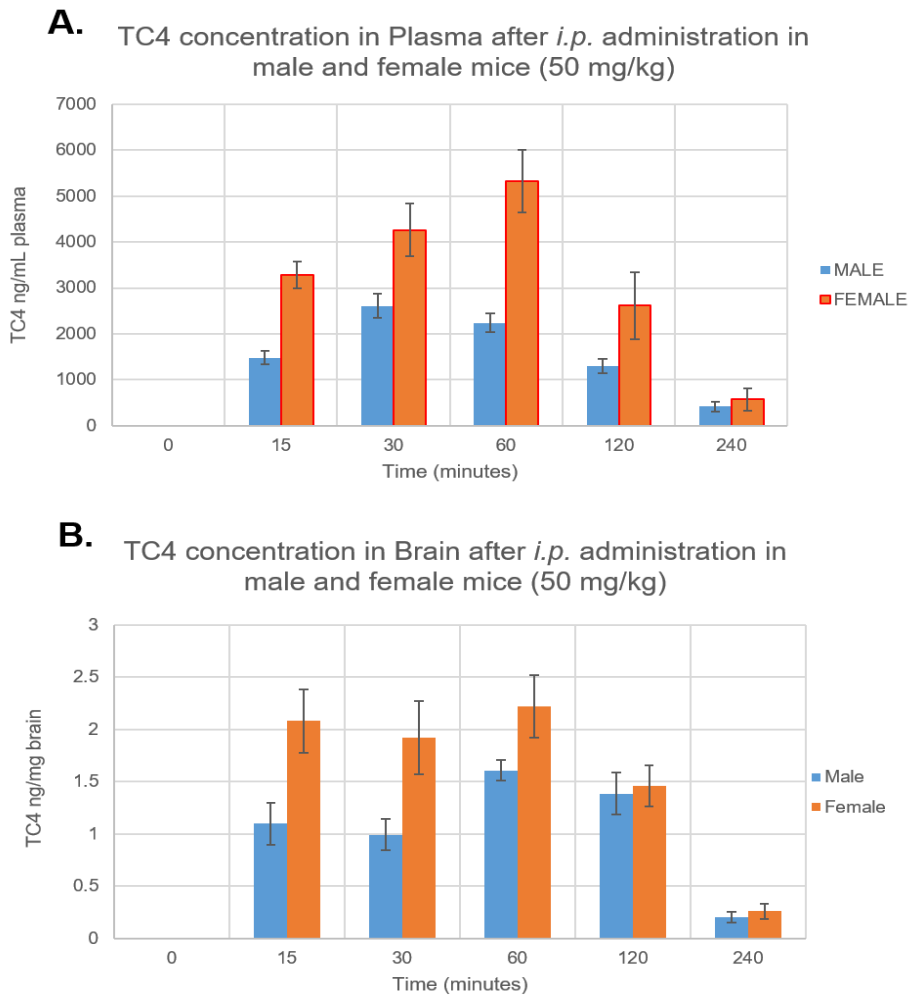

Figure 27: Experimentally determined concentration levels of TC4 in male and female mice (A.) Plasma and (B.) Brain samples in the time range of 0-240 minutes after *i.p.* administration of TC4 (50 mg/kg). Results are expressed as average values and the error bars represent the standard deviation.

Nevertheless, it is noteworthy that CRC was not detected in any plasma or brain sample following the *i.p.* administration as it is demonstrated in Figure 23. On the contrary, it has been reported that TC4 quickly hydrolyzes to CRC after *p.o*. administration [220], [222], [223], [224]. Therefore, in order to evaluate the distinct biological role of TC4, an *i.p.* administration scheme should be employed, since any observed biological effects are not overlapped by the presence of CRC in plasma. Furthermore, the levels obtained by this administration route are capable of clearly evaluating its biological role and any possible toxicological side effects.

Brain:

Experimentally determined TC4 levels in the brain of the studied mice in the predefined time points regarding both administration doses are shown in Figure 27 and Figure 28. The results demonstrate the bioavailability of TC4 in mice brain in a time range of 0-240 minutes. It should be noted that some measured amount of TC4 in the brain tissue could be due to the blood perfusing the brain because capillary depletion prior to brain homogenates was not performed, as it has been previously noted by W.M. Pardridge and others [233]–[236]. It seems that there is a time phase delay between blood and brain peak concentrations suggesting that there is indeed BBB crossing and distribution in brain tissue. Therefore, we believe that this study provides preliminary evidence on TC4's ability to penetrate the BBB as it is demonstrated in Figure 24. Considering the hydrophilic nature of the TC4 molecule, this transport is probably achieved through an active receptor-mediated transport (RMT) process with the aid of protein carriers.

Our study shows that there are sustained levels of TC4 built up in the brain [i.e., **mean 3.03 (±0.23) ng/ mg** brain for 120 min], indicating its' potential role as a neuroactive agent. As a matter of fact, Figure 27 and Figure 28 show that the levels of TC4 obtained in the Brain have reached a nearly steady state from 15-120 min. Moreover, the fact that no circulating CRC levels have been found (Figure 23 and Figure 24) may suggest that an alteration to the administration route (from *p.o*. to *i.p*.) could lead to the maintenance of TC4 circulating levels for a longer period of time allowing the application of its pharmacological activities in other organs such as the brain.

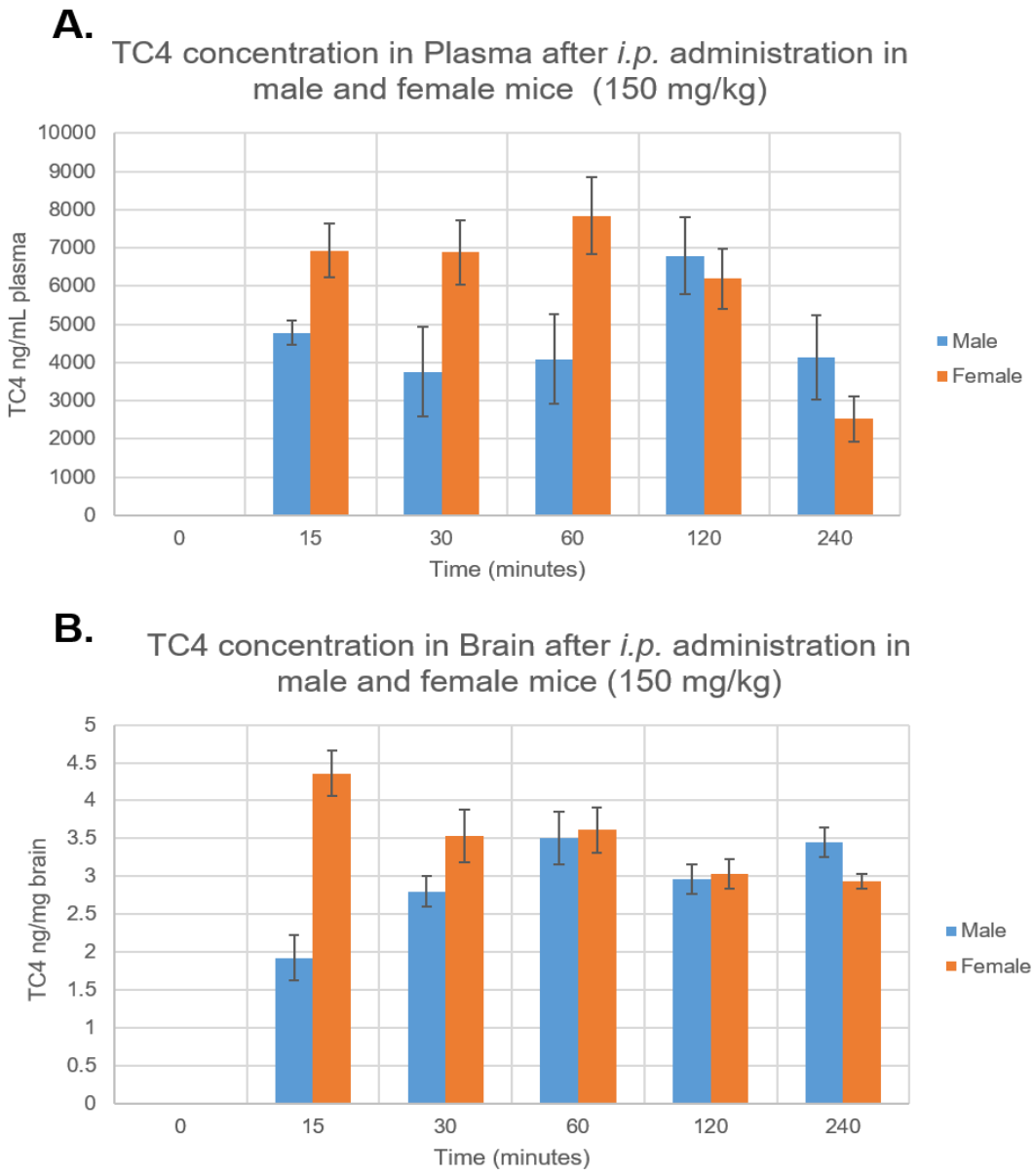

Figure 28: Experimentally determined concentration levels of TC4 in male and female mice (A.) Plasma and (B.) Brain samples in the time range of 0-240 minutes after *i.p.* administration of TC4 (150 mg/kg). Results are expressed as average values and the error bars represent the standard deviation.

3.5 CONCLUSION

The main goal of the current study was to develop two UPLC-PDA analytical methodologies for the sensitive and simultaneous determination of *trans*-crocin-4 and CRC in mice plasma and brain, taking into account the reduced analytical cost and the ease of adoptability from the pharmaceutical industries. The developed methodologies featured short analysis time (2.5 min incl. equilibration) and excellent resolution between TC4, CRC and ISTD. Thus, the UPLC separation procedure has been evaluated as a method capable of allowing ultra-high resolution chromatographic runs in a significantly restricted analysis time. After full validation according to EMA, FDA and ICH guidelines, the developed methodology, due to its sensitivity, allows the determination and monitoring of low analyte concentrations, often observed after natural products *i.p.* administration. This has allowed us to successfully apply the developed methodology to an exploratory quantitative study of TC4 and CRC in mouse plasma and brain. As far as the plasma is concerned, the bioavailability of TC4 in plasma was found to be in considerably high levels probably due to the application of *i.p.* administration where the first-pass metabolism and/or gastric hydrolysis were bypassed. In addition, this study shows the advantage of the *i.p.* administration, where detection of TC4 in mouse brains was observed for the first time, thus providing preliminary evidence on TC4's ability to penetrate the BBB, albeit its extremely hydrophilic character. In addition, no circulating CRC levels were detected in either plasma or brain samples. Finally, these results indicate that TC4 could serve as an active pharmaceutical ingredient, even though an extensive evaluation is needed in order to assess its efficacy and safety as a neuroprotective agent, as well as elucidate its mechanism of action.

3.6 ACKNOWLEDGEMENTS

We would like to acknowledge Despoina Papasavva for technical assistance in the animal experiments, and *Cooperative De Safran* (Krokos Kozanis, West Macedonia, Greece) for providing saffron samples.

3.7 FUNDING

This research was funded by the TreatAD SYN21-1003 ESPA Grant.

CHAPTER FOUR

UHPLC-HRMS-based plasma metabolomics study of *trans*-crocin 4 after *i.p.* administration in a mice model

4.1 ABSTRACT

Trans-crocin 4 (TC4) is an important carotenoid constituent of saffron showing remarkable activity against Alzheimer's disease due to its antioxidant and antiamyloidogenic properties. Metabolomics is an emerging scientific field that enhances biomarker discovery and reveals underlying biochemical mechanisms aiming towards the early subclinical diagnosis of diseases. So far, there have been scarce data demonstrating changes induced to mice plasma metabolome after TC4 administration. Thus, an untargeted UPLC-HRMS metabolomics approach has been employed to determine the alteration to the metabolic fingerprint after *i.p* administration of TC4 in male and female mice. Therefore, blood samples from fifty-six (56) mice administered with TC4, including control animals, were analyzed by UPLC-HRMS (Orbitrap Discovery XL). Statistical evaluation of the results was achieved by multivariate analysis (MVA) i.e. principal component analysis (PCA), Partial-Least Squares−Discriminant Analysis (PLS-DA) in order to discover the variables that contributed to the discrimination between treated and untreated groups whereas the variables contributing to the discrimination, were identified using comparisons to online databases (e.g. Metlin, HMDB, KEGG) aided by chemometric processing e.g. adduct and fragment identification, covariance searching etc. It should be noted that due to the high variability imposed by various factors e.g. sex of the animals participating in the study, administration dose and time-points of sacrifice, multilevel sparse PLS–DA analysis e.g. splitting variation to each individual component, has proven to be a more efficient approach for such designs.

By this methodology, the time sequence of metabolome changes due to the administration of TC4 has been made apparent. Furthermore, a sex-related effect on the metabolome has been proven to exist, denoting that the administration in both genders is indispensable in order to acquire safe conclusions as reliable metabolome pictures.

4.2 INTRODUCTION

Crocus sativus L. is a perennial stemless herb belonging to the family Iridaceae and its dried stigmas are commonly known as “Saffron”. The genus *Crocus* comprises some 85–100 species, while phytogeographically, the majority of species occur within the Mediterranean floristic region, extending eastward into the Irano-Turanian region. [237] The particularly specific climate prerequisites in order to cultivate *Cr. sativus* successfully, leading to the limitation of the potential cultivating areas, in combination with the confined production of each flower in stigmas, as well as the manual labor required during the harvesting period, have established Saffron as the highest priced value agricultural product in the world (HVAP). [238] The main constituents of saffron are carotenoids, glucosides, flavonoids, monoterpenes and other volatile compounds etc. [124] However, the most significant bioactive components are; apocarotenoids such as crocins, safranal and picrocrocin, while each of them is responsible for a particular organoleptic characteristic of saffron. Crocins are responsible for the intense red color, safranal for the odor and picrocrocin offers the bitter taste.

Crocins, which are highly water-soluble carotenoid metabolites, are mono- and bis-esters of crocetin (apocarotenoid) with glucose and/or gentiobiose and they are considered to be the most abundant constituents of saffron. [174] According to the number of sugars conjugated with the aglycon (crocetin), they are characterized as crocin-1. -2, -3, -4, -5 and they can be identified as either *-cis* or -*trans* isomers. *Trans*-crocin-4 (TC4) (digentiobiosyl 8, 8′-diapocarotene-8, 8′-oate; $C_{44}H_{64}O_{24}$), a diester of crocetin with gentiobiose, is the most abundant crocin possessing numerous pharmacological activities. The beneficial role of TC4 has been demonstrated regarding the treatment of several diseases due to its large array of biological activities, as it is involved in many pharmacological pathways. TC4 has been shown to exhibit free radical scavenging activity therefore antioxidant properties [149], and interestingly is responsible for scavenging ROS (Reactive Oxygen Species) involved in the memory impairment. Furthermore, its antioxidant effects were superior to those of α-tocopherol at the same concentration suggesting that, crocin is a unique and potent antioxidant that combats oxidative stress in neurons.[239] Crocin also possesses antitumor activity by inhibiting the proliferation and tumorigenicity of HL-60 cells, which may be mediated by the induction of apoptosis, given that this procedure in tumor cells is considered to be very useful in the management and therapy as well as in the prevention of cancer. [240] Recent findings suggest that crocin can regulate Hypothalamic-Pituitary-Adrenal (HPA) axis

activity in post-traumatic stress disorders (PTSD), thus it may serve as an effective treatment for subjects experiencing a traumatic event. [241] Also, saffron and its major constituent crocin, has been found to have a more significant impact on the Beck Depression Inventory-Second Edition (BDI-II) than the placebo on mothers suffering from mild-to-moderate postpartum depressive disorder. [242] Another really significant scientific discovery is that crocin has a positive effect in Obsessive-Compulsive Disorder (OCD) pointing towards the possibility of a functional interaction between crocin and the serotonergic system. [243] These results should be taken into consideration along with the findings of studies suggesting that saffron and its major bioactive components including crocin, could ameliorate Metabolic Syndrome (MetS) symptoms in both animal and clinical studies. [244] Along with the plethora of biological activities of crocin, it should also be emphasized the fact that TC4 has significant results against neurodegenerative diseases. The anti-inflammatory effects of crocin demonstrated in animal models of neuronal degeneration could be mediated by its direct effects on microglia homeostasis. [245] Furthermore, the amphiphilic character of crocin was found to make it more effective in preventing accumulation of toxic amyloid structures. [246] The inhibition of the neurotoxic effects of D-gal mediated by the improvement of spatial learning and memory functions as well as the reduction of Midbrain dopaminergic (MDA) levels that TC4 can cause, suggest TC4 as a healthcare product against prevention of age-related brain diseases such as Alzheimer's. [130] It is well known that the aggregation of intra-and/or extracellular misfolded proteins as amyloid fibrils, comprises a significant characteristic of more than 20 amyloid-related diseases. Therefore, preventing or reversing amyloid aggregation employing small molecules, is considered as a promising approach to the treatment or modification of these diseases. [247] It has been found that TC4 is able to inhibit Aβ-fibrillogenesis at lower concentrations as well as to control Aβ42-mediated amyloid fibril formation *in vitro*, probably through the stabilization of the helical structure, which prevents fibril formation and dissolves previously formed aggregates. [208] These observations suggest that TC4 could potentially be utilized as a bioactive pharmacological agent responsible for the inhibition of aggregation and deposition of Aβ in the human brain and capable of retarding amyloid fibril formation in Alzheimer's disease. [128][208]

Metabolomics can provide detailed information on the patterns of metabolite change in an entire metabolic network under the imposition of a stress condition.[248] It is a high throughput analysis of a complete set of small molecules allowing the identification and quantification of a biological system's endogenous low molecular weight compounds (e.g., <1500 Da) aiming towards the

understanding of biological processes that alter between the treated and untreated population. [249][250] Metabolomics rely essentially on the two most commonly used techniques currently applied to metabolomics analysis: Mass Spectrometry (MS) and Nuclear Magnetic Resonance (NMR). [248] During the last 10 years, liquid chromatography coupled with tandem mass spectrometry (LC-MS/MS) has been widely used owing to its superior sensitivity and selectivity for application to biological samples. Furthermore, LC-MS/MS allows the simultaneous measurement of multiple analytes in a single run within short separation time, providing a clear depiction of the metabolome in a particular condition but also aiming towards the identification of metabolites that are altered, in response to the application of the under-study-factor. [251] [252] In other words, metabolomics facilitates the complete depiction of the potential circulating metabolites practically in all biological sources (e.g. blood, urine and tissue etc.) needing to applied in, at least, two conditions (treated vs. untreated) followed by the statistical evaluation of the differences between the two states. This approach aims towards revealing the metabolites that are either up- or down-regulated as a result of an exogenous factor such as the administration of the compound of interest.

An ordinary pipeline of metabolomics analysis comprises of the following steps; sample preparation (e.g. protein precipitation employing various techniques), data acquisition (instrumental analysis of the previously processed samples with LC-MS or NMR experiments), data analysis using specific experimental tools and programs. The final interpretation and biological evaluation of the results is performed usually but not exclusively, employing multivariate statistical analysis (MVA), e.g. PCA, PLS-DA etc.

Multivariate statistics -in strict statistical terminology- differ from univariate methods in that they are able of simultaneously analyzing more than one dependent variable. A MVA approach is often used in order to discover the relationship between the samples analyzed and to identify the existence of any kind of clustering and connection amongst the population studied. Classification, clustering, and pattern recognition are different closely related terms that refer to statistical processes. They are used to specify samples in a set of categories while these categories can be pre-specified (often referred to as supervised classification) or not pre-specified (often referred to as unsupervised classification). [253]

Occasionally, in order to reveal all the minor difficultly noticeable treatment effects, it is useful to divide the total experimentally observed variance into its two constituent sources of variance i.e. between subjects variation and within subjects variation. Nevertheless, a commonly occurring problem is that the existing

variations among the subjects outweigh the changes induced by the administration of the compound of interest, and that is the obstacle that the most common multivariate analysis techniques (e.g. Principal Component Analysis (PCA), Partial Least Squares (PLS) and Partial-Least Squares−Discriminant Analysis (PLS−DA)) fail to overcome in order to successfully interpret the obtained results. Consequently, this limitation in the evaluation of the results requires the adoption of more complex analysis methodologies, one of them being the Multi Level - Multi Variate Analysis (ML-MVA) approach, that separates the variation within the subjects from the variation among them, in order to find the variation with the highest impact on the data sets, facilitating thus the identification of possible metabolites as the most differentiating biomarkers and ultimately leading better and more clear clustering of the studied groups.

As a result, since the interest in natural bioactive products emerges and constantly evolves but also based on the evidence that TC4 has been found to play a crucial role in the treatment or the modification of several neurodegenerative diseases, a UHPLC-HRMS based plasma metabolomics study was designed in order to characterize the metabolomics based fingerprinting after *trans*-crocin 4 administration as well as to identify metabolites that might participate in the biomolecular mechanisms of a disease inception and progress. (Figure 29).

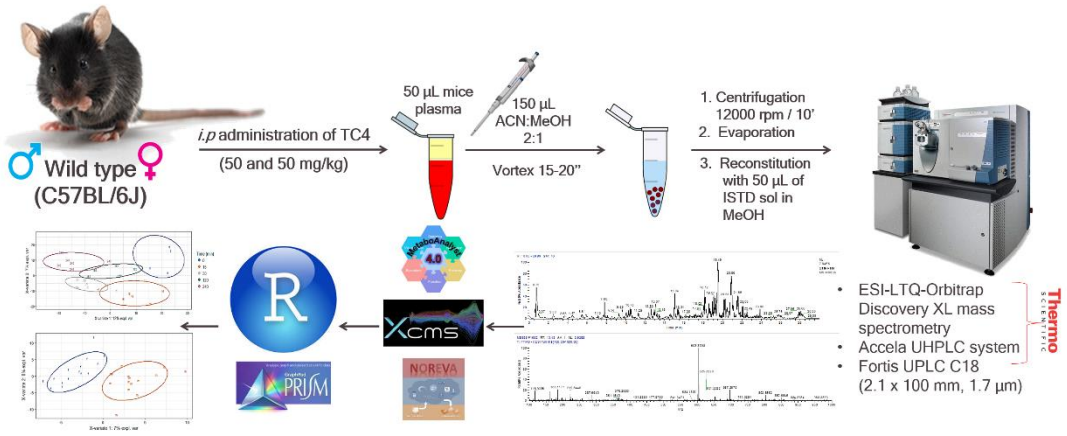

Figure 29: UHPLC-HRMS based plasma metabolomics experimental workflow

4.3 MATERIALS AND METHODS

4.3.1 Animal study design

The mice study was conducted under medical supervision at National and Kapodistrian University of Athens Medical School. Fifty-six (56) wild type (C57BL/6J) mice were divided into three groups. The treatment groups were as follow: 21 mice (15 female-6 male) were treated with 50 mg/kg pure TC4 (dissolved in 0.9% aqueous NaCl) through *i.p.* administration; 30 mice (18 female-12 male) were treated with 150 mg/kg pure TC4 (dissolved in 0.9% aqueous NaCl) through *i.p.* administration; 5 mice (3 female-2 male) were used as control animals. The protocol was approved by the ethical committee of the National and Kapodistrian University of Athens and was conducted according to the ICH-GCP guidelines (ICH GCP, 1996). The study received a permit from the Veterinary Directorate of the Prefecture of Athens (Approval #: 478/ 2014) according to the Greek legislation conforming to the 2010/53/ EU Council Directive.

4.3.2 Biofluid Collection

Plasma samples of all the mice were collected by authorized personnel at predefined time points (0, 15, 30, 60, 120 and 240 minutes after *i.p.* administration), have been gently shaken and centrifuged at 4000 rpm for 10 min at 25 ^{o}C. After the collection of serum with a plastic pipette, the plasma samples were immediately stored in EDTA containing vacutainers at -80 ^{o}C.

4.3.3 Chemical and Analytical Reagents

The analytical reference standard of *trans*-crocin 4 (TC4) was isolated from *Crocus sativus* stigmas following a procedure previously developed and described in our laboratory. [229] Plant material, *Cr. sativus* dried stigmas (saffron), were kindly provided by the *Cooperative De Safran* (Krokos Kozanis, West Macedonia, Greece). In brief, the necessary amount of TC4 in order to perform the following experiments was isolated from saffron stigmas by Fast Centrifugal Partition Chromatography (FCPC) employing a rapid and selective isolation protocol. With the aid of HPLC-PDA analysis employing the continuous peak purity approach, the purity of the isolated TC4 was found to be more than 90% and the verification of its structure was conducted by ^{1}H Nuclear Magnetic Resonance (NMR) spectroscopy. The isolated TC4 was further administered to the mice in order to perform the metabolomics study. All solvents were of LC-MS grade. Acetonitrile (ACN),

methanol (MeOH) and water, were purchased from Avantor ® (Gliwice, Poland), whereas formic acid (FA) was purchased from Sigma-Aldrich ®. The compounds reserpine, yohimbine and m-amino-phenol used as Internal Standards were purchased from Sigma-Aldrich ®.

4.3.4 Instrumentation

The metabolomic analysis was performed employing an ESI-LTQ-Orbitrap Discovery XL mass spectrometry (Thermo Scientific, Germany) connected to an Accela UHPLC system (Thermo Scientific, Germany). The UHPLC system was equipped by an autosampler, a vacuum degasser, a binary pump and a temperature-controlled column. The centrifugation of the plasma samples during the sample pretreatment procedure was performed with the aid of a Mikro 200R centrifuge (Hettich Lab Technology, Germany) while the evaporation of the precipitation solvent was performed by a GeneVac HT-4X EZ-2 series evaporator Lyospeed ENABLED (Genevac Ltd, UK).

4.3.5 Sample pretreatment

The mice plasma samples were prepared according to the sample preparation protocol that is described below. The plasma samples, that were kept frozen at -80 °C, were allowed to thaw slowly in an ice box at 4-5 °C for ~15-30 min. In order to proceed to the precipitation of the plasma proteins, an aliquot of 50 μL of each plasma sample was transferred into a labeled 1.5 mL eppendorf tube and then, 150 μL of a mixture of cold ACN:MeOH in a ratio 2:1 was added followed by vortexing for ~15-20 sec. The protein precipitation solvent system was constantly kept stored at an ice box in order to maintain its temperature, since the cold solution was found to have a higher protein precipitation capability compared to that kept at room temperature. Subsequently, the samples were centrifuged at 12000 rpm for 10 min at 4 °C and afterwards, 150 μL aliquot from the supernatant of each sample were transferred into an eppendorf tube and then they were completely evaporated in the GeneVac apparatus for 90 min at 40 °C under full vacuum. Finally, the residue was reconstituted with 50 μL of a methanolic solution containing m-amino-phenol, reserpine and yohimbine at a concentration of 2 μg/mL each, that were used as Internal Standards (ISTDs); the mixture was vortexed for ~20 sec and it was centrifuged at 12000 rpm for 10 min at 4 °C. At last, the supernatant was transferred to UPLC vials (in 200 μL inserts) and were stored until analysis.

4.3.6 UHPLC-HRMS Analysis

A Fortis UPLC C18 (2.1 x 100 mm, 1.7 µm) reversed phase column (Fortis Technologies Ltd.) was used for the chromatographic separation of the plasma metabolites. The system was run in a binary gradient solvent mode consisting of 0.1% (v/v) formic acid/water (solvent A) and acetonitrile (solvent B). Sample analysis was carried out in both the positive (ESI+) and the negative (ESI-) ion modes. The flow rate was 0.4 mL/min. A 30 min gradient method was employed as follows: 0 to 24 min: 95% A: 5% B, 24 to 28 min: 5% A: 95% B, 28 to 30 min: 95% A: 5% B. The column temperature was maintained at 40°C while the autosampler tray temperature was kept at 8 °C. The injection volume was 10 µL. For the positive ion mode, the capillary temperature and voltage was set at 320 °C and 40 V, respectively. The sheath gas flow was set to 40 arb. units and the aux gas flow to 8 arb. units. The spray voltage was set to 3.6 kV and the tube lens voltage to 120 V. For the negative ion mode, the capillary temperature and voltage was set at 320 °C and -40 V, respectively. The sheath gas flow was set to 40 arb. units and the aux gas flow to 8 arb. units. The spray voltage was set to 2.7 kV and tube lens voltage to -120 V. In both positive and negative ion modes, analysis was performed using the Fourier transform mass spectrometry (FTMS) full scan ion mode, applying mass scan range of 115-1000 m/z and a resolution of 30000 FWHM (Full width at half maximum) while acquisition of the spectra was performed in centroid mode. (Table 6)

UPLC parameters

Column: Fortis UPLC C18 (2.1 x 100 mm, 1.7 µm) Reversed Phase
Mobile phase: Water, 0.1% (v/v) Formic Acid (A) and Acetonitrile (B)
Flow rate: 0.4 mL/min ESI (+) / 0.4 mL/min ESI (-)
Column temperature: 40 °C
Autosampler Tray temperature: 8 °C
Injection volume: 10 µL

	Gradient Program		
	Time (min)	**A%**	**B%**
ESI (+) & ESI (-)	0	95	5
	24	95	5
	24	5	95
	28	5	95
	28	95	5
	30	95	5

MS parameters

Mode; ESI
Resolution; 30000 FWHM
Spectra Acquisition Mode; Centroid
Mass Scan Range: 115-1000 m/z

ESI (+)	Capillary temperature (°C): 320 Capillary voltage (V): 40 Sheath gas flow (arb. units): 40 Aux gas flow (arb. units): 8 Spray voltage (kV): 3.6 Tube lens (V): 120
ESI (-)	Capillary temperature (°C): 320 Capillary voltage (V): -40 Sheath gas flow (arb. units): 40 Aux gas flow (arb. units): 8 Spray voltage (kV): 2.7 Tube lens (V): -120

Table 6: UHPLC-HRMS parameters (ESI LTQ Orbitrap Discovery XL mass spectrometry connected to an Accela UHPLC system) used in the plasma metabolomics approach in both ESI (+) and ESI (-) modes.

4.3.7 Quality Control samples

For the untargeted metabolomics approach, the most common practice to monitor the experimental variability, as well as that of the analytical instrumentation, is to analyze quality control samples (QCs) inserted periodically in the analysis sequence. [254] The application of QCs provides a mechanism to evaluate the quality and calculate the analytical variance. A proper QC sample should represent the entire average of all the metabolomes analyzed in the metabolomics study. The ideal QC sample is a pooled sample, produced by mixing a small aliquot of each biological sample included in the metabolomics study. The pooled QC samples essentially contain all the metabolites present in the samples and could therefore be used to evaluate their variability due the analytical instrumentation. Frequently, the samples are of sufficient quantity in order to be analyzed both as unknowns and to be mixed as QC samples.

In the current study, the pooled QC methodology was employed. In details, each QC sample was prepared by mixing equal aliquots (30 μL) of each sample to be analyzed. The quantity of the aliquot of each sample was determined by the initial quantity of the plasma that was available to be analyzed. The combined aliquots from all the studied samples were thoroughly vortexed for 1 min to achieve protein precipitation following the same method as in the individual samples for analysis that was previously described. The analytical sequence was designed so as to include five blank samples and 2 QCs at the beginning of each batch and one QC and one blank placed intermittently every seven samples during the sequence.

Additionally, in order to ensure the quality of the obtained results, all the data have been subjected to normalization and correction with the application of algorithms and the aid of appropriate software. As a result, the obtained data could be evaluated regarding their distribution and repeatability, possible outliers could easily be identified whereas this is considered an excellent way to monitor the instrumental performance.

4.3.8 Data pre-processing

Data pre-processing was performed employing Proteowizard (http://proteowizard.sourceforge.net/), a set of modular and extensible open-source, cross-platform tools and software libraries that facilitate metabolomics data analysis, R software (https://www.r-project.org/), Microsoft Excel 2013, GraphPad Prism v 7.0.1 (https://www.graphpad.com/scientific-software/prism/) and the free

web platforms; (a) MetaboAnalyst 4.0 suite (http://www.metaboanalyst.ca) and (b) NOREVA (NORmalization and EVAluation of MS-based metabolomics data) http://idrb.zju.edu.cn/noreva/.

At first, with the aid of Proteowizard, the generated UPLC-HRMS raw files (*.raw) were converted into the mzXML format (*.mzXML) so as to be compatible for direct uploading to XCMS platform. Subsequently, the R-statistical programming language based software package IPO (Isotopologue Parameter Optimization), was employed in order to optimize the parameters used by XCMS since the outcome of XCMS data processing strongly depends on the parameter settings. [255] Subsequently, the XCMS R-package was used in order to preprocess data for high-throughput, untargeted metabolite profiling. XCMS incorporates novel nonlinear retention time alignment, matched filtration, peak detection, and peak matching.[256]–[258] The above described procedure generated a file (*.csv) containing a peak list of mass (m/z) and retention time (t_R) combined with corresponding intensities for all detected peaks for each uploaded data file. Until this step of analysis, data deriving from both ESI(+) and ESI(-) ionization, were analyzed following the same procedure. However, the consequent steps of analysis differ between the data deriving from positive and negative ionization.

Regarding ESI(+), the generated peak list was imported to the free web platform MetaboAnalyst 4.0 suite following the commands and instructions provided in each step. In details: [1st step] Removal of features with >50% missing values and application of the KNN (k-nearest neighbor) algorithm in order to impute the possible missing values; [2nd step] data-filtering through the QC samples using the relative standard deviation (RSD = SD/mean), as a robust estimator of the baseline noise, leading to the identification and removal of the variables that are unlikely to be of use when modeling the data. Normalization of the data was performed through the R-statistical language employing two suitable R-algorithms based on the application of multiple ISTDs to monitor the systematic error; Cross-Contribution Compensating Multiple Standard Normalization (CCMN) [259] and Normalization using Optimal selection of Multiple Internal Standards (NOMIS). [260] The results generated from the two approaches were evaluated and finally subjected to multivariate statistical analysis e.g. Principal Component Analysis (PCA), Partial Least Square-Discriminant Analysis (PLS-DA) and Orthogonal Projections to Latent Structures Discriminant Analysis (OPLS DA).

As far as the data occurring from ESI(-) are concerned, the XCMS generated peak list was imported to the free web platform NOREVA following the commands and instructions provided in each step. In details: [1st step] A dataset with QC

samples included was uploaded while data pre-processing was performed with 0.8 Filter criterion and 0.75 Bias-variance tradeoff, Local polynomial fits and KNN imputation algorithm; [2nd step] Data normalization was performed employing various methods (Pareto scaling, total sum etc. The results generated from the approaches were evaluated and finally subjected to multivariate statistical analysis e.g. PCA, PLS-DA and OPLS-DA.

Finally, all the .csv files deriving from both the above described procedures that included the generated peak list of mass and retention time as well as the corresponding intensities for all detected peaks from each data file, were imported to Microsoft Excel 2013 and were appropriately converted employing the commands; “ROUND”, “CONCATENATE” and “TRANSPOSE”.

4.3.9 Chemometrics and Data analysis

Chemometrics is the application of statistical and mathematical methods in order to facilitate the interpretation of chemical information and the correlation between quality parameters or physical properties and data deriving from analytical instruments. The aim of the chemometric analysis is to model patterns in the analyzed data while these models can then be applied to future data in the same way so as to predict parameters of the same quality.

The initial step of a chemometric analysis procedure is to discover the existence of any kind of clustering between the analyzed sample groups. Hence, PCA was the first multivariate statistical analysis technique applied, since PCA offers the ability to reveal the existing variation between the datasets and the possible outliers as well as the visual examination of the QC distribution in the 2D score plot.

Thus, the MS data were subjected to multivariate statistical analysis using SIMCA P+14.1 (Umetrics, Umea, Sweden) as well as the package MixOmics (http://mixomics.org/) [260] as implemented to the R statistical language, in order to perform PCA, PLS-DA and OPLS-DA analyses. Additionally to PCA analysis, PLS-DA is a valuable tool for the identification of the potential clustering between the studied populations and for the detection of the most influential metabolites that are responsible for the classification between the studied groups. PLS-DA and OPLS-DA results were validated by the application of permutation testing employing 100 random permutations for both methodologies. The optimal number of principal components allowed to characterize the statistical model adequately, resulted from the R^2 and Q^2 values while intending to minimize the difference between the two

values. Consequently, the variable importance in projection (VIP) values from the PLS-DA and OPLS-DA models that achieved a VIP scoring > 1.0 were identified. These VIP features (AMRT's coded as m/z_t_R) represented the metabolites/parameters that contributed the most in the clustering of the studied groups and the 20 first hierarchically ordered by the magnitude of the VIP variables were selected. Hence, attempting to adjust the model too closely to the data (e.g. selection of too many variables in a multivariate model) can lead to the introduction of substantial errors and to overfitting of the model which consequents to the reduction of its predictive power. Thus, the application of multivariate models requires the development of a parallel validation protocol based on univariate statistical analysis tools. [261]

Consequently, in order to statistically evaluate the results and to validate the importance of the VIP features from the MVA, several normality tests have been performed employing GraphPad Prism and Microsoft Excel 2013. The t-test verification was performed on Microsoft Excel 2013 while the p-value was set at ≤ 0.05 in order to point out a significant statistical difference between the two studied groups. ROC analysis and creation of univariate plots (box-plots) was performed employing GraphPad Prism. Furthermore, the R-statistical language package "sda" was employed for the construction of the t-test and the "CAT" scores so as to identify the significant features.

4.3.10 Annotation of potential metabolites

The significant VIP features (m/z_t_R) that fulfilled all the experimentally set criteria were compared with the aid of online databases in order to complement the selected m/z values and the corresponding metabolites. Specifically, the following free online MS spectra databases including spectra of metabolites were used; (a) METLIN Metabolomics Database (http://metlin.scripps.edu/index.php), (b) Human Metabolome Data Base (HMDB) (http://www.hmdb.ca/), (c) Kyoto Encyclopedia of Genes and Genomes (KEGG) (http://www.genome.jp/kegg/), (d) ChemSpider free chemical structure database (http://www.chemspider.com) and (e) LIPID MAPS (http://www.lipidmaps.org). Moreover, additional data were taken into consideration in order to evaluate the VIP features through the Identification point System proposed to the EC [262] e.g. isotopic pattern and RDB value which provides the unsaturation degree of a molecule. Finally, deconvolution has been performed to the acquired spectra, employing the Mass Frontier Spectral Interpretation Software 7.0 in order to elucidate potential in source fragmentation.

4.3.11 Metabolic Pathway Analysis

Metabolic Pathway analysis was performed employing the free online web platform MetaboAnalyst 4.0 in order to detect if any metabolic pathway was significantly affected as a consequence of the administration of the studied compound. The annotated *m/z* features that were statistically different among the populations were imported to the online platform as HMDB compound names and the potential participation of some features in the associated pathways was examined. The pathway analysis is based on three criteria; the selection of the correct pathway library regarding the studied organism (e.g. human, mouse, rat etc.), the pathway enrichment analysis algorithm and the topological analysis algorithm. [263] The p-value (deriving from the pathway enrichment analysis) indicates the statistical significance of the differentiated metabolites association within the pathway, while the pathway impact is calculated as the sum of the importance measures of the matched metabolites normalized by the sum of the importance measures of all metabolites in each pathway. [263] As a result, the pathways with a p-value < 0.05 or an impact value of >0.1 were considered to be significant.

4.4 RESULTS AND DISCUSSION

4.4.1 Metabolomic analysis of the samples in ESI-LTQ-Orbitrap Discovery XL mass spectrometer

4.4.1.1 Selection of Internal Standards

Prior to LC/MS analysis, the reconstitution of the previously extracted mice plasma samples was performed with a methanolic solution containing three Internal Standards (ISTDs) in order to eliminate the systematic error and to facilitate the normalization of the acquired data by the appropriate algorithms. In details, the selected ISTDs were 2-amino-phenol (MW: 109.0522), Yohimbine (MW: 354.1938) and Reserpine (MW: 608.2728) and they were selected as suitable ISTDs due to the fact that under no circumstances could they be related to the mice plasma metabolome. Furthermore, the main reason for using three ISTDs instead of one ISTD is that the aim of the study was to afford one ISTD in the retention time as well as in the MW axes (low, medium, high) thus facilitating the alignment procedure and the correction of the mass spectra in the total scan range of 100–1000 m/z. It also should be noted that all three compounds are ionized in both + and – ESI.

4.4.1.2 Mass Spectra Processing

Equally important to the state-of-the-art equipment in metabolomics, is the choice or even the development of techniques for the effective interpretation of the results. A first crucial part in such analyses is the normalization issue, where the most fit-for-purpose methodology needs to be implemented in order to eliminate the sample preprocessing and the instrumental drifts, in the effort to uncover the biological meaning of the experiment.

4.4.1.2.1 UHPLC-(+/-)ESI-HRMS analysis of the TC4 mice plasma samples

The MS data (.raw) acquired from the ESI-LTQ-Orbitrap were converted to .mzXML format in order to be compatible with the XCMS requirements according to the directions provided by the XCMS package in R-statistical language. The primary step for the processing of the MS data is to construct a matrix table including information about m/z and retention time of all the identified features. The XCMS package was selected as a suitable approach as it incorporates novel nonlinear retention time alignment, matched filtration, peak detection, and peak matching. Initially, the method has the ability to identify a large amount of endogenous features/metabolites and to calculate a nonlinear retention time correction profile for

each sample. Subsequently, the relative metabolite ion intensities are evaluated in order to detect potential alterations to some of the endogenous metabolites leading to the identification of potential biomarkers. [257]

Moreover, XCMS offers the ability to align many chromatographic traces, handle large data sets and discover novel differences between two sample groups provided that it has the right parameters. As a result, the key characteristic of a successful metabolomics approach is the optimization of the algorithm parameters in order to afford the best possible outcome of the data otherwise the result would be estimated as biased or even subjective. Consequently, another R-based program, namely IPO, was employed for the optimization of peak picking parameters. IPO automatically optimizes the XCMS parameters by using natural, stable ^{13}C isotopes. The optimum correction of the retention time is performed by minimizing the relative retention time differences within features whereas the optimization of the grouping parameters is performed by maximizing the number of features showing exactly one peak from each injection of a pooled sample. The different parameter settings are achieved by the design of experiments methodology (DoE) based on response surface modeling. [264] The outcome of the XCMS experiment, after optimization with IPO, was evaluated by detection of the ISTDs peaks in both ESI(-) and ESI(+) mode. As a result, the observation of the ISTDs in each analyzed sample as well as the QCs was essential in order to evaluate the XCMS result.

The .csv file as exported from the XCMS processing was accordingly modified in order to be imported to MetaboAnalyst 4.0 in an attempt to perform missing values estimation. The following step was the normalization of the data, an indispensable procedure that should indefinitely be incorporated into a metabolomics workflow. It is well known that each step of the metabolomics analysis can significantly affect the quantitative results and thus should be performed with great caution. Furthermore, the total sample amount or concentration of metabolites can be considerably diverse between the samples. Thus, it is vital to reduce or even minimize the effect of total sample amount variation on quantification of individual metabolites [265] as well as the systematic error caused by experimental conditions. Therefore, a fundamental step of the metabolomics workflow is to develop a normalization method in order to remove unwanted analytical variation occurring during the analytical measurements thus increasing the power of the forthcoming statistical analysis. [266] There are many different normalization protocols described in the literature therefore according to the experimental conditions the most adequate should be selected. [265] Hence, regarding the

current study, in an effort to utilize different exploration protocols for negative and positive MS data, various data normalization methods have been employed.

Regarding ESI(+) data, the .csv files containing the m/z_retention time data, as exported from MetaboAnalyst 4.0, were further imported to R-studio web platform and have been subjected to normalization by application of two normalization algorithms that were included in the R-package “Metabolomics”, NOMIS and CCMN. [267] The results obtained by the two normalization methods were subsequently evaluated by further multivariate statistical analysis importing the data in SIMCA P+ 14.1, where PCA and PLS-DA analyses were carried out. The most suitable normalization method was selected based on the clustering of the QCs. More specifically, the normalization approach that allowed a closer clustering of the QCs has been selected, as it reduced the possible instrumental instability improving the reliability of the analysis. Between the two normalization approaches, CCMN proved to be the most effective regarding both administration doses (50 mg/kg and 150 mg/kg) as it is clearly depicted in Figure 30.

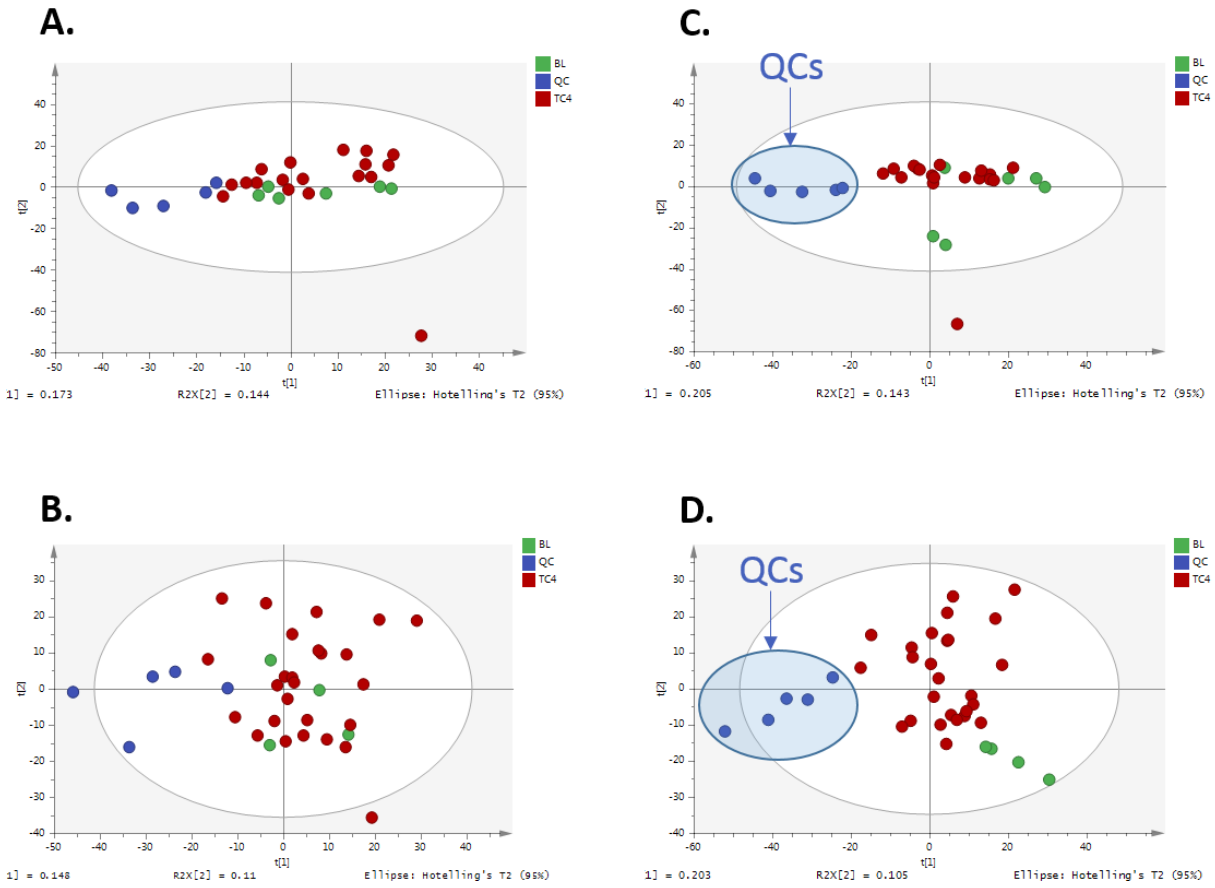

Figure 30: PCA scores plots of the plasma samples obtained from UHPLC-(+)ESI-HRMS analysis after UV scaling. Blue dots represent the QC samples while red and green dots represent the control and tested samples. (A) PCA scores plot of samples administered with 50 mg/kg after normalization with NOMIS (B) PCA scores plot of samples administered with 150 mg/kg after normalization with NOMIS (C) PCA scores

plot of samples administered with 50 mg/kg after normalization with CCMN (D) PCA scores plot of samples administered with 150 mg/kg after normalization with CCMN. Regarding both administration doses, the CCMN algorithm resulted in more tightly clustered QCs thus it was selected as a more suitable normalization approach.

Regarding ESI(-) data, the XCMS generated peak list was imported to the free web platform NOREVA where various normalization methods have been employed (Auto Scaling, Pareto scaling, total sum etc. The evaluation was performed by collectively considering five different criteria for assessing the normalization performance; (a) Method's capability of reducing intragroup variation among samples was calculated by the following common measurements including pooled coefficient of variation (PCV), pooled estimate of variance (PEV) and pooled median absolute deviation (PMAD) (b) Method's effect on differential metabolic analysis where the differential significance of metabolites between 2 groups was measured by P-values (c) Method's consistency of the identified metabolic markers among different datasets, where a consistency score was defined to quantitatively measure the overlap of identified metabolic markers among different partitions of a given dataset (d) Method's influence on classification accuracy where Receiver Operating Characteristic (ROC) curve together with Area Under the Curve (AUC) values based on support vector machine (SVM) were provided and finally (e) Level of correspondence between normalized and reference data.

The results generated from the approaches were evaluated and finally, among the studied normalization approaches, Pareto scaling proved to be the most suitable one as it revealed a tighter clustering of the QC samples. (Figure 31)

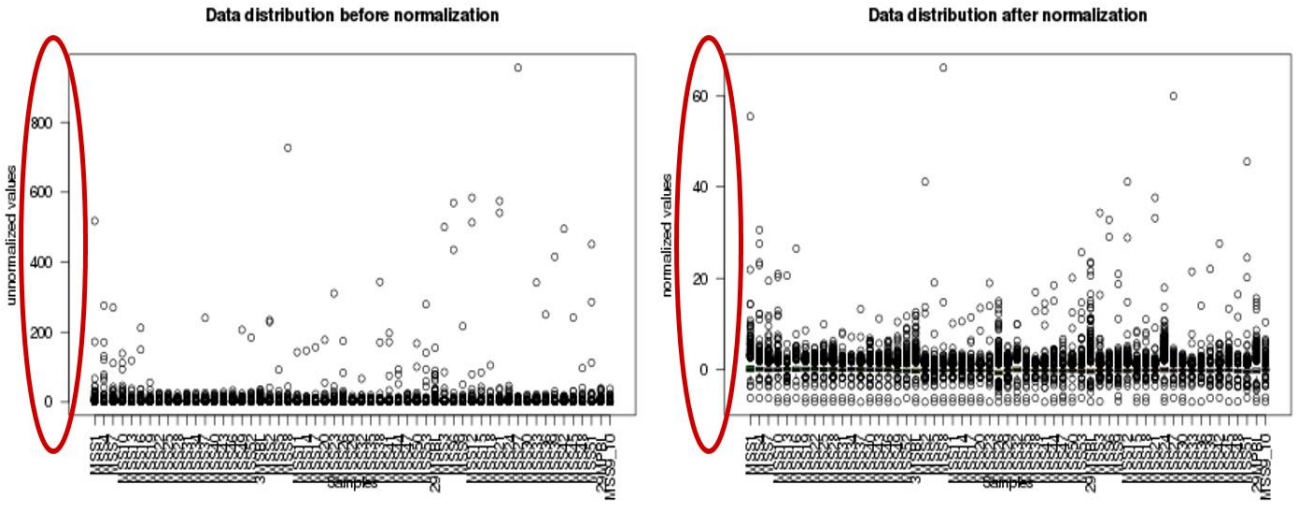

Figure 31: Data distribution of UHPLC-(-)ESI-HRMS data before and after normalization with Pareto scaling from the web-online platform NOREVA thus indicating the necessity to perform normalization procedures before further handling the MS data

4.4.1.3 Chemometric analysis of ESI-LTQ-Orbitrap data

In an attempt to detect a potential tendency in the clustering of the studied MS data, a number of multivariate statistical methodologies have been employed e.g. PCA, PLS-DA, OPLS-DA.

4.4.1.3.1 Multivariate analysis of ESI(+) data of mice plasma samples after *i.p.* administration of TC4

Initially, PCA was the first-pass methodology in order to identify chemical differences between high-dimensional spectral measurements and to detect a potential clustering between the studied groups. Furthermore, PCA experiments were also applied so as to explore the QC clustering and to verify the stability in the analytical conditions and the instrumental repeatability. In order to achieve the best clustering capacity, many parameters have been evaluated as an attempt to describe the studied model in the best possible way without overfitting. PCA has been performed with many combinations in the experimental parameters such as employing different scaling techniques (e.g. UV, Pareto). As it is clearly depicted in Figure 32, the UV scaling methodology offered an enhanced clustering capacity between the treated and untreated groups in both studied doses, thus it was selected as a the most suitable approach.

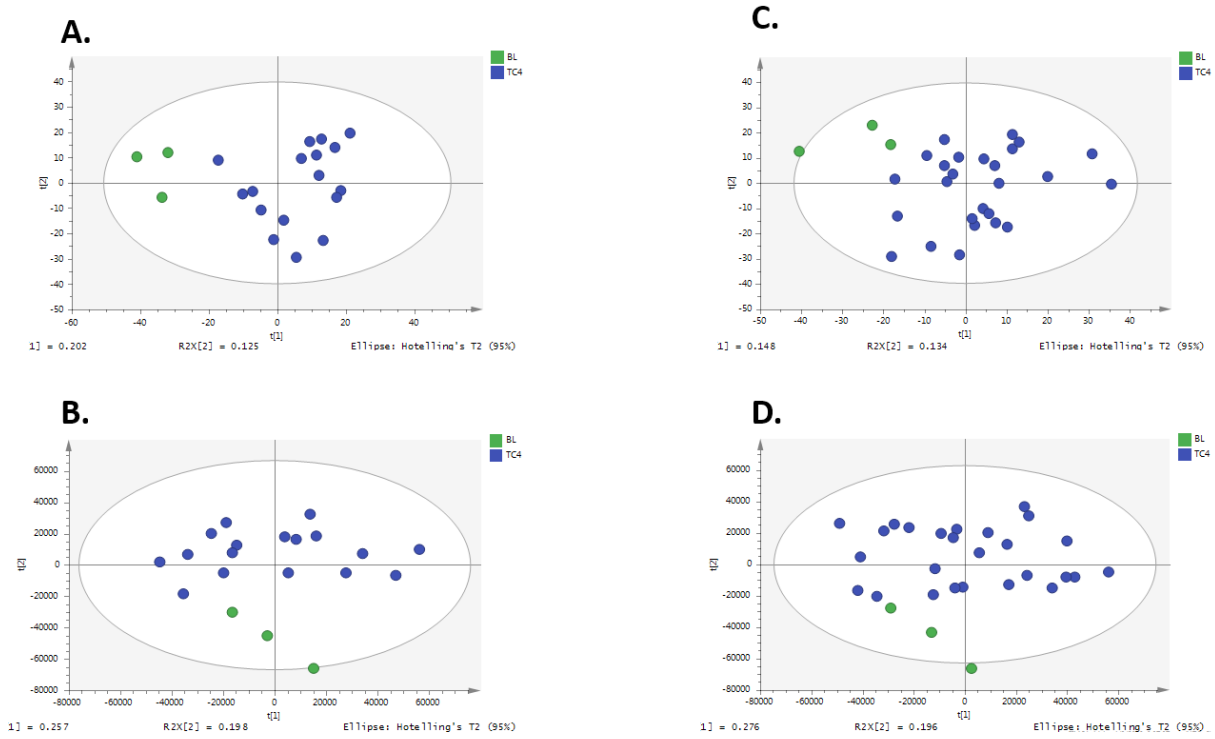

Figure 32: PCA scores plots of the plasma samples obtained from UHPLC-(+)ESI-HRMS analysis after UV and Pareto scaling in both administration doses. Blue dots represent the treated samples while green dots represent the control samples. PCA scores plot of samples administered with 50 mg/kg after (A) UV scaling and (B) Pareto scaling; PCA scores plot of samples administered with 150 mg/kg after (C) UV scaling and (D) Pareto scaling. Regarding both scaling approaches the UV scaling methodology offered an enhanced clustering capacity between the treated and untreated groups in both studied doses, thus it was selected as a the most suitable approach

For all the studied models, the number of PCs employed for the description of the models was limited to the minimum number in order to explain the variance sufficiently since the inclusion of more PCs would only lead to overfitting. As a result, regarding both administration doses, only the first five PCs have been taken into consideration. The evaluation of the PCA model was performed by the R^2X (cum) and Q^2X (cum) values. R^2 is the percent of variation of the training set with PCA that is explained by the model and it is a measure of the goodness of fit, i.e. how well the model fits the data. Q^2 is the percent of variation of the training set with PCA that is predicted by the model according to cross validation while Q^2 indicates how well the model predicts new data, employing in the current case the notion of 7-fold cross validation. For the classification, the R^2X (cum) and Q^2X (cum) values were: [For dose 50 mg/kg] R^2=0.525 and Q^2=0.178; [For dose 150 mg/kg] R^2=0.544 and Q^2=0.22.

Additional classification of the data was achieved by the application of further supervised multivariate statistical methodologies i.e. PLS-DA and OPLS-DA. As it is clearly depicted in Figure 33, there is a distinct clustering between the treated and the untreated populations while preliminary data indicate also an underlying "interior" clustering among the studied time points. (Figure 33) However, there is a need for more animals in each studied time point in order to be able to draw safe conclusions.

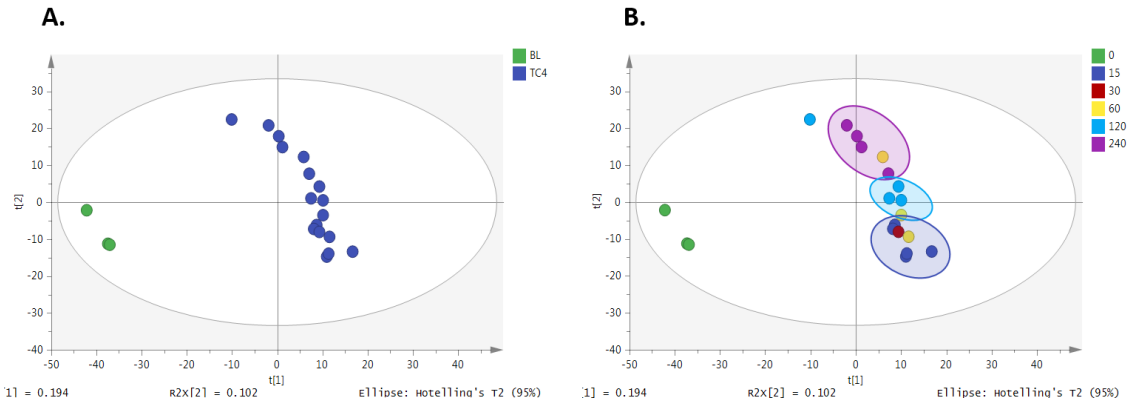

Figure 33: PLS-DA scores plot of the plasma samples (50 mg/kg) obtained from UHPLC-(+)ESI-HRMS analysis. Blue dots represent the treated samples while green dots represent the control samples. (A) Distinct clustering between treated and untreated samples is observed. Furthermore, (B) preliminary data point towards an underlying interior clustering among the studied time points (0' -240').

For 50 mg/kg dose , the R^2X (cum), R^2Y (cum) and Q^2X (cum) values of the PLS-DA model were 0.363, 0.997 and 0.902 respectively, employing 3 principal components in ESI(+); for the 150 mg/kg dose, the respective values of the PLS-DA model were 0.307, 0.987 and 0.865, employing 3 principal components.

However, PLS-DA is a multivariate methodology that will nearly always yield scores-space classification based on the assigned group associations while eagerly overfits the data and forces separation between experimental groups, therefore thorough validation is indispensable. [268] Moreover, careless use of the multivariate methodologies without validation or awareness of the association of PCA with PLS models can lead to statistically insignificant conclusions about the underlying chemistry.[269] Consequently, in an effort to verify the PLS-DA and OPLS-DA analyses and to validate the clustering results, the "clValid" package, as implemented in R, was employed in combination with permutation testing employing 100 random permutations. The R-package "clValid" evaluates the clustering results taking into consideration three values: (a) Connectivity; which corresponds to what extent items are placed in the same cluster as their nearest neighbors in the data space (b) Dunn index; which indicates the separation of the clusters; if the data set contains compact and well-separated clusters, the diameter of the clusters is expected to be small and the distance between the clusters is expected to be large and (c) Silhouette analysis; which measures how well an observation is clustered and it estimates the average distance between clusters thus observations with a large S_{index} (almost 1) are very well clustered. [270] The "clValid" plots are presented in Figure 34 and the internal validation values (Connectivity, Dunn index and Silhouette analysis) are presented in Table 7.

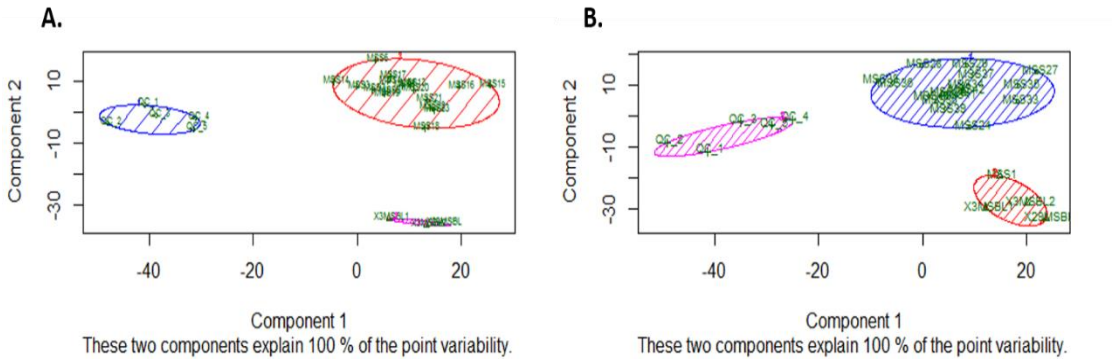

Figure 34: Clustering plots of PLS-DA models obtained from UHPLC-(+)ESI-HRMS analysis, employing R-package "clValid". (A) Dose 50 mg/kg; (B) Dose 150 mg/kg

Ionization	Administration Dose	Internal Validation Index	Value
ESI (+)	50 mg/kg	Connectivity	8.7941
		Dunn	0.5465
		Silhouette	0.6703
	150 mg/kg	Connectivity	8.842
		Dunn	0.5633
		Silhouette	0.7031
ESI (-)	50 mg/kg	Connectivity	4.2869
		Dunn	0.7863
		Silhouette	0.7008
	150 mg/kg	Connectivity	4.3869
		Dunn	0.6783
		Silhouette	0.7709

Table 7: The optimal values of the internal validation; Connectivity, Dunn and Silhouette as calculated by the clValid packet in ESI(+) and ESI(-).

Subsequently, a supervised OPLS-DA model has been applied in order to achieve enhanced classification between the studied groups regarding the TC4 administration and to enable the identification of the metabolites responsible for the clustering. As it is clearly depicted in Figure 35, the applied OPLS-DA model afforded an adequate discrimination of the studied groups thus demonstrating that the metabolic profiles of the treated mice have significantly been altered due to the administration of TC4 in both doses. For dose 50 mg/kg, the R^2X (cum), R^2Y (cum) and Q^2X (cum) values of the corresponding OPLS-DA model were 0.363, 0.997 and 0.851 respectively, whereas for dose 150 mg/kg, the R^2X (cum), R^2Y (cum) and Q^2X (cum) values of the corresponding OPLS-DA model were 0.307, 0.987 and 0.88 respectively indicating very good clustering.

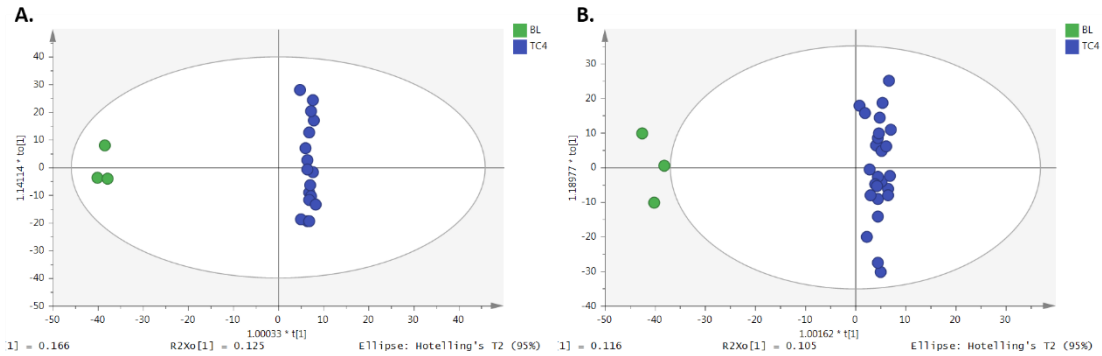

Figure 35: OPLS-DA scores plots of the plasma samples (A) 50 mg/kg and (B) 150 mg/kg, obtained from UHPLC-(+)ESI-HRMS analysis. Blue dots represent the treated samples while green dots represent the control samples. Excellent clustering between treated and untreated samples is observed.

4.4.1.3.2 Features' selection and Identification of metabolites

The next step of the study was to select the significant features that contributed the most to the discrimination of the studied groups and at the end, to annotate the metabolites that were significantly altered due to the *i.p.* administration of TC4.

With the aid of SIMCA P+ 14.1 software, based on the PLS-DA models, a list of features with a VIP value >1.0 that contributed the most to the clustering of the groups was created. Furthermore, an S-plot was employed in order to figure out visually the features responsible for the classification. As it is demonstrated in Figure 36, the more distant from the center and closer to the vertical axes of the S-plot a metabolite is, the more it contributes to the separation of the groups (x axis) with high reliability (y axis).

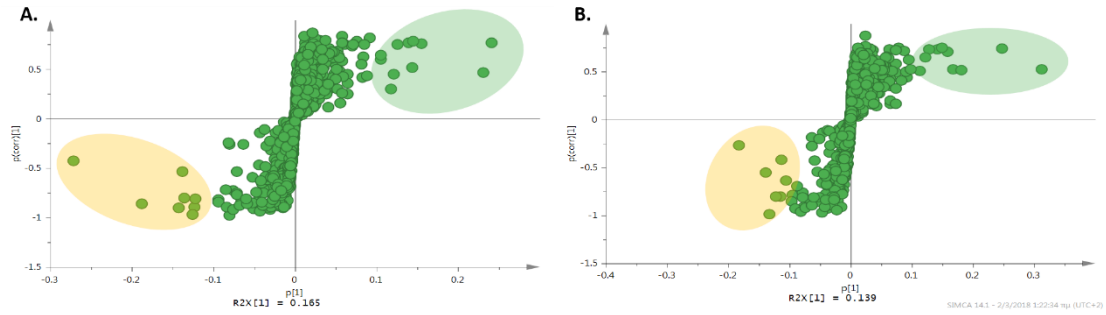

Figure 36: S-plots from OPLS-DA (Pareto) modes for treated and untreated groups subjected in UHPLC-(+)ESI-HRMS analysis (A) 50 mg/kg and (B) 150 mg/kg. The greed dots represent the metabolites contributing the most to the separation of the groups.

In order to validate the prediction accuracy during statistical tests, and to assess the risk of the current PLS-DA model being spurious, permutation tests were performed allowing 100 random permutations. (Figure 37) The permutation tests demonstrated that the goodness of fit as well as the predictive ability (R^2 / Q^2) of the studied models are higher than those of the permuted ones in both administration doses. Moreover, it is worth noting that when all green R^2-values to the left, each one corresponding to random permuted model, are lower than the original point to the right, this is also an indication for the validity of the original model. In combination with another essential prerequisite, indicating that all blue Q^2-values, the permuted models, to the left should be lower than the original points to the right while the blue regression line of the Q^2-points should intersect the vertical axis (on the left) at, or below zero.

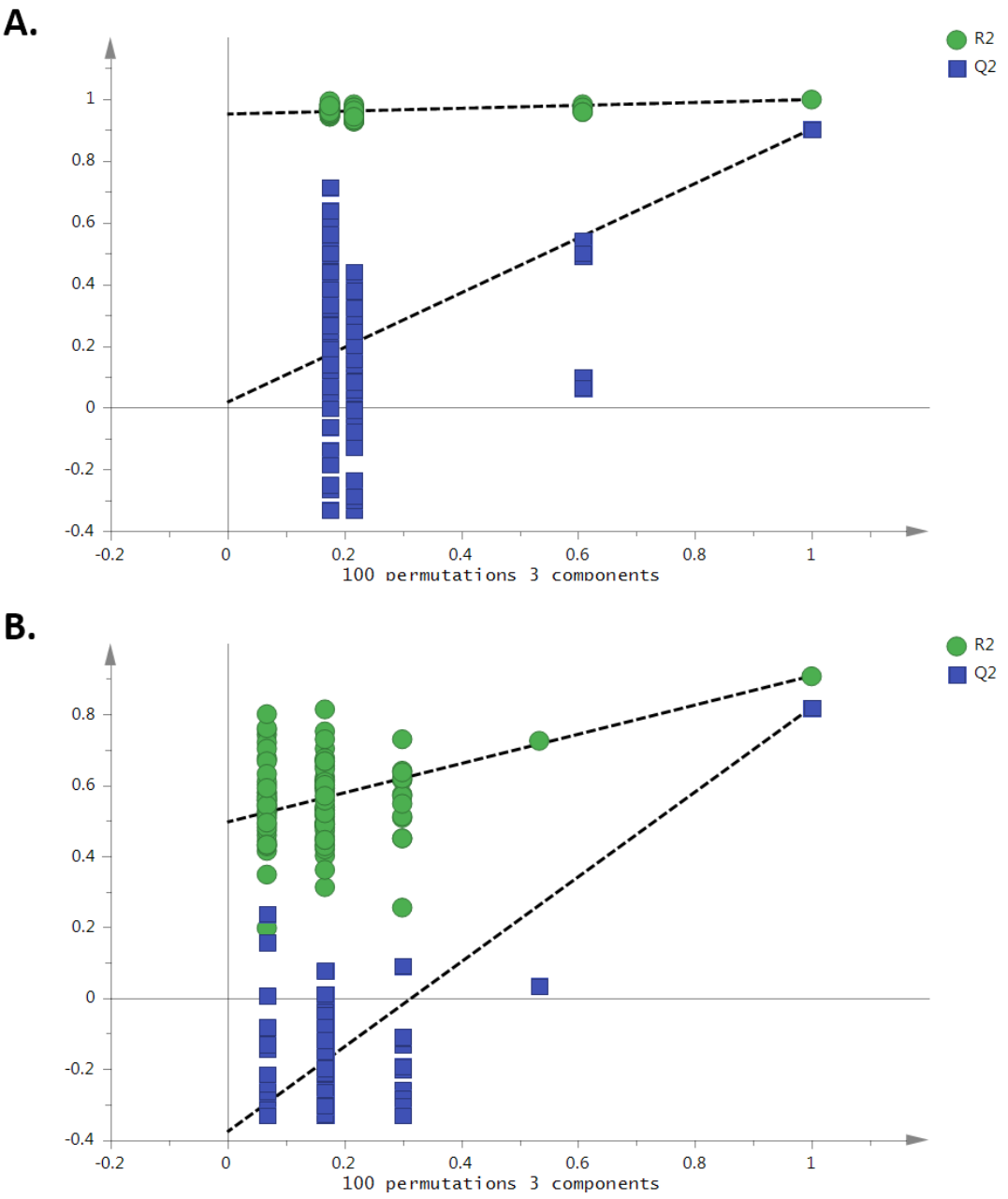

Figure 37: Permutation tests, allowing 100 random permutations, for PLS-DA models performed in samples subjected to UHPLC-(+)ESI-HRMS analysis (A) 50 mg/kg and (B) 150 mg/kg.

The selection of the features that contributed to the discrimination of the studied groups was based on the following statistical tests in order to minimize the number of features. With the aid of the R-package “sda” the t-test and the “CAT” scores were constructed where the first 25 features of either t-test or cat-test were considered to be significant. In association with the VIP list as well as the distinct metabolites as indicated by the S-plot, a list of all the significant metabolites/features was constructed regarding each studied case. Finally, as a further verification step of the selected features, ROC analysis and univariate statistical analysis visualized by the creation of univariate plots (box-plots) was performed employing GraphPad Prism, in order to evaluate the differences between the studied groups.

4.4.1.3.3 Multivariate analysis of ESI(-) data of mice plasma samples after *i.p.* administration of TC4

A different approach was selected in order to explore the initial information from the ESI(-) data. The normalized data as exported from the NOREVA web platform, were subjected to multivariate statistical analysis in order to identify potential clustering between the treated and untreated populations.

Initially, PCA experiments were performed in both administration datasets in order to obtain visual estimation of the quality of the acquired data. Many parameters have been assessed e.g. scaling method (UV or Pareto) and calculation of the optimal R^2 and Q^2 values, so as to adequately describe the largest possible variance contribution of the model without overfitting it. Finally, the PCA models created with Pareto scaling offered tighter clusters of the groups, enabling enhanced classification. As depicted in Figure 38, PCA models afforded a clear separation of the studied groups, thus demonstrating the ability of PCA to cluster the examined samples after TC4 administration. Therefore, since a clear group separation in scores-space is obtained, allowed further data analysis with supervised methodologies such as PLS-DA and OPLS-DA.

The evaluation of the PCA model was performed by the R^2X (cum) and Q^2X (cum) values. For the classification, the R^2X (cum) and Q^2X (cum) values were: [For dose 50 mg/kg] R^2=0.506 and Q^2=0.112; [For dose 150 mg/kg] R^2=0.4 and Q^2=0.087. However, regarding dose 150 mg/kg, the low Q^2 value indicates poor predictive ability of the model.

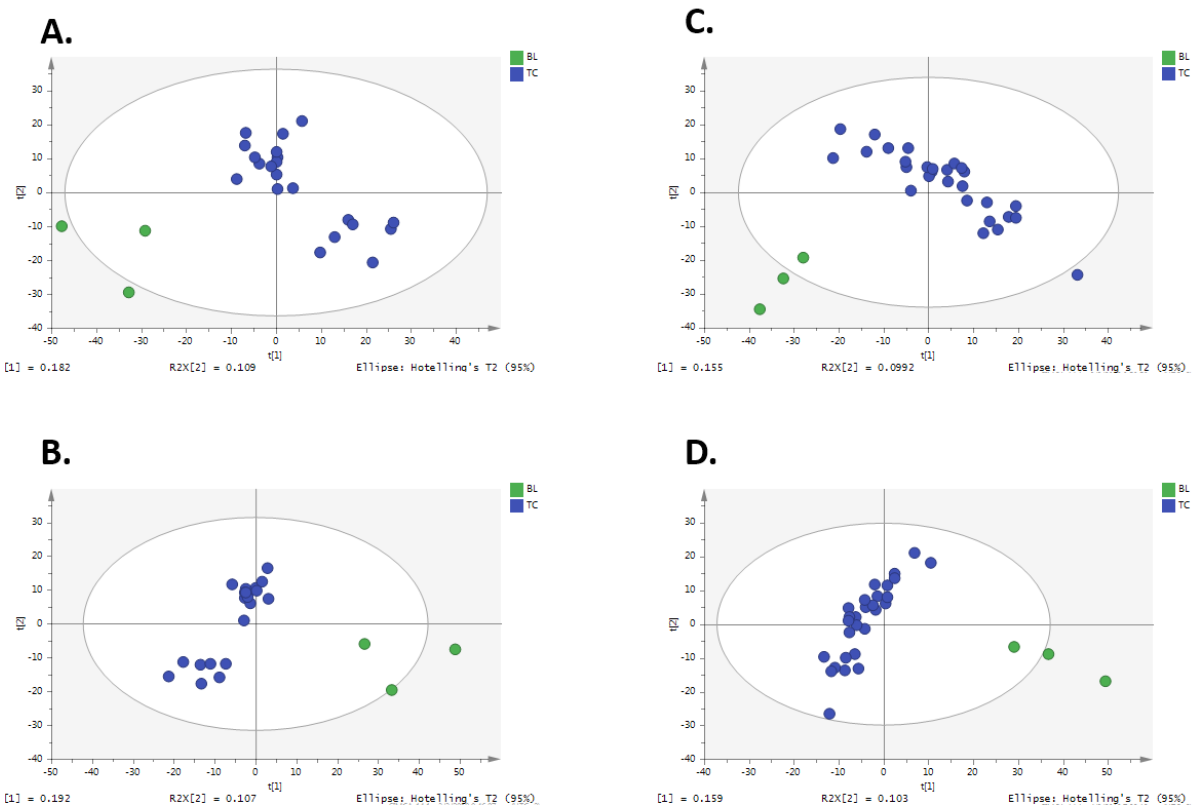

Figure 38: PCA scores plots of the plasma samples obtained from UHPLC-(-)ESI-HRMS analysis after UV and Pareto scaling in both administration doses. Blue dots represent the treated samples while green dots represent the control samples. PCA scores plot of samples administered with 50 mg/kg after (A) UV scaling and (B) Pareto scaling; PCA scores plot of samples administered with 150 mg/kg after (C) UV scaling and (D) Pareto scaling. Regarding both scaling approaches, Pareto scaling methodology offered an enhanced clustering capacity between the treated and untreated groups in both studied doses, thus it was selected as a the most suitable approach

In an attempt to achieve the maximum differentiation between the studied groups leading to robust classification, the PLS-DA and OPLS-DA models have been created. The combined application of PCA and (O)PLS-DA to spectral datasets yields valuable insights on both general spectral trends (PCA) and group-predictive spectral features (PLS). [269] For the PLS-DA model, UV scaling was performed in order to afford sufficient clustering between treated and untreated groups. According to the PLS-DA model, there is a distinct clustering between treated and untreated groups while for dose 50 mg/kg, the R^2X (cum), R^2Y (cum) and Q^2X (cum) values of the PLS-DA model were 0.318, 0.97 and 0.404 respectively, employing 3 principal components in ESI(+); Considering dose 150 mg/kg, the R^2X (cum), R^2Y (cum) and Q^2X (cum) values of the PLS-DA model were 0.234, 0.914 and 0.646 respectively, employing 2 principal components.

As it is previously reported for the of ESI(+) data analysis, further verification of the PLS-DA and OPLS-DA models and validation of the clustering results was performed with application of the “clValid” R package and the results were further verified by permutation testing employing 100 random permutations. The “clValid” plots are presented in Figure 39 and the internal validation values (Connectivity, Dunn index and Silhouette analysis) are presented in Table 7.

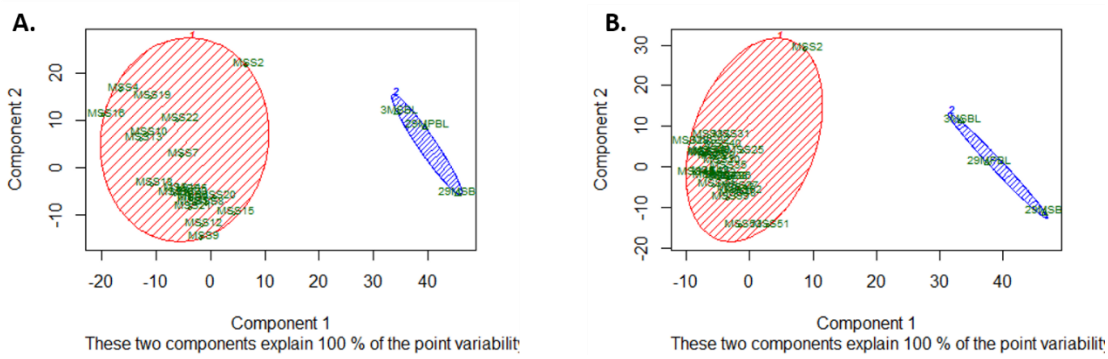

Figure 39: Clustering plots of PLS-DA models obtained from UHPLC-(-)ESI-HRMS analysis, employing R-package “clValid”. (A) Dose 50 mg/kg; (B) Dose 150 mg/kg

Subsequently, in an effort to perform a more sufficient class estimation of the analyzed data, PLS-DA analysis was performed with the intention to achieve better clustering of the studied groups. As it is depicted in Figure 40, PLS-DA models exhibited discrimination between the examined populations (treated *vs.* untreated), while the observed samples tend to form separate and distinct groups and to be further categorized according to the time point of the sacrifice. However, no specific clustering was observed when a classification based on the sex of the animals was attempted. (Figure 40)

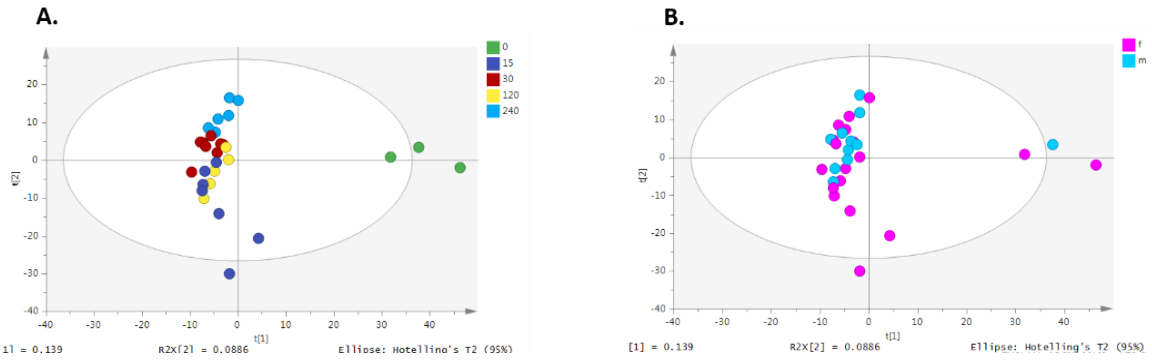

Figure 40: PLS-DA scores plots of the plasma samples of dose 150 mg/kg, obtained from UHPLC-(-)ESI-HRMS analysis colored (A) according to the time point of the sacrifice (min) and (B) according to the sex of the animals participating in the study. Regarding the time point analysis, a decent clustering was observed among the studied time points whereas considering the sex of the animals no specific clustering was observed.

4.4.1.3.4 Multilevel-Multivariate Analysis of ESI(+/-) data

As previously described, the MVA analysis of the ESI(+/-) data was capable of providing discrimination between the treated and untreated populations. However, in almost all cases, supervised approaches such as PLS-DA as well as OPLS-DA did not reveal any “inner” clustering regarding either the different administration time points or the sex of the administered animal. As the biological variation is much larger than the variation due to the administration of TC4, it could actually be considered as the driving force of the PLS-DA analysis. Consequently, since the existing variations among the subjects outweigh the changes induced by the administration of TC4, the Multi-Level-Multivariate Analysis (ML-MVA) might offer the chance to separate the variation within the subjects from the variation among them, in order to find the variation with the highest impact on the data sets, to achieve better and more clear clustering of the studied groups and finally to enable the identification of possible metabolites as those contributing the most to the clustering as well as the differentiation of the groups. Therefore, the total variance is split into its constituent parts, a fact that allows the detection of the effects or the alterations caused in the metabolome by the administration of TC4.

For the ML-MVA the R-package “mixOmics” was employed as it offers a wide range of unique multivariate methods. In more details, in the same data sets as in the classical MVA, a ML-PLS-DA analysis was performed with the aid of “mixOmics”, resulting in clear clustering between the studied groups. In order to investigate the effect of the time-point of sacrifice within the subjects, the variation

caused by the sex of the animals of the study was deducted while the variation within the subjects (treated *vs.* untreated animals) was kept unaffected. Interestingly, as it is presented in Figure 41, a ML-PLS-DA model proved to be significantly informative for the clustering of the groups regarding the time-point of the sacrifice. Although, the necessity for more samples is inevitable in order to reach safe conclusions, a sufficient clustering is observed as well as the fact that the clusters of the samples follow an almost circular/elliptic pattern indicating the time progression of the metabolome.

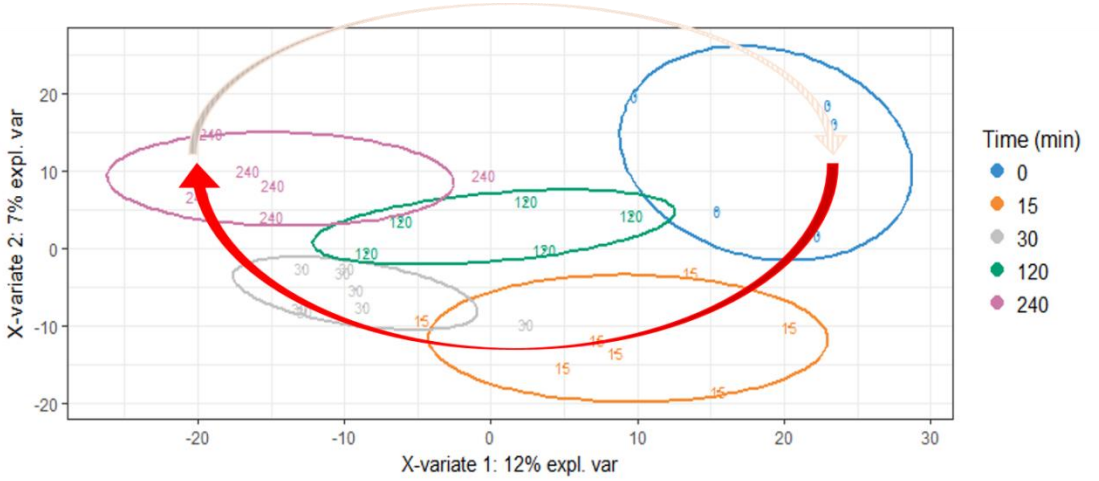

Figure 41: ML-PLS-DA scores plots of the plasma samples of dose 150 mg/kg, obtained from UHPLC-(-)ESI-HRMS analysis colored according to the time point of the sacrifice (min). Regarding the time-point analysis, an excellent clustering was observed among the studied time-points. Furthermore, the clusters of the samples follow an almost circular/elliptic pattern indicating the time progression of the metabolome.

Moreover, in an attempt to investigate the effect of the sex of the animals regardless of the time-point of the sacrifice, another ML-PLS-DA model was evaluated. In this case, ML-sPLS-DA (sparse PLS-DA) was performed in order to detect the features (in “mixOmics” they are called ‘loadings’) that are responsible for the clustering and allow the sufficient variable selection. Hence, similarly to the first approach to split the total into separate sub-variances, the applied ML-sPLS-DA model succeeded in performing classification leading to the creation of two separate groups (male, female). (Figure 42)

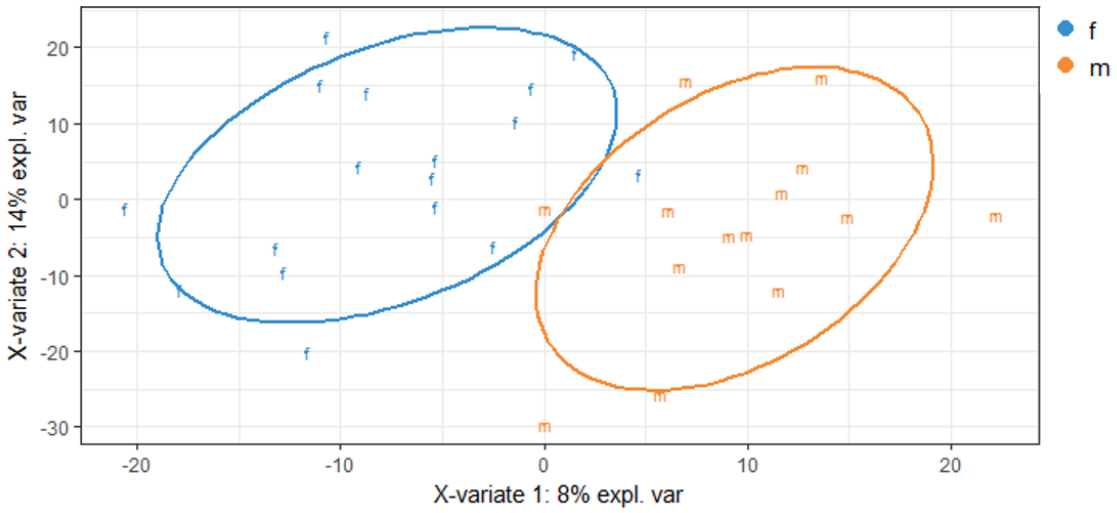

Figure 42: ML-sPLS-DA scores plots of the plasma samples of dose 150 mg/kg, obtained from UHPLC-(-)ESI-HRMS analysis colored according to the sex of the administered animals. Blue dots represent the male mice while orange dots represent the female mice samples. Excellent clustering was observed among the studied populations.

Consequently, considering the clustering results of the two ML-(s)PLS-DA approaches in comparison with the results of the previously described PLS-DA models, it is evident that the administration effect has been relatively concealed under the variance caused by the time point of the sacrifice as well as the sex of the administered animals. Similar results have been observed regarding the ML-(s)PLS-DA approaches performed on the results deriving from the ESI(+) ionization. Thus, in order to reveal the outcome of the administration of TC4 alone, excluding the variance deriving from other factors and essentially evaluate the loadings responsible for the differentiation between the studied time points, the deduction of the parallel co-existing data variations is indispensable.

4.4.2 Annotation of potential metabolites

4.4.2.1 Evaluation of the selected features from ESI(+/-)

As it was previously described, the applied ML-(s)PLS-DA models were capable of achieving sufficient clustering of the metabolic profiles of the studied populations in both ionization modes. Furthermore, a successful ML-(s)PLS-DA approach leads to the identification of the metabolites that contributed the most to the discrimination of the groups. As a result, the loadings deriving from these models are subjected to further analysis and finally a created list of the most significant loadings, indicates the most important metabolites that are significantly altered after the administration of TC4.

The aforementioned significant loadings are selected by the ML-(s)PLS-DA plot of variables. In more details, the plot of loadings is an elliptic diagram with an external ellipsis including all the loadings and an adjustable same-centered internal one that is manipulated according to a desired level of metabolite significance. The initial distance of the two ellipses started from 0.9 and it was manually decreased by 0.1 each time. All the significant variables were included in the space between the two ellipses, while the most important ones were located between the ellipses located to the space between 0.9 and 1. A corresponding plot of variables deriving from ML-(s)PLS-DA approach for the clustering of groups according to their sex is depicted in Figure 43.

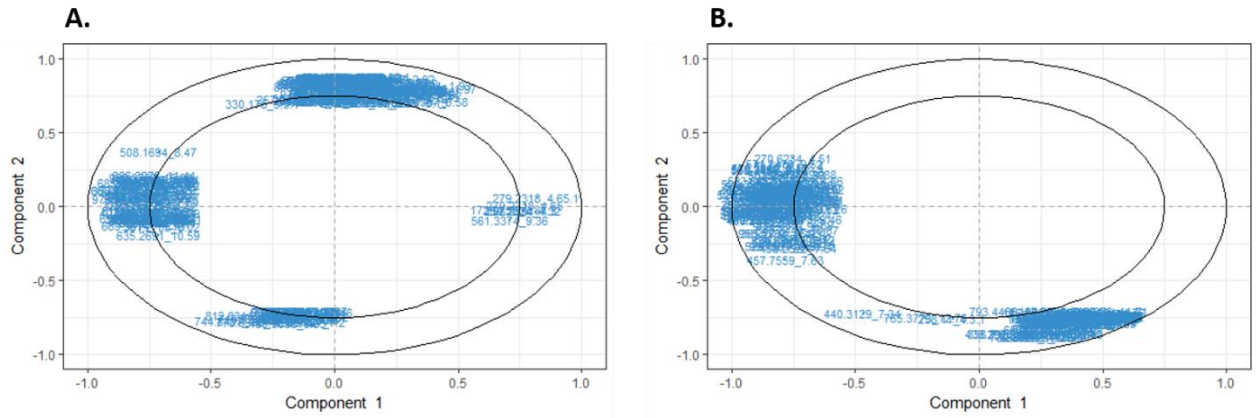

Figure 43: Plots of variables deriving from ML-PLS-DA approaches for the clustering of groups as far as A. their sex and B. the time-point of the sacrifice are concerned. Data obtained from UHPLC-(-)ESI-HRMS analysis.

All the loadings contributing the most to the classifications described above (according to sex and according to time-points) were further evaluated by univariate analysis, in order to verify their actual significance and creating a list of potential metabolites. The selected features are included in Table 8 along with additional information (e.g. m/z, t_R, $\Delta_{(ppm)}$, RDB etc.). Analysis of the putative adducts (e.g. M-H, M+Na-2H, M+Cl, M+K-2H, M+FA-H, M+H, M+Na, M+FA etc.) was also performed. The adduct annotation was performed with the aid of the R-package "CAMERA" which enables the detection of adducts, fragments and isotopes and finally indicates the actual molecular weight of a metabolite.

Subsequently, the following step was to identify the statistically significant VIP features deriving from all the above described procedures. Each of the previous ML-MVA approaches resulted in the creation of a feature list contributing to the separation of the studied groups. However, although these metabolites are estimated as "key-features" for the group clustering, this estimation could be

incorrect if these features do not pass a series of statistical tests. As a result, all the VIP features were subjected to further univariate analysis techniques in order to verify their actual importance, thus a significantly shrunk list of potential metabolites was created, proving the need of additional verification steps in order to draw safe conclusions. Therefore, the t-test and q-values for all the selected VIP features from all the individual ML-MVA techniques, have been estimated [271]–[273]; t-test calculates the statistical significance of the change of the mean (p-value) before and after administration and provides the probability of a false positive on a single test. The q-value is a p-value that has been adjusted for the False Discovery Rate (FDR) while the FDR is the proportion of false positives expected from a test. Practically, the FDR approach to p-values allocates a modified p-value for each test which is translated as the "q-value". Furthermore, a p-value of 0.05 (or 5%) means that 5% of the performed test will result in false positives, however a q-value of 0.05 (or 5%) indicates that 5% of the already significant results (those owing a p-value > 0.05) are false positives. Thus, the initial VIP lists were significantly reduced leading to the estimation of only the truly important features. The t-test has been performed with Microsoft Excel 2013 and the q-values have been estimated by the online platform "q-value estimation for FDR control" http://qvalue.princeton.edu/ , an implementation of the qvalue R package.

As a result, the features that fulfilled both the above described criteria were subjected to Receiver Operating Characteristic (ROC) analysis and then univariate plots (box-plots) were created. The Area Under the ROC Curve (AUC) provides a measurement of the accuracy of the model where, the closer an AUC value to 1.0 is, the more valid the diagnostic ability of discrimination between groups is. For each of the selected variables, an AUC value of ~1.0 represents the perfect test while an AUC value of 0.5 or less indicated random discrimination. Therefore, ROC analysis employing GraphPad Prism was performed, in order to evaluate the discriminating capacity of each significant feature between treated and untreated groups. The results indicated that the selected significant features were capable of discriminating the treated with TC4 population from the untreated ones.
(Figure 44, Figure 45, Figure 46, Figure 47, Figure 48, Figure 49, Figure 50, Figure 51)

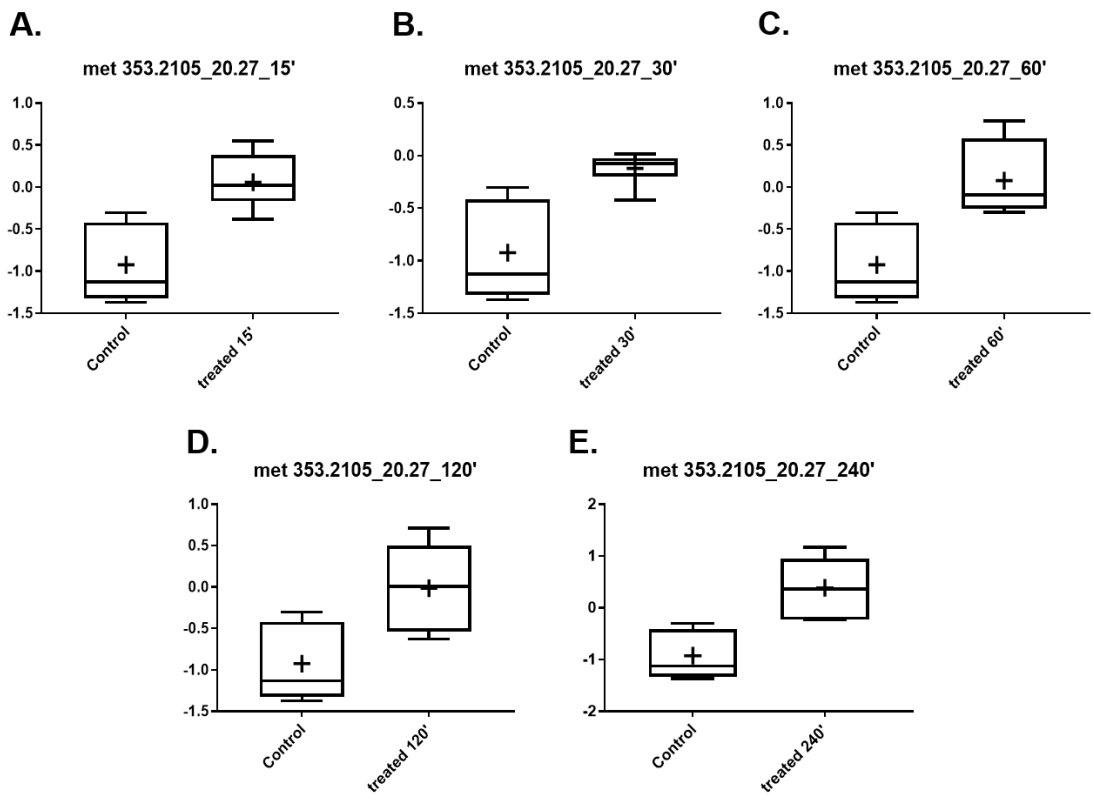

Figure 44: Box plots of the variable 353.2105_20.27 which is progressively altered depending on the time point of the sacrifice (A-E). This metabolite derives from the VIP scoring after univariate statistical analysis between the control and TC4 administered group (150 mg/kg) employing UHPLC-HRMS (Orbitrap) analysis in negative ion mode. The crosses correspond to the means while the horizontal lines that divide the boxes into two parts represent the medians. The upper and lower limits of the boxes represent the third and first quartiles respectively. The upper and lower whiskers represent scores outside the middle 50% and indicate the maximum values of each group.

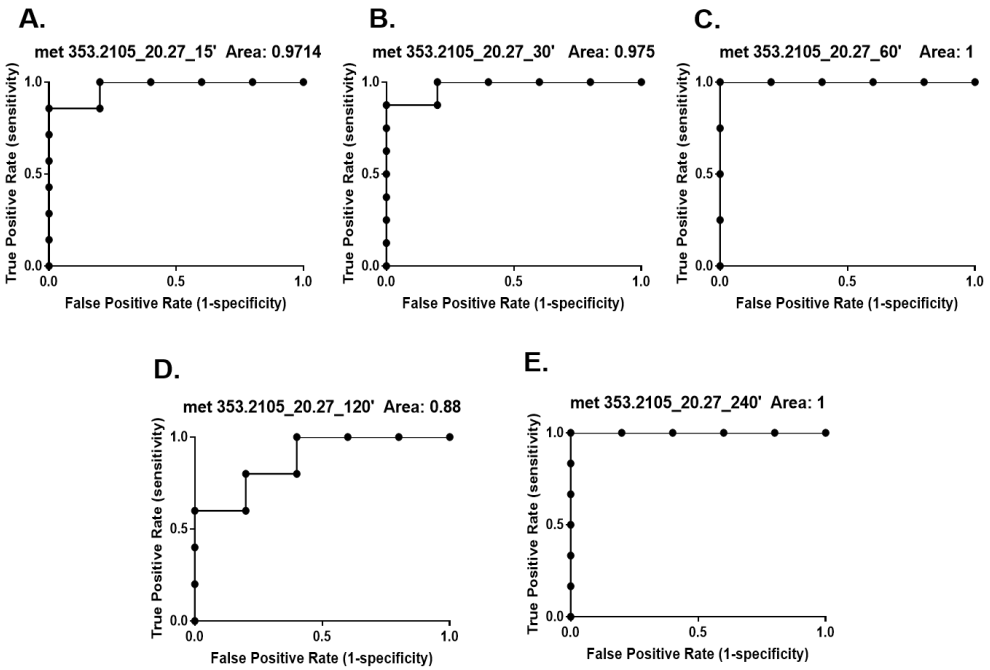

Figure 45: ROC curves of the variable 353.2105_20.27 regarding the time points of sacrifice have been constructed employing the GraphPad Prism. All ROC curves (A-E) bared an acceptable AUC value > 0.5 indicating that the selected significant feature was capable of discriminating the treated with TC4 population from the untreated ones in all studied time points.

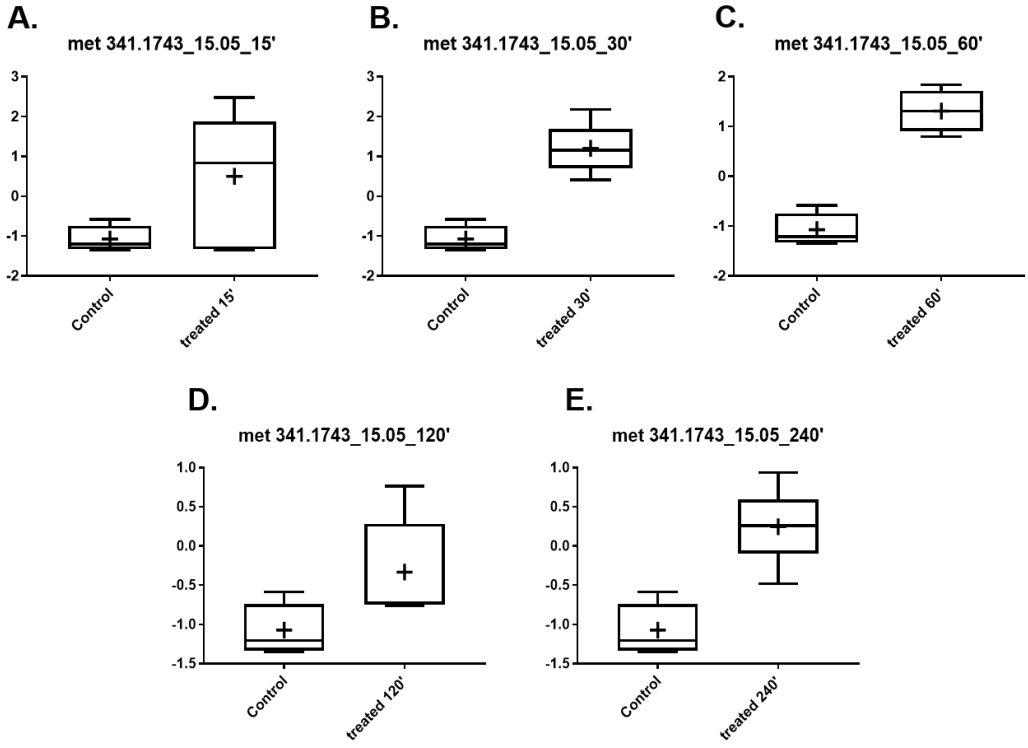

Figure 46: Box plots of the variable 341.1743_15.05 which is progressively altered depending on the time point of the sacrifice (A-E). This metabolite derives from the VIP scoring after univariate statistical analysis between the control and TC4 administered group (150 mg/kg) employing UHPLC-HRMS (Orbitrap) analysis in negative ion mode. The crosses correspond to the means while the horizontal lines that divide

the boxes into two parts represent the medians. The upper and lower limits of the boxes represent the third and first quartiles respectively. The upper and lower whiskers represent scores outside the middle 50% and indicate the maximum values of each group.

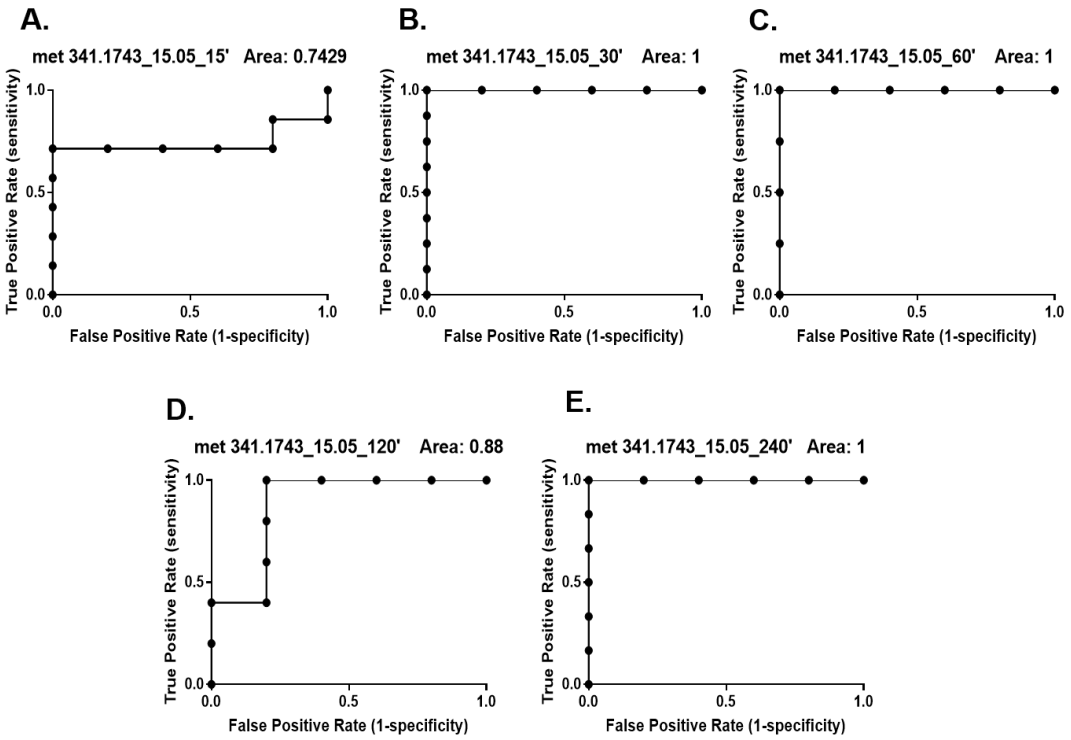

Figure 47: ROC curves of the variable 341.1743_15.05 regarding the time points of sacrifice have been constructed employing the GraphPad Prism. All ROC curves (A-E) bared an acceptable AUC value > 0.5 indicating that the selected significant feature was capable of discriminating the treated with TC4 population from the untreated ones in all studied time points.

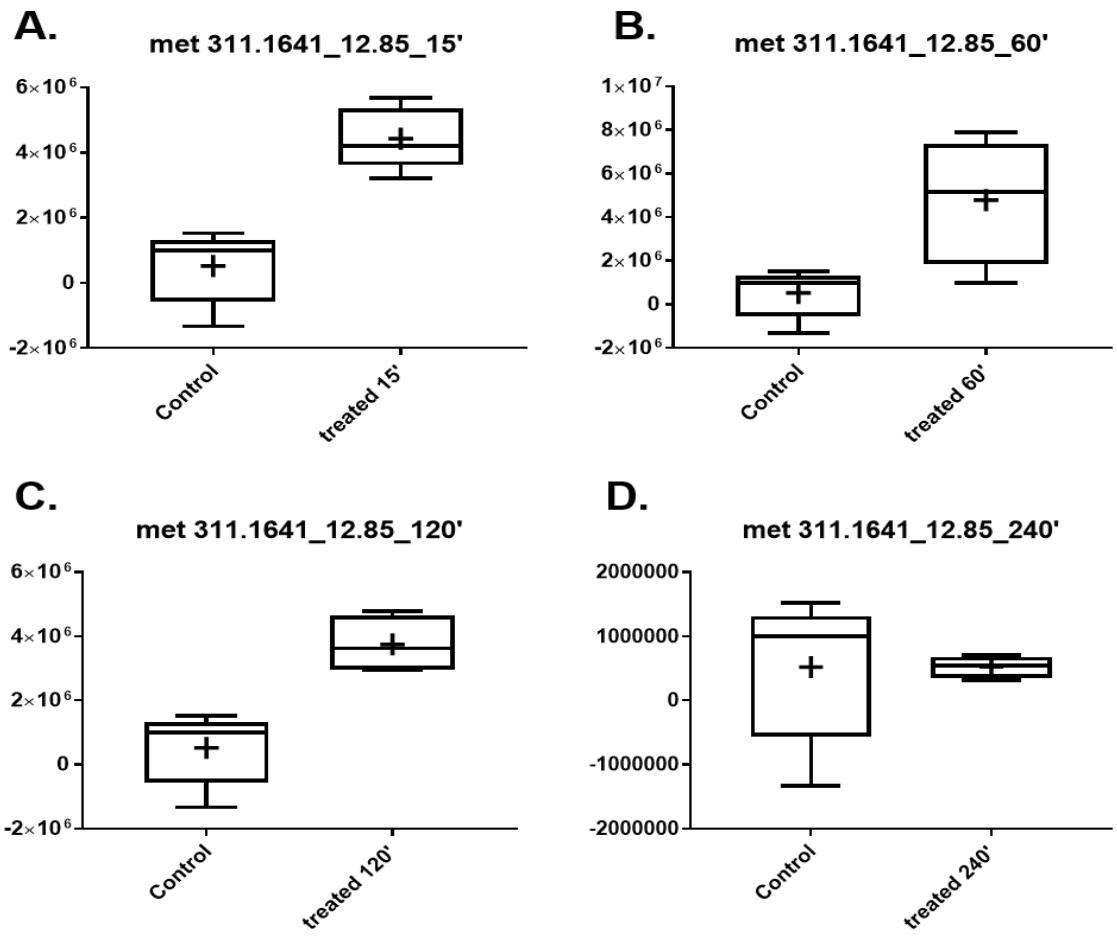

Figure 48: Box plots of the variable 311.1641_12.85 which is progressively altered depending on the time point of the sacrifice (A-E). This metabolite derives from the VIP scoring after univariate statistical analysis between the control and TC4 administered group (50 mg/kg) employing UHPLC-HRMS (Orbitrap) analysis in positive ion mode. The crosses correspond to the means while the horizontal lines that divide the boxes into two parts represent the medians. The upper and lower limits of the boxes represent the third and first quartiles respectively. The upper and lower whiskers represent scores outside the middle 50% and indicate the maximum values of each group.

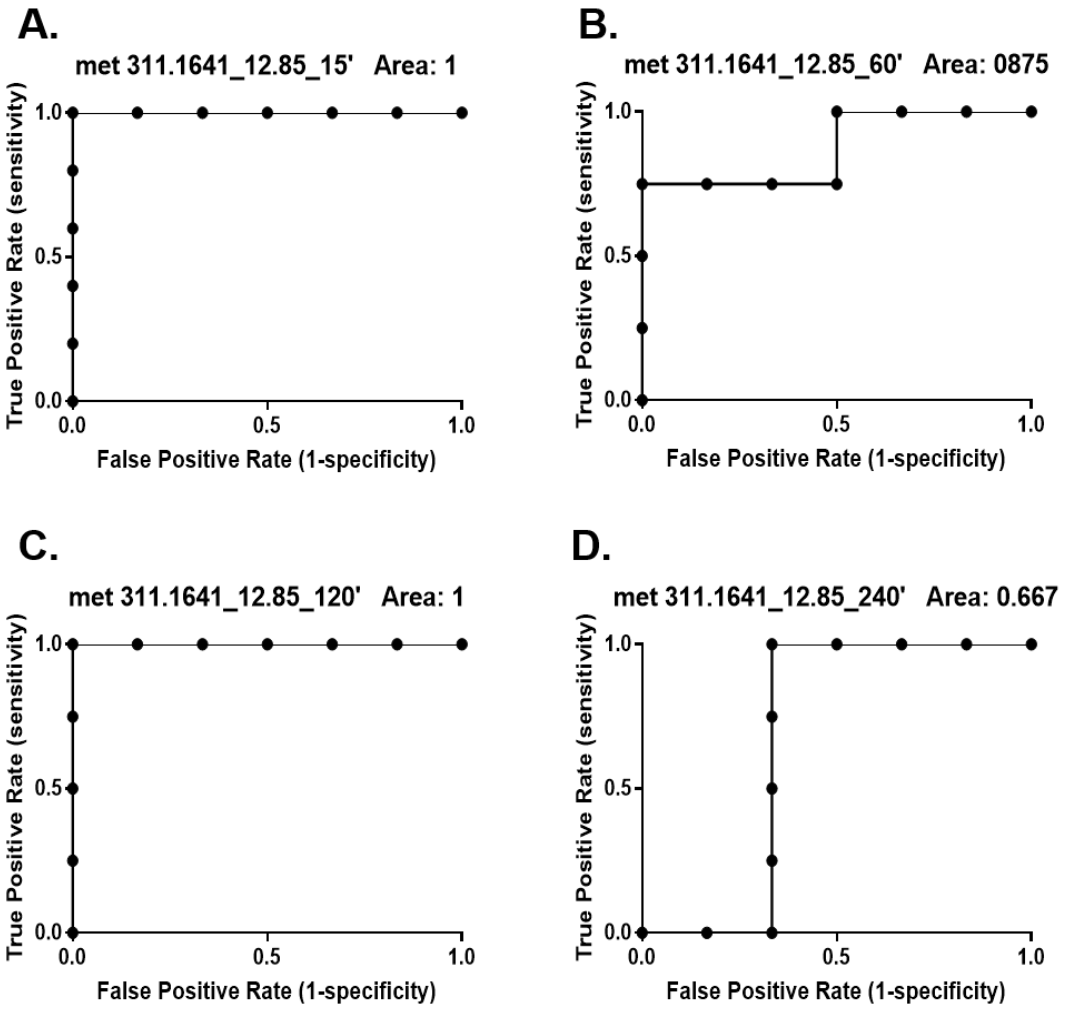

Figure 49: ROC curves of the variable 311.1641_12.85 regarding the time points of sacrifice have been constructed employing the GraphPad Prism. All ROC curves (A-D) bared an acceptable AUC value > 0.5 indicating that the selected significant feature was capable of discriminating the treated with TC4 population from the untreated ones in all studied time points.

Regarding the features contributing to the discrimination of the studied groups according to sex, the BOX plots of two representative metabolites have been demonstrated indicating the differences in the metabolites circulation between male and female mice in all the studied time points (Figure 50 and Figure 51).

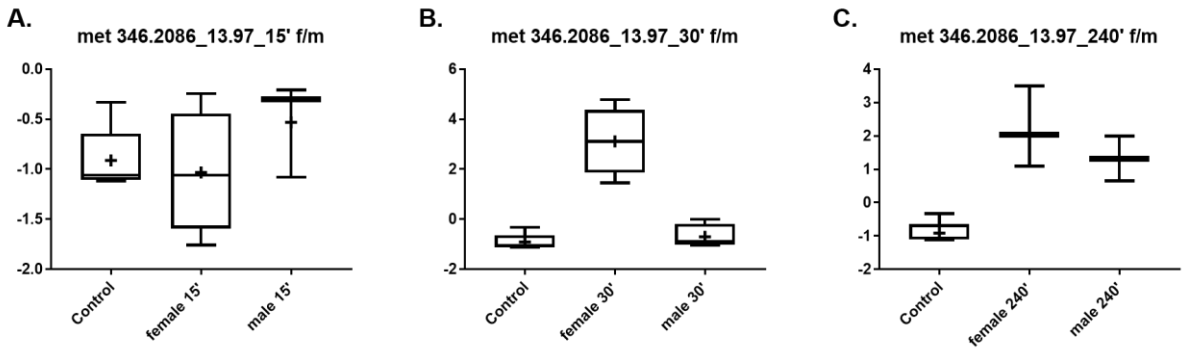

Figure 50: Box plots of the variable 346.2086_13.97 which is differently altered as far as the sex of the animals participating in the study is concerned. This metabolite derives from the VIP scoring after univariate statistical analysis between the control and TC4 administered group (150 mg/kg) employing UHPLC-HRMS (Orbitrap) analysis in negative ion mode. The crosses correspond to the means while the horizontal lines that divide the boxes into two parts represent the medians. The upper and lower limits of the boxes represent the third and first quartiles respectively. The upper and lower whiskers represent scores outside the middle 50% and indicate the maximum values of each group.

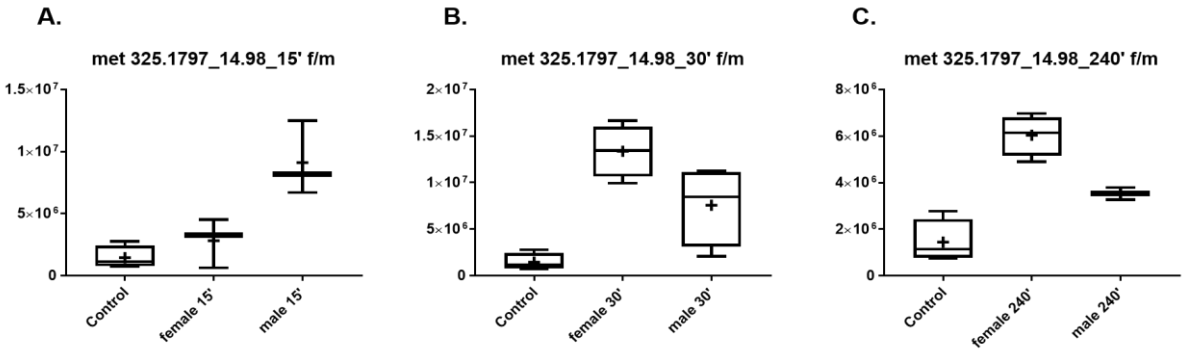

Figure 51: Box plots of the variable 325.1797_14.98 which is differently altered as far as the sex of the animals participating in the study is concerned. This metabolite derives from the VIP scoring after univariate statistical analysis between the control and TC4 administered group (150 mg/kg) employing UHPLC-HRMS (Orbitrap) analysis in positive ion mode. The crosses correspond to the means while the horizontal lines that divide the boxes into two parts represent the medians. The upper and lower limits of the boxes represent the third and first quartiles respectively. The upper and lower whiskers represent scores outside the middle 50% and indicate the maximum values of each group.

4.4.2.2 Annotation of the selected metabolites from mice plasma after *i.p.* administration of TC4

For the annotation of the significant features that were considerably altered after the administration of TC4, the METLIN, the Human Metabolome Data Base (HMDB) and the KEGG on-line databases were used along with the results from the CAMERA algorithm in order to facilitate the discovery of the potential metabolites. The adopted procedure is as follows; the selected features were matched, regarding their mass accuracy, with metabolites from the on-line databases, using a predefined mass accuracy window defined in ppm. The mass window was evaluated from the repeatability and the mass accuracy of the instruments performance regarding selected metabolites. Subsequently, the selected features were evaluated in terms of fulfilling additional criteria such as the isotopic pattern and the RDB (the degree of the molecule's unsaturation). In more details, the isotopic pattern of the expected metabolite should match those of the measured one according to the EC directive (Figure 52) while the RDB should agree with the proposed structure.

The exploration of the selected features was also facilitated with the employment of the "xMSannotator" R-package which uses a multi-criteria scoring scheme and provides an interface to perform annotation of High-Resolution Mass Spectral data using KEGG, HMDB, T3DB and LipidMaps. The multilevelannotation() function employs a multi-criteria approach based on data-driven modules, retention time, adducts, isotopes, mass detect, and various chemical rules and ratio checks for assigning annotations into different confidence levels: high (3), medium (2), low (1), and none (0). [263]

In more details, the final selected features that met all the necessary prerequisites were uploaded to online databases (METLIN and HMDB) in order to be annotated. Regarding the annotation of the features deriving from both ion modes, the same procedure was followed which will be thoroughly discussed below for a representative number of features.

Finally, as a further verification step, the Mass Frontier software was employed for spectral deconvolution so as to elucidate a potential fragmentation of the Molecular Ion that happens in the source (pseudo-fragmentation). Furthermore Xcalibur has been used in order to compare the MSMS spectra derived from DDA scanning to the experimental spectra information.

mz	t_R	comp1	ttest	qvalue	metlin	Dppm	isotopic pattern	Pseudo MS/MS ions	MS/MS from Xcalibur	Molecular Formula	Adduct	Trend	Dataset
635.2691	**13.11**	2.41	9.19E-05	0.0042	*trans*-crocin 2	1	100/37/9 vs. 100/34/6 (sim)			$C_{32}H_{44}O_{14}$	$[M+H-H_20]+$	↑	d.50 ESI(+) According to Time
815.3327	**10.46**	2.30	4.90E-05	0.0028	*trans*-crocin 3	0	100/40 vs. 100/40/1 (sim)			$C_{38}H_{54}O_{19}$	$[M+H]+$	↑	d.50 ESI(+) According to Time
311.1641	**12.85**	2.26	0.0004	0.0089	17-epiestriol	7	100/20/2 vs 100/20/0.6 (sim).	213/199/ 157/159	213	$C_{18}H_{24}O_3$	$[M+Na]+$	↑	d.50 ESI(+) According to Time
275.1430	**14.94**	2.02	0.0002	0.0067	Glutarylcarnitine	8	100/15/3 vs. 100/13/1 (sim)			$C_{12}H_{21}NO_6$	$[M+H]+$	↑	d.50 ESI(+) According to Time
491.2268	**10.4**	1.98	0.0001	0.0060	*trans*-crocin 1	1	100/28 vs. 100/26 (sim)			$C_{26}H_{34}O_9$	$[M+H]+$	↑	d.50 ESI(+) According to Time
152.1067	**2.17**	1.80	0.0018	0.0143	DL-Norephedrine	1	100/10 vs. 100/10 (sim)	134/118		$C_9H_{13}NO$	$[M+H]+$	↑	d.150 ESI(+) According to Time
279.2318	**18.11**	1.41	0.0050	0.0324	α-Linolenic Acid	0	100/16 vs. 100/20 (sim)			$C_{18}H_{30}O_2$	$[M+H]+$	↓	d.150 ESI(+) According to Time
325.1797	**14.98**	2.32	0.0008	0.0073	19-Hydroxyandrost-4-ene-3,17-dione	7	100/20/2 vs. 100/20/2 (sim)	267/257/ 249/243/ 145	267/257/ 249/243/ 145	$C_{19}H_{26}O_3$	$[M+Na]+$	↑	d.150 ESI(+) According to Sex
553.3109	**19.1**	2.58	0.0018	0.0429	PG	6	100/26/4 vs. 100/28/2 (sim)			$C_{26}H_{51}O_{10}P$	$[M-H]-$	↑	d.50 ESI(-) According to Time
612.3281	**18.77**	2.31	0.0022	0.0457	LysoPE(24:6(6Z,9Z, 12Z,15Z,18Z,21Z)/0:0)	3	100/34/7 vs. 100/31/5 (sim)			$C_{29}H_{48}NO_7P$	$[M+CH_3COO]-$	↑	d.50 ESI(-) According to Time

mz	t_R	comp1	ttest	qvalue	metlin	Dppm	isotopic pattern	Pseudo MS/MS ions	MS/MS from Xcalibur	Molecular Formula	Adduct	Trend	Dataset
269.2476	**24.42**	2.16	0.0014	0.0372	Nonyl octanoate	3	100/17/1 vs. 100/18/0.4 (sim)	269/251 /169		$C_{17}H_{34}O_2$	[M-H]-	↑	d.50 ESI(-) According to Time
711.2837	**15.05**	2.00	5.12E-07	0.0001	*trans*-crocin 2	4	100/36/9 vs. 100/36/6 (sim)			$C_{32}H_{44}O_{14}$	[M+CH_3COO]-	↑	d.50 ESI(-) According to Time
200.1286	**9.32**	1.86	0.0002	0.0089	Capryloylglycine	3	100/10/1 vs. 100/10/0.6	182/156		$C_{10}H_{19}NO_3$	[M-H]-	↑	d.50 ESI(-) According to Time
239.1644	**16.56**	1.37	9.06E-06	0.0011	Tetradecanedioic acid	1	100/15/0.5 vs. 100/15/0.8 (sim)	221/195/ 155/141		$C_{14}H_{26}O_4$	[M-H_2O-H]-	↑	d.50 ESI(-) According to Time
239.1644	**16.56**	1.37	9.06E-06	0.0011	Tetradecanedioic acid	1	100/15/0.5 vs. 100/15/0.8 (sim)	221/195/ 155/141		$C_{14}H_{26}O_4$	[M-H_2O-H]-	↑	d.50 ESI(-) According to Sex
697.2682	**13.08**	2.32	0.0023	0.0318	*trans*-crocin 2	4	100/37/9 vs. 100/34/6 (sim)			$C_{32}H_{44}O_{14}$	[M+FA-H]-	↑	d.150 ESI(-) According to Time
353.2105	**20.27**	2.22	0.0066	0.0472	21-Hydroxypregnenolone	1	100/23/5 vs. 100/23/3 (sim)	295		$C_{21}H_{32}O_3$	[M+Na-2H]-	↑	d.150 ESI(-) According to Time
421.1343	**7.61**	2.15	0.0009	0.0168	Riboflavin (Vitamin B2)	5	100/22/6 vs. 100/19/2 (sim)	375/255		$C_{17}H_{20}N_4O_6$	[M+FA-H]-	↑	d.150 ESI(-) According to Time
959.4600	**15.03**	2.09	0.0001	0.0035	PIP(20:4(8Z,11Z,14Z,17Z)/16:0)	7	100/48/18 vs. 100/48/11 (sim)			$C_{45}H_{80}O_{16}P_2$	[M+Na-2H]-	↑	d.150 ESI(-) According to Time
614.3343	**19.1**	2.01	0.0042	0.0472	PC(22:6(4Z,7Z,10Z, 13Z,16Z,19Z)/0:0)	3	100/33/5 vs. 100/33/5 (sim)			$C_{30}H_{50}NO_7P$	[M+FA-H]-	↑	d.150 ESI(-) According to Time

mz	t_R	comp1	ttest	qvalue	metlin	Dppm	isotopic pattern	Pseudo MS/MS ions	MS/MS from Xcalibur	Molecular Formula	Adduct	Trend	Dataset
524.3336	**19.66**	1.97	0.0035	0.0426	PC(O-16:1(9E)/0:0)[U]	4	100/23/7 vs. 100/27/3 (sim)			$C_{24}H_{50}NO_6P$	[M+FA-H]-	↓	d.150 ESI(-) According to Time
246.0954	**8.87**	1.77	0.0033	0.0413	Alpha-N-Phenylacetyl-L-glutamine	2	100/13/0.9 vs. 100/14/0.9 (sim)	203/201/ 186/116/98		$C_{13}H_{16}N_2O_4$	[M-H_2O-H]-	↑	d.150 ESI(-) According to Time
239.1644	**16.56**	1.37	9.06E-06	0.0011	Tetradecanedioic acid	1	100/15/0.5 vs. 100/15/0.8 (sim)	221/195/155/141		$C_{14}H_{26}O_4$	[M-H_2O-H]-	↑	d.150 ESI(-) According to Time
341.1743	**15.05**	1.66	8.13E-06	0.0004	cortisone	2	100/21/2 vs. 100/22/2 (sim)	299/257/ 205/203/ 175		$C_{21}H_{28}O_5$	[M-H_2O-H]-	↑	d.150 ESI(-) According to Time
206.0815	**8.21**	2.69	0.0036	0.0426	N-Acetyl-L-phenylalanine	3	100/10/2 vs. 100/10/2 (sim)	164/147		$C_{11}H_{13}NO_3$	[M-H]-	↑	d.150 ESI(-) According to Sex
237.1488	**15.35**	2.29	3.40E-05	0.0011	12-Hydroxydodecanoic acid	6	100/13 vs. 100/13 (sim)			$C_{12}H_{24}O_3$	[M+Na-2H]-	↑	d.150 ESI(-) According to Sex
239.1644	**16.56**	1.37	9.06E-06	0.0011	Tetradecanedioic acid	1	100/15/0.5 vs. 100/15/0.8 (sim)	221/195/ 155/141		$C_{14}H_{26}O_4$	[M-H2O-H]-	↑	d.150 ESI(-) According to Sex
289.1643	**9.61**	1.56	1.84E-05	0.0007	Dodecanedioic acid	4	100/15 vs. 100/15/1 (sim)	229/209		$C_{12}H_{22}O_4$	[M+CH_3COO]-	↑	d.150 ESI(-) According to Sex
524.3336	**19.66**	1.38	0.0035	0.0426	PC(O-16:1(9E)/0:0)[U]	4	100/23/7 vs. 100/27/3 (sim)			$C_{24}H_{50}NO_6P$	[M+FA-H]-	↓	d.150 ESI(-) According to Sex
346.2086	**13.97**	1.18	0.0016	0.0258	Dihydrocortisol	3	100/21/3 vs. 100/22/3			$C_{21}H_{32}O_5$	[M-H_2O-H]-	↑	d.150 ESI(-) According to Sex

Table 8: Potential annotated metabolites from both administration doses of TC4 (50 and 150 mg/kg) obtained from both ESI (+) and ESI(-) UPLC-HRMS analyses.

4.4.2.2.1 Feature 311.1641_12.85 (mz_t_R)

The feature with **m/z=311.1641** and **t_R=12.85 min** resulted from the positive ion mode. Initially, the mz = 311.1641 was searched against METLIN allowing a Δppm ≤ 10 and a number of hits (19 hits) were provided according to this particular mass. However, after careful evaluation, most of them were discarded since they were irrelevant with the current study and the target organism. As a result, $C_{18}H_{24}O_3$ was chosen as a putative molecular formula. According to METLIN and HMDB the proposed molecular formula corresponded to "estriol" and "17-epiestriol". Calculation of the isotopic ratios was performed with the aid of Xcalibur 2.1 and the results are presented in Table 8 indicating that the isotopic pattern of the expected metabolite matched those of the measured one. Finally, METLIN and HMDB online data bases revealed that the feature 311.1641_12.85 is 17-epiestriol as a sodium adduct $[M+Na]^+$ while, based on the MS/MS spectra provided from METLIN and the deconvoluted MS spectra provided from Mass Frontier, **17-epiestriol** was found to be the potential annotated metabolite since the 213/199/159/157 ions have been successfully recognized.

4.4.2.2.2 Feature 279.2318_18.11 (mz_t_R)

The feature with **m/z=279.2318** and **t_R=18.11 min** resulted from positive ion mode. Likewise, it was searched against METLIN with many hits arranged by Δppm (109 hits). The first hit that afforded a Δppm=0 and also was closely related to the object of the current study was **α-Linolenic Acid** with proposed molecular formula $C_{18}H_{30}O_2$. Similarly to the procedure followed in the previous feature, the isotopic ratio calculation was performed and the isotopic pattern of the expected metabolite matched those of the measured one (Table 8). However, the Mass Frontier algorithm did not success in providing any deconvoluted MS spectra.

4.4.2.2.3 Feature 341.1743_15.05 (mz_t_R)

The feature with **m/z=341.1743** and **t_R=15.05 min** resulted from negative ion mode. According to the CAMERA algorithm, this feature was a potential adduct of $[M+Cl]^-$305.2016 and $[M-H_2O-H]$-359.1917. After searching of potential association of this feature with a known compound, METLIN provided several hits (21 hits) including the $[M-H_2O-H]^-$ adduct of Cortisone with molecular formula $C_{21}H_{28}O_5$ and the $[M+Cl]^-$ adduct of 2alpha-Fluoro-17beta-hydroxyandrost-4-en-3-one with molecular formula $C_{19}H_{27}FO_2$. Both of them were examined regarding the isotopic pattern of the proposed compounds in comparison with the isotopic pattern of the measured feature. However, as it was clearly observed in the mass spectrum

of the selected feature, the M+2 isotope did not have the necessary intensity ratio for a molecule that includes a -Cl (1/3 of the observed intensity of the Molecular ion-M) thus the hypothesis of 2alpha-Fluoro-17beta-hydroxyandrost-4-en-3-one was rejected. Furthermore, the application of the Mass Frontier algorithm provided the deconvoluted MS spectra leading to the successful recognition of the following pseudoMS ions (341/299/257/205/203/175) thus leading to **Cortisone** as the potential annotated metabolite.

Similarly to the previously described features, all the identified metabolites afforded the same isotopic pattern with the proposed metabolites in each case. However not all the m/z_t_R hits that were statistically significant ended up in an annotated metabolite since some m/z did not correspond to any METLIN hit thus they are regarded as unknown features.

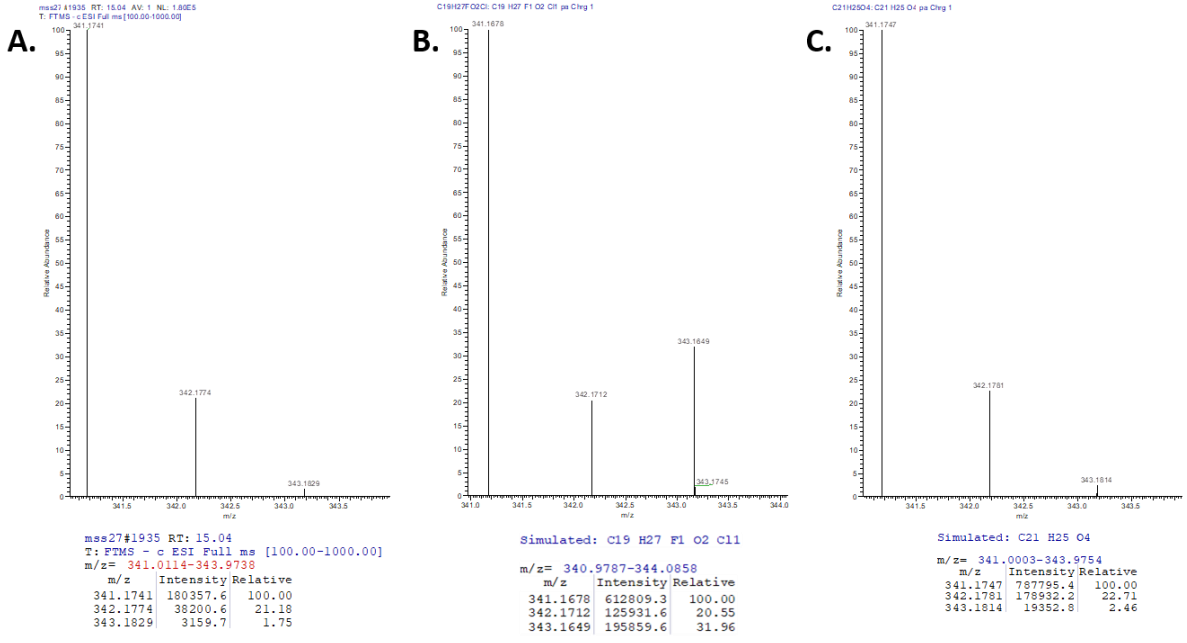

Figure 52: MS spectra representing the isotopic patterns of (A) the feature with *m/z* 341.1743 (B) the simulated ion of the proposed molecular formula $C_{19}H_{27}FO_2$ as $[M+Cl]^-$ adduct and (C) the simulated ion of the proposed molecular formula $C_{21}H_{28}O_5$ as $[M-H_2O-H]^-$ adduct indicating the absence of -Cl in the actual spectrum as the M/M+2 isotopic ratio is not 3:1. The isotopic pattern of the expected metabolite (C.) matched those of the measured one (A.) thus demonstrating that the feature with *m/z* 341.1743 corresponds to Cortisone as $[M-H_2O-H]^-$ adduct

4.4.3 Metabolic Pathway Analysis

In an effort to detect the potential involvement of the annotated metabolites in biological pathways, the identified metabolites were imported to MetaboAnalyst 4.0 which offers the ability to explore the contribution of the compounds of interest in biological pathways. The annotated metabolites were uploaded according to their HMDB exact names and if necessary, the names of some hits were further standardized, then the appropriate pathway library was selected; in this case *Mus musculus* (mouse). The Over Representation Analysis and the Pathway Topology Analysis have been performed with the Hypergeometric test and Relative-betweeness Centrality algorithms respectively, resulting to the metabolic pathways outcomes.

The interpretation of the results was performed after taking into consideration either a p-value < 0.05 or an impact value > 0.1 thus indicating that the metabolic pathways in which some of the annotated compounds are involved are the following: Steroid hormone biosynthesis, alpha-Linolenic acid metabolism and Starch and sucrose metabolism
(Table 9)

	Total	Expected	Hits	Raw p	Holm p	FDR	Impact
Steroid hormone biosynthesis	72	0.81299	5	2.7604E-4	0.2264	0.2264	0.08483
alpha-Linolenic acid metabolism	9	0.10162	1	0.097415	1	1	1
Riboflavin metabolism	11	0.12421	1	0.11782	1	1	0
Starch and sucrose metabolism	19	0.21454	1	0.19519	1	1	0.16647
Fructose and mannose metabolism	21	0.23712	1	0.21351	1	1	0
Galactose metabolism	26	0.29358	1	0.25762	1	1	0.00169
Glycolysis or Gluconeogenesis	26	0.29358	1	0.25762	1	1	0.00778
Amino sugar and nucleotide sugar metabolism	37	0.41778	1	0.34664	1	1	0
Tryptophan metabolism	40	0.45166	1	0.36912	1	1	0
Biosynthesis of unsaturated fatty acids	42	0.47424	1	0.3837	1	1	0
Purine metabolism	68	0.76782	1	0.54668	1	1	0.04219

Table 9: The obtained metabolic pathways from the Metabolic Pathway Analysis from the MetaboAnalyst 4.0 online platform. Total is the total number of compounds included in the pathway; the Hits are the number of the matched compounds from those initially uploaded; the Raw p is the original p value calculated from the pathway enrichment analysis; the FDR is the False Discovery Rate; the Impact is the cumulative percentage from the matched metabolite nodes calculated from pathway topology analysis. The pathways that were altered are represented in bold-blue lines and have been selected based on the criteria of either p-value < 0.05 or impact value > 0.1.

A clear "metabolome view" of the potential pathways is depicted below. (Figure 53) It comprises of all the matched pathways (the metabolome) arranged by p-values (from pathway enrichment analysis) on Y-axis, and pathway impact values (from pathway topology analysis) on X-axis. The node color is based on its p-value and the node radius is determined based on their pathway impact values.

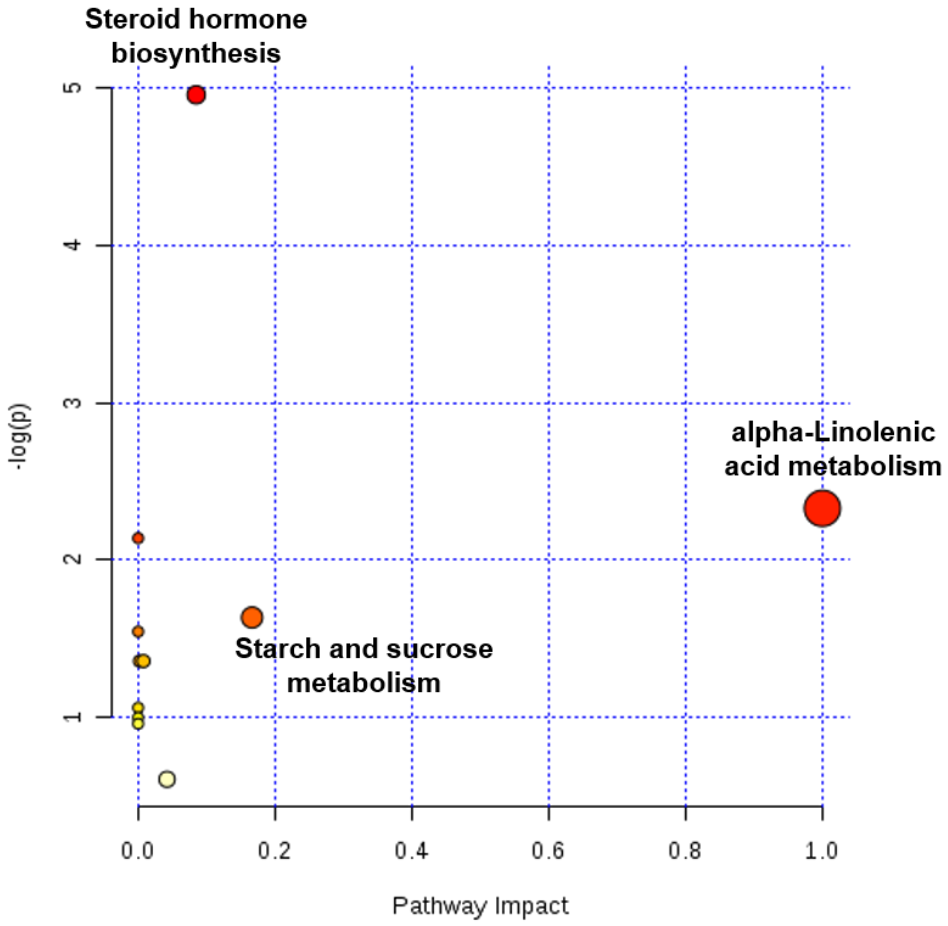

Figure 53: A “metabolome view” of the selected pathways that were altered due to the *i.p.* administration of TC4 in mice. The matched pathways are depicted as nodes where the node color is based on its p-value and the node radius is determined by their pathway impact values.

4.4.4 Biological evaluation of the results

After the annotation of the metabolites responsible for the differentiation between the treated and untreated populations as well as the significant features that have been altered due to the *i.p.* administration of TC4 it is evident that the TC4 increases some specific circulating steroids in the studied plasma samples. (Figure 54)

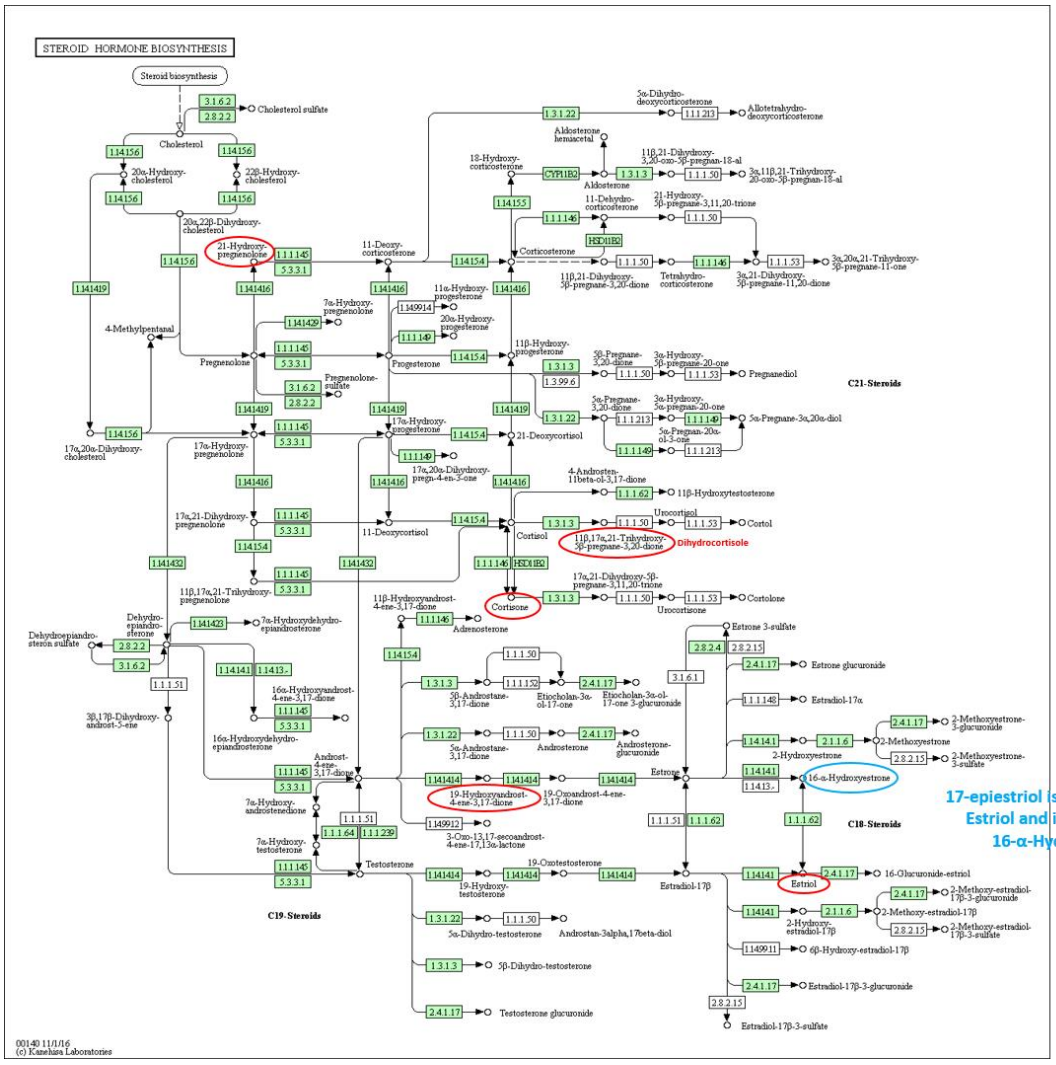

Figure 54: Steroid hormone biosynthesis - *Mus musculus* (mouse). The annotated metabolites that have been affected due the administration of TC4 are marked with red circles. 16-a-Hydroxyestrone (marked with a light blue circle) is responsible for the formation of the annotated metabolite 17-epiestriol which is a 17-a-epimer of estriol.

One of the annotated metabolites participating in the steroid biosynthesis pathway is **17-epiestriol**, also known as 16α-hydroxy-17α-estradiol, which is a minor and weak endogenous estrogen, and the 17α-epimer of estriol (which is 16α-hydroxy-17β-estradiol), formed from 16α-hydroxyestrone. In contrast to other endogenous estrogens like estradiol, 17α-epiestriol is a selective agonist of the Estrogen Receptor beta (ERβ). [274] ER-β is found throughout the brain at various concentrations in different neuron clusters. [275] It has been demonstrated that the genetic variation in ERβ is both sex and age dependent while the ERβ polymorphism has been accused for cognitive impairment, accelerated brain aging, and development of AD pathology. Furthermore, the risk of AD development in post-menopausal women is significantly increased mainly due to the decrease in the amount of the available estrogens, a situation closely related to the proper aging of the hippocampus, the neurons' survival and regeneration, as well as the amyloid metabolism since ERβ mRNA is highly expressed in hippocampal formation, a brain area closely associated with memory. [276]

As a result, the normal expression of ERβ mRNA leads to enhanced survival of the neurons while offering neuroprotection against neurodegenerative diseases. Furthermore, ERβ has the ability to control the accumulation of amyloid beta peptide (Aβ) since it up-regulates the insulin-degrading enzyme (IDE) and maintains the APP. IDE regulates the Aβ degradation in case of extraordinary accumulation. In the case of AD, the lack of ERβ results in insufficient degradation which subsequently allows Aβ to form the senile-plaques. Moreover, the activation of ERβ offers protection against AD also by regulating APOE, thus estrogen therapy via an ERβ-targeted approach, so as to overcome the antagonistic actions of interactions between ERα and ERβ inside the brain, can be used as a prevention method for AD either before or at the onset of menopause. [277]

Furthermore, therapeutically the treatment with ERβ agonists can also offer neuroprotective benefits since it can reverse the inhibition of brain plasticity due to the low estrogen levels and it can enhance the proliferation of progenitor cells to create new neurons. Finally, ERβ-agonists can be used in both men and women to support the treatment of neurodegenerative diseases since they offer neuroprotection as well as enhance the regulation of plaques inside the brain. [277]

Another annotated metabolite participating in the steroid biosynthesis pathway is **21-Hydroxypregnenolone** (3β,21-dihydroxypregn-5-en-20-one) a naturally occurring and endogenous pregnane steroid and an intermediate in the biosynthesis of 11-deoxycorticosterone (21-hydroxyprogesterone), corticosterone (11β,21-dihydroxyprogesterone) and other corticosteroids. On the other hand, 11-deoxycorticosterone is considered to be a proneurosteroid of Tetrahydrodeoxycorticosterone (abbreviated as THDOC; 3α,21-dihydroxy-5α-pregnan-20-one) which is synthesized from the adrenal hormone deoxycorticosterone by the action of two enzymes, 5α-reductase type I and 3α-hydroxysteroid dehydrogenase. [278] It has been demonstrated that 3a, 5a-THDOC interacts with GABA type A (GABAA) receptors by increasing the frequency and/or duration of openings of the GABA-gated chloride channel thus modulating neuronal excitability. [279] Moreover, in preclinical studies, 3a-reduced neuroactive steroids have been found capable of modulating anxiety and depression related behavior as well as influencing the neurochemical responses to acute or chronic stress conditions. [279] As a result, alterations to neuroactive steroid concentrations might enhance the therapeutic effects of certain psychopharmacological drugs. [280]

4.5 CONCLUSIONS

This study demonstrates an integrated UHPLC-HRMS-based metabolomics approach that has been utilized for the analysis of mice plasma samples after *i.p.* administration of TC4, a natural compound of saffron. The data analysis was performed employing two different approaches, a MVA and a ML-MVA methodology. Regarding both ionization techniques (positive and negative) the MVA allowed sufficient clustering between the treated and the untreated animals. However, MVA analysis was incapable of allowing internal clustering of the treated population e.g. classification regarding the different time points of the sacrifice as well as the sex of the treated animals. As a result, the need to apply ML-MVA approaches was indispensable so as to perform exploration between the studied subjects. Consequently, due to the high variability imposed by various factors e.g. sex, administration dose, and time points, the ML-(s)PLS–DA, e.g., splitting variation to each individual component, has proven to be the only effective approach. Furthermore, a preliminary sex-related effect on the metabolome has been proven to exist, denoting that the administration in both genders is indispensable in order to acquire safe conclusions as reliable metabolome pictures. However, in order to be able to reach certain and safer conclusions, the experimental design should include equal number of animals of both sexes in order to evaluate the results and to monitor the metabolic differences induced by the administration of TC4. Finally, this UPLC-HRMS-based methodology clearly demonstrates that the time sequence of metabolome changes is due to the administration of TC4. In accordance with the results provided by various statistical softwares, the selected features were identified and were further implemented to online databases so as to annotate them and to identify potential metabolites. Overall, 25 metabolites were annotated and were afterwards inspected so as to identify if they were altering any biological metabolic pathway. The results demonstrated that five annotated metabolites were involved in the steroid biosynthesis pathway while two of them might be considered as neuroprotective agents.

To sum up, *i.p* administration of TC4 proved capable of causing alterations to the metabolic profiles of the mice participating in the current study. Furthermore, a ML-MVA approach revealed internal differences among the treated populations, which are related to either their sex (male, female) or the time-point of the sacrifice. To our current knowledge, this is the first time that such an untargeted metabolomics approach has been applied for the analysis of plasma samples after

i.p. administration of TC4. However, no matter how promising these results could be, they are considered to be preliminary evidence, thus metabolomics studies with participation of more animals in total and more animals of both sexes in each group are essential so as to reach safe conclusions and to be capable of revealing the underlying mechanisms of metabolic alterations caused by the administration of TC4.

4.6 ACKNOWLEDGEMENTS

We would like to acknowledge Despoina Papasavva for technical assistance in the animal experiments, and *Cooperative De Safran* (Krokos Kozanis, West Macedonia, Greece) for providing saffron samples.

BIBLIOGRAPHY

[1] G. M. Cragg and D. J. Newman, “Biodiversity: A continuing source of novel drug leads*,” *Pure Appl. Chem*, vol. 77, no. 24, pp. 7–24, 2005.

[2] D. A. Dias, S. Urban, and U. Roessner, “A historical overview of natural products in drug discovery.,” *Metabolites*, vol. 2, no. 2, pp. 303–36, Apr. 2012.

[3] G. Farré, D. Blancquaert, T. Capell, D. Van Der Straeten, P. Christou, and C. Zhu, “Engineering Complex Metabolic Pathways in Plants,” *Annu. Rev. Plant Biol.*, vol. 65, no. 1, pp. 187–223, Apr. 2014.

[4] I. Lavi *et al.*, “Stress and marital adjustment in families of children with cancer,” *Psychooncology.*, Mar. 2018.

[5] S. Catt, R. Starkings, V. Shilling, and L. Fallowfield, “Patient-reported outcome measures of the impact of cancer on patients’ everyday lives: a systematic review,” *J. Cancer Surviv.*, vol. 11, no. 2, pp. 211–232, 2017.

[6] E. Espinosa, P. Zamora, J. Feliu, and M. González Barón, “Classification of anticancer drugs - A new system based on therapeutic targets,” *Cancer Treat. Rev.*, vol. 29, no. 6, pp. 515–523, 2003.

[7] J. F. Buyel, “Plants as sources of natural and recombinant anti-cancer agents,” *Biotechnol. Adv.*, vol. 36, no. 2, pp. 506–520, 2018.

[8] J. M. Landete, “Updated Knowledge about Polyphenols: Functions, Bioavailability, Metabolism, and Health,” *Crit. Rev. Food Sci. Nutr.*, vol. 52, no. 10, pp. 936–948, Oct. 2012.

[9] S. TABREZ *et al.*, “Cancer Chemoprevention by Polyphenols and Their Potential Application as Nanomedicine,” *J. Environ. Sci. Heal. Part C*, vol. 31, no. 1, pp. 67–98, Jan. 2013.

[10] M. Asensi, A. Ortega, S. Mena, F. Feddi, and J. M. Estrela, “Natural polyphenols in cancer therapy,” *Crit. Rev. Clin. Lab. Sci.*, vol. 48, no. 5–6, pp. 197–216, Dec. 2011.

[11] Z. Habli, G. Toumieh, M. Fatfat, O. Rahal, and H. Gali-Muhtasib, “Emerging Cytotoxic Alkaloids in the Battle against Cancer: Overview of Molecular Mechanisms,” *Molecules*, vol. 22, no. 2, p. 250, Feb. 2017.

[12] M. Schnekenburger, M. Dicato, and M. Diederich, “Plant-derived epigenetic modulators for cancer treatment and prevention,” *Biotechnol. Adv.*, vol. 32, no. 6, pp. 1123–1132, Nov. 2014.

[13] “Definition of cardiovascular diseases,” Mar. 2018.

[14] I. Dagla *et al.*, “Alteration in the liver metabolome of rats with metabolic syndrome after treatment with Hydroxytyrosol. A Mass Spectrometry And

Nuclear Magnetic Resonance - based metabolomics study," *Talanta*, vol. 178, no. May 2017, pp. 246–257, 2018.

[15] P. J. Barnes, "Chronic Obstructive Pulmonary Disease," *N. Engl. J. Med.*, vol. 343, no. 4, pp. 269–280, Jul. 2000.

[16] E. D. Bateman *et al.*, "Global strategy for asthma management and prevention: GINA executive summary.," *Eur. Respir. J.*, vol. 31, no. 1, pp. 143–78, Jan. 2008.

[17] X. Guihua, L. Shuyin, G. Jinliang, and S. Wang, "Naringin Protects Ovalbumin-Induced Airway Inflammation in a Mouse Model of Asthma," *Inflammation*, vol. 39, no. 2, pp. 891–899, Apr. 2016.

[18] J. Li and B. Zhang, "Apigenin protects ovalbumin-induced asthma through the regulation of Th17 cells," *Fitoterapia*, vol. 91, pp. 298–304, Dec. 2013.

[19] E. Conte, E. Fagone, M. Fruciano, E. Gili, M. Iemmolo, and C. Vancheri, "Anti-inflammatory and antifibrotic effects of resveratrol in the lung," vol. 30, no. 5, pp. 523–529, 2015.

[20] V. R. Askari *et al.*, "Evaluation of the effects of Iranian propolis on the severity of post operational-induced peritoneal adhesion in rats," *Biomed. Pharmacother.*, vol. 99, pp. 346–353, Mar. 2018.

[21] M. J. Ball, W. J. Lukiw, E. M. Kammerman, and J. M. Hill, "Intracerebral propagation of Alzheimer's disease: strengthening evidence of a herpes simplex virus etiology.," *Alzheimers. Dement.*, vol. 9, no. 2, pp. 169–75, Mar. 2013.

[22] D. Hober, F. Sane, H. Jaïdane, K. Riedweg, A. Goffard, and R. Desailloud, "Immunology in the clinic review series; focus on type 1 diabetes and viruses: role of antibodies enhancing the infection with Coxsackievirus-B in the pathogenesis of type 1 diabetes.," *Clin. Exp. Immunol.*, vol. 168, no. 1, pp. 47–51, Apr. 2012.

[23] C.-M. Yang, H.-Y. Cheng, T.-C. Lin, L.-C. Chiang, and C.-C. Lin, "Hippomanin a from acetone extract ofPhyllanthus urinaria inhibited HSV-2 but not HSV-1 infectionin vitro," *Phyther. Res.*, vol. 21, no. 12, pp. 1182–1186, Dec. 2007.

[24] M. A. Huber, "Herpes simplex type-1 virus infection.," *Quintessence Int.*, vol. 34, no. 6, pp. 453–67, Jun. 2003.

[25] M. Fatahzadeh and R. A. Schwartz, "Human herpes simplex labialis," *Clin. Exp. Dermatol.*, vol. 32, no. 6, pp. 625–630, Nov. 2007.

[26] F. Morfin and D. Thouvenot, "Herpes simplex virus resistance to antiviral drugs.," *J. Clin. Virol.*, vol. 26, no. 1, pp. 29–37, Jan. 2003.

[27] J. Hudson and S. Vimalanathan, "Echinacea—A Source of Potent Antivirals for Respiratory Virus Infections," *Pharmaceuticals*, vol. 4, no. 7, pp. 1019–1031,

Jul. 2011.

[28] C. A. J. Erdelmeier, J. Cinatl, H. Rabenau, H. W. Doerr, A. Biber, and E. Koch, “Antiviral and antiphlogistic activities of Hamamelis virginiana bark,” *Planta Med.*, vol. 62, no. 3, pp. 241–245, 1996.

[29] M. S. Ghannad, S. M. Hosseini, and A. Gharib, “The efficacy and mechanism of herbals action on herpes simplex virus type 1: A review,” vol. 9, no. 1, pp. 77–81, Jan. 2016.

[30] M. T. H. Khan, A. Ather, K. D. Thompson, and R. Gambari, “Extracts and molecules from medicinal plants against herpes simplex viruses,” *Antiviral Res.*, vol. 67, no. 2, pp. 107–119, Aug. 2005.

[31] R. M. Fairhurst *et al.*, “Artemisinin-resistant malaria: research challenges, opportunities, and public health implications.,” *Am. J. Trop. Med. Hyg.*, vol. 87, no. 2, pp. 231–41, Aug. 2012.

[32] A. Lubbe, I. Seibert, T. Klimkait, and F. van der Kooy, “Ethnopharmacology in overdrive: The remarkable anti-HIV activity of Artemisia annua,” *J. Ethnopharmacol.*, vol. 141, no. 3, pp. 854–859, Jun. 2012.

[33] M. T. Lin and M. F. Beal, “Mitochondrial dysfunction and oxidative stress in neurodegenerative diseases,” *Nature*, vol. 443, no. 7113, pp. 787–795, 2006.

[34] W. Poewe, “Non-motor symptoms in Parkinson’s disease,” *Eur. J. Neurol.*, vol. 15, no. s1, pp. 14–20, Apr. 2008.

[35] J. W. Langston, “The Parkinson’s complex: Parkinsonism is just the tip of the Iceberg,” *Ann. Neurol.*, vol. 59, no. 4, pp. 591–596, 2006.

[36] D. M. Radhakrishnan and V. Goyal, “Parkinson’s disease: A review.,” *Neurol. India*, vol. 66, no. Supplement, pp. S26–S35, 2018.

[37] D. W. Dickson *et al.*, “Neuropathological assessment of Parkinson’s disease: refining the diagnostic criteria.,” *Lancet. Neurol.*, vol. 8, no. 12, pp. 1150–7, Dec. 2009.

[38] F. Miraglia, L. Betti, L. Palego, and G. Giannaccini, “Parkinson’s Disease and Alpha-Synucleinopathies: from Arising Pathways to Therapeutic Challenge,” *Cent. Nerv. Syst. Agents Med. Chem.*, vol. 15, no. 2, pp. 109–116, May 2015.

[39] M. Bourdenx, N. S. Koulakiotis, D. Sanoudou, E. Bezard, B. Dehay, and A. Tsarbopoulos, “Protein aggregation and neurodegeneration in prototypical neurodegenerative diseases: Examples of amyloidopathies, tauopathies and synucleinopathies,” *Prog. Neurobiol.*, vol. 155, pp. 171–193, Aug. 2017.

[40] D. Chang *et al.*, “A meta-analysis of genome-wide association studies identifies 17 new Parkinson’s disease risk loci.,” *Nat. Genet.*, vol. 49, no. 10, pp. 1511–1516, Oct. 2017.

[41] E. Kara *et al.*, “Assessment of Parkinson’s disease risk loci in Greece,” *Neurobiol. Aging*, vol. 35, no. 2, 2014.

[42] I. J. Siddiqui, N. Pervaiz, and A. A. Abbasi, “The Parkinson Disease gene SNCA: Evolutionary and structural insights with pathological implication,” *Sci. Rep.*, vol. 6, 2016.

[43] D. G. Hernandez *et al.*, “Genome wide assessment of young onset Parkinson’s disease from Finland.,” *PLoS One*, vol. 7, no. 7, p. e41859, 2012.

[44] K. Y. Mok, G. Koutsis, L. V. Schottlaender, J. Polke, M. Panas, and H. Houlden, “High frequency of the expanded C9ORF72 hexanucleotide repeat in familial and sporadic Greek ALS patients,” *Neurobiol. Aging*, vol. 33, no. 8, p. 1851.e1, 2012.

[45] “Genetics of Parkinson’s disease: alpha-synuclein and other insights from Greece.”

[46] E. Sidransky and G. Lopez, “The link between the GBA gene and parkinsonism.,” *Lancet. Neurol.*, vol. 11, no. 11, pp. 986–98, Nov. 2012.

[47] K. Kalinderi, S. Bostantjopoulou, C. Paisan-Ruiz, Z. Katsarou, J. Hardy, and L. Fidani, “Complete screening for glucocerebrosidase mutations in Parkinson disease patients from Greece,” *Neurosci. Lett.*, vol. 452, no. 2, pp. 87–89, Mar. 2009.

[48] A. Lwin, E. Orvisky, O. Goker-Alpan, M. E. Lamarca, and E. Sidransky, “Glucocerebrosidase mutations in subjects with parkinsonism.”

[49] E. Rogaeva and J. Hardy, “Gaucher and Parkinson diseases: unexpectedly related.,” *Neurology*, vol. 70, no. 24, pp. 2272–3, Jun. 2008.

[50] J. Jankovic, “Parkinson’s disease: clinical features and diagnosis,” *J. Neurol. Neurosurg. Psychiatry*, vol. 79, no. 4, pp. 368–376, Apr. 2008.

[51] W. J. Weiner, “Initial Treatment of Parkinson Disease,” vol. 61, pp. 1966–1969, 2013.

[52] J. Jankovic and L. G. Aguilar, “Current approaches to the treatment of Parkinson’s disease.,” *Neuropsychiatr. Dis. Treat.*, vol. 4, no. 4, pp. 743–57, Aug. 2008.

[53] R. Pahwa and K. E. Lyons, “Outpatient titration of carbidopa/levodopa enteral suspension (Duopa),” *Int. J. Neurosci.*, vol. 127, no. 5, pp. 459–465, May 2017.

[54] R. A. Hauser, “Future Treatments for Parkinson’s Disease: Surfing the PD Pipeline,” *Int. J. Neurosci.*, vol. 121, no. sup2, pp. 53–62, Sep. 2011.

[55] L. Dezsi and L. Vecsei, “Monoamine Oxidase B Inhibitors in Parkinson’s Disease,” *CNS Neurol. Disord. - Drug Targets*, vol. 16, no. 4, pp. 425–439, Jul. 2017.

[56] N. Schendzielorz, A. Rysa, I. Reenila, A. Raasmaja, and P. T. Mannisto, “Complex estrogenic regulation of catechol-O-methyltransferase (COMT) in rats.,” *J. Physiol. Pharmacol.*, vol. 62, no. 4, pp. 483–90, Aug. 2011.

[57] C. W. Olanow and F. Stocchi, “COMT inhibitors in Parkinson’s disease: can they prevent and/or reverse levodopa-induced motor complications?,” *Neurology*, vol. 62, no. 1 Suppl 1, pp. S72-81, Jan. 2004.

[58] M. G. Spillantini, M. L. Schmidt, V. M.-Y. Lee, J. Q. Trojanowski, R. Jakes, and M. Goedert, “alpha-Synuclein in Lewy bodies,” *Nature*, vol. 388, no. 6645, pp. 839–840, 1997.

[59] J.-C. Rochet, B. A. Hay, and M. Guo, “Molecular Insights into Parkinson’s Disease,” in *Progress in molecular biology and translational science*, vol. 107, 2012, pp. 125–188.

[60] T. Bachhuber *et al.*, “Inhibition of amyloid-β plaque formation by α-synuclein,” *Nat. Med.*, vol. 21, no. 7, pp. 802–807, Jul. 2015.

[61] J. Lewis *et al.*, “In vivo silencing of alpha-synuclein using naked siRNA.,” *Mol. Neurodegener.*, vol. 3, p. 19, Nov. 2008.

[62] J. M. Cooper *et al.*, “Systemic exosomal siRNA delivery reduced alpha-synuclein aggregates in brains of transgenic mice.,” *Mov. Disord.*, vol. 29, no. 12, pp. 1476–85, Oct. 2014.

[63] L. Fonseca-Ornelas *et al.*, “Small molecule-mediated stabilization of vesicle-associated helical α-synuclein inhibits pathogenic misfolding and aggregation,” *Nat. Commun.*, vol. 5, p. 5857, 2014.

[64] L. Breydo, J. W. Wu, and V. N. Uversky, “α-Synuclein misfolding and Parkinson’s disease,” *Biochim. Biophys. Acta - Mol. Basis Dis.*, vol. 1822, no. 2, pp. 261–285, 2012.

[65] W. Zhou, K. Bercury, J. Cummiskey, N. Luong, J. Lebin, and C. R. Freed, “Phenylbutyrate Up-regulates the DJ-1 Protein and Protects Neurons in Cell Culture and in Animal Models of Parkinson Disease,” *J. Biol. Chem.*, vol. 286, no. 17, pp. 14941–14951, Apr. 2011.

[66] S. S. Karuppagounder, S. Brahmachari, Y. Lee, V. L. Dawson, T. M. Dawson, and H. S. Ko, “The c-Abl inhibitor, Nilotinib, protects dopaminergic neurons in a preclinical animal model of Parkinson’s disease,” *Sci. Rep.*, vol. 4, no. 1, p. 4874, May 2015.

[67] J. Bieschke *et al.*, “EGCG remodels mature α-synuclein and amyloid-β fibrils and reduces cellular toxicity,” *Proc. Natl. Acad. Sci.*, vol. 107, no. 17, pp. 7710–7715, Apr. 2010.

[68] D. Games *et al.*, “Reducing C-terminal-truncated alpha-synuclein by

immunotherapy attenuates neurodegeneration and propagation in Parkinson's disease-like models.," *J. Neurosci.*, vol. 34, no. 28, pp. 9441–54, Jul. 2014.

[69] A. Burns and S. Iliffe, "Alzheimer's disease.," *BMJ*, vol. 338, p. b158, Feb. 2009.

[70] I. S. Shin, M. Carter, D. Masterman, L. Fairbanks, and J. L. Cummings, "Neuropsychiatric symptoms and quality of life in Alzheimer disease," *Am. J. Geriatr. Psychiatry*, vol. 13, no. 6, pp. 469–474, 2005.

[71] J. Neugroschl and S. Wang, "Alzheimer's disease: diagnosis and treatment across the spectrum of disease severity.," *Mt. Sinai J. Med.*, vol. 78, no. 4, pp. 596–612, 2011.

[72] V. M.-Y. Lee, M. Goedert, and J. Q. Trojanowski, "Neurodegenerative Tauopathies," *Annu. Rev. Neurosci.*, vol. 24, no. 1, pp. 1121–1159, Mar. 2001.

[73] T. Guo, W. Noble, and D. P. Hanger, "Roles of tau protein in health and disease," *Acta Neuropathol.*, vol. 133, no. 5, pp. 665–704, 2017.

[74] D. P. Perl, "Neuropathology of Alzheimer ' s Disease," *Mt Sinai J Med*, vol. 77, no. 1, pp. 32–42, 2010.

[75] J. Nunan *et al.*, "The C-terminal fragment of the Alzheimer's disease amyloid protein precursor is degraded by a proteasome-dependent mechanism distinct from gamma-secretase.," *Eur. J. Biochem.*, vol. 268, no. 20, pp. 5329–36, Oct. 2001.

[76] M. P. Murphy and H. Levine III, "Alzheimer's Disease and the Amyloid-beta Peptide.," *J. Alzheimers. Dis.*, vol. 19, pp. 311–323, 2010.

[77] K. H. Ashe and A. Aguzzi, "Prions, prionoids and pathogenic proteins in Alzheimer disease.," *Prion*, vol. 7, no. 1, pp. 55–9, 2013.

[78] M. Jucker and L. C. Walker, "Pathogenic protein seeding in alzheimer disease and other neurodegenerative disorders," *Ann. Neurol.*, vol. 70, no. 4, pp. 532–540, Oct. 2011.

[79] H. Braak and E. Braak, "Neuropathological stageing of Alzheimer-related changes," *Acta Neuropathol.*, vol. 82, no. 4, pp. 239–259, 1991.

[80] H. Braak, I. Alafuzoff, T. Arzberger, H. Kretzschmar, and K. Del Tredici, "Staging of Alzheimer disease-associated neurofibrillary pathology using paraffin sections and immunocytochemistry.," *Acta Neuropathol.*, vol. 112, no. 4, pp. 389–404, Oct. 2006.

[81] J. Kim, J. M. Basak, and D. M. Holtzman, "The role of apolipoprotein E in Alzheimer's disease.," *Neuron*, vol. 63, no. 3, pp. 287–303, Aug. 2009.

[82] Z. Guo *et al.*, "Apolipoprotein E genotypes and the incidence of Alzheimer's disease among persons aged 75 years and older: variation by use of antihypertensive medication?," *Am. J. Epidemiol.*, vol. 153, no. 3, pp. 225–31,

Feb. 2001.

[83] “FDA-approved treatments for Alzheimer’s.”

[84] M. B. Colovic, D. Z. Krstic, T. D. Lazarevic-Pasti, A. M. Bondzic, and V. M. Vasic, “Acetylcholinesterase Inhibitors: Pharmacology and Toxicology,” *Curr. Neuropharmacol.*, vol. 11, no. 3, pp. 315–335, 2013.

[85] J. S. Birks and J. Grimley Evans, “Rivastigmine for Alzheimer’s disease,” in *Cochrane Database of Systematic Reviews*, no. 4, J. S. Birks, Ed. Chichester, UK: John Wiley & Sons, Ltd, 2015, p. CD001191.

[86] J. Olin and L. Schneider, “Galantamine for dementia due to Alzheimer’s disease,” in *The Cochrane Database of Systematic Reviews*, no. 3, Chichester, UK: John Wiley & Sons, Ltd, 2002, p. CD001747.

[87] D. S. Geldmacher, “Donepezil (Aricept®) for treatment of Alzheimer´s disease and other dementing conditions,” *Expert Rev. Neurother.*, vol. 4, no. 1, pp. 5–16, Jan. 2004.

[88] W. J. Deardorff and G. T. Grossberg, “A fixed-dose combination of memantine extended-release and donepezil in the treatment of moderate-to-severe Alzheimer’s disease.,” *Drug Des. Devel. Ther.*, vol. 10, pp. 3267–3279, 2016.

[89] B. Solomon, R. Koppel, D. Frankel, and E. Hanan-Aharon, “Disaggregation of Alzheimer beta-amyloid by site-directed mAb.,” *Proc. Natl. Acad. Sci. U. S. A.*, vol. 94, no. 8, pp. 4109–12, Apr. 1997.

[90] F. Bard *et al.*, “Peripherally administered antibodies against amyloid beta-peptide enter the central nervous system and reduce pathology in a mouse model of Alzheimer disease.,” *Nat. Med.*, vol. 6, no. 8, pp. 916–919, Aug. 2000.

[91] D. Schenk *et al.*, “Immunization with amyloid-β attenuates Alzheimer-disease-like pathology in the PDAPP mouse,” *Nature*, vol. 400, no. 6740, pp. 173–177, Jul. 1999.

[92] J.-M. Orgogozo *et al.*, “Subacute meningoencephalitis in a subset of patients with AD after Abeta42 immunization.,” *Neurology*, vol. 61, no. 1, pp. 46–54, Jul. 2003.

[93] C. H. van Dyck, “Anti-Amyloid-β Monoclonal Antibodies for Alzheimer’s Disease: Pitfalls and Promise,” *Biol. Psychiatry*, vol. 83, no. 4, pp. 311–319, Feb. 2018.

[94] C. Li and J. Götz, “Tau-based therapies in neurodegeneration: Opportunities and challenges,” *Nat. Rev. Drug Discov.*, vol. 16, no. 12, pp. 863–883, 2017.

[95] C. M. Wischik, P. C. Edwards, R. Y. Lai, M. Roth, and C. R. Harrington, “Selective inhibition of Alzheimer disease-like tau aggregation by phenothiazines.,” *Proc. Natl. Acad. Sci. U. S. A.*, vol. 93, no. 20, pp. 11213–8,

Oct. 1996.

[96] E. E. Congdon *et al.*, “Methylthioninium chloride (methylene blue) induces autophagy and attenuates tauopathy in vitro and in vivo,” *Autophagy*, vol. 8, no. 4, pp. 609–622, Apr. 2012.

[97] M. Jaime Toro, “Is IVIg of Any Use in the Treatment of Alzheimer Disease?,” *NEJM J. Watch*, vol. 2017, Apr. 2017.

[98] Y. Shi, H. Inoue, J. C. Wu, and S. Yamanaka, “Induced pluripotent stem cell technology: a decade of progress,” *Nat. Rev. Drug Discov.*, vol. 16, no. 2, pp. 115–130, Feb. 2017.

[99] T. Kondo *et al.*, “iPSC-Based Compound Screening and In Vitro Trials Identify a Synergistic Anti-amyloid β Combination for Alzheimer’s Disease,” *Cell Rep.*, vol. 21, no. 8, pp. 2304–2312, 2017.

[100] D. Tewari *et al.*, “Ethnopharmacological Approaches for Dementia Therapy and Significance of Natural Products and Herbal Drugs,” *Front. Aging Neurosci.*, vol. 10, p. 3, Feb. 2018.

[101] R. Guan *et al.*, “Draft genome of the living fossil Ginkgo biloba,” *Gigascience*, vol. 5, no. 1, p. 49, 2016.

[102] F. V DeFeudis and K. Drieu, “Ginkgo biloba extract (EGb 761) and CNS functions: basic studies and clinical applications.,” *Curr. Drug Targets*, vol. 1, no. 1, pp. 25–58, Jul. 2000.

[103] J. Kobus, E. Flaczyk, A. Siger, M. Nogala-Kałucka, J. Korczak, and R. B. Pegg, “Phenolic compounds and antioxidant activity of extracts of Ginkgo leaves,” *Eur. J. Lipid Sci. Technol.*, vol. 111, no. 11, pp. 1150–1160, 2009.

[104] C. Rendeiro, J. D. T. Guerreiro, C. M. Williams, and J. P. E. Spencer, “Postgraduate Symposium: Flavonoids as modulators of memory and learning: Molecular interactions resulting in behavioural effects,” *Proc. Nutr. Soc.*, vol. 71, no. 2, pp. 246–262, 2012.

[105] P. Huang *et al.*, “Effects of food and gender on the pharmacokinetics of ginkgolides A, B, C and bilobalide in rats after oral dosing with ginkgo terpene lactones extract,” *J. Pharm. Biomed. Anal.*, vol. 100, pp. 138–144, Nov. 2014.

[106] Q. Yuan, C. wen Wang, J. Shi, and Z. xiu Lin, “Effects of Ginkgo biloba on dementia: An overview of systematic reviews,” *J. Ethnopharmacol.*, vol. 195, no. December 2016, pp. 1–9, 2017.

[107] C. Shi, J. Liu, F. Wu, and D. T. Yew, “Ginkgo biloba extract in Alzheimer’s disease: from action mechanisms to medical practice.,” *Int. J. Mol. Sci.*, vol. 11, no. 1, pp. 107–23, Jan. 2010.

[108] M. Panepistēmio tēs Krētēs. *et al.*, *International journal of molecular medicine.*,

vol. 39, no. 3. University of Crete, Faculty of Medicine, 2017.

[109] F. Chen, E. A. Eckman, and C. B. Eckman, “Reductions in levels of the Alzheimer’s amyloid β peptide after oral administration of ginsenosides,” *FASEB J.*, vol. 20, no. 8, pp. 1269–1271, Jun. 2006.

[110] C. A. Anastasiou *et al.*, “Mediterranean diet and cognitive health: Initial results from the Hellenic Longitudinal Investigation of Ageing and Diet,” *PLoS One*, vol. 12, no. 8, pp. 1–18, 2017.

[111] J. Rodríguez-Morató, L. Xicota, M. Fitó, M. Farré, M. Dierssen, and R. de la Torre, “Potential Role of Olive Oil Phenolic Compounds in the Prevention of Neurodegenerative Diseases,” *Molecules*, vol. 20, no. 3, pp. 4655–4680, Mar. 2015.

[112] A. H. Abuznait, H. Qosa, B. A. Busnena, K. A. El Sayed, and A. Kaddoumi, “Olive-oil-derived oleocanthal enhances β-amyloid clearance as a potential neuroprotective mechanism against Alzheimer’s disease: in vitro and in vivo studies.,” *ACS Chem. Neurosci.*, vol. 4, no. 6, pp. 973–82, Jun. 2013.

[113] M. Caruana, R. Cauchi, and N. Vassallo, “Putative Role of Red Wine Polyphenols against Brain Pathology in Alzheimer’s and Parkinson’s Disease.,” *Front. Nutr.*, vol. 3, p. 31, 2016.

[114] X. Wang and E. K. Michaelis, “Selective neuronal vulnerability to oxidative stress in the brain.,” *Front. Aging Neurosci.*, vol. 2, p. 12, 2010.

[115] H. Jick, G. L. Zornberg, S. S. Jick, S. Seshadri, and D. A. Drachman, “Statins and the risk of dementia.,” *Lancet (London, England)*, vol. 356, no. 9242, pp. 1627–31, Nov. 2000.

[116] K. K. Borowicz, B. Piskorska, M. Banach, and S. J. Czuczwar, “Neuroprotective actions of neurosteroids.,” *Front. Endocrinol. (Lausanne).*, vol. 2, p. 50, 2011.

[117] S. Giatti, M. Boraso, R. C. Melcangi, and B. Viviani, “Neuroactive steroids, their metabolites, and neuroinflammation.,” *J. Mol. Endocrinol.*, vol. 49, no. 3, pp. R125-34, Dec. 2012.

[118] R. C. Melcangi *et al.*, “Role of neuroactive steroids in the peripheral nervous system.,” *Front. Endocrinol. (Lausanne).*, vol. 2, p. 104, 2011.

[119] R. Cosimo Melcangi and L. M. Garcia-Segura, “Sex-specific therapeutic strategies based on neuroactive steroids: In search for innovative tools for neuroprotection,” *Horm. Behav.*, vol. 57, no. 1, pp. 2–11, Jan. 2010.

[120] K. P. Datla, H. E. Murray, A. V Pillai, G. E. Gillies, and D. T. Dexter, “Differences in dopaminergic neuroprotective effects of estrogen during estrous cycle.,” *Neuroreport*, vol. 14, no. 1, pp. 47–50, Jan. 2003.

[121] L. C. Turtzo and L. D. McCullough, “Sex differences in stroke.,” *Cerebrovasc.*

Dis., vol. 26, no. 5, pp. 462–74, 2008.

[122] M. COSKUN, M. GOK, and S. COSKUN, “Climate Characteristics of Safranbolu (Karabuk) and Saffron Cultivation,” *Int. J. Geogr. Geol.*, vol. 6, no. 3, pp. 58–69, 2017.

[123] A. R. Gohari, S. Saeidnia, and M. K. Mahmoodabadi, “An overview on saffron, phytochemicals, and medicinal properties.,” *Pharmacogn. Rev.*, vol. 7, no. 13, pp. 61–6, Jan. 2013.

[124] P. Winterhalter and M. Straubinger, “Saffron—Renewed Interest in an Ancient Spice,” *Food Rev. Int.*, vol. 16, no. 1, pp. 39–59, 2000.

[125] B. P. V Sunanda, B. Rammohan, and A. Kumar, “The effective study of aqueous extract of Crocus sativus Linn.(Saffron) in depressed mice,” *Int. J. PharmTech Res.*, vol. 6, no. 3, pp. 1143–1152, 2014.

[126] A. Poma, G. Fontecchio, G. Carlucci, and G. Chichiriccò, “Anti-inflammatory properties of drugs from saffron crocus.,” *Antiinflamm. Antiallergy. Agents Med. Chem.*, vol. 11, no. 1, pp. 37–51, 2012.

[127] S. Samarghandian and A. Borji, “Anticarcinogenic effect of saffron (Crocus sativus L.) and its ingredients.,” *Pharmacognosy Res.*, vol. 6, no. 2, pp. 99–107, Apr. 2014.

[128] M. a. Papandreou *et al.*, “Inhibitory activity on amyloid-β aggregation and antioxidant properties of Crocus sativus stigmas extract and its crocin constituents,” *J. Agric. Food Chem.*, vol. 54, no. 23, pp. 8762–8768, 2006.

[129] C. G. Vasilopoulou *et al.*, “Phytochemical composition of ‘mountain tea’ from Sideritis clandestina subsp. clandestina and evaluation of its behavioral and oxidant/antioxidant effects on adult mice,” *Eur. J. Nutr.*, vol. 52, no. 1, pp. 107–116, Feb. 2013.

[130] S. Heidari, S. Mehri, and H. Hosseinzadeh, “Memory enhancement and protective effects of crocin against D-galactose aging model in the hippocampus of wistar rats,” *Iran. J. Basic Med. Sci.*, vol. 20, no. 11, pp. 1250–1259, 2017.

[131] H. Hosseinzadeh, G. Karimi, and M. Niapoor, “Antidepressant effect of Crocus sativus L. stigma extracts and their constituents, crocin and saffranal, in mice,” *Acta Hortic.*, no. 650, pp. 435–445, May 2004.

[132] N. Pitsikas, S. Zisopoulou, P. A. Tarantilis, C. D. Kanakis, M. G. Polissiou, and N. Sakellaridis, “Effects of the active constituents of Crocus sativus L., crocins on recognition and spatial rats’ memory.,” *Behav. Brain Res.*, vol. 183, no. 2, pp. 141–6, Nov. 2007.

[133] R. Mehdizadeh, M. Parizadeh, A.-R. Khooei, S. Mehri, and H. Hosseinzadeh, “Cardioprotective Effect of Saffron Extract and Safranal in Isoproterenol-

Induced Myocardial Infarction in Wistar Rats," *Mashhad Univ. Med. Sci.*, vol. 16, no. 1, pp. 56–63, Jan. 2013.

[134] S. N. Goyal *et al.*, "Preventive effect of crocin of Crocus sativus on hemodynamic, biochemical, histopathological and ultrastuctural alterations in isoproterenol-induced cardiotoxicity in rats," *Phytomedicine*, vol. 17, no. 3–4, pp. 227–232, Mar. 2010.

[135] M. Imenshahidi, H. Hosseinzadeh, and Y. Javadpour, "Hypotensive effect of aqueous saffron extract (Crocus sativus L.) and its constituents, safranal and crocin, in normotensive and hypertensive rats," *Phyther. Res.*, vol. 24, no. 7, p. n/a-n/a, Jul. 2009.

[136] M. Kamalipour and S. Akhondzadeh, "Cardiovascular effects of saffron: an evidence-based review.," *J. Tehran Heart Cent.*, vol. 6, no. 2, pp. 59–61, 2011.

[137] H. Hosseinzadeh and H. M. Younesi, "Antinociceptive and anti-inflammatory effects of Crocus sativus L. stigma and petal extracts in mice.," *BMC Pharmacol.*, vol. 2, p. 7, Mar. 2002.

[138] M. Hemshekhar *et al.*, "A dietary colorant crocin mitigates arthritis and associated secondary complications by modulating cartilage deteriorating enzymes, inflammatory mediators and antioxidant status," *Biochimie*, vol. 94, no. 12, pp. 2723–2733, Dec. 2012.

[139] Q. Ding *et al.*, "Anti-arthritic effects of crocin in interleukin-1β-treated articular chondrocytes and cartilage in a rabbit osteoarthritic model," *Inflamm. Res.*, vol. 62, no. 1, pp. 17–25, Jan. 2013.

[140] H. Mollaei, R. Safaralizadeh, E. Babaei, M. R. Abedini, and R. Hoshyar, "The anti-proliferative and apoptotic effects of crocin on chemosensitive and chemoresistant cervical cancer cells," *Biomed. Pharmacother.*, vol. 94, pp. 307–316, Oct. 2017.

[141] H. Hosseinzadeh and H. R. Sadeghnia, "Effect of Safranal, a Constituent of *Crocus sativus* (Saffron), on Methyl Methanesulfonate (MMS)–Induced DNA Damage in Mouse Organs: An Alkaline Single-Cell Gel Electrophoresis (Comet) Assay," *DNA Cell Biol.*, vol. 26, no. 12, pp. 841–846, Dec. 2007.

[142] H. Bakshi *et al.*, "DNA fragmentation and cell cycle arrest: a hallmark of apoptosis induced by crocin from kashmiri saffron in a human pancreatic cancer cell line.," *Asian Pac. J. Cancer Prev.*, vol. 11, no. 3, pp. 675–9, 2010.

[143] K. Bajbouj, J. Schulze-Luehrmann, S. Diermeier, A. Amin, and R. Schneider-Stock, "The anticancer effect of saffron in two p53 isogenic colorectal cancer cell lines," *BMC Complement. Altern. Med.*, vol. 12, no. 1, p. 1100, Dec. 2012.

[144] A. Amin, K. Bajbouj, A. Koch, M. Gandesiri, and R. Schneider-Stock, "Defective

autophagosome formation in p53-null colorectal cancer reinforces crocin-induced apoptosis.," *Int. J. Mol. Sci.*, vol. 16, no. 1, pp. 1544–61, Jan. 2015.

[145] H. Hosseinzadeh, T. Ziaee, and A. Sadeghi, "The effect of saffron, Crocus sativus stigma, extract and its constituents, safranal and crocin on sexual behaviors in normal male rats," *Phytomedicine*, vol. 15, no. 6–7, pp. 491–495, Jun. 2008.

[146] H. H. M. M. M. Vahabazadeh, "Clinical Applications of Sa ff ron (Crocus sativus) and its Constituents : A Review," pp. 287–295, 2015.

[147] H. Hosseinzadeh, G. Karimi, and M. Niapoor, "Antidepressant effects of Crocus sativus stigma extracts and its constituents, crocin and safranal, in mice," *J. Med. Plants*, vol. 3, no. 11, pp. 48–58, 2004.

[148] B. Mousavi *et al.*, "Safety evaluation of saffron stigma (Crocus sativus L.) aqueous extract and crocin in patients with schizophrenia.," *Avicenna J. phytomedicine*, vol. 5, no. 5, pp. 413–9.

[149] a N. Assimopoulou, Z. Sinakos, and V. P. Papageorgiou, "Radical scavenging activity of Crocus sativus L. extract and its bioactive constituents.," *Phytother. Res.*, vol. 19, no. 11, pp. 997–1000, 2005.

[150] M.-B. Ebrahim-Habibi, M. Amininasab, A. Ebrahim-Habibi, M. Sabbaghian, and M. Nemat-Gorgani, "Fibrillation of α-lactalbumin: Effect of crocin and safranal, two natural small molecules from Crocus sativus," *Biopolymers*, vol. 93, no. 10, pp. 854–865, Apr. 2010.

[151] S. Purushothuman *et al.*, "Saffron pre-treatment offers neuroprotection to Nigral and retinal dopaminergic cells of MPTP-Treated mice.," *J. Parkinsons. Dis.*, vol. 3, no. 1, pp. 77–83, 2013.

[152] G. D. Geromichalos *et al.*, "Saffron as a source of novel acetylcholinesterase inhibitors: Molecular docking and in vitro enzymatic studies," *J. Agric. Food Chem.*, vol. 60, no. 24, pp. 6131–6138, 2012.

[153] C. A. Ross and M. A. Poirier, "Protein aggregation and neurodegenerative disease," *Nat. Med.*, vol. 10, no. 7, pp. S10–S17, Jul. 2004.

[154] J. A. Hardy and G. A. Higgins, "Alzheimer's disease: the amyloid cascade hypothesis.," *Science*, vol. 256, no. 5054, pp. 184–5, Apr. 1992.

[155] S. T. Ferreira and W. L. Klein, "The Aβ oligomer hypothesis for synapse failure and memory loss in Alzheimer's disease," *Neurobiol. Learn. Mem.*, vol. 96, no. 4, pp. 529–543, Nov. 2011.

[156] C. Ballard, S. Gauthier, A. Corbett, C. Brayne, D. Aarsland, and E. Jones, "Alzheimer's disease," *Lancet*, vol. 377, no. 9770, pp. 1019–1031, Mar. 2011.

[157] K. J. A. Davies, "Degradation of oxidized proteins by the 20S proteasome,"

Biochimie, vol. 83, no. 3–4, pp. 301–310, Mar. 2001.

[158] F. N. Bazoti, J. Bergquist, K. E. Markides, and A. Tsarbopoulos, “Noncovalent interaction between amyloid-β-peptide (1-40) and oleuropein studied by electrospray ionization mass spectrometry,” *J. Am. Soc. Mass Spectrom.*, vol. 17, no. 4, pp. 568–575, 2006.

[159] J. Jerabek *et al.*, “Tacrine-resveratrol fused hybrids as multi-target-directed ligands against Alzheimer’s disease,” *Eur. J. Med. Chem.*, vol. 127, pp. 250–262, 2017.

[160] S.-Y. Park, “Potential therapeutic agents against Alzheimer’s disease from natural sources,” *Arch. Pharm. Res.*, vol. 33, no. 10, pp. 1589–1609, 2010.

[161] W. Song and D. K. Lahiri, “Melatonin alters the metabolism of the β-amyloid precursor protein in the neuroendocrine cell line PC12,” *J. Mol. Neurosci.*, vol. 9, no. 2, pp. 75–92, Oct. 1997.

[162] R.-Y. Liu, J.-N. Zhou, J. van Heerikhuize, M. A. Hofman, and D. F. Swaab, “Decreased Melatonin Levels in Postmortem Cerebrospinal Fluid in Relation to Aging, Alzheimer’s Disease, and Apolipoprotein E-ε4/4 Genotype [1],” *J. Clin. Endocrinol. Metab.*, vol. 84, no. 1, pp. 323–327, Jan. 1999.

[163] F. N. Bazoti, A. Tsarbopoulos, K. E. Markides, and J. Bergquist, “Study of the non-covalent interaction between amyloid-beta-peptide and melatonin using electrospray ionization mass spectrometry.,” *J. Mass Spectrom.*, vol. 40, no. 2, pp. 182–192, 2005.

[164] F. N. Bazoti, J. Bergquist, K. Markides, and A. Tsarbopoulos, “Localization of the Noncovalent Binding Site Between Amyloid-β-Peptide and Oleuropein Using Electrospray Ionization FT-ICR Mass Spectrometry,” *J. Am. Soc. Mass Spectrom.*, vol. 19, no. 8, pp. 1078–1085, 2008.

[165] N. S. Koulakiotis, D. Anagnostopoulos, I. Chalatsa, D. Sanoudou, and A. Tsarbopoulos, *GSTF Journal of Advances in Medical Research JAMR*, vol. 1 pp.10–15, no. 3. 2015.

[166] H. Caballero-Ortega, R. Pereda-Miranda, and F. I. Abdullaev, “HPLC quantification of major active components from 11 different saffron (Crocus sativus L.) sources,” *Food Chem.*, vol. 100, no. 3, pp. 1126–1131, 2007.

[167] R. Hamidpour, S. Hamidpour, M. Hamidpour, and M. Shahlari, “Effect of Crocus sativus and its active compounds for the treatment of several diseases : A review,” *Int. J. Case Reports Images*, vol. 4, no. 12, pp. 666–670, 2013.

[168] A. H. Mohammadpour, M. Ramezani, N. Tavakoli Anaraki, B. Malaekeh-Nikouei, S. Amel Farzad, and H. Hosseinzadeh, “Development and Validation of HPLC Method for Determination of Crocetin, a constituent of Saffron, in

Human Serum Samples.," *Iran. J. Basic Med. Sci.*, vol. 16, no. 1, pp. 47–55, 2013.

[169] M. R. Khazdair, M. H. Boskabady, M. Hosseini, R. Rezaee, and A. M Tsatsakis, "The effects of Crocus sativus (saffron) and its constituents on nervous system: A review.," *Avicenna J. phytomedicine*, vol. 5, no. 5, pp. 376–91, Jan. .

[170] N. P. G Georgiadou, V. Grivas, P.A. Tarantilis, "Crocins, the active constituents of Crocus Sativus L., counteracted ketamine–induced behavioural deficits in rats," *Psychopharmacology (Berl).*, vol. 231, pp. 717–726, 2014.

[171] G.-F. Zhang, Y. Zhang, and G. Zhao, "Crocin protects PC12 cells against MPP(+)-induced injury through inhibition of mitochondrial dysfunction and ER stress.," *Neurochem. Int.*, vol. 89, pp. 101–10, Oct. 2015.

[172] S. V. Rao, Muralidhara, S. C. Yenisetti, and P. S. Rajini, "Evidence of neuroprotective effects of saffron and crocin in a Drosophila model of parkinsonism.," *Neurotoxicology*, vol. 52, pp. 230–242, Dec. 2015.

[173] D. G. Chryssanthi, F. N. Lamari, G. Iatrou, A. Pylara, N. K. Karamanos, and P. Cordopatis, "Inhibition of breast cancer cell proliferation by style constituents of different Crocus species.," *Anticancer Res.*, vol. 27, no. 1A, pp. 357–362, 2007.

[174] N. S. Koulakiotis, E. Gikas, G. Iatrou, F. N. Lamari, and A. Tsarbopoulos, "Quantitation of crocins and picrocrocin in saffron by hplc: Application to quality control and phytochemical differentiation from other crocus taxa," *Planta Med.*, vol. 81, no. 7, pp. 606–612, 2015.

[175] W. Murayama, T. Kobayashi, Y. Kosuge, H. Yano, Y. Nunogaki, and K. Nunogaki, "A new centrifugal counter-current chromatograph and its application," *J. Chromatogr. A*, vol. 239, no. C, pp. 643–649, 1982.

[176] A. P. Foucault, *Centrifugal Partition Chromatography*. 1995.

[177] A. Berthod, *Countercurrent Chromatography: The Support-Free Liquid Stationary Phase (Comprehensive Analytical Chemistry)*. 2002.

[178] L. Marchal, J. Legrand, and A. Foucault, "Centrifugal partition chromatography: A survey of its history, and our recent advances in the field," *Chem. Rec.*, vol. 3, no. 3, pp. 133–143, 2003.

[179] A. Berthod, M. J. Ruiz-Ángel, and S. Carda-Broch, "Countercurrent chromatography: People and applications," *J. Chromatogr. A*, vol. 1216, no. 19, pp. 4206–4217, 2009.

[180] A. B. J. M. K. F. N. Mekaoui, "Solvent Selection in Countercurrent Chromatography Using Small-Volume Hydrostatic Columns."

[181] S. Chollet, L. Marchal, Jérémy Meucci, J.-H. Renault, J. Legrand, and A. Foucault, "Methodology for optimally sized centrifugal partition chromatography

columns," *J. Chromatogr. A*, vol. 1388, pp. 174–183, Apr. 2015.

[182] K. Skalicka-Woźniak and I. Garrard, "Counter-current chromatography for the separation of terpenoids: a comprehensive review with respect to the solvent systems employed," *Phytochem. Rev.*, vol. 13, no. 2, pp. 547–572, Jun. 2014.

[183] K. Hostettmann, A. Marston, and M. Hostettmann, "Introduction," in *Preparative Chromatography Techniques*, Berlin, Heidelberg: Springer Berlin Heidelberg, 1998, pp. 1–2.

[184] G. F. Pauli, S. M. Pro, and J. B. Friesen, "Countercurrent separation of natural products - Supporting information," *J. Nat. Prod.*, vol. 71, no. 8, pp. 1489–1508, 2008.

[185] K. D. Yoon, Y.-W. Chin, and J. Kim, "Centrifugal Partition Chromatography: Application To Natural Products in 1994–2009," *J. Liq. Chromatogr. Relat. Technol.*, vol. 33, no. 9–12, pp. 1208–1254, 2010.

[186] S. A. Mohajeri, H. Hosseinzadeh, F. Keyhanfar, and J. Aghamohammadian, "Extraction of crocin from saffron (Crocus sativus) using molecularly imprinted polymer solid-phase extraction," *J. Sep. Sci.*, vol. 33, no. 15, pp. 2302–2309, 2010.

[187] F. Hadizadeh, S. a. Mohajeri, and M. Seifi, "Extraction and purification of crocin from saffron stigmas employing a simple and efficient crystallization method," *Pakistan J. Biol. Sci.*, vol. 13, no. 14, pp. 691–698, 2010.

[188] H. Choi, "Isolation and characterization of the major colorant in Gardenia fruit," *Dye. Pigment.*, vol. 49, no. 1, pp. 15–20, 2001.

[189] P. A. Tarantilis, A. Beljebbar, M. Manfait, and M. Polissiou, "FT-IR, FT-Raman spectroscopic study of carotenoids from saffron (Crocus sativus L.) and some derivatives," *Spectrochim. Acta Part A Mol. Biomol. Spectrosc.*, vol. 54, no. 4, pp. 651–657, 1998.

[190] A. Rubio Moraga, O. Ahrazem, J. L. Rambla, A. Granell, and L. Gómez Gómez, "Crocins with High Levels of Sugar Conjugation Contribute to the Yellow Colours of Early-Spring Flowering Crocus Tepals," *PLoS One*, vol. 8, no. 9, 2013.

[191] M. Straubinger, M. Jezussek, R. Waibel, and P. Winterhalter, "Novel Glycosidic Constituents from Saffron," *J. Agric. Food Chem.*, vol. 45, no. 5, pp. 1678–1681, 1997.

[192] M. Straubinger, B. Bau, S. Eckstein, M. Fink, and P. Winterhalter, "Identification of novel glycosidic aroma precursors in saffron (Crocus sativus L.)," *J. Agric. Food Chem.*, vol. 46, no. 8, pp. 3238–3243, 1998.

[193] W. D. and R. J. P. Conway, *Modern countercurrent chromatography*. 1995.

[194] M. Lautenschläger, M. Lechtenberg, J. Sendker, and A. Hensel, "Effective

isolation protocol for secondary metabolites from Saffron: Semi-preparative scale preparation of crocin-1 and trans-crocetin," *Fitoterapia*, vol. 92, pp. 290–295, 2014.

[195] Z. Liang *et al.*, "Isolation and Purification of Geniposide, Crocin-1, and Geniposidic Acid from the Fruit of *Gardenia jasminoides* Ellis by High-Speed Counter-Current Chromatography," *Sep. Sci. Technol.*, vol. 49, no. 9, pp. 1427–1433, 2014.

[196] M. Lechtenberg, D. Schepmann, M. Niehues, N. Hellenbrand, B. Wünsch, and A. Hensel, "Quality and functionality of saffron: Quality control, species assortment and affinity of extract and isolated saffron compounds to NMDA and σ1(Sigma-1) receptors," *Planta Med.*, vol. 74, no. 7, pp. 764–772, 2008.

[197] X. Chu, A. Sun, and R. Liu, "Preparative isolation and purification of five compounds from the Chinese medicinal herb Polygonum cuspidatum Sieb. et Zucc by high-speed counter-current chromatography," *J. Chromatogr. A*, vol. 1097, no. 1–2, pp. 33–39, 2005.

[198] Y. Zhang, C. Liu, Z. Zhang, Y. Qi, G. Wu, and S. Li, "Solvent gradient elution for comprehensive separation of constituents with wide range of polarity in Apocynum venetum leaves by high-speed counter-current chromatography," *J. Sep. Sci.*, vol. 33, no. 17–18, pp. 2743–2748, 2010.

[199] S. Ignatova, N. Sumner, N. Colclough, and I. Sutherland, "Gradient elution in counter-current chromatography: A new layout for an old path," *J. Chromatogr. A*, vol. 1218, no. 36, pp. 6053–6060, 2011.

[200] S. Ignatova, P. Wood, D. Hawes, L. Janaway, D. Keay, and I. Sutherland, "Feasibility of scaling from pilot to process scale," *J. Chromatogr. A*, vol. 1151, no. 1–2, pp. 20–24, 2007.

[201] I. A. Sutherland, "Recent progress on the industrial scale-up of counter-current chromatography," *J. Chromatogr. A*, vol. 1151, no. 1–2, pp. 6–13, 2007.

[202] A. Angelis, A. Urbain, M. Halabalaki, N. Aligiannis, and A.-L. Skaltsounis, "One-step isolation of γ-oryzanol from rice bran oil by non-aqueous hydrostatic countercurrent chromatography," *J. Sep. Sci.*, vol. 34, no. 18, pp. 2528–2537, Sep. 2011.

[203] S. Zheng, Z. Qian, L. Sheng, and N. Wen, "Crocetin Attenuates Atherosclerosis in Hyperlipidemic Rabbits Through Inhibition of LDL Oxidation," *J. Cardiovasc. Pharmacol.*, vol. 47, no. 1, pp. 70–76, 2006.

[204] I.-A. Lee, J. H. Lee, N.-I. Baek, and D.-H. Kim, "Antihyperlipidemic effect of crocin isolated from the fructus of Gardenia jasminoides and its metabolite Crocetin.," *Biol. Pharm. Bull.*, vol. 28, no. 11, pp. 2106–10, 2005.

[205] S.-Y. He, Z.-Y. Qian, N. Wen, F.-T. Tang, G.-L. Xu, and C.-H. Zhou, “Influence of Crocetin on experimental atherosclerosis in hyperlipidamic-diet quails,” *Eur. J. Pharmacol.*, vol. 554, no. 2–3, pp. 191–195, Jan. 2007.

[206] S. Llorens *et al.*, “Effects of crocetin esters and crocetin from crocus sativus L. on aortic contractility in rat genetic hypertension,” *Molecules*, vol. 20, no. 9, pp. 17570–17584, 2015.

[207] M. Agha-Hosseini *et al.*, “Crocus sativus L. (saffron) in the treatment of premenstrual syndrome: a double-blind, randomised and placebo-controlled trial,” *BJOG An Int. J. Obstet. Gynaecol.*, vol. 115, no. 4, pp. 515–519, Mar. 2008.

[208] A. Ghahghaei, S. Z. Bathaie, H. Kheirkhah, and E. Bahraminejad, “The protective effect of crocin on the amyloid fibril formation of Aβ42 peptide in vitro.,” *Cell Mol Biol Lett.*, vol. 18, no. 3, pp. 328–39, 2013.

[209] S. Akhondzadeh *et al.*, “ORIGINAL ARTICLE: Saffron in the treatment of patients with mild to moderate Alzheimer’s disease: a 16-week, randomized and placebo-controlled trial,” *J. Clin. Pharm. Ther.*, vol. 35, no. 5, pp. 581–588, 2010.

[210] A. Talaei, M. Hassanpour Moghadam, S. A. Sajadi Tabassi, and S. A. Mohajeri, “Crocin, the main active saffron constituent, as an adjunctive treatment in major depressive disorder: A randomized, double-blind, placebo-controlled, pilot clinical trial,” *J. Affect. Disord.*, vol. 174, pp. 51–56, 2015.

[211] H. B. Bostan, S. Mehri, and H. Hosseinzadeh, “Toxicology effects of saffron and its constituents: a review.,” *Iran. J. Basic Med. Sci.*, vol. 20, no. 2, pp. 110–121, Feb. 2017.

[212] A. H. Mohamadpour, Z. Ayati, M. R. Parizadeh, O. Rajbai, and H. Hosseinzadeh, “Safety evaluation of crocin (a constituent of saffron) tablets in healthy volunteers,” *Iran. J. Basic Med. Sci.*, vol. 16, no. 1, pp. 39–46, 2013.

[213] H. Hosseinzadeh, V. M. Shariaty, A. K. Sameni, and M. Vahabzadeh, “Acute and sub-acute toxicity of crocin, a constituent of Crocus sativus L. (safron), in mice and rats,” *Pharmacologyonline*, vol. 2, pp. 943–951, 2010.

[214] B. Ghadrdoost *et al.*, “Protective effects of saffron extract and its active constituent crocin against oxidative stress and spatial learning and memory deficits induced by chronic stress in rats,” *Eur. J. Pharmacol.*, vol. 667, no. 1, pp. 222–229, 2011.

[215] M.-B. Ebrahim-Habibi, M. Amininasab, A. Ebrahim-Habibi, M. Sabbaghian, and M. Nemat-Gorgani, “Fibrillation of alpha-lactalbumin: effect of crocin and safranal, two natural small molecules from Crocus sativus.,” *Biopolymers*, vol. 93, no. 10, pp. 854–65, Oct. 2010.

[216] J. H. Ahn, Y. Hu, M. Hernandez, and J. R. Kim, “Crocetin inhibits beta-amyloid fibrillization and stabilizes beta-amyloid oligomers,” *Biochem. Biophys. Res. Commun.*, vol. 414, no. 1, pp. 79–83, 2011.

[217] X. Bie, Y. Chen, X. Zheng, and H. Dai, “The role of crocetin in protection following cerebral contusion and in the enhancement of angiogenesis in rats,” *Fitoterapia*, vol. 82, no. 7, pp. 997–1002, 2011.

[218] V. Magesh, J. P. V. Singh, K. Selvendiran, G. Ekambaram, and D. Sakthisekaran, “Antitumour activity of crocetin in accordance to tumor incidence, antioxidant status, drug metabolizing enzymes and histopathological studies,” *Mol. Cell. Biochem.*, vol. 287, no. 1–2, pp. 127–135, Jul. 2006.

[219] L. Xi, Z. Qian, P. Du, and J. Fu, “Pharmacokinetic properties of crocin (crocetin digentiobiose ester) following oral administration in rats,” *Phytomedicine*, vol. 14, no. 9, pp. 633–636, Sep. 2007.

[220] A. Asai, T. Nakano, M. Takahashi, and A. Nagao, “Orally administered crocetin and crocins are absorbed into blood plasma as crocetin and its glucuronide conjugates in mice,” *J. Agric. Food Chem.*, vol. 53, pp. 7302–7306, 2005.

[221] M. Lautenschläger *et al.*, “Intestinal formation of trans-crocetin from saffron extract (Crocus sativus L.) and in vitro permeation through intestinal and blood brain barrier.,” *Phytomedicine*, vol. 22, no. 1, pp. 36–44, Jan. 2015.

[222] N. Umigai *et al.*, “The pharmacokinetic profile of crocetin in healthy adult human volunteers after a single oral administration.,” *Phytomedicine*, vol. 18, no. 7, pp. 575–8, 2011.

[223] Y. Zhang *et al.*, “Sensitive analysis and simultaneous assessment of pharmacokinetic properties of crocin and crocetin after oral administration in rats,” *J. Chromatogr. B*, vol. 1044–1045, pp. 1–7, Feb. 2017.

[224] D. G. Chryssanthi, F. N. Lamari, C. D. Georgakopoulos, and P. Cordopatis, “A new validated SPE-HPLC method for monitoring crocetin in human plasma--application after saffron tea consumption.,” *J. Pharm. Biomed. Anal.*, vol. 55, no. 3, pp. 563–8, 2011.

[225] Y. Chen, J. C. Sullivan, A. Edwards, and A. T. Layton, “Sex-specific Computational Models of the Spontaneously Hypertensive Rat Kidneys: Factors Affecting Nitric Oxide Bioavailability,” *Am. J. Physiol. - Ren. Physiol.*, 2017.

[226] K. H. van Het Hof, C. E. West, J. A. Weststrate, and J. G. Hautvast, “Dietary factors that affect the bioavailability of carotenoids.,” *J. Nutr.*, vol. 130, no. 3, pp. 503–6, Mar. 2000.

[227] A. Cassidy *et al.*, “Factors affecting the bioavailability of soy isoflavones in humans after ingestion of physiologically relevant levels from different soy

foods.," *J. Nutr.*, vol. 136, no. 1, pp. 45–51, Jan. 2006.

[228] P. V Turner, T. Brabb, C. Pekow, and M. a Vasbinder, "Administration of substances to laboratory animals: routes of administration and factors to consider," *J Am Assoc Lab Anim Sci*, vol. 50, no. 5, pp. 600–613, 2011.

[229] E. Karkoula *et al.*, "Development and validation of a UPLC method for quantifying trans-crocin 4 and crocetin from saffron in plasma: A pharmacokinetic study," *Planta Med.*, vol. 81, no. S 01, pp. S1–S381, Dec. 2016.

[230] C. Gonzalez-Riano, A. Garcia, and C. Barbas, "Metabolomics studies in brain tissue: A review," *J. Pharm. Biomed. Anal.*, vol. 130, pp. 141–168, 2016.

[231] F. X. Pi-Sunyer, "The epidemiology of central fat distribution in relation to disease.," *Nutr. Rev.*, vol. 62, no. 7 Pt 2, pp. S120-6, Jul. 2004.

[232] N. Kokras, C. Dalla, and Z. Papadopoulou-Daifoti, "Sex differences in pharmacokinetics of antidepressants," *Expert Opin. Drug Metab. Toxicol.*, vol. 7, no. 2, pp. 213–226, Feb. 2011.

[233] W. M. Pardridge, "Blood–brain barrier delivery," *Drug Discov. Today*, vol. 12, no. 1–2, pp. 54–61, Jan. 2007.

[234] W. M. Pardridge, "Molecular Trojan horses for blood–brain barrier drug delivery," *Curr. Opin. Pharmacol.*, vol. 6, no. 5, pp. 494–500, Oct. 2006.

[235] W. M. Pardridge, "The blood-brain barrier: bottleneck in brain drug development.," *NeuroRx*, vol. 2, no. 1, pp. 3–14, Jan. 2005.

[236] D. Triguero, J. Buciak, and W. M. Pardridge, "Capillary depletion method for quantification of blood-brain barrier transport of circulating peptides and plasma proteins.," *J. Neurochem.*, vol. 54, no. 6, pp. 1882–8, Jun. 1990.

[237] R. B. Saxena, "Botany, Taxonomy and Cytology of Crocus sativus series.," *Ayu*, vol. 31, no. 3, pp. 374–81, Jul. 2010.

[238] M. Z. Tsimidou, "SaffronOMICS: the international dimension and impact of the scientific achievements of a European COST ACTION project," *Acta Hortic.*, no. 1184, pp. 1–10, Nov. 2017.

[239] T. Ochiai, S. Ohno, S. Soeda, H. Tanaka, Y. Shoyama, and H. Shimeno, "Crocin prevents the death of rat pheochromyctoma (PC-12) cells by its antioxidant effects stronger than those of α-tocopherol," *Neurosci. Lett.*, vol. 362, no. 1, pp. 61–64, May 2004.

[240] Y. Sun *et al.*, "Crocin Exhibits Antitumor Effects on Human Leukemia HL-60 Cells In Vitro and In Vivo.," *Evid. Based. Complement. Alternat. Med.*, vol. 2013, p. 690164, 2013.

[241] S. Asalgoo, M. Tat, H. Sahraei, and G. Pirzad Jahromi, "The Psychoactive

Agent Crocin Can Regulate Hypothalamic-Pituitary-Adrenal Axis Activity," *Front. Neurosci.*, vol. 11, p. 668, Dec. 2017.

[242] J. Tabeshpour *et al.*, "A double-blind, randomized, placebo-controlled trial of saffron stigma (Crocus sativus L.) in mothers suffering from mild-to-moderate postpartum depression," *Phytomedicine*, vol. 36, pp. 145–152, Dec. 2017.

[243] G. Georgiadou, P. a. Tarantilis, and N. Pitsikas, "Effects of the active constituents of Crocus Sativus L., crocins, in an animal model of obsessive-compulsive disorder," *Neurosci. Lett.*, vol. 528, no. 1, pp. 27–30, 2012.

[244] M. Shafiee *et al.*, "Saffron against Components of Metabolic Syndrome: Current Status and Prospective," *J. Agric. Food Chem.*, vol. 65, no. 50, pp. 10837–10843, 2017.

[245] M. A. Yorgun, K. Rashid, A. Aslanidis, C. Bresgen, K. Dannhausen, and T. Langmann, "Crocin, a plant-derived carotenoid, modulates microglial reactivity," *Biochem. Biophys. Reports*, vol. 12, no. September, pp. 245–250, 2017.

[246] S. H. Alavizadeh and H. Hosseinzadeh, "Bioactivity assessment and toxicity of crocin: a comprehensive review.," *Food Chem. Toxicol.*, vol. 64, pp. 65–80, 2014.

[247] T. N. Joloudar, A. A. Saboury, M. D. Shasaltaneh, S. Bahramikia, M. A. Ebrahimi, and A. Ghasemi, "Inhibitory effect of safranal and crocin, two principle compounds of Crocus sativus, on fibrillation of lysozyme," *J. Iran. Chem. Soc.*, vol. 14, no. 11, pp. 2407–2416, 2017.

[248] S. Padmanabhan, K. Burgess, N. Rankin, and S. Weidt, "Chapter 10 – Metabolomics," in *Handbook of Pharmacogenomics and Stratified Medicine*, 2014, pp. 181–205.

[249] "Chapter 1 – Biomarker Discovery: Study Design and Execution," in *Proteomic and Metabolomic Approaches to Biomarker Discovery*, 2013, pp. 1–16.

[250] B. Ivarez-Sánchez, F. Priego-Capote, and L. de Castro, "Metabolomics analysis I. Selection of biological samples and practical aspects preceding sample preparation," *Trends Anal. Chem.*, vol. 29, pp. 111–119.

[251] B. Zhu *et al.*, "A simultaneously quantitative method to profiling twenty endogenous nucleosides and nucleotides in cancer cells using UHPLC-MS/MS," *Talanta*, vol. 179, pp. 615–623, Mar. 2018.

[252] J. Stanstrup, M. Gerlich, L. O. Dragsted, and S. Neumann, "Metabolite profiling and beyond: Approaches for the rapid processing and annotation of human blood serum mass spectrometry data Metabolomics and Metabolite Profiling," *Anal. Bioanal. Chem.*, vol. 405, no. 15, pp. 5037–5048, 2013.

[253] A. H. Pripp, "Application of Multivariate Analysis: Benefits and Pitfalls," in

Statistics in Food Science and Nutrition, New York, NY: Springer New York, 2013, pp. 53–64.

[254] M. Calderón-Santiago, M. A. López-Bascón, Á. Peralbo-Molina, and F. Priego-Capote, “MetaboQC: A tool for correcting untargeted metabolomics data with mass spectrometry detection using quality controls,” *Talanta*, vol. 174, pp. 29–37, Nov. 2017.

[255] G. Libiseller *et al.*, “IPO: a tool for automated optimization of XCMS parameters,” *BMC Bioinformatics*, vol. 16, no. 1, p. 118, Dec. 2015.

[256] H. P. Benton, E. J. Want, and T. M. D. Ebbels, “Correction of mass calibration gaps in liquid chromatography-mass spectrometry metabolomics data,” *Bioinformatics*, vol. 26, no. 19, pp. 2488–2489, 2010.

[257] C. a Smith, E. J. Want, G. O’Maille, R. Abagyan, G. Siuzdak, and and G. S. CA Smith, J Elizabeth, G O’Maille,Ruben Abagyan, “XCMS: processing mass spectrometry data for metabolite profiling using Nonlinear Peak Alignment,Matching,and Identification,” *ACS Publ.*, vol. 78, no. 3, pp. 779–87, 2006.

[258] R. Tautenhahn, C. Bottcher, and S. Neumann, “Highly sensitive feature detection for high resolution LC/MS,” *BMC Bioinformatics*, vol. 9, no. 1, p. 504, Nov. 2008.

[259] H. Redestig *et al.*, “Compensation for systematic cross-contribution improves normalization of mass spectrometry based metabolomics data,” *Anal. Chem.*, vol. 81, no. 19, pp. 7974–7980, 2009.

[260] M. Sysi-Aho, M. Katajamaa, L. Yetukuri, and M. Orešič, “Normalization method for metabolomics data using optimal selection of multiple internal standards,” *BMC Bioinformatics*, vol. 8, pp. 1–17, 2007.

[261] M. Vinaixa, S. Samino, I. Saez, J. Duran, J. J. Guinovart, and O. Yanes, “A Guideline to Univariate Statistical Analysis for LC/MS-Based Untargeted Metabolomics-Derived Data.,” *Metabolites*, vol. 2, no. 4, pp. 775–95, Oct. 2012.

[262] 96/23/Ec Commission Decision, “96/23/EC COMMISSION DECISION of 12 August 2002 implementing Council Directive 96/23/EC concerning the performance of analytical methods and the interpretation of results (notified under document number C(2002) 3044)(Text withEEA relevance) (2002/657/EC),” *96/23/Ec Comm. Decis.*, p. 29, 2002.

[263] T. Package and A. K. Uppal, “Package ‘ xMSannotator ,’” pp. 1–14, 2017.

[264] A. Gunnar Libiseller, C. Magnes, T. Riebenbauer, and M. Thomas Riebenbauer, “Package ‘IPO’ Title Automated Optimization of XCMS Data Processing parameters,” 2018.

[265] Y. Wu and L. Li, “Sample normalization methods in quantitative metabolomics,” *J. Chromatogr. A*, vol. 1430, pp. 80–95, Jan. 2016.

[266] X. Shen *et al.*, “Normalization and integration of large-scale metabolomics data using support vector regression,” *Metabolomics*, vol. 12, no. 5, p. 89, May 2016.

[267] A. Alysha, M. De Livera, J. B. Bowne, and M. Alysha, “Package ‘metabolomics’ Title Analysis of Metabolomics Data,” 2015.

[268] J. A. ; Westerhuis *et al.*, “UvA-DARE (Digital Academic Repository) Assessment of PLSDA cross validation Assessment of PLSDA cross validation,” *Metabolomics*, vol. 4, no. 1, pp. 81–89, 2008.

[269] B. Worley and R. Powers, “PCA as a practical indicator of OPLS-DA model reliability.,” *Curr. Metabolomics*, vol. 4, no. 2, pp. 97–103, 2016.

[270] S. Theodoridis and K. Koutroumbas, *Pattern recognition*. Academic Press, 2009.

[271] J. D. Storey, “The positive false discovery rate: A Bayesian interpretation and the q-value,” *Ann. Stat.*, vol. 31, no. 6, pp. 2013–2035, 2003.

[272] Storey J.D., “A direct approach to false discovery rates John,” *J. R. Stat. Soc.*, vol. 64, no. Part 3, pp. 479–498, 2002.

[273] J. D. Storey, J. E. Taylor, and D. Siegmund, “Strong control, conservative point estimation and simultaneous conservative consistency of false discovery rates: A unified approach,” *J. R. Stat. Soc. Ser. B Stat. Methodol.*, vol. 66, no. 1, pp. 187–205, 2004.

[274] G. V. (Gajanan V. . Sherbet, *Therapeutic strategies in cancer biology and pathology*. Elsevier, 2013.

[275] J. Q. Zhang, W. Q. Cai, D. S. Zhou, and B. Y. Su, “Distribution and differences of estrogen receptor beta immunoreactivity in the brain of adult male and female rats.,” *Brain Res.*, vol. 935, no. 1–2, pp. 73–80, May 2002.

[276] R. Li, J. Cui, and Y. Shen, “At the Cutting Edge Brain sex matters: Estrogen in cognition and Alzheimer’s disease,” 2014.

[277] L. Zhao, S. K. Woody, and A. Chhibber, “Estrogen receptor β in Alzheimer’s disease: From mechanisms to therapeutics,” *Ageing Res. Rev.*, vol. 24, pp. 178–190, 2015.

[278] R. C. Agís-Balboa *et al.*, “Characterization of brain neurons that express enzymes mediating neurosteroid biosynthesis,” 2006.

[279] R. H. Purdy, A. L. Morrow, P. H. Moore, S. M. Paul, and S. M. Paul, “Stress-induced elevations of gamma-aminobutyric acid type A receptor-active steroids in the rat brain.,” *Proc. Natl. Acad. Sci. U. S. A.*, vol. 88, no. 10, pp. 4553–7, May 1991.

[280] D. Eser *et al.*, “Neuroactive steroids as modulators of depression and anxiety,” *Neuroscience*, vol. 138, no. 3, pp. 1041–1048, Mar. 2006.

ACKNOWLEDGEMENTS

I would like to express my sincere gratitude to all the people that contributed to the completion of this doctoral thesis.

First of all, my special thanks and appreciation go to my supervisor and my mentor Associate Prof. Anthony Tsarbopoulos for his constant support, his advice, and his constant consulting towards every aspect of the current thesis. Moreover, I would like to gratefully thank him for all the times that I “fell” and he lifted me up one more time. I feel very proud of being a member of his team.

I sincerely thank the members of the examining scientific committee;
Prof. Constantinos Pantos, Prof. Alexios-Leandros Skaltsounis, Prof. Jonas Bergquist, Associate Prof. Nikolaos Skarmeas, Assistant Prof. Evagelos Gikas and Assistant Prof. Christina Dalla for the academic support, their excellent comments and suggestions and of course, for the time they have spent in reading my thesis in spite of their busy schedules.

I would like to express my gratefulness, my happiness and my sincere thanks to Assistant Prof. Vagelis Gikas for his constant, even late-night, support, his never ending passion that managed to blow me with and all his encouragement, even when things were not going that well. It was an honor working with him not only because he was a tremendous teacher and ready to impart all of his knowledge to me, but also a great friend to all of us.

Since I never forget my initial scientific family, I would like to sincerely thank Prof. Alexios-Leandros Skaltsounis for his enormous scientific support, his financial support and of course for the opportunity to participate in three international congresses in the last 4 years. A special thanks for the almost 10 years of collaboration and appreciation.

From the team of Athens Medical School I would like to gratefully acknowledge Assistant Prof. Christina Dalla and Dr. Nikolaos Kokras, Scientific Associate of the 1st Psychiatric Clinic, Eginition Hospital, National and Kapodistrian University of Athens, for their scientific support, their positivity even when we faced difficult situations as well as their brilliant suggestions and advice regarding my PhD thesis.

Despoina Papasavva is gratefully acknowledged for her help in all the animal experiments as well as her positivity and her pleasantness during our collaboration.

Assistant Prof. Maria Halabalaki is gratefully acknowledged for her substantial scientific support and contribution to the progress of my PhD thesis as well as the publications occurred.

I would like to thank my professors Panagiotis Marakos and Nicole Pouli for their substantial contribution and constructive suggestions towards my decision to start this PhD thesis and their constant support and interest on me.

Special thanks to The Goulandris Natural History Museum and all the working stuff for the financial support and the effective help they have offered me whenever I faced a difficult situation.

My dear colleagues have been kind enough to offer me a helping hand each and every time that I have asked them to, thus I would like to thank them all for all the time that we have spent together and for their true friendship. My work would not have been the same if it had not been for Dr. Apostolis Angelis, Dr. Nikos Lemonakis, Dr. Nikos Koulakiotis and Dr. Job Tchoumtchoua. Their constant support has boosted my energy and has made me a better scientist.

My warmest thanks go to my friends, Nikitia, Marianna, Rozalia, Job, Katerina, Pinelopi and Eva Dina for all the things we have shared and seen together, for their support and their love.

My deepest gratefulness goes to my friends Eirini and Ioanna for their support and their love. Nothing would have been the same if they haven’t been around me to constantly cheer me up, to help me overcome the difficulties, to encourage me and to love me.

Τέλος θα ήθελα να ευχαριστήσω την οικογένειά μου για την αγάπη τους, την ανιδιοτελή στήριξη, για την υποστήριξη, για την ανοχή, για τη βοήθεια που μου παρείχαν στο να πραγματοποιήσω το όνειρό μου και για τις όλες τις θυσίες που έκαναν τα 12 χρόνια των σπουδών μου.

Λουτσιάνο, Βασίλη, Κατερίνα, Χριστίνα, Χρήστο και Νίνα

ΣΑΣ ΕΥΧΑΡΙΣΤΩ ΑΠΟ ΤΑ ΒΑΘΗ ΤΗΣ ΚΑΡΔΙΑΣ ΜΟΥ